

**Key Roles of Essential Genes in Mycobacterial Glycoconjugate
Biosynthesis: *otsB2* and *Rv0225***

Inaugural dissertation

for the attainment of the title of doctor
in the Faculty of Mathematics and Natural Science
at the Heinrich Heine University Düsseldorf

presented by
Jan Korte
from Nottuln

Düsseldorf, November 2019

from the Institute of Pharmaceutical Biology and Biotechnology
at the Heinrich Heine University Düsseldorf

Published by permission of the
Faculty of Mathematics and Natural Sciences at
Heinrich Heine University Düsseldorf

Supervisor: Prof. Dr. Rainer Kalscheuer
Co-supervisor: Prof. Dr. Karl-Erich Jaeger
Date of the oral examination: 26.05.2020

„Inmitten der Schwierigkeiten liegt die Möglichkeit.“

(Albert Einstein)

Acknowledgement

First and foremost, I would like to express my sincere gratitude to Prof. Dr. Rainer Kalscheuer. His professionalism, broad knowledge, patience and thoroughness guided me through scientific questions and contributed immensely to my personal development. I appreciate the funding and all his inspiring ideas, which made my Ph.D. thesis, productive and stimulating. It has been a great honor to be one of his Ph.D. students and being part of such an excellent and successful institute.

I cordially like to thank Prof. Dr. Karl-Erich Jaeger for his willingness being my co-supervisor and sharing with me his diverse expertise during my Ph.D.

I am very thankful for the generous funding of the Jürgen Manchot Stiftung and the Graduate School „Molecules of Infection“. Undoubtedly, it enriched my interdisciplinary way of thinking and my scientific education.

I am especially grateful to my whole working group, for the joy and enthusiasm. Thank you for advice and collaboration during the whole period. Especially, I would like to thank Lasse van Geelen, Hendrik Koliwer-Brandl, Milena Hänisch, Nidja Rehberg, Lisanna Hülse, Kathrin Sommer and Dieter Meyer. Many thanks also to Heike Goldbach-Gecke. It has been a pleasure working with you. Thank you for all the interesting discussions, reliability and establishing an efficient atmosphere in busy times.

I would like to acknowledge honorary the whole Institute of Medical Microbiology and Hospital Hygiene, especially Prof. Dr. Klaus Pfeffer for his support. His lab has been a source of collaboration, scientific interactions and friendships. Thanks to Daniel Degrandi and Tim Mehlhorn for the time, we have spent together in the lab. Thanks to Prof. Dr. Heiner Schaal and Björn Wefers. Your commitment around the BSL3 laboratory was impeccable. I enjoyed the teamwork and professionalism in handling pathogens.

I am much obliged to the whole Institute of Pharmaceutical Biology and Biotechnology, in particular Prof. Dr. Peter Proksch for giving me the opportunity to obtain more insights into the world of drug discovery.

Lastly, thanks to my mother for her encouragement and unlimited support. Thanks a million to Frank for sharing my enthusiasm to biology and backing all our family pursuits.

And most importantly, I would finally express my deepest gratitude and love to my wonderful wife Lisa. She is the most impressive person and I am more than thankful to spend my life with her and our family. For these reasons, I would like to dedicate my scientific work to her. Your faithful support during my whole doctoral thesis is so appreciated. Thank you!

Summary

(Parts of this summary related to *OtsB2* has been published in *PLoS Pathog* 12(12): e1006043)

On a global perspective, *Mycobacterium tuberculosis*, the etiologic agent of tuberculosis, represents the most devastating bacterial pathogen. Multi-drug resistance is a major force causing the exacerbation of the global tuberculosis pandemic. Strains are emerging worldwide at an alarming rate which are resistant to most available antitubercular drugs and which are very difficult to control. The whole structure of the mycobacterial cell wall is of considerable complexity and thickness, which confers high intrinsic resistance against antibiotics. First-line drugs such as isoniazid and ethambutol target the mycobacterial cell wall and have been used for the clinical treatment since many decades, justifying the ongoing research on the mycobacterial cell wall assembly to identify novel drug targets. In order to contribute to *Mycobacterium tuberculosis* research, two projects were in focus of this doctoral thesis investigating key roles of the essential mycobacterial cell wall associated genes *otsB2* and *Rv0225*. Both genes are likely involved in a direct or indirect manner in the mycolic acid metabolism in mycobacteria. Mycolic acids are the major component of the mycobacterial cell wall and occur in different forms of glycoconjugates that together form a highly hydrophobic layer.

Project 1 „Trehalose-6-Phosphate-Mediated Toxicity Determines Essentiality of *OtsB2* in *Mycobacterium tuberculosis* in Vitro and in Mice“ deals with mycolic acid-containing trehalose glycoconjugates, which are essential for mycomembrane formation. Generally, trehalose biosynthesis is considered an attractive target for the development of antimicrobials against fungal, helminthic and bacterial pathogens including *Mycobacterium tuberculosis*. The most common biosynthetic route involves the trehalose-6-phosphate (T6P) synthase *OtsA* and T6P phosphatase *OtsB2* that generate trehalose from ADP/UDP-glucose and glucose-6-phosphate. In order to assess the drug target potential of T6P phosphatase, we generated a conditional mutant of *Mycobacterium tuberculosis* allowing the regulated gene silencing of the T6P phosphatase gene *otsB2*. We found that *otsB2* is essential for growth of *Mycoacterium tuberculosis in vitro* as well as for the acute infection phase in mice following aerosol infection. By contrast, *otsB2* is not essential for the chronic infection phase in mice, highlighting the substantial remodelling of trehalose metabolism during infection by *Mycobacterium tuberculosis*. Blocking *OtsB2* resulted in the accumulation of its substrate T6P, which appears to be toxic, leading to the self-poisoning of cells. Accordingly, blocking T6P production in a Δ *otsA* mutant abrogated *otsB2* essentiality. T6P accumulation elicited a global upregulation of more than 800 genes, which might result from an increase in RNA stability implied by the enhanced neutralization of toxins exhibiting ribonuclease activity. Surprisingly, overlap with the stress

response caused by the accumulation of another toxic sugar phosphate molecule, maltose-1-phosphate, was minimal. A genome-wide screen for synthetic lethal interactions with *otsA* identified numerous genes, revealing additional potential drug targets synergistic with OtsB2 suitable for combination therapies that would minimize the emergence of resistance to OtsB2 inhibitors.

Project 2 „Functional Analysis of the Putative Essential Glycosyltransferase Rv0225 in a Cell Wall Associated Gene Cluster in *Mycobacterium* Species“ describes the functional analysis of the annotated glycosyltransferase Rv0225, which might play a role in synthesis of methylglucose lipopolysaccharides (MGLPs), which in turn are supposed to affect mycolic acid metabolism in the mycobacterial cell. Since MGLPs are only found in slow-growing mycobacteria, they likely play an essential role in bacterial growth for *Mycobacterium tuberculosis*. Studies suggest that the polymer has a regulatory function for the fatty acid synthase I (FAS-I). Its biological function and structure are not completely understood. We hypothesized that Rv0225 might elongate the proximal part of the MGLP glucan backbone. Our results based on conditional gene silencing demonstrate that *Rv0225* is strictly essential for *in vitro* growth in *Mycobacterium smegmatis* strain mc2155, *Mycobacterium bovis* BCG-Pasteur and, more important, also for the virulent *Mycobacterium tuberculosis* strain H37Rv. *In vitro* killing kinetics revealed that inactivation of *Rv0225* is bactericidal, resulting in rapid loss of viability upon gene silencing. Partially silenced conditional *Mycobacterium bovis* and *Mycobacterium smegmatis* mutants exhibited a different colony morphology in comparison to the fully induced mutants, indicative of an altered cell wall structure. A transcriptome profiling of the conditional *Mycobacterium tuberculosis* *Rv0225* mutant using RNAseq points towards cell wall stress in partially silenced cells, which is in agreement with the mentioned altered colony morphology. High-resolution mass spectroscopy ESI-MS (electron spray ionisation-mass spectrometry) revealed a subtle but significant loss of prominent α -mycolic acids under partial silenced gene expression conditions, highlighting a cell wall associated function of Rv0225. Further gene editing experiments on the *Rv0225* conserved mycobacterial gene cluster *Rv0224c* -*Rv0228*, showed the dispensability of the putative methyltransferase *Rv0224c* for *in vitro* growth. On the contrary, the conditional *Mycobacterium tuberculosis* *Rv0226c* mutant showed impaired growth on solid medium under completely silenced gene expression conditions, suggesting a partial essential role of the putative transmembrane protein for *in vitro* growth. Strikingly, when the orthologue of *Rv0226c* was partially silenced in *Mycobacterium bovis*, the mutant exhibited the same alteration in cellular morphology compared to the partial silenced *Rv0225* mutant. This also suggests a cell wall associated function for Rv0226c, possibly in the same pathway with Rv0225.

Table of Contents

Acknowledgement	1
Summary	2
Table of Contents.....	4
1 List of Figures.....	8
2 Table Directory	9
3 Introduction	10
3.1 Robert Koch	10
3.2 Pathogenesis of Tuberculosis	11
3.3 Prevalence / Epidemiology of Tuberculosis	12
3.4 Vaccination.....	15
3.5 Antibiotics	16
3.6 The mycobacterial cell envelope: cell wall and capsule.....	16
3.7 Trehalose	19
3.7.1 Trehalose as a carrier molecule during the mycobacterial cell wall assembly and the recycling function of the LpqY-SugABC transporter	20
3.7.2 Trehalose containing glycolipids and their immunological functions.....	21
3.7.3 The trehalose biosynthetic pathways.....	23
3.7.4 α -Glucans and α -glucan pathways	25
3.8 MGLP-Synthesis	27
3.8.1 MGLPs chemical structure and function	27
3.8.2 Genetics of MGLP synthesis	29
4 Aims of the thesis.....	31
4.1 Trehalose-6-phosphate-mediated toxicity determines essentiality of OtsB2 in <i>M. tuberculosis</i> in vitro and in mice.....	31
4.2 Characterization of the putative essential glycosyltransferase Rv0225 in a cell wall associated gene cluster in <i>Mycobacterium</i> species.	31

5	Material and Methods	33
5.1	List of abbreviations	33
5.2	Generation of targeted gene deletion and conditional mutants	34
5.2.1	Oligonucleotides	35
5.3	Instruments, Kits and consumables.....	44
5.4	Strains and growth conditions	45
5.4.1	Cultivation of mycobacterial strains	45
5.4.2	Cultivation of <i>E. coli</i>	45
5.4.3	Harvesting and washing of bacteria.....	46
5.4.4	Generation of glycerol stocks of Mycobacteria and <i>E. coli</i>	46
5.5	Genetical and analytical methods	46
5.5.1	Plasmid isolation.....	46
5.5.2	Polymerase chain reaction (PCR)	46
5.5.3	Agarose gel electrophoresis	48
5.5.4	DNA extraction out of agarose gel.....	48
5.5.5	Sequencing for plasmid quality control	49
5.5.6	Restriction of DNA	49
5.5.7	Ligation.....	50
5.5.8	Generation of site-specific gene deletion mutants.....	50
5.5.9	Generation of conditional mycobacterial mutants.....	50
5.5.10	Genetic complementation.....	52
5.5.11	Hidden Markov Models (HMMs) for non-gene-centric comparative analysis of Tn-seq data	52
5.5.12	Resazurin microplate assay (REMA) for growth quantification of ATc dependant mycobacterial growth.....	53
5.5.13	Isolation of genomic DNA	54
5.5.14	Southern Blot.....	56
5.5.15	Transformation of <i>E. coli</i> via heat shock.....	56
5.5.16	Transformation of mycobacteria	56
5.5.17	Mouse infection: OtsB2 study.....	57
5.5.18	Thin-layer chromatography (TLC) and ¹ H-NMR analysis of carbohydrates for OtsB2.	57
5.5.19	Extraction and TLC analysis of Mycolic Acid Methyl Esters (MAMEs).....	57
5.5.20	Extraction and TLC analysis of cell wall associated lipids in BCG.....	58
5.5.21	Transcriptome profiling of conditional OtsB2 and Rv0225 mutants	58

6	Results	59
6.1	Trehalose-6-phosphate-mediated toxicity determines essentiality of OtsB2 in <i>Mycobacterium tuberculosis</i> <i>in vitro</i> and in mice.....	59
6.1.1	OtsB2 is essential for the <i>in vitro</i> growth of <i>M. tuberculosis</i>	59
6.1.2	T6P-associated toxicity is the cause of OtsB2 essentiality	61
6.1.3	Insights into the T6P-induced stress response	63
6.1.4	OtsB2 is essential for <i>M. tuberculosis</i> to establish an acute infection in mice.....	66
6.1.5	Genome wide screen for synthetic lethal interactions.....	68
6.2	Characterization of the putative essential glycosyltransferase Rv0225 in a cell wall associated gene cluster in <i>Mycobacterium</i> species	69
6.2.1	Sublethal <i>Rv0225</i> gene-silencing in conditional <i>Mycobacterium</i> species leads to an altered colony morphology and α -mycolic acid composition	73
6.2.2	Thin layer chromatography- and mass spectroscopy analysis on mycobacterial lipids	74
6.2.3	Genome-wide characterization of the <i>Rv0225</i> -elicited stress response profile.....	76
7	Discussion	79
7.1	Trehalose-6-phosphate-mediated toxicity determines essentiality of OtsB2 in <i>Mycobacterium tuberculosis</i> <i>in vitro</i> and in mice.....	79
7.2	Characterization of the putative essential glycosyltransferase <i>Rv0225</i> in a cell wall associated gene cluster in <i>Mycobacterium</i> species	81
8	Supplementary Information	86
8.1	List of Figures (Supplementary Information)	86
8.2	Table Directory (Supplemental Information)	87
8.3	OtsB2 study	88
8.4	Rv0225 study	99
9	References	119
10	Statement of project contribution	129

11 Research contributions.....	132
11.1 Journal publications	132
11.2 Talks and Poster	132
12 Curriculum Vitae.....	133
13 Eidesstattliche Erklärung.....	134

1 List of Figures

Fig 1. Estimated TB incidence rates (2015), reproduced from WHO (2016) [12].	13
Fig 2. Percentage of new TB cases with multi-drug resistant/rifampicin-resistant (MDR/RR)-TB, reproduced from WHO (2016) [12].	14
Fig 3. The mycobacterial cell wall.	17
Fig 4. Chemical structure of trehalose.	19
Fig 5. Reactions of the OtsA-OtsB2 pathway for trehalose synthesis.	24
Fig 6. Revised model of GlgE-mediated intracellular and capsular α -glucan synthesis in mycobacteria.	26
Fig 7. Methylglucose Lipopolysaccharides (MGLPs) in <i>M. tuberculosis</i> .	28
Fig 8. OtsB2 is essential for <i>in vitro</i> growth of <i>M. tuberculosis</i> .	60
Fig 9. Silencing of <i>otsB2</i> leads to T6P accumulation in <i>M. tuberculosis</i> .	62
Fig 10. Genome-wide characterization of the T6P-elicited stress response profile.	64
Fig 11. OtsB2 is required for <i>M. tuberculosis</i> to establish an acute infection in mice but dispensable for survival during the chronic phase.	67
Fig12. The <i>Rv0225</i> homologue <i>MSMEG_0311</i> is essential for <i>in vitro</i> growth of <i>M. smegmatis</i> .	71
Fig 13. The <i>Rv0225</i> homologue <i>Mb0230</i> is essential for <i>in vitro</i> growth of <i>M. bovis</i> .	72
Fig 14. <i>Rv0225</i> is essential for <i>in vitro</i> growth of <i>M. tuberculosis</i> .	73
Fig 15. ATc dosis dependent partial gene silencing of the <i>Rv0225</i> homologous locus <i>MSMEG_0311</i> in <i>M. smegmatis</i> leads to differences in cell morphology.	74
Fig 16. Mycolic acid analysis of <i>M. tuberculosis</i> c- <i>Rv0225</i> -tet-on via mass spectroscopy ESI-MS (electron spray ionisation-mass spectrometry).	75
Fig 17. Insights into the <i>Rv0225</i> -induced stress response in <i>M. tuberculosis</i> using RNAseq.	77
Fig 18. Confirmation of RNAseq via qRT-PCR.	78

2 Table Directory

Table 1. Oligonucleotides used for generation of allelic exchange substrates in the OtsB2 study	35
Table 2. Strains used in the OtsB2 study	35
Table 3. Oligonucleotides used for pMV361 complementation plasmid in the OtsB2 study	37
Table 4. Oligonucleotides used for generation of allelic exchange substrates in the Rv0225 study	37
Table 5. Mycobacterial strains used in the Rv0225 study.	38
Table 6. Oligonucleotides used for pMV361 complementation plasmids in the Rv0225 study	42
Table 7. Overview of used <i>E. coli</i> strains used for the OtsB2 and Rv0225 studies	42
Table 8. Oligonucleotides used for qRT-PCR of <i>M. tuberculosis</i> transcripts (OtsB2 study)	43
Table 9. Oligonucleotides used for qRT-PCR of <i>M. tuberculosis</i> transcripts (Rv0225 study)	43
Table 10. Instruments, kits and consumables used in this study	44
Table 11. Kits	44
Table 12. Consumables.....	44
Table 13. Overview of the used PCR-Protocol for defined DNA fragment amplification...	47
Table 14. Quantitative real time PCR	47
Table 15. Tris-Acetate-EDTA-buffer (TAE-buffer)	48
Table 16. Oligonucleotides used for sequencing reactions for verification of plasmids. .	49
Table 17. Applied restriction enzymes.....	49
Table 18. Anhydrotetracycline culturing conditions for dosis dependant gene silencing of conditional mycobacterial mutants.....	54
Table 19. List of the ten most differentially up- and downregulated genes in T6P-stressed <i>M. tuberculosis</i> cells.	65
Table 20. Genes differentially essential in the <i>M. tuberculosis</i> Δ otsA mutant in absence of trehalose supplementation.	69

3 Introduction

3.1 Robert Koch

Robert Koch (1843-1910) is known as the founder of modern bacteriology. The discoveries of the German microbiologist made significant contributions to the development of new experimental methods to test whether a particular microorganism is the cause of a disease. Indeed, he was the first scientist to report the successful isolation of the causative agent of the tuberculosis disease (TB) in 1882, named one year later as "*Mycobacterium tuberculosis*" (*M. tuberculosis*).

R. Koch became popular at a meeting of the Physiological Society in Berlin in March 24 in 1882 by holding his famous lecture: "The Etiology of Tuberculosis". He brought his entire laboratory to the lecture room and illustrated the identification of the microscopic rod-shaped bacterium by demonstrating tissue dissections from *M. tuberculosis* infected guinea pigs. These test animals were infected with tuberculous material, obtained from several sources: material from infected apes (lungs), from humans who either had died from blood-borne tuberculosis (brains and lungs) or were chronically infected (cheesy masses from lungs) and lastly from *M. tuberculosis* infected cattle (abdominal cavities).

Independent from the source of the isolated tuberculous material, the experimentally infected guinea pigs developed the same disease severity, and the cultures of bacteria taken from the infected guinea pigs were identical. These observations led to the formulation of the Koch's postulates at the end of the 19th century. First, bacilli can be isolated from tuberculous tissues. Second, the infectious agent can be cultured *in vitro*. Third, the administration of cultured bacilli to a non-infected animal reproduces the same morbid conditions.

In summary, R. Koch clearly demonstrated that TB is acquired through *M. tuberculosis* transmission from a patient or an animal, invaded by this bacterial pathogen.

R. Koch further contributed to the microscopic identification of the acid-fast mycobacteria, including not only *M. tuberculosis* but also *Mycobacterium leprae* and other mycobacterial pathogens. He and others optimized the alcohol-methylene blue staining (Karl Weigert, 1875). Franz Ziehl and Friedrich Neelsen finalized the technique in 1885. The Ziehl-Neelsen stain is still used in the clinics for detection of a broad range of acid-fast mycobacteria.

Additionally, R. Koch published his concept of primary and secondary infection in guinea pigs and discovered the tuberculin - a glycerol extract from dead *M. tuberculosis* cells, later applied as the "Tuberculin Skin Test" (TST) to identify TB infection.

Finally, “for his investigations and discoveries in relation to tuberculosis”, he was presented with the Nobel Prize in Physiology or Medicine in 1905. Undoubtedly, his research shows that transmission and identification of pathogens are important issues in order to treat patients efficiently and prevent devastating pathogenic outbreaks, saving human beings. Certainly, his enthusiasm was driven by the mortality rate of TB. At that time in 1882, he estimated that one in seven of all human beings died from TB. Furthermore, if one only considered the productive middle-age groups, tuberculosis carried away one-third, and often more [1].

3.2 Pathogenesis of Tuberculosis

What makes a successful pathogen in ancient times when people mostly lived in small communities in rather sparsely populated rural areas? It is transmitted via aerosols, very efficiently infects individuals, and causes predominantly latent infection and active disease only in a limited number of infected individuals to allow transmission. *M. tuberculosis* matches all those criteria, which likely contributes to the global spread of this human pathogen.

The only known environmental reservoir of *M. tuberculosis* is humans, implying a long evolutionary adaption of complex host-pathogen interactions, which are still not completely understood [2, 3]. *M. tuberculosis* is commonly known as a pulmonary pathogen, although it can cause disease throughout the body affecting various organs and tissues. The dynamic lifestyle of *M. tuberculosis* can range from asymptomatic infection to a life-threatening disease. In this regard, patients are categorized as having either latent TB infection (LTBI) or active TB disease. In the latent state, the infection has not been cleared entirely by the immune system after exposure. Residual bacteria can switch to a dormant state of infection, persisting for weeks up to several decades in the human body until the infection can progress to clinical disease [4].

Several *in vivo* experiments in small mammals (such as mice, guinea pigs and rabbits) and non-human primates helped to investigate the route and matter of infection. After inhalation of *M. tuberculosis*, the route of infection passes to the lower respiratory tract and bacteria encounter alveolar macrophages, which are the dominant cell type that *M. tuberculosis* infects [2, 3]. Once internalized by receptor-mediated phagocytosis, *M. tuberculosis* actively blocks phagosome fusion with lysosomes, ensuring its survival. In addition to that, the ESX-1 secretion by *M. tuberculosis* can disrupt the phagosomal membrane causing its escape and release of bacterial products, including mycobacteria DNA, into the macrophage cytosol. An important research priority is decoding the advantages of delivering bacterial products into the cytosol. For instance, it has been associated with the activation of the cytosolic surveillance pathway in order to facilitate promotion of intracellular bacterial growth [5, 6]. Hence, the first line of defending alveolar macrophages, dendritic cells or monocytes fail to eliminate the bacteria, and

M. tuberculosis gains access to the lung interstitium, possibly via transmigration of *M. tuberculosis* infected alveolar macrophages across the alveolar epithelium to the lung parenchyma or by directly infecting alveolar epithelial cells. Subsequently, *M. tuberculosis* is transported by either dendritic cells or inflammatory monocytes to pulmonary lymph nodes for T cell priming, leading to granuloma formation [2]. These are characteristic structures during the latent state of infection with equilibrium of replicating and killed bacterial cells by the immune system. With these granulomas, the host tries to “wall-off” the infection from the rest of the body [2], reducing substantial tissue pathology outside these immune structures [7, 8]. Based on this latent state of infection, under certain conditions such as malnutrition, diabetes, immune senescence or co-infection with other pathogens (e.g.: HIV), *M. tuberculosis* can become reactivated [9]. In case of active TB and from the bacterial perspective, it is a growing collection of phagocytic cells to infect and replicate within. If the bacterial load becomes too great, the granulomas fail to contain the infection and bacteria can enter the bloodstream or re-enter the respiratory tract to be released. The disease turns into an active disease: the host is infectious and symptomatic [2].

3.3 Prevalence / Epidemiology of Tuberculosis

Globally, TB remains a major killer. Since even more than 130 years after R. Koch’s findings, TB still belongs to one of the top 10 causes of death. The world’s population is currently estimated at 7.32 billion people. Roughly, about one-third of the world's population has latent TB (2.44 billion people), which means people have been infected by TB bacteria but are not (yet) ill with the disease and cannot transmit the disease [10]. The pathogen is not completely eliminated by the immune system, but rather survives in an asymptomatic dormant status of infection, possible for decades until reactivation [4, 11]. It is startling that in 2015, approximately 1.8 million people died by TB infection without any significant co-infections.

On a global perspective in 2015, the number of new and relapse cases of TB was 142 cases per 100,000 population (incidence rate) (Fig 1). In total, approximately 10.4 million people have been newly infected with *M. tuberculosis* in 2015. Importantly, 87% of all estimated incident cases worldwide are accounted by the 30 high TB burden countries. The following six countries had the largest number of incident cases in 2015 in descending order: India, Indonesia, China, Nigeria, Pakistan and South Africa (combined, 60% of the global total TB cases 2015). Although these countries in particular show high TB incidence rates, multidrug-resistant (MDR) strains are emerging worldwide at an alarming rate. These strains are resistant to rifampicin and isoniazid and very difficult to control. Globally in 2015, approximately 480,000 people were

suffering by a MDR-strain [12]. Most cases of MDR-TB are estimated to reflect transmission rather than initial acquisition [2, 13].

Estimated TB incidence rates, 2015

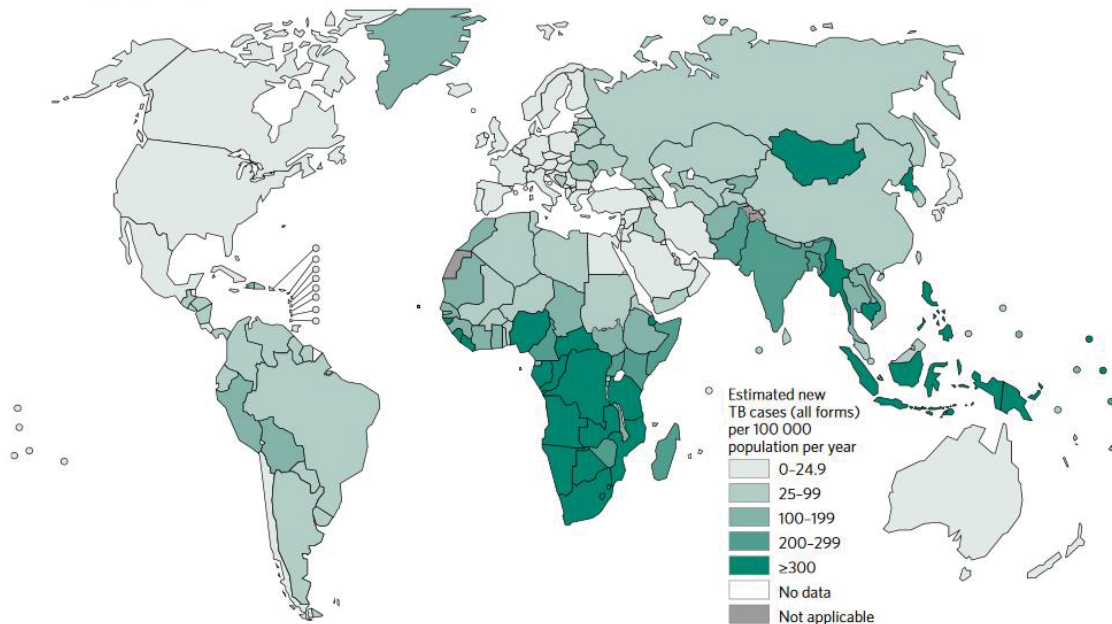
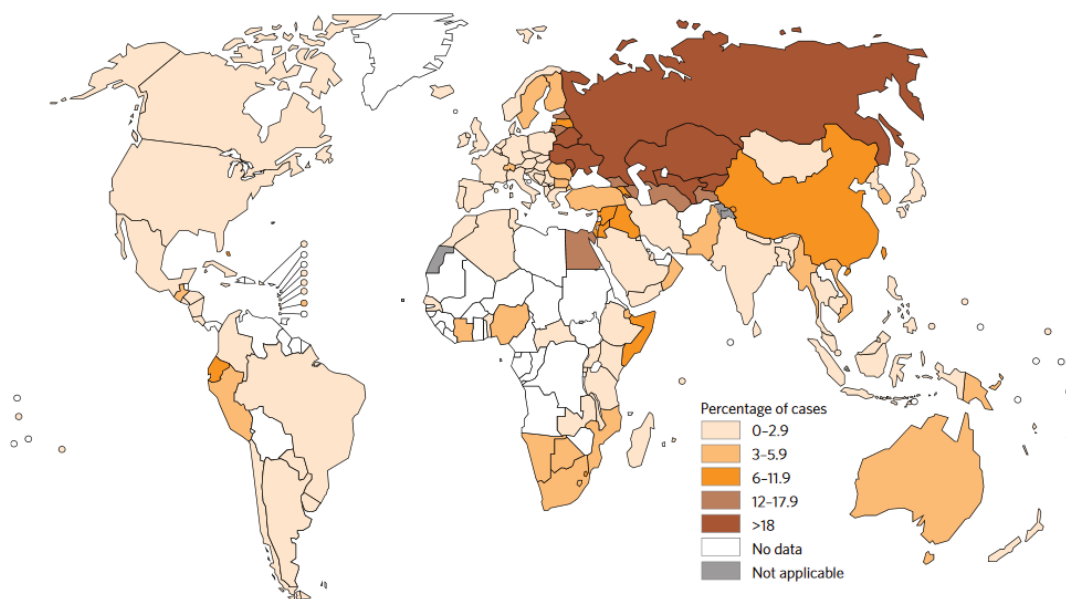


Fig 1. Estimated TB incidence rates (2015), reproduced from WHO (2016) [12].

For instance, the highest incidence rates occur in Russia, Kazakhstan, Ukraine and Belarus. In 2015, in these countries more than 18% of newly estimated TB-cases were related to MDR-strains (Fig 2). In addition, the TB-incidence in China is of a particular concern where one-quarter of all active TB disease cases are resistant to either isoniazid or rifampicin [2, 13].

Percentage of new TB cases with MDR/RR-TB^a

^a Figures are based on the most recent year for which data have been reported, which varies among countries. Data reported before the year 2001 are not shown.

Fig 2. Percentage of new TB cases with multi-drug resistant/rifampicin-resistant (MDR/RR)-TB, reproduced from WHO (2016) [12].

MDR-strains are resistant to isoniazid and rifampicin with or without resistance to other first-line drugs and have been reported in virtually all countries [14]. *M. tuberculosis* can also acquire extensively drug resistance (XDR). These strains are very difficult to control and, in addition to resistances to the two most powerful anti-TB drugs isoniazid and rifampicin, involve further resistance to any of the fluoroquinolones (such as levofloxacin or moxifloxacin) and to at least one of the three injectable second-line drugs (amikacin, capreomycin or kanamycin). Also frightening, India witnessed the emergence of so-called totally drug-resistant strains which have been described to show resistance to nine or even more different anti-TB drugs [2, 15].

Furthermore, HIV co-infections play a significant role in TB-disease incidence and progression [2, 16, 17]. Hence, circa 0.4 million HIV co-infected people died in 2015. TB is clearly a poverty related disease given the fact that over 95% of TB deaths occur in low- and middle-income countries [12]. In these countries, the HIV incidence is increased in comparison to high-income countries due to insufficient medication, malnutrition, a lack of knowledge of HIV transmission routes and poor patient's compliance [18]. HIV patients co-infected with *M. tuberculosis* are 20 to 30 times more likely to develop active TB compared to people with an *M. tuberculosis* infection alone. For this reason, TB is known to be a leading killer of HIV-positive people. In 2015, 35% of HIV deaths were due to TB [12]. Furthermore, many people with HIV in Africa likely die of undiagnosed TB [19].

In general, TB is frequently fatal in the absence of treatment. Approximately 50% of individuals who develop active TB disease will succumb to it. Although the TB incidence has fallen by an average of 1.5% per year since 2000, MDR and XDR strains cause great concern due to an ineffective TB-treatment [12]. Thus, a high priority for the response to drug-resistant TB is to identify and target 'hotspots' of MDR-TB transmission [20] and to develop a broad spectrum of antibiotics.

3.4 Vaccination

What are the reasons for the worldwide TB pandemic more than 130 years after the discovery of *M. tuberculosis* by Robert Koch? Certainly, one answer would be decades of neglect in the development of new vaccines. In 1928, more than 90 ago, an attenuated live vaccine derived from *Mycobacterium bovis* (*M. bovis*) was the first anti-TB vaccine, mainly developed at the Pasteur Institute by Albert Calmette and Camille-Guérin (BCG-Pasteur) [21]. Notably, for almost a century now, BCG is administrated to prevent life threatening clinical forms of TB in >90% of infants per year, globally [2, 22]. Infants and children under 5 years of age are likely to be protected against severe, extrapulmonary forms of active TB and TB morbidity (such as TB meningitis) and mortality [23]. Unfortunately, BCG vaccination has been ineffective in controlling the global TB epidemic because it provides insufficient protection against the major form of the disease, i.e. pulmonary TB in adults. The BCG vaccine is administered once at birth, and its protection is unlikely to extend consistently into adolescence, probably only up to ten years with vaccine efficacy waning over time [22]. Hence, the risk of progression from infection to active TB disease in adults remains high [12]. Furthermore, BCG vaccination is not recommended for HIV-exposed infants [2]. Retrospective studies from Argentina and South Africa show there is a substantiated higher risk of disseminated BCG disease developing in children infected with HIV who are vaccinated at birth and who later developed AIDS [24]. Both the slow decline in TB incidence globally and the persistent threat of MDR-TB highlight the critical need for new TB vaccines that are more effective than the BCG vaccine in preventing TB. At the moment, there are 13 advanced candidates in the TB vaccine development pipeline. Nevertheless, a new TB vaccine is not expected to be approved in the near future. Research is focused on recombinant BCGs, whole-cell derived vaccines, recombinant viral-vectored platforms, protein and adjuvant combinations, and mycobacterial extracts either in order to prevent infection (pre-exposure) or to prevent primary progression into disease or reactivation of LTBI (post-exposure). Finally, TB infection does not guarantee resistance to a subsequent second infection - a reason why further vaccines and antibiotics must be developed [12].

3.5 Antibiotics

Anti TB-treatment relies on targeting essential mycobacterial compartments and processes such as interrupting the DNA coiling (fluoroquinolones: inhibition of DNA-gyrase), transcription (rifampicin: RNA-synthesis) [25], inhibition of energy catabolism (bedaquiline: inhibition of ATP synthase) and cell wall synthesis (isoniazid / delamanid: inhibition of mycolic acid synthesis; ethambutol: inhibition of arabinogalactan and lipoarabinomannan synthesis) [2].

The slow growth rate of *M. tuberculosis* (generation time *E. coli* 20 min, *M. tuberculosis* 20 – 24 h) correlates with a slow killing rate. Hence, the standard TB-treatment for new patients with pulmonary TB includes a long combination therapy of six months (2HRZE/4HR), comprising treatment with isoniazid (H, introduced in 1952), rifampicin (R, 1963), pyrazinamide (Z, 1954) and ethambutol (E, 1961) over two months, followed by isoniazid and rifampicin treatment over a duration of four month [26]. The optimal dosing frequency is daily throughout the course of therapy. Patients suffering from MDR-TB must be treated with second line antibiotics (such as capreomycin, kanamycin, fluoroquinolones, streptomycin and amikacin) and the individual treatment is based on the respective resistances. The cost intensive MDR and XDR-TB treatment often takes 18 to 24 month and over two years, respectively [27]. The more resistances are acquired, the worse is the therapeutic success.

Returning to the initial question why *M. tuberculosis* still remains a major problem in human health: all of the first-line drugs of today were discovered between 1952 (isoniazid) and 1963 (rifampicin). TB drug discovery flourished in the mid-20th century, but since 1963, discoveries of novel anti-mycobacterial lead structures have been elusive. First hope raised in the year 2014 after approximately five decades, when the anti-TB drug bedaquiline representing a new chemical class (diarylquinoline) became available. Together with the new compound delamanid (a nitroimidazo-oxazole derivative), the US Food and Drug Administration (US FDA) conditionally approved the drugs for treatment of adults with pulmonary MDR-TB in 2014. However, the persistent threat of MDR and XDR-TB highlight the critical need of novel drug targets and new anti-mycobacterial lead structures in order to defend one of the most devastating pathogens. Additionally, there is a strong need for new TB vaccines that are more effective than the BCG vaccine [12].

3.6 The mycobacterial cell envelope: cell wall and capsule

The expansively structured Gram-positive mycobacterial cell wall (Fig 3) provides an intrinsic barrier to a huge range of antibiotics. The composition is rich of lipids and glycoconjugates and not only serves as a permeability barrier, providing protection against hydrophilic compounds, but also it is vital in supporting cell growth and virulence [28]. The mycobacterial cell wall

consists of three distinct layers between the inner most cytoplasm membrane and the outermost capsule: a cross-linked polymer of peptidoglycan, anchored to the cytoplasm membrane, followed by a highly branched arabinogalactan polysaccharide. Characteristic and unique within the Gram-positive bacteria, a thick waxy coat comprised of a layer of long-chain mycolic acids forms the third layer, called the mycomembrane, and completes the so-called **mycolyl-arabinogalactan-peptidoglycan** (mAGP) complex [28, 29]. The cytoplasm membrane composition is typical for bacteria and includes phospholipids such as phosphatidylethanolamine, phosphatidyl-*myo*-inositol (PI), cardiolipin, phosphatidylserine and phosphatidylglycerol [30]. As in all bacteria, phospholipids form the basic structure of a bio membrane in order to maintain bilayer fluidity and stability.

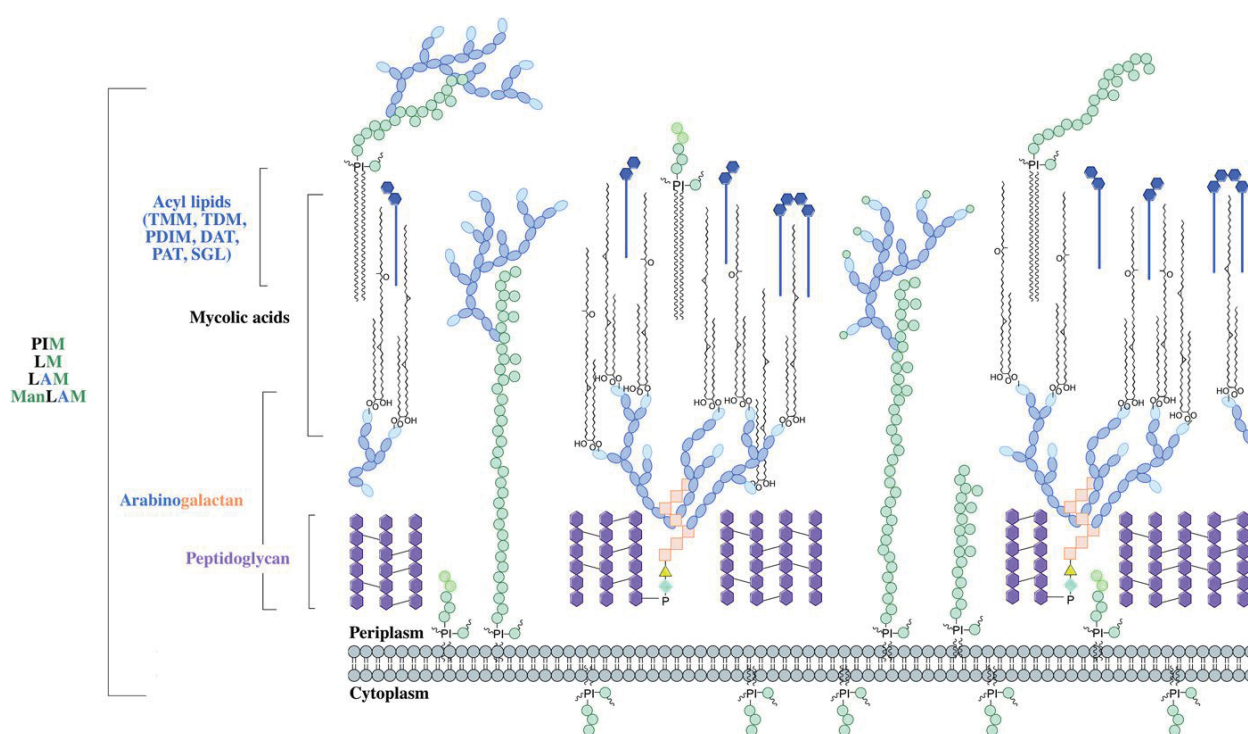


Fig 3. The mycobacterial cell wall.

A schematic representation of the mycobacterial cell wall, depicting the prominent features including glycolipids (PIMs, phosphatidyl-*myo*-inositol mannosides; LM, lipomannan; LAM, lipoarabinomannan; ManLAM, mannosylated lipoarabinomannan), peptidoglycan, arabinogalactan and mycolic acids. Intercalated into the mycolate layer are the acyl lipids (including TMM, trehalose monomycolate; TDM, trehalose dimycolate; DAT, diacyltrehalose; PAT, polyacyltrehalose; PDIM, phthiocerol dimycocerosate; SGL, sulfoglycolipid). The capsular material is not illustrated. Figure reproduced from Besra, G.S [31].

However, certain phospholipids might possess specialized functions. It has been reported that the non-covalently linked PIs are essential for *M. tuberculosis* survival [32], indicating their importance. In addition to their localization in the inner cytoplasmic membrane, PI-based glycoconjugates can also be found in the mycomembrane of all *Mycobacterium* species, where they are anchored with their PI moiety [31, 33]. The mannosylated forms of PIs are

phosphatidyl-myo-inositol mannosides (PIMs), glycopospholipids with attached carbohydrates. They serve as a structural component for lipoglycans (lipids with attached carbohydrates), called lipomannans (LMs), lipoarabinomannans (LAMs) and mannosylated (mannose caps) lipoarabinomannans (ManLAMs) [34]. LMs and LAMs are associated with *M. tuberculosis* pathogenicity as they represent modulators of host pathogen interactions during infection [35-38].

The peptidoglycan layer ensures shape and rigidity, and it is also responsible for counteracting turgor pressure [39]. All Gram-positive bacteria share the same basic core structure: a glycan backbone and short cross-linked peptide side chains. Peptidoglycan is a polymer of alternating N-acetylglucosamine and N-acetylmuramic acid, whereas mycobacterial peptidoglycan includes N-glycolyl- and N-acetylmuramic acid residues, amidation of the carboxylic acids in the peptide stems and additional glycine or serine residues [39, 40].

The arabinogalactan is attached to peptidoglycan via a single linker unit [41]. Arabinogalactan is a layer of highly branched macromolecules, the major cell wall polysaccharide [31]. As the name suggest, it is composed predominantly of galactose (Gal) and arabinose sugar (Ara) residues [42]. A linear chain of approximately 30 galactan residues built the galactan core, which in turn is attached to 30 arabinose residues [31]. The non-reducing termini of the arabinose chain acts as attachment site for mycolic acids [43, 44].

The so-called mycomembrane forms an outer membrane-like structure. It is the outermost component of the mycobacterial cell wall and is attached to the arabinogalactan layer. It contributes to the fluidity, permeability [45], integrity, virulence [46] and hydrophobicity of the acid fast mycobacterial cell wall. Mycolic acids are characterized by C₅₄ to C₆₃ α -alkyl β -hydroxy fatty acids bearing C₂₀ to C₂₄ α -side chains [47], divided in three distinct structural classes in *M. tuberculosis*: α -, methoxy- and keto-mycolic acids. The α -mycolic acids are the most abundant form (>70%), whereas methoxy- and keto-mycolic acids are minor components (15% each) [48]. The mycolic acid biosynthesis is catalyzed by a complex interaction of several enzymes [28]. Briefly, the **fatty acid synthase I (FAS-I)** catalysis the *de novo* synthesis of short-chain fatty acids (C₁₆₋₂₄) from acetyl-CoA [47]. These fatty acids are released as CoA derivatives. It has been proposed that C₂₀₋₂₄ fatty acids serve as a starting point where the **fatty acid synthase II (FAS-II)** system takes over for the synthesis of the very-long-chain mero segment (C₅₄ to C₆₃) mycolic acids. Desaturases or dehydratases/isomerases and methyl transferases modify the proximal and distal ends of the meromycoloyl chain, introducing double bonds, cyclopropyl, methoxy and keto functionalities [49]. Both non-elongated released α side chains and modified meromycoloyl chains are coupled by the acyl-AMP ligase FadD32 and polyketide synthase Pks13 [47] in order to produce α -alkyl- β -keto-mycolic acids [50]. Mycolic acids also occur in form of glycoconjugates, namely trehalose-6,6'-dimycolate TDM (also known as „cord factor“)

and as the carrier molecule trehalose-6-monomycolate (TMM) in the outer cell envelope. Both forms fulfill structural and immunomodulatory functions [51, 52].

Further cell wall associated molecules are glycolipids, glycoproteins and other factors such as phthioceroldimycocerosates (PDIMs) [53], which are located in the outer membrane of the mycobacterial cell wall [31, 54]. The cell envelope of *M. tuberculosis* is completed by an outer membrane segment, also referred to as capsule. It is composed of solvent-extractable lipids, polysaccharides and proteins forming a loosely bound mesh [31]. The mesh is dominated by a glycogen-like polysaccharide (α -glucan glucose polymer), but it also contains secreted proteins that include lipases, proteases, secretion systems and porins. As a whole, the capsule is thought to be involved in mycobacterial–host interactions or in the maintenance of the typical *M. tuberculosis* intracellular lifestyle [55, 56].

3.7 Trehalose

Trehalose (Fig 4) has been an important focus of research over the last 60 years. It is widely distributed in nature and found in all domains of life, including several eukaryotic organisms (fungi, nematodes, insects, crustaceans and plants) and members of the prokaryotic domains Bacteria and Archaea [57]. In 1832, H.A.L. Wiggers discovered the non-reducing natural glucose disaccharide (α -D-glucopyranosyl-1 \rightarrow 1- α -D-glucopyranoside) in the fungus *Claviceps purpurea*. Twenty-six years later, the same sugar was isolated from ‘trehala manna’, the sweet-tasting cocoons of *Larinus* beetles, and named trehalose [58]

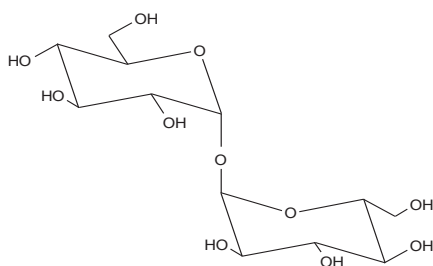


Fig 4. Chemical structure of trehalose.

Trehalose (α -D-glucopyranosyl-1 \rightarrow 1- α -D-glucopyranoside) is an abundant disaccharide found in many different groups of organisms with the notable exemption of mammals.

It has been shown that trehalose is the primary sugar in insects' haemolymph and the main source of energy required for flight [59]. It is also considered an universal stress-bioprotectant, synthesized and accumulated in response to stimuli such as osmotic, heat, cold, dehydration and other stresses in order to prevent denaturation and to maintain intracellular integrity [57, 60, 61]. In this regard, trehalose plays an essential role in *Escherichia coli* (*E. coli*) resistance to cold [62, 63]. In *Candida albicans*, trehalose accumulates in response to oxidative stress, and

its absence was shown to accelerate H₂O₂-triggered apoptosis [64]. In *Propionibacterium freudenreichii*, the accumulation of trehalose was a common response to acid stress, osmotic pressure and oxidative insults [65]. Notably, studies have shown that trehalose is required for the viability and/or virulence of several fungal, helminthic and many bacterial pathogens. Trehalose biosynthesis has recently been considered a potent virulence factor of the plant pathogen *Pseudomonas aeruginosa* PA14 by allowing its replication in the plant intercellular environment [66]. Overall, trehalose is an extremely versatile molecule, often an essential element in many organisms.

A century after its original discovery, Mary Pangborn and Rudolph Anderson purified trehalose from a *Mycobacterium* strain for the first time (Pangborn & Anderson, 1933). Today it is known that trehalose is conserved in over 160 species within the class of actinobacteria– not only within the genus *Mycobacterium*, but also in genera such as *Corynebacterium* and *Nocardia* [57]. As already indicated, it is a crucial player in the assembly and architecture of the remarkable mycobacterial cell envelope as a structural component of several highly antigenic glycolipids, namely the above-mentioned TDM and TMM. These molecules fulfil crucial roles in the formation of the mycolic acid cell wall layer either as a structural component TDM or as a carrier molecule TMM that shuttles mycolic acids from their site of biosynthesis in the cytoplasm to the periplasm, where they serve as substrates of the antigen 85 complex [51, 67]. Free trehalose has been detected in the mycobacterial cytoplasm and occasionally in oligosaccharides with unknown function. However, since gluconeogenesis is reported to be essential for *M. tuberculosis* virulence during infection, it is likely that *M. tuberculosis* is not able to uptake trehalose from the host [68, 69]. Furthermore, trehalose is not synthesized in mammals (although trehalases for the specific hydrolysis of the trehalose present in food sources such as plants, mushrooms, crustaceans or insects are expressed in the intestinal epithelia). Thus, trehalose biosynthesis is considered an attractive target for the development of antimicrobial drugs [51, 70-77].

3.7.1 Trehalose as a carrier molecule during the mycobacterial cell wall assembly and the recycling function of the LpqY-SugABC transporter

Trehalose is recognized as an important structural component within the cell-wall assembly. Briefly, undergoing several processing steps, mature mycolic acids are synthesized in the cytoplasm, which finally form complexes with trehalose to yield TMM. TMM serves as a carrier molecule of the mycolyl group [47, 78]. Via the membrane transporter MmpL3, TMM is transported through the cell membrane. Extracellularly, the periplasmic TMM serves as a substrate of the mycolyltransferases of the antigen 85 complex, which is described to act in two ways. It transfers the mycolate moiety either (i) to the arabinogalactan layer to form cell-wall-

bound mycolates or (ii) to another TMM molecule, resulting in the formation of TDM [79]. The latter case includes the concomitantly release of a trehalose molecule, which was shown to get reimported to the cytoplasm by the LpqY-SugA-SugB-SugC ABC transporter. *M. tuberculosis* Δ lpqY and Δ sugC mutants secreted substantial amounts of trehalose in the supernatant during growth on glycerol, whereas no trehalose was detected in control experiments with the respective complemented mutant strains or the *M. tuberculosis* wild-type strain. This strongly suggests a trehalose recycling mechanism, mediated by the LpqY-SugA-SugB-SugC ABC transporter. Importantly, the *M. tuberculosis* Δ lpqY and Δ sugC mutants were strongly attenuated for virulence in mice during the early phase of infection but were still able to persist in mice during the chronic infection phase. This indicates that trehalose recycling via the LpqY-SugA-SugB-SugC ABC transporter plays a significant role during the acute infection phase but is largely dispensable for the chronic infection phase in mice [68].

3.7.2 Trehalose containing glycolipids and their immunological functions

The innate immunity plays an important role during the first contact with *M. tuberculosis*. Macrophages and dendritic cells recognize various pathogen-associated molecular patterns of mycobacteria through pattern recognition receptors, including Toll-like receptors, Nod-like receptors, and C-type lectin receptors (CLR) [52, 80, 81]. Mycobacterial cell wall components such as Man-LAM, LAM, LM, acylated LM, glycerol monomycolate, PIM, AcPIM2 as well as cytosolic DNA are recognized by distinct pattern recognition receptors [52]. There is accumulating evidence demonstrating that CLRs play an essential role in the recognition of mycobacteria. They are mainly defined as a family of proteins binding sugar containing ligands, including Macrophage-Inducible C-Type Lectin (Mincle), Macrophage C-Type Lectin, Dendritic Cell Immunoactivating Receptor, Dectin-2 and Dectin 1 [52]. In context of the crucial role of trehalose in the mycobacterial cell wall and its immunogenic properties, the glycolipid TDM has been described to be a Mincle ligand, which is proposed to activate NF- κ B via the Syk–CARD9–Bcl10–Malt1 pathway, resulting in the maturation of antigen-presenting cells. Additionally and likely, TDM binding by Mincle promotes Th1/Th17T-cell responses, as revealed by *in vitro* studies employing the synthetic TDM analogue trehalose-6,6-dibehenate [82, 83]. In this regard, also the precursor TMM can bind to mincle receptor as a weak ligand [52, 84-86]. Furthermore, it has also been reported that mycobacteria preferentially produce glucose monomycolate (GMM) in host cells instead of TDM, since glucose is proposed to be more abundant compared with other environments [87]. However, GMM is only weakly recognized by Mincle as compared to TDM, suggesting a hypothetical mycobacterial strategy to escape host immunity [84].

Other immunoregulatory molecules containing trehalose in *M. tuberculosis* are sulfoglycolipids, which have been suggested to interact with TDM during infection. Originally, they were

discovered in 1959 in strains of *M. tuberculosis* virulent to humans (H37Rv) or cattle (Vallée) [88]. Like TDM and TMM, the sulfoglycolipids are abundant glycolipids located in the outer membrane of *M. tuberculosis*. Structurally, they consist of multi-acylated forms of trehalose sulfate that differ by the number, structure, and location of acyl moieties [89]. Sulfolipid 1 (SL-1) is known as the major sulfolipid. It was chemically characterized as 2,3,6,6'-tetraacyl- α - α' -trehalose-2'-sulfate acylated by two hydroxyphthioceranates (HPA), one phthioceranate (PA), and one palmitate (C₁₆) or stearate (C₁₈). There are other minor tetra-acylated forms of sulfolipids differing from SL-1 by the fatty acyl composition, namely SL-I', SL-II, and SL-II', and one tri-acylated form, SL-III [90, 91]. SL-IV was tentatively assigned to be 2,3-diacyltrehalose-2'-sulfate. It was isolated from clinical isolates of *M. tuberculosis* [92] and proposed to correspond to the more polar uncharacterized sulfatide observed [93]. However, the compound was finally shown to lack a sulfate ester group [94, 95], meaning it does not represent a sulfatide [96].

Since sulfolipids are integral components of the cell wall, they are likely to interact with host cells during the course of infection. Interestingly, sulfolipids are present in the virulent laboratory strain *M. tuberculosis* H37Rv but absent from the avirulent strain *M. tuberculosis* H37Ra [88]. Their role in virulence is highlighted by a highly significant correlation between the production of sulfolipids in culture of 60 clinical *M. tuberculosis* isolates obtained from different geographical origins and their relative virulence in a guinea pig infection model. The attenuated strains were strongly deficient in sulfolipid production, whereas the virulent strains were generally prolific producers of sulfolipids [97-100]. Nevertheless, authors were careful to make a clear conclusion, since the data included also some outliers, meaning that the presence of sulfolipids may be a necessary but not a sufficient requirement for virulence [97, 98]. Results of Rousseau et al. suggest that SL-1 deficient *M. tuberculosis* H37Rv mutants show no phenotype in mice and guinea pigs or in cultured macrophages [100]. Further studies revealed that even injection of purified high doses of *M. tuberculosis* SL-1 into mice were innocuous. SL-1 was non-toxic and non-granulomatogenic. Additionally, after co-administration of SL-1 with TDM into mice, SL-1 prevented TDM induced granuloma formation [101].

Apart from the cross talk between TDM and SL, *in vitro* studies showed that SL-1 induced swelling and disruption of mitochondrial membranes and strongly inhibited mitochondrial oxidative phosphorylation [99]. Sulfolipids are described to be capable of preventing phagosome-lysosome fusion in cultured macrophages [102]. This suggests a major role for sulfolipids in one of the most distinctive pathogenic functions of the tubercle bacillus [100]. In terms of their ability to influence production and effects of cytokines, several *in vitro* studies showed their ability to modulate the oxidative response and the cytokine secretion in treated human monocytes and neutrophils [103-105]. A remarkable property of sulfolipids and an important factor underlying their biological activities is their anionic character, disturbing the

functions of phagosomal and lysosomal membranes by distorting their structure. They may also inactivate lysosomal hydrolases by interacting with the cationic sites of these enzymes [98].

3.7.3 The trehalose biosynthetic pathways

(This paragraph has been published in *PLoS Pathog* 12(12): e1006043)

Based on bioinformatic analyses and enzymatic *in vitro* characterizations, it appeared that three alternative pathways for trehalose biosynthesis are potentially present in *M. tuberculosis*: the OtsA-OtsB2, the TreY-TreZ and the TreS pathways [106]. However, our group has recently demonstrated that trehalose biosynthesis is mediated in mycobacteria only by two alternative routes: the OtsA-OtsB2 and the TreY-TreZ pathway. Both pathways synthesize trehalose *de novo* either from glycolytic intermediates or from α -glucans (glycogen like structures) [56]. On the otherhand, the TreS pathway is involved in the conversion of trehalose to linear/ branched cytoplasmic and/or branched capsular α -glucans and therefore consumes, rather than produces this disaccharide [106, 107].

The TreY-TreZ pathway releases trehalose from intracellular linear α -glucan storages. The maltooligosyltrehalose synthase TreY converts the terminal α -1,4-glycosidic linkage at the reducing end of an α -1,4-glucan into an α -1,1-bond yielding maltooligosyltrehalose. The trehalohydrolase TreZ then hydrolytically liberates trehalose. In the OtsA-OtsB2 pathway (Fig. 5), the trehalose-6-phosphate (T6P) synthase (OtsA) catalyzes the transfer of nucleoside diphosphate-activated glucose (UDP-glucose/ ADP-glucose) to G6P to yield T6P with the release of ADP/UDP. Subsequently, T6P phosphatase OtsB2 dephosphorylates T6P to trehalose [56]. The OtsA-OtsB2 and TreY-TreZ pathways do not contribute equally to trehalose production. A Δ otsA (Rv3490) gene deletion mutant was significantly attenuated for *in vitro* growth in trehalose-free medium and in a mouse infection model, indicating that the OtsA-OtsB2 pathway is the dominant route for trehalose formation *in vitro* and *in vivo* [108]. Surprisingly, in contrast to the genetic dispensability of *otsA* and the growth defect of the Δ otsA mutant, the *otsB2* gene (Rv3372) is strictly essential in *M. tuberculosis* because the gene could not be inactivated even in the presence of exogenous trehalose to chemically complement the biosynthetic defect [108].

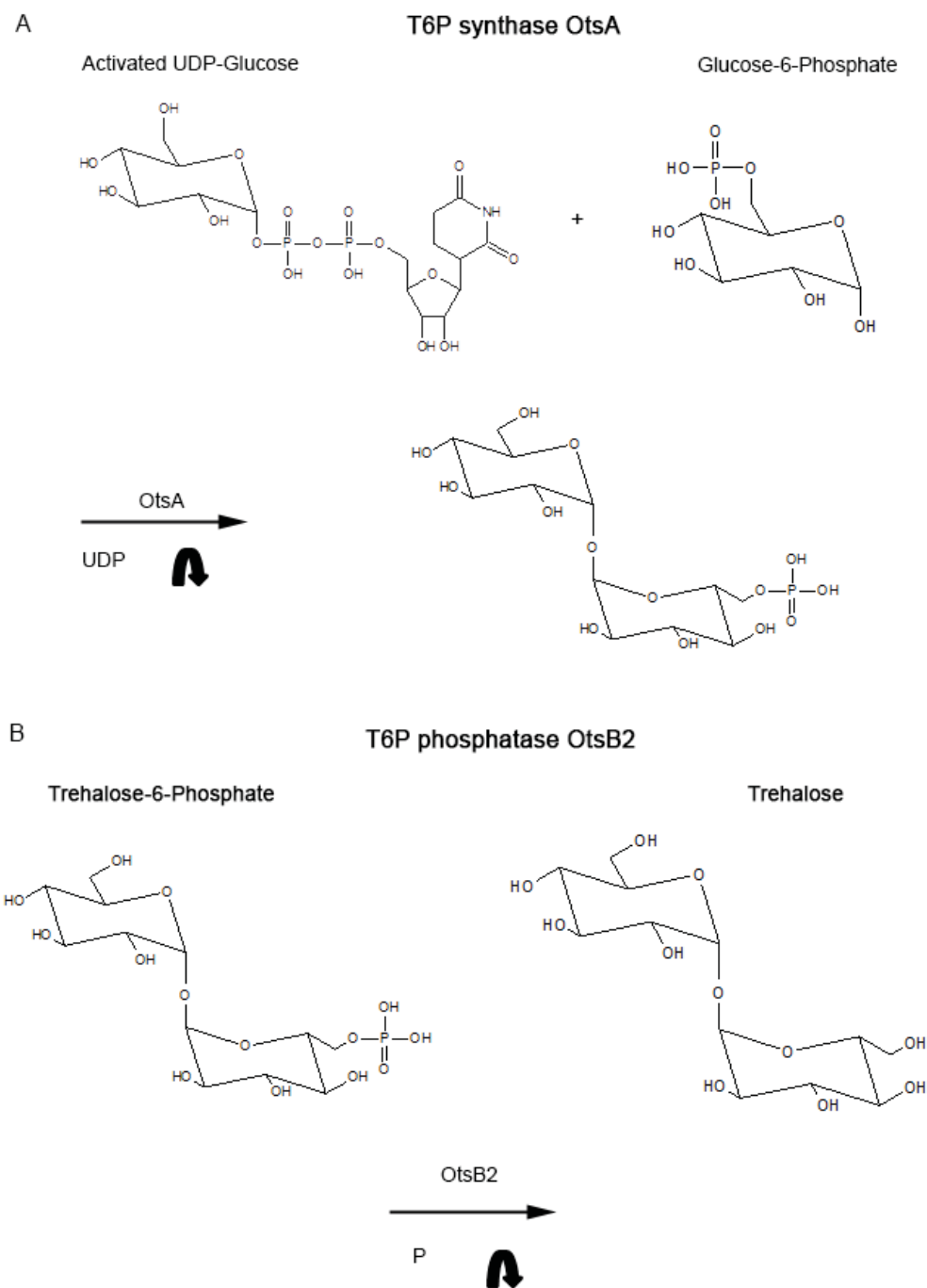


Fig 5. Reactions of the OtsA-OtsB2 pathway for trehalose synthesis.

(A) Trehalose-6-phosphate (T6P) synthase (OtsA) catalyzes the transfer of nucleoside diphosphate-activated glucose (UDP-glucose/ ADP-glucose) to G6P to yield T6P with the release of ADP/UDP. Subsequently, T6P phosphatase OtsB2 dephosphorylates T6P to trehalose (B).

3.7.4 α -Glucans and α -glucan pathways

Most studies have focused on the role of cell wall components, but reports have suggested the presence of a capsular layer surrounding mycobacteria for a long time [109, 110]. General infection experiments showed that bacterial binding of *M. bovis* and *M. smegmatis* cells to human monocyte-derived macrophages is significantly reduced, after the bacteria were chemically treated for capsule removal [111]. Since α -glucans represent a major constituent of the capsule [112, 113], they received more interest. It is well described that α -glucans play a role in immune evasion and virulence [55, 56, 114-116]. *M. tuberculosis* α -glucans are reported as a ligand for the C-type lectin receptor DC-SIGN [114] and not TLR2, as shown for α -glucans of the fungus *Pseudallescheria boydii* [117]. Ligand-receptor binding in LPS-activated monocyte-derived dendritic cells shows stimulated IL-10 production, an interleukin known as an immunosuppressive mediator and indicating an immune evasion mechanism [114]. Other studies suggest that capsular glucans of *M. tuberculosis* strains inhibit complement receptor 3 (CR3) interactions in highly expressing CR3 chinese hamster ovary (CHO-Mac-1) cells, considering CR3 as an additional receptor interacting with capsular glucans of *M. tuberculosis* [115]. Further, Gagliardi et al. described a blockage of CD1 molecules expression during the differentiation of monocytes to dendritic cells when they were treated with isolated mycobacterial α -glucans, suggesting a negative regulation of CD1 expression and inhibiting the antigen presentation to memory T-cells and naive T-cells [118].

Taken together, there are various evidences that capsular α -glucans are of importance for *M. tuberculosis* during host-interaction to escape the immune response and ensure mycobacterial survival, by influencing the immune response. However, the precise role in its virulence remains elusive.

The α -glucans are typically assembled intracellularly in a glycogen-like storage form. As already indicated, two α -glucan synthesizing pathways, the TreS-Pep2-GlgE and the GlgC-GlgA-GlgE pathway are closely involved in the network of trehalose metabolism. However and very strikingly, both pathways, probably in all mycobacteria, utilize the common building block of M1P (Fig 6). In detail, the TreS-Pep2 pathway consumes trehalose by isomerization to maltose by the trehalose synthase TreS [107, 119, 120], followed by an ATP-driven phosphorylation of maltose to M1P by a maltokinase Pep2 [120-122]. The GlgC-GlgA pathway catalyzes the production of M1P from ADP-glucose and G1P. The common intermediate of both pathways, M1P, serves as the substrate for the maltosyltransferase GlgE which transfers maltosyl units from the donor substrate M1P to the non-reducing end of α -glucan acceptors molecules, leading to linear α -1,4-chain elongation [123, 124]. With other words, GlgE polymerizes the α -maltose 1-phosphate building block. Subsequently, linear α -glucans can be branched by the branching enzyme GlgB in order to get exported to the capsule. On the other hand, linear α -glucans can

serve as a storage polymer (glycogen like structure), metabolized to trehalose via the TreY-TreZ pathway or to G1P by the glycogen phosphorylase GlgP [56]. As needed, G1P might then be used in order to enhance trehalose biosynthesis (OtsA-OtsB2 pathway), followed by production of trehalose mycolates or any other trehalose-derived glycolipids.

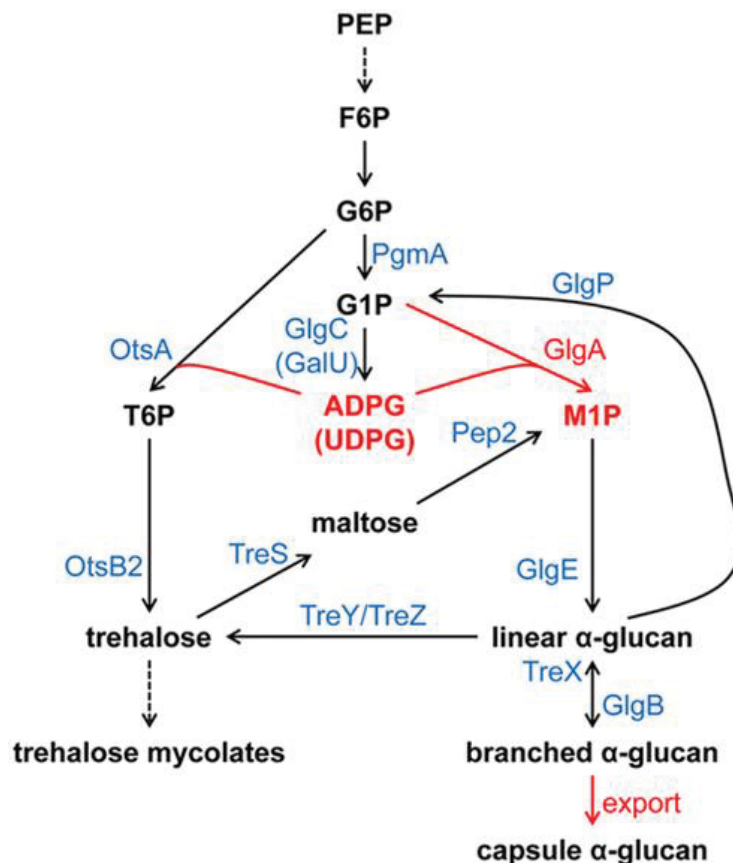


Fig 6. Revised model of GlgE-mediated intracellular and capsular α -glucan synthesis in mycobacteria.

The M1P building block for the maltosyltransferase GlgE is formed via two alternative routes, TreS-Pep2 and GlgC-GlgA. Both routes are connected via the shared use of ADP-glucose by GlgA and OtsA, the latter providing the trehalose substrate for the TreS-Pep2 pathway. GlgA, like OtsA, is also capable of using UDP-glucose as a donor, which in turn is produced from G1P by GalU, but this appears to be less significant *in vivo*. GlgE is essential for intracellular and capsular α -glucan synthesis and generates linear maltooligosaccharides as the substrates for the branching enzyme GlgB. α -Glucans are produced intracellularly with partial coupling to secretion by unknown transport mechanisms. Steps highlighted in red are new findings as described in this report. G6P, glucose 6-phosphate; G1P, glucose 1-phosphate; M1P, α -maltose 1-phosphate; T6P, trehalose 6-phosphate; ADPG, ADP-glucose; UDPG, UDP-glucose. Figure reproduced from Koliwer-Brandl H [56].

Importantly, as one key enzyme in the α -glucan biosynthetic pathway, GlgA homologues from microorganisms were considered to synthesize glycogen using the classical GlgC-GlgA pathway [55, 125, 126]. However, recently it has been shown that GlgA catalyzes M1P from ADP-glucose and G1P, 1000-fold more efficiently than its hitherto described glycogen synthase activity [56]. Considering the maltosyltransferase GlgE (see above), the GlgC-GlgA-GlgE and the TreS-Pep2-GlgE pathways have redundant roles in α -glucan formation. While the TreS-

Pep2-GlgE route dominates under standard laboratory culture conditions, the GlgC-GlgA-GlgE appears to be more active during infection in mice [56]. A third pathway has been suggested to contribute to α -glucan biosynthesis, the Rv3032 pathway [55]. However, it has been shown that Rv3032 is dispensable for α -glucan biosynthesis. For instance, gene deletion of Rv3032 resulted in no significant impact on the levels of either intracellular or capsular α -glucans. This glycosyltransferase has been reported to contribute to the production of higher-molecular weight α -glucans in *M. tuberculosis*. Its main role appears to be the formation of specialized oligomeric glucan derivatives, known as methylglucose lipopolysaccharides (MGLPs) [127-130].

3.8 MGLP-Synthesis

3.8.1 MGLPs chemical structure and function

Mycobacteria produce a family of intracellular alpha-glucan oligomers, which belong to the class of polymethylated polysaccharides (PMPS) [131]. Mycobacteria produce two types of cytoplasmic PMPS, 3-O-methylmannose polysaccharides (MMPs, MW: 2100) and 6-O-methylglucose lipopolysaccharides (MGLPs, MW: 3700) [128, 132]. The latter form possesses an α -glucan core structure, whereas MMPs constitute mannan derivatives. The O-methylation renders them slightly hydrophobic [130, 133]. Both forms occur simultaneously in the fast growing species whereas MGLPs are only found in the slow growers, suggesting that MGLPs might play an essential role in bacterial growth of *M. tuberculosis* [128, 129]. PMPS were initially isolated from the fast growing species *Mycobacterium phlei* (*M. phlei*) in Clinton Ballou's laboratory in the 60s [133]. The variants differ in their degree of glycosylation, number of methylation sites, and in the nature and frequency of the esterified acyl chains [129, 134]. The longer-chain PMPS are composed of 15–20 hexoses residues (glucose or mannose) [129]. Since MGLPs (Fig. 7) are the only PMPS present in pathogenic slow-growing mycobacteria, they are particularly interesting for identification of new drug targets, but what is their physiological role? Mycobacterial MMPs and MGLPs have been reported to markedly stimulate fatty acid synthesis and mycolic acid metabolism in mycobacteria. First evidences arose by Gray and Ballou in 1971: the MGLPs and MMPs were isolated from the water-soluble portion of crude lipids of *M. phlei* purified by chromatography techniques. Importantly, the polysaccharides and fatty acyl-CoA were eluted in a single peak, indicating formation of a molecular complex [132, 135]. They have the ability to form *in vitro* stable 1:1 complexes (1 mol of fatty acyl-CoA per mol of polysaccharide) [132]. The formation of these novel complexes may result from hydrophobic interactions between the paraffin chains of the acyl-CoA derivatives and O-methyl-sugar residues of the polysaccharides. However, due to their structure, MGLPs adopt a helical

conformation in solution. Depending on the degree of methyl groups facing the inner part of the coil, a cylindrical hydrophobic cavity is formed. This coiled helix model allows the assumption

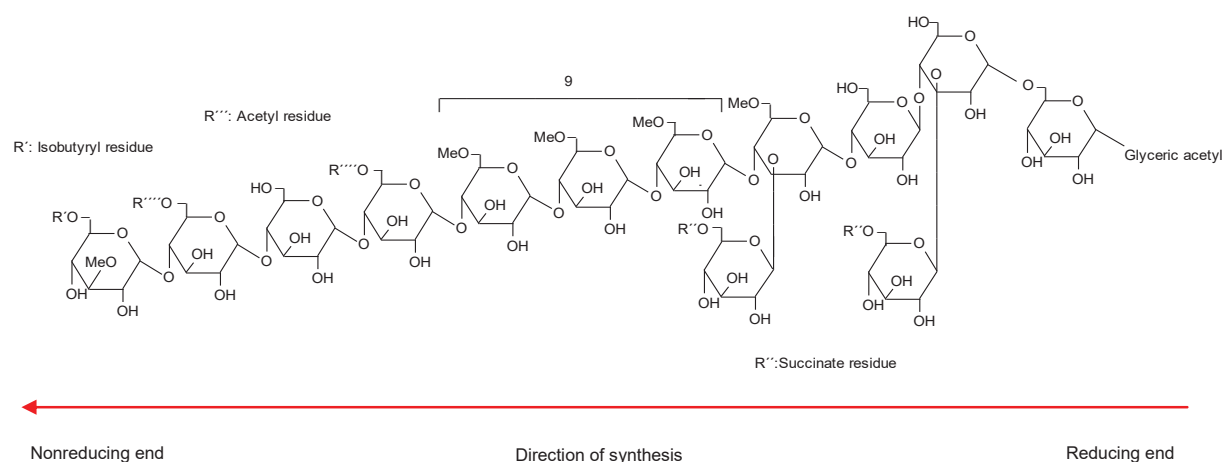


Fig 7. Methylglucose Lipopolysaccharides (MGLPs) in *M. tuberculosis*.

MGLPs are predominantly composed of α -1,4-linked glucose and 6-O-methylglucose units, building most part of the MGLP backbone. Glucosylglycerate serves as the starter unit at the reducing end. The second and fourth glucose molecules are substituted at position 3 by single β -1,3-linked glycosyl units each conjugated with a succinate moiety. The nonreducing end consist of a methylated glycosyl unit modified with an isobutyryl residue, followed by an acetylated unit.

that via hydrophobic interactions a “guest molecule”, free or enzyme-bound, can be accommodated within the polymer, such as an apolar long-chain fatty acid derivative (acyl-CoA) [129]. Based on hypothetical calculation of all cytoplasmic PMPS (1 mM) in *M. smegmatis* and concentrations of long-chain acyl-CoAs (0.3 mM), every long chain fatty acid may be complexed with PMPS. PMPS are also called “fatty acid carriers”. Consequently, PMPS protect long chain acyl-CoAs from degradation by cytoplasmic lipolytic enzymes [129]. It has been shown that PMPS preferentially interact with fatty acids with chain length ranging from C₁₆–C₂₂, while the interaction with immediately shorter or longer fatty-acyl chains has a significantly lower affinity. Due to this observation, it might be doubtful to reach a total 1:1 molar ratio (fatty acyl-CoA: polysaccharide) [129].

Anecdotal reports suggested that PMPS regulate the activity of the mycobacterial fatty acid synthase I (FAS-I) [135]. MGLPs are reported to decrease the Michaelis constant (K_m) of the FAS-I for acyl-CoA substrates. Hence, the synthesis of fatty acids can continue at low substrate concentrations, allowing a higher enzyme turnover by promoting faster chain release and terminating the elongation [129, 136].

Collectively, PMPS might serve as “fatty acid carriers” protecting acyl-CoAs from degradation by cytoplasmic lipolytic enzymes, and they might regulate fatty acid elongation by influencing the FAS-I activity until their termination, allowing diffusion of newly-synthesized acyl chains.

3.8.2 Genetics of MGLP synthesis

The participation of mainly two gene clusters in *M. tuberculosis*, *Rv1208–Rv1213* [55, 128, 130] and *Rv3030–Rv3037c* [137] has been suggested to contribute to MGLP biosynthesis. Importantly, most of the research has been done in the fast-growing nonpathogenic *M. smegmatis* and data for pathogenic *M. tuberculosis* remains largely elusive. In the following, the MGLP-synthesis is illustrated in its putative order of enzymatic reaction steps.

Studies reported that glucosylglycerate (GG) is the most relevant starting substrate for MGLP biosynthesis [136]. GG is synthesized in a two-step reaction: first, the glucosyl-3-phosphoglycerate synthase GpgS (Rv1208) is capable to catalyze the reaction to glucosyl-3-phosphoglycerate (GPG) using predominantly UDP-activated glucose and D-3-phosphoglyceric acid as donor substrates [128]. Rv1208 is proposed to be an essential gene for growth in *M. tuberculosis*, since the inactivation of its ortholog in *M. smegmatis* (MSMEG_5084) led to dramatically reduced MGLPs levels. In view of an immense decrease, but not complete loss, in the MGLP synthesis in the MSMEG_5084-deficient *M. smegmatis* mutant, there could be an alternative enzyme capable of synthesizing GPG [128]. Next, the second step in GG synthesis comprises the dephosphorylation of GPG by the glucosyl-3-phosphoglycerate phosphatase (GpgP), encoded by the gene Rv2419c [138].

After provision of the starter molecule for MGLP synthesis, the further putative reaction steps include the formation of diglucosylglycerate (DGG) [139] by a so far unknown enzyme. A putative diglucosylglycerate synthase (DggS) could be encoded by the gene Rv3031. Hypothetically, Rv3031 forms the α -1,6-linkage between a glucose molecule and GG [129]. Alternatively, this enzymatic step could be performed by the mentioned glycogen-branching enzyme GlgB (Rv1326c) [129]. However, since Rv3031 is clustered with Rv3032, this is a strong hint that Rv3031 might fulfill this function. Gene deletion studies of Rv3032 in *M. tuberculosis* showed a dramatic decrease in all forms of MGLPs, whereas overexpression experiments of this gene in *M. smegmatis* stimulated the production of mature forms of MGLPs. Thus, Rv3032 very likely encodes an α -1,4-glycosyltransferase responsible for MGLP elongation. Rv3032 can utilize ADP-glucose as well as UDP-glucose as activated donor substrates and starts the polymerization at the α -1,4-glycosidic chain, beginning at the DGG moiety [127].

Although the glycogen synthase GlgA (Rv1212c) has been previously suggested to possess at least partially redundant function to Rv3032 [129, 130], it has recently been shown that it has no α -glucan polymerase activity but rather catalyzes the production of maltose-1-phosphate (M1P) from ADP-glucose and G1P 1000-fold more efficiently than its hitherto described glycogen synthase activity [56]. Further genes within the gene cluster of *Rv3030–Rv3037c* are two

putative S-adenosylmethionine-dependent methyltransferase (SAMs), encoded by Rv3030 and Rv3037c, and Rv3034c, a putative acetyltransferase.

Collectively, although a few enzymatic steps for MGLP synthesis are well described, a complete understanding remains elusive. A significant contribution in understanding the elongation of the MGLPs was achieved by finding the key glycosyltransferase gene (Rv3032) in *M. tuberculosis* [127]. Rv3032 is likely involved in the production of higher-molecular weight α -glucans derivatives but not in lower-molecular weight glucan biosynthesis as already mentioned above. Therefore, Rv3032 might not be the only glycosyltransferase involved in synthesizing the MGLP backbone. Likely, further gene products fulfill further modifications and elongation steps of this putative cell wall regulatory complex molecule. In this context, we investigated the essentiality of the putative glycosyltransferase Rv0225 and the neighbouring genes in order to study potential co-participation in the MGLP biosynthetic pathway. The putative glycosyltransferase Rv0225 could elongate the proximal part of the sugar backbone of the molecule, whereas the non-essential glycosyltransferase Rv3032 covers the distal part. Neighboring genes, Rv0224c (a putative methyltransferase) and Rv0228 (a putative acyltransferase) might fulfill a modifying role during the MGLP maturing steps.

4 Aims of the thesis

4.1 Trehalose-6-phosphate-mediated toxicity determines essentiality of OtsB2 in *M. tuberculosis* in vitro and in mice.

The mycobacterial cell wall is a rich source of targets for clinically used antibiotics such as isoniazid, ethambutol and delamanid. It contains large amounts of long-chain mycolic acids forming a hydrophobic layer that confers high intrinsic resistance against antibiotics. Mycolic acids form an outer membrane-like structure, the so-called mycomembrane. Abundant trehalose (α -D-glucopyranosyl-1 \rightarrow 1- α -D-glucopyranoside)-based cell wall molecules and other intracellular glycoconjugates play crucial roles within cell wall assembly. Thus, for biogenesis of the mycomembrane, the disaccharide trehalose is considered an attractive target for development of antimycobacterial drugs [51]. Mycolic acid-containing trehalose glycoconjugates are essential for mycomembrane formation in two regards: as the structural component trehalose-6,6'-dimycolate (TDM, also known as „cord factor“) and as the carrier molecule trehalose-6-monomycolate (TMM), which shuttles mycolic acids from their site of biosynthesis in the cytoplasm to the periplasm where they serve as substrate of the antigen 85 complex. Our work group has recently demonstrated that trehalose biosynthesis in mycobacteria relies predominantly on trehalose-6-phosphate (T6P) synthase (OtsA) and T6P phosphatase (OtsB2) mediating trehalose formation from UDP-glucose and glucose-6-phosphate (OtsA-OtsB2 pathway) [107]. Based on this work, we aimed to generate a conditional *M. tuberculosis* mutant for the T6P phosphatase gene *otsB2* allowing regulated gene silencing in order to assess the drug target potential of OtsB2 and elucidate the mechanism of essentiality *in vitro* as well as for the acute and chronic infection phase in mice *in vivo*.

4.2 Characterization of the putative essential glycosyltransferase Rv0225 in a cell wall associated gene cluster in *Mycobacterium* species.

In addition to the aforementioned trehalose-based cell wall molecules, mycobacteria also produce two types of cytoplasmic PMPS, MMPs and MGLPs. Both forms occur simultaneously in the fast-growing species whereas MGLPs are only found in the slow growers, suggesting that MGLPs might play an essential role in bacterial growth of *M. tuberculosis*. MGLPs can form stable *in vitro* complexes with fatty acids, thereby potentially regulating fatty acid synthase I

(FAS I) and mycolic acid metabolism in mycobacteria. MGLP biosynthesis is poorly understood, with several enzymatic steps being elusive. Thus, in a second project of my doctoral thesis, we wanted to study a conserved mycobacterial gene cluster (*Rv0224c* - *Rv0228*), which might be involved in MGLP synthesis providing a premature polymethylated and acylated α -1,4-glucan derivative. Initial gene silencing experiments by our workgroup showed that *Rv0225* is essential *in vitro*. *Rv0225* encodes a putative glycosyltransferase. We hypothesized that *Rv0225* plays a role in elongation of the proximal part of the MGLP glucan backbone, whereas *Rv3032* covers the distal elongation. In this context, we also wanted to investigate the essentiality of *Rv0225* neighbouring genes in order to study potential co-participation in the same biosynthetic pathway or if they are clustered by coincidence.

5 Material and Methods

5.1 List of abbreviations

°C	DegreeCelsius
Apra	Apramycin
ATc	Anyhydrotetracycline
ATP/ADP/AMP	Adenosin-(tri)-(di)-(mono)-phosphate
BCG	Bacille Calmette Guerin
BSA	Bovine Serum Albumin
CFU	Colony forming units
DANN	Desoxyribonucleic acid
EMB	Ethambutol
G3P	Glycerol-3-phosphate
GTP/GDP/GMP	Guanosin-(tri)-(di)-(mono)-phosphate
HIV	Human immunodeficiency virus
Hyg	Hygromycin
IFN	Interferon
IL	Interleukin
Kann	Kanamycin
(K)bp	(Kilo) base pairs
LAM	Lipoarabinomannan
LM	Lipomannan
mAGP	Mycolyl-Arabinogalactan-Peptidoglycan
MAME	Mycolic acid methyl ester
Man	Mannose
Man-LAM	Mannosylated lipoarabinomannan
mRNA	Messenger ribonucleoid acid
M. tuberculosis	<i>Mycobacterium tuberculosis</i>
NADH+	Nicotinamide adenine dinucleotide
OD	Optical density
OM	Outer membrane
ORF	Open reading frame
PBS	Phosphate buffered saline
PCR	Polymerase chain reaction
PDIM	Phthioceroldimycocerosate
PFU	Plaque forming unit
PIM	Phosphatidyl- <i>myo</i> -inositolmannoside
RNA	Ribonucleic acid
TAE	Tris-acetate-EDTA
tetO	Tet-operator
tetR	Tet-repressor
TLC	Thin layer chromatography
TLR	Toll-like receptor
TNF	Tumor necrosis factor
TRIS	Tri(hydromethyl)aminomethane
UTP/UDP/UMP	Uracil-(Tri)-(Di)-(Mono) phosphate
UV	Ultraviolet
XDR-TB	extensively drug-resistant M. tuberculosis strain
WT	Wildtype
TB	Tuberculosis
MGLP	Methylglucose Lipopolysaccharide
GT	Glycosyltransferase
GpgS	Glycosylphosphoglycerate-Synthase
FAS	Fatty acid synthase
Dggs	Diglycosylglycerate-Synthase
AES	Allelic exchange substrate
AcTr	Acyltransferase
3-PGA	3-Phosphoglycerate

5.2 Generation of targeted gene deletion and conditional mutants

Mutants of *M. tuberculosis* were generated by allelic exchange using specialized transduction principally as described [140, 141]. Details on the generation of mutants and genetic complementation are described in 5.5.9 using oligonucleotides listed in Table 1 (OtsB2 study) and Table 4 (Rv0225 study) for constructing specific allelic exchange substrates.

5.2.1 Oligonucleotides

Table 1. Oligonucleotides used for generation of allelic exchange substrates in the OtsB2 study

	Upstream flanking sequence			Downstream flanking sequence			Resulting phage
	5' primer	3' primer	Restriction site	5' primer	3' primer	Restriction site	
Δ otsA	5' TTTTCCATAAAATTGGGCG-TGGCTGACCAAGAAGT 3'	5' TTTTCCATTTCCTTGGTCGATTGGC-TACCACCACGA 3'	<i>Van91I</i>	5' TTTTGCATAGATTGCCTGG-GCACAGTCGTTTCTCG 3'	5' TTTTGCATCTTTTGCCA-CCTGGAAGGTCCACAGCA 3'	<i>BstAPI</i>	phcRv3490S
Δ otsB2	5' TTTTGCATAAAATTGCC-CTATCTCCCCGTCGAGTACGAC 3'	5' TTTTGCATTTCCTTGGAGTTGCCG-GACCAGTTCCTGGG 3'	<i>BstAPI</i>	5' TTTTGCATAGATTGGGC-ACTGTTTGCCTGGACAGTCC 3'	5' TTTTGCATCTTTTGCCATG-CGGTGTTCGGAAGTCCCTTG 3'	<i>Van91I</i>	phcRv3372S
c-otsB2	5' TTTTGCATAAAATTGCCA-TGTCGGCGGCCACCTGCTG 3'	5' TTTTGCATTTCCTTGCACCCACCT-CTCACGGGGGTC 3'	<i>Van91I</i>	5' TTTTGCATAGATTGCATGC-GCAA-TTGGGCCCGGTC 3'	5' TTTTGCATCTTTTGCTT-CTGCAGTGGCCTCCAAGGC 3'	<i>Van91I</i>	phcRv3372-4xtetO

Primers listed here were used for generation of gene deletion or knock-in plasmids/ phasmids. Phasmids were packaged into bacteriophages and delivered into mutants of *M. tuberculosis* H37Rv listed in Table 2 by specialized transduction as described in 5.5.8 and 5.5.9.

Table 2. Strains used in the OtsB2 study

RKSC-Nr.	Strain	Alternative designation	Relevant characteristics	Source or reference
<i>M. tuberculosis</i> H37Rv strains				
1	WT			W.R. Jacobs Jr., AECOM, Bronx, NY
214	WT pMV361(Kan):: <i>otsB2</i>	<i>otsB2</i> merodiploid strain	Constitutive <i>otsB2</i> expression from the <i>groEL2</i> (hsp60) promoter on integrative plasmid pMV361; Kan ^r	This study
320	Δ otsB2 pMV361(Kan):: <i>otsB2</i>		Δ otsB2:: <i>yōres-sacB-hyg-yōres</i> ; constitutive <i>otsB2</i> expression from the <i>groEL2</i> (hsp60) promoter on integrative plasmid pMV361; Hyg ^r , Kan ^r	This study
86	c-otsB2-4xtetO		Knock-in mutant harboring <i>hyg-Pmyc1-4xtetO</i> cassette upstream of <i>otsB2</i> start codon; Hyg ^r	This study
165	c-otsB2-4xtetO pMV261(Kan)		Knock-in mutant harboring <i>hyg-Pmyc1-4xtetO</i> cassette upstream of <i>otsB2</i> start codon; empty episomal vector pMV261; Hyg ^r , Kan ^r	This study
175	c-otsB2-4xtetO pMV261(Kan)::tetR-G	c-otsB2-tet-on	Conditional mutant harboring <i>hyg-Pmyc1-4xtetO</i> cassette upstream of <i>otsB2</i> start codon; constitutive expression of <i>E. coli</i> Tn10 <i>tetR</i> from the <i>groEL2</i> (hsp60) promoter on episomal plasmid pMV261; Hyg ^r , Kan ^r	This study

Material and Methods

316	c-otsB2-4xtetO pMV261(Kan)::tetR-G pMV361(Apra)::otsB2	c-otsB2-tet-on pMV361::otsB2	Complemented conditional mutant harboring <i>hyg-Pmyc1-4xtetO</i> cassette upstream of <i>otsB2</i> start codon; constitutive expression of <i>E. coli</i> Tn10 <i>tetR</i> from the <i>groEL2</i> (hsp60) promoter on episomal plasmid pMV261; constitutive <i>otsB2</i> expression from the <i>groEL2</i> (hsp60) promoter on integrative plasmid pMV361; Hyg ^r , Kan ^r , Apra ^r	This study
89	Δ otsA		Δ otsA:: γ ores-sacB-hyg- γ ores; Hyg ^r	This study
315	Δ otsA _u		Δ otsA:: γ ores	This study
318	Δ otsA _u Δ otsB2		Δ otsA:: γ ores Δ otsB2:: γ ores-sacB-hyg- γ ores; Hyg ^r	This study
319	Δ otsA _u c-otsB2-4xtetO		Δ otsA:: γ ores; Knock-in mutant harboring <i>hyg-Pmyc1-4xtetO</i> cassette upstream of <i>otsB2</i> start codon; Hyg ^r	This study
323	Δ otsA _u c-otsB2-4xtetO pMV261(Kan)::tetR-G	Δ otsA _u c-otsB2-tet-on	Δ otsA:: γ ores; Conditional mutant harboring <i>hyg-Pmyc1-4xtetO</i> cassette upstream of <i>otsB2</i> start codon; constitutive expression of <i>E. coli</i> Tn10 <i>tetR</i> from the <i>groEL2</i> (hsp60) promoter on episomal plasmid pMV261; Hyg ^r , Kan ^r	This study
71	Δ panCD _u		Δ panCD:: γ ores	W.R. Jacobs Jr., AECOM, Bronx, NY
159	Δ panCD _u c-otsB2-4xtetO			This study
215	Δ panCD _u c-otsB2-4xtetO pMV261(Kan)::tetR-G::panCD	Δ panCD _u c-otsB2-tet-on		This study
<i>E. coli</i>				
215	pc-otsB2-4xtetO		Generation of an <i>otsB2</i> knock-in mutant	This study
213	pc- Δ otsB2		Generation of an <i>otsA</i> knock-out mutant	This study
212	pc- Δ otsA		Generation of an <i>otsB2</i> knock-out mutant	This study
227	phAE159::c-otsB2-4xtetO		Generation of an <i>otsB2</i> knock-in mutant	This study
224	phAE159:: Δ otsA		Generation of an <i>otsA</i> knock-out mutant	This study
225	phAE159:: Δ otsB2		Generation of an <i>otsB2</i> knock-out mutant	This study

Mutants were generated by allelic exchange employing specialized transduction as described in 5.5.8. Abbreviations: WT, wild-type; Kan^r, kanamycin resistant; Hyg^r, hygromycin resistant; Apra^r, apramycin resistant.

Table 3. Oligonucleotides used for pMV361 complementation plasmid in the OtsB2 study

Gene	Forward Primer	Restriction site	Reverse Primer	Restriction site
<i>otsB2</i>	5' TTTT <u>TTAATTAA</u> GTGCGCAAGTTGGGCCCGGTC 3'	5' <i>PacI</i>	5' TTTT <u>AAGCTT</u> TCACGTTGCCCGCAGGGGAGC 3'	3' <i>HindIII</i>

The restriction sites to establish the cloning are underlined.

Table 4. Oligonucleotides used for generation of allelic exchange substrates in the Rv0225 study

	Upstream flanking sequence			Downstream flanking sequence			Resulting phage
	5' primer	3' primer	Restriction site	5' primer	3' primer	Restriction site	
<i>M. tuberculosis/ M. bovis</i>							
<i>c-Rv0224c</i>	5'TTTTTC <u>CCATAAA</u> TGGACAT-GCCCGTGAAAGGTAAC 3'	5'TTTTTC <u>CAATTCT</u> TGGCCGCCA-GTGTGCGATAGAACCGTG 3'	<i>Van91I</i>	5'TTTTTC <u>CATAGAT</u> TGGATGG-CGG-TCACCGATGTGTTTCG 3'	5'TTTTTC <u>CAATC</u> TTTTGGGC-CGAA-CGCGAAACGAGAAC 3'	<i>Van91I</i>	phcRv0224 c-4xtetO
<i>c-Rv0225</i>	5'TTTTTC <u>CCATAAA</u> TGGGTC-ATGGCGTCACCCCTACCCAAG 3'	5'TTTTTC <u>CAATTCT</u> TGGTGGTC-GATAGCCTAGCGGGCCG3'		5'TTTTTCATAGATTGGAATG-TCTGCTCTGCGCTCGGTGTT-G 3'	5'TTTTTCATCTTTTGGGACA-TGCCCGTGAAAGGTAAC 3'	<i>Van91I</i>	phcRv0225 -4xtetO
<i>c-Rv0226c</i>	5'TTTTTC <u>CCATAAA</u> TGGCAC-CGAGAAGAAGACATACC 3'	5'TTTTTC <u>CAATTCT</u> TGGGTCGCGC-TGATTAGCGCGCTC 3'	<i>Van91I</i>	5'TTTTTC <u>CATAGAT</u> TGGATGC-GCTGG-TTCCGACCGGGGTAC 3'	5'TTTTTC <u>CAATC</u> TTTTGGCC-ACCATGGCGAGTAGTACGAC 3'	<i>Van91I</i>	phcRv0226 c-4xtetO
<i>c-Rv0227c</i>	5'TTTTTC <u>GCATAAA</u> TGCTAGG-CCCCTCGCGCAGCAACATT-C 3'	5'TTTTTC <u>GCA</u> TTTCTTGCGACTG-C-CCGGTTACCTGCGCCG 3'	<i>BstAPI</i>	5'TTTTTC <u>CATAGAT</u> TGGATGT-TGCGGTTGCGCCGCTGCGG 3'	5'TTTTTC <u>CAATC</u> TTTTGGCG-GCCGCGGTGAATGTAATC3'	<i>Van91I</i>	phcRv0227 c-4xtetO
<i>c-Rv0228</i>	5'TTTTTC <u>CCATAAA</u> TGGGCG-GTATGTGGTTAAACCGTTG 3'	5' TTT <u>CCATTCT</u> TGGACGCT-CTGCTGTTAGGGTCAAACGG 3'	<i>Van91I</i>	5' TTTTTC <u>GCATAGAT</u> TGCATG-GGCCCGCGGACGAATCGGG 3'	5' TTTTTC <u>GCATC</u> TTTTGGCG-GTCTTACC CGCAATTGTGC 3'	<i>BstAPI</i>	phcRv0228- i4xtetO
Δ Rv0224c	5'TTTTTC <u>CCATAAA</u> TGGCGA-CATGCCCGTGAAAGGTAAC 3'	5'TTTTTC <u>CAATTCT</u> TGGAGCCA-CAGATCGCCGATCATTG 3'	<i>Van91I</i>	5'TTTTTCACAGAGTGGCGTG-AGTTCCTGGTGAGCAATCTG 3'	5'TTTTTC <u>CACCT</u> TGTGACTT-GCCGCGAGTTCTAAGGTG 3'	<i>DrallI</i>	phRv0224cS

Material and Methods

<i>M. smegmatis</i>							
c-MSMEG0311	5'TTTTTCATAAATTGGGTG-TCATGCGGTTACACTACTC 3'	5'TTTTTCATTCTTGGTGCGC-C-GATGCGCTGCACGTACG 3'	Van91I	5'TTTTTCATAGATTGGATG-TCTGCCCGGCCGAGTCTGC 3'	5'TTTTTCATCTTTTGGCTGC-GTTGCAGTACACGATGTTTG 3'	Van91I	phc-MSMEG0311-4xtetO
ΔMSMEG0051	5'TTTTTCATAAATTGGGCGA-GGCATCCTCGGAAAC 3'	5'TTTTTCATTCTTGGGCAT-GCTGTTGCTCCTGTTAG 3'	Van91I	5'TTTTTCATAGATTGGCCTTC-GCGCTCAAGCAGCTTCGT 3'	5'TTTTTCATCTTTTGGCACA-TCGTGCGGGCCGTAATGG 3'	Van91I	phc-MSMEG0051S

Oligonucleotides used for generation of allelic exchange substrates in the Rv0225 study. Primer listed here were used for generation of gene deletion or knock-in plasmids/ phasmids, conserved in plasmid-harboring recombinant *E. coli* glycerol stocks. Phasmids were packaged into bacteriophages and delivered into cells of *M. tuberculosis* H37Rv listed in Table 5 by specialized transduction as described in 5.5.8 and 5.5.9.

Table 5. Mycobacterial strains used in the Rv0225 study.

RKSC-Nr.	Strain	Alternative designation	Relevant characteristics	Source or reference
<i>M. tuberculosis</i> H37Rv strains				
1	WT			W.R. Jacobs Jr., AECOM, Bronx, NY
253	c-Rv0224c-4xtetO		Knock-in mutant harboring <i>hyg</i> – <i>Pmyc1</i> -4xtetO cassette upstream of <i>Rv0224c</i> start codon; Hyg ^r	This study
399	c-Rv0224c-4xtetO pMV261 (Kan)		Knock-in mutant harboring <i>hyg</i> – <i>Pmyc1</i> -4xtetO cassette upstream of <i>Rv0224c</i> start codon; empty episomal vector pMV261; Hyg ^r , Kan ^r	This study
254	c-Rv0224c-4xtetO pMV261(Kan)::tetR-E	c-Rv0224c-tet-on	Conditional mutant harboring <i>hyg</i> - <i>Pmyc1</i> -4xtetO cassette upstream of <i>Rv0224c</i> start codon; constitutive expression of <i>E. coli</i> Tn10 <i>tetR</i> from the <i>groEL2</i> (hsp60) promoter on episomal plasmid pMV261; Hyg ^r , Kan ^r	This study
365	ΔRv0224c		ΔRv0224c::yōres-sacB-hyg-yōres; Hyg ^r	This study
71	ΔpanCD _u		ΔpanCD::yōres	W.R. Jacobs Jr., AECOM, Bronx, NY
363	ΔpanCD _u c-Rv0225c-4xtetO		Knock-in mutant harboring <i>hyg</i> – <i>Pmyc1</i> -4xtetO cassette upstream of <i>Rv0225</i> start codon; ΔpanCD	This study
352	ΔpanCD _u c-Rv0225c-4xtetO-(Kan)::tetR-D::panCD	ΔpanCD _u c-Rv0225-tet-on	::yōres; Hyg ^r	This study

Material and Methods

353	<i>ΔpanCD_u</i> c-Rv0225c-4xtetO pMV261 (Kan)::tetR-D::panCD pMV361 (Apra)::Rv0225	<i>ΔpanCD_u</i> c-Rv0225-tet-on pMV361::Rv0225	Complemented conditional mutant harboring hyg-Pmyc1-4xtetO cassette upstream of Rv0225 start codon; constitutive expression of <i>E. coli</i> Tn10 tetR from the groEL2 (hsp60) promoter on episomal plasmid pMV261; constitutive Rv0225 expression from the groEL2 (hsp60) promoter on integrative plasmid pMV361; Hyg ^r , Kan ^r , Apra ^r	This study
364	<i>ΔpanCD_u</i> c-Rv0225c-4xtetO pMV261 (Kan)::tetR-D::panCD pMV361 (Apra)::	<i>ΔpanCD_u</i> c-Rv0225-tet-on pMV361::	Conditional integrative control vector mutant harboring hyg-Pmyc1-4xtetO cassette upstream of Rv0225 start codon; constitutive expression of <i>E. coli</i> Tn10 tetR from the groEL2 (hsp60) promoter on episomal plasmid pMV261; empty integrative plasmid pMV361; Hyg ^r , Kan ^r , Apra ^r	This study
178	c-Rv0225c-4xtetO pMV261 (Kan)		Knock-in mutant harboring hyg -Pmyc1-4xtetO cassette upstream of Rv0225c start codon; empty episomal vector pMV261; Hyg ^r , Kan ^r	This study
255	c-Rv0226c-4xtetO		Knock-in mutant harboring hyg -Pmyc1-4xtetO cassette upstream of Rv0226c start codon; Hyg ^r	This study
400	c-Rv0226c-4xtetO pMV261 (Kan)		Knock-in mutant harboring hyg -Pmyc1-4xtetO cassette upstream of Rv0226c start codon; empty episomal vector pMV261; Hyg ^r , Kan ^r	This study
256	c-Rv0226c-4xtetO pMV261(Kan)::tetR-E	c-Rv0226c-tet-on	Conditional mutant harboring hyg-Pmyc1-4xtetO cassette upstream of Rv0226c start codon; constitutive expression of <i>E. coli</i> Tn10 tetR from the groEL2(hsp60) promoter on episomal plasmid pMV261; Hyg ^r , Kan ^r	This study
349	pMV361: Rv0226c		Merodiploid Rv0226c strain with integrative plasmid pMV361 in wild-type background; Apra ^r	This study
216	c-Rv0228-4xtetO		Knock-in mutant harboring hyg -Pmyc1-4xtetO cassette upstream of Rv0228 start codon; Hyg ^r	This study
249	c-Rv0228-4xtetO pMV261 (Kan)		Knock-in mutant harboring hyg -Pmyc1-4xtetO cassette upstream of Rv0228 start codon; empty episomal vector pMV261; Hyg ^r , Kan ^r	This study
250	c-Rv0228-4xtetO pMV261(Kan)::tetR-E		Conditional mutant harboring hyg-Pmyc1-4xtetO cassette upstream of Rv0228 start codon; constitutive expression of <i>E. coli</i> Tn10 tetR from the groEL2(hsp60) promoter on episomal plasmid pMV261; Hyg ^r , Kan ^r	This study
M. bovis BCG Pasteur				
297	<i>ΔMb0229c</i>		<i>ΔMb0229c::yδres-sacB-hyg-yδres</i> ; Hyg ^r	This study
286	c-Mb0231c-4xtetO		Knock-in mutant harboring hyg -Pmyc1-4xtetO cassette upstream of Mb0231c start codon; Hyg ^r	This study
293	c-Mb0231c-4xtetO pMV261 (Kan)		Knock-in mutant harboring hyg -Pmyc1-4xtetO cassette upstream of Mb0231c start codon; empty episomal vector pMV261; Hyg ^r , Kan ^r	This study
288	c- Mb0231c -4xtetO pMV261(Kan)::revtetR-D	c- Mb231c-tet-off	Conditional mutant harboring hyg-Pmyc1-4xtetO cassette upstream of Mb0231c start codon; constitutive expression of <i>E. coli</i> Tn10 tetR from the groEL2(hsp60) promoter on episomal plasmid pMV261; Hyg ^r , Kan ^r	This study
80	c-Mb0230-4xtetO		Knock-in mutant harboring hyg -Pmyc1-4xtetO cassette upstream of Mb0230 start codon; <i>ΔpanCD</i> ::yδres; Hyg ^r	This study
141	c-Mb0230-4xtetO-(Kan)::revtetR-F	c- Mb0230-tet-off		This study

Material and Methods

295	c-Mb0230-4xtetO pMV261 (Kan)::revtetR-F pMV361 (Apra)::Rv0225	c-Mb0230-tet-off pMV361::Rv0225	Complemented conditional mutant harboring hyg-Pmyc1-4xtetO cassette upstream of Mb0230 start codon; constitutive expression of <i>E. coli</i> Tn10 <i>tetR</i> from the <i>groEL2</i> (hsp60) promoter on episomal plasmid pMV261; constitutive <i>Rv0225</i> expression from the <i>groEL2</i> (hsp60) promoter on integrative plasmid pMV361; Hyg ^r , Kan ^r , Apra ^r	This study
296	c-Mb0230-4xtetO- pMV261 (Kan)::revtetR-F pMV361 (Apra)::	c- Mb0230-tet-off pMV361::	Conditional integrative control vector mutant harboring hyg-Pmyc1-4xtetO cassette upstream of Mb0230 start codon; constitutive expression of <i>E. coli</i> Tn10 <i>tetR</i> from the <i>groEL2</i> (hsp60) promoter on episomal plasmid pMV261; empty integrative plasmid pMV361; Hyg ^r , Kan ^r , Apra ^r	This study
127	c-Mb0230-4xtetO pMV261 (Kan)		Knock-in mutant harboring hyg -Pmyc1-4xtetO cassette upstream of Mb0230 start codon; empty episomal vector pMV261; Hyg ^r , Kan ^r	This study
97	c-Mb0233-4xtetO		Knock-in mutant harboring hyg -Pmyc1-4xtetO cassette upstream of Mb0233 start codon; Hyg ^r	This study
130	c-Mb0233-4xtetO pMV261 (Kan)		Knock-in mutant harboring hyg -Pmyc1-4xtetO cassette upstream of Mb0233 start codon; empty episomal vector pMV261; Hyg ^r , Kan ^r	This study
138	c- Mb0233-4xtetO - pMV261(Kan)::revtetR-D		Conditional mutant harboring hyg-Pmyc1-4xtetO cassette upstream of Mb0233 start codon; constitutive expression of <i>E. coli</i> Tn10 <i>tetR</i> from the <i>groEL2</i> (hsp60) promoter on episomal plasmid pMV261; Hyg ^r , Kan ^r	This study
M. smegmatis				
185	c-MSMEG0311-4xtetO		Knock-in mutant harboring hyg -Pmyc1-4xtetO cassette upstream of Rv0225 start codon; ΔpanCD ::γδres; Hyg ^r	This study
186	c- MSMEG0311-4xtetO-(Kan)::tetR-D	c-Rv0225-tet-on		This study
191	c-MSMEG0311-4xtetO pMV261 (Kan)::tetR-D pMV361 (Apra)::Rv0225	c-Rv0225-tet-on pMV361::Rv0225	Complemented conditional mutant harboring hyg-Pmyc1-4xtetO cassette upstream of MSMEG0311 start codon; constitutive expression of <i>E. coli</i> Tn10 <i>tetR</i> from the <i>groEL2</i> (hsp60) promoter on episomal plasmid pMV261; constitutive <i>Rv0225</i> expression from the <i>groEL2</i> (hsp60) promoter on integrative plasmid pMV361; Hyg ^r , Kan ^r , Apra ^r	This study
228	c- MSMEG0311-4xtetO- pMV261 (Kan)::tetR-D pMV361 (Apra)::	c-Rv0225-tet-on pMV361::	Conditional integrative control vector mutant harboring hyg-Pmyc1-4xtetO cassette upstream of MSMEG0311 start codon; constitutive expression of <i>E. coli</i> Tn10 <i>tetR</i> from the <i>groEL2</i> (hsp60) promoter on episomal plasmid pMV261; empty integrative plasmid pMV361; Hyg ^r , Kan ^r , Apra ^r	This study
190	c-MSMEG0311-4xtetO pMV261 (Kan)		Knock-in mutant harboring hyg -Pmyc1-4xtetO cassette upstream of MSMEG0311 start codon; empty episomal vector pMV261; Hyg ^r , Kan ^r	This study
234	ΔMSMEG0051		ΔMSMEG0051::γδres-sacB-hyg-γδres; Hyg ^r	This study
E. coli				
343	pc-Rv0224c-4xtetO		Generation of a Rv0224c knock-in mutant	This study
353	phc-Rv0224c-4xtetO		Generation of a Rv0224c knock-in mutant	This study

Material and Methods

426	pc-ΔRv0224c		Generation of a <i>Rv0224c</i> knock-out mutant	This study
434	phc-ΔRv0224c		Generation of a <i>Rv0224c</i> knock-out mutant	This study
117	pc-Rv0225-4xtetO		Generation of a <i>Rv0225</i> knock-in mutant	This study
129	phc-Rv0225-4xtetO		Generation of a <i>Rv0225</i> knock-in mutant	This study
343	pc-Rv0226c-4xtetO		Generation of a <i>Rv0226c</i> knock-in mutant	This study
354	phc-Rv0226c-4xtetO		Generation of a <i>Rv0226c</i> knock-in mutant	This study
427	pc-ΔRv0226c		Generation of a <i>Rv0226c</i> knock-out mutant	This study
435	phc-ΔRv0226c		Generation of a <i>Rv0226c</i> knock-out mutant	This study
157	pc-Rv0228-i4xtetO		Generation of a <i>Rv0228</i> knock-in mutant	This study
159	phc-Rv0228-i4xtetO		Generation of a <i>Rv0228</i> knock-in mutant	This study
469	pc-ΔRv0228		Generation of a <i>Rv0228</i> knock-out mutant	This study
485	phc-ΔRv0228		Generation of a <i>Rv0228</i> knock-out mutant	This study
421	pMV361 (Apra ^r): <i>Rv0224c</i>		Complementation	This study
433	pMV361 (Apra ^r): <i>Rv0225</i>		Complementation	This study
281	pMV361 (Kan ^r): <i>Rv0225</i>		Complementation	This study
423	pMV361 (Apra ^r): <i>Rv0226c</i>		Complementation	This study
419	pc-MSMEG_0311-4xtetO		Generation of a <i>MSMEG0311</i> knock-in mutant	This study
420	phc-MSMEG_0311-4xtetO		Generation of a <i>MSMEG0311</i> knock-in mutant	This study
468	pc-ΔMSMEG_0051		Generation of a <i>MSMEG_0051</i> knock-out mutant	This study
484	phc-ΔMSMEG_0051		Generation of a <i>MSMEG_0051</i> knock-out mutant	This study

Mutants were generated by allelic exchange employing specialized transduction as described in 5.5.8 and 5.5.9. Abbreviations: WT, wild-type; Kan^r, kanamycin resistant; Hyg^r, hygromycin resistant; Apra^r, apramycin resistant.

Table 6. Oligonucleotides used for pMV361 complementation plasmids in the Rv0225 study

Gene	Forward Primer	Restriction site	Reverse Primer	Restriction site
<i>M. tuberculosis</i>				
<i>Rv0224c</i>	5' TTTT <u>TTAATT</u> AATGGCGGTCACCGATGTGTTG- GCG 3'	5' <i>Pacl</i>	5' TTTT <u>AAGCTT</u> AGGGTGTGAGCACCAATACC- AG 3'	3' <i>HindIII</i>
<i>Rv0225</i>	5' TTTT <u>TTAATT</u> AAATGTCTGCTCTGCGCTCGGT- GTTG 3'	5' <i>Pacl</i>	5' TTTT <u>AAGCTT</u> TCAAACCACGCCGCTGACAA- AAC 3'	3' <i>HindIII</i>
<i>Rv0226c</i>	5' TTTT <u>TTAATT</u> AATGCGCTGGTCCGACCGGG- TAC 3'	5' <i>Pacl</i>	5' TTTT <u>AAGCTT</u> AATCCTGGGCGCGGCTCGC- CG 3'	3' <i>HindIII</i>
<i>Rv0228</i>	5' TTTT <u>TTAATT</u> AATGGGCCCGCGGACGAATCG- GG 3'	5' <i>Pacl</i>	TTT <u>TAAAGCTT</u> CAGGGTGCAATCGCTCCGCC- TG 3'	3' <i>HindIII</i>

Oligonucleotides used for pMV361 complementation plasmids in the Rv0225 study. Plasmids harbor an additional gene copy to complement conditional mutants. The restriction sites to establish the cloning are underlined.

Table 7. Overview of used *E. coli* strains used for the OtsB2 and Rv0225 studies

RKSC-Nr.	Strain	Alternative designation	Relevant characteristics	Source or reference
<i>E. coli</i> strains				
8	phAE159		Temperature sensitive shuttle plasmid; derivative of mycobacteriophage TM4 (<i>Apra</i> ^r)	Kalscheuer lab
9	pRv0004S		Temperature sensitive shuttle plasmid; derivative of mycobacteriophage TM4 (<i>Hyg</i> ^r)	Kalscheuer lab
19	pMV361		Shuttle plasmid (<i>Apra</i> ^r) for generation of merodiploid strains	Kalscheuer lab
201	pMV261::tetR_RBS-Mut.D		Shuttle plasmids for the generation of conditional tetON-mutants; Gradual translation rate of tetR mediated through modified ribosomal binding sites	Kalscheuer lab
202	pMV261::tetR_RBS-Mut.E			
203	pMV261::tetR_RBS-Mut.F			
204	pMV261::tetR_RBS-Mut.G			
317	pMV261::tetR_RBS-Mut.E::panCD		Shuttle plasmids for the generation of conditional tetOFF-mutants; Gradual translation rate of tetR mediated through modified ribosomal binding sites; plasmids harbour panCD gene copy to complement the auxotrophy of Δ panCD mutant strains	Kalscheuer lab
318	pMV261::tetR_RBS-Mut.G::panCD			
414	pMV261::revtetR_RBS-Mut.D		Shuttle plasmids for the generation of conditional tetOFF-mutants; Gradual translation rate of tetR mediated through modified ribosomal binding sites	Kalscheuer lab
415	pMV261::revtetR_RBS-Mut.E			
416	pMV261::revtetR_RBS-Mut.F			
417	pMV261::revtetR_RBS-Mut.G			
323	pMV261::revtetR_RBS-Mut.D::panCD		Shuttle plasmids for the generation of conditional tetOFF-mutants; Gradual translation rate of tetR mediated through modified ribosomal binding sites; plasmids harbour panCD gene copy to complement the auxotrophy of Δ panCD mutant strains	Kalscheuer lab
332	pMV261::revtetR_RBS-Mut.E::panCD			
330	pMV261::revtetR_RBS-Mut.F::panCD			
331	pMV261::revtetR_RBS-Mut.G::panCD			

Table 8. Oligonucleotides used for qRT-PCR of *M. tuberculosis* transcripts (OtsB2 study)

Gene	Forward Primer	Reverse Primer
<i>vapB43</i> (Rv2871)	5' ACCGCGAGGTGAAAGCAAAGG 3'	5' AAGTGCGGCGTTGGACGATAG
<i>vapB7</i> (Rv0662)	5' AATGGCCTCACGCACGACGGTG 3'	5' TACGCGTGCCTATCGACGCTAC
<i>Rv1258c</i>	5' CCGATGGCCGGGCGGACAATAA- AG 3'	5' AACGTGCTGGTGCTGGCCGTAT- GG 3'
<i>Rv1655</i> (<i>argD</i>)	5' GACGTGGACGGCAGAACCTATAT- C 3'	5' GCCGGAGTTGCAGAAGAACAC- CG 3'
<i>Rvnc0036a</i> (MTS2823)	5' AAGGCTCGATCCAGAAGAGAAG- G 3'	5' CAACACGGTTCTCGGTTACCA- AG 3'
<i>Rv3371</i> (<i>otsB2</i>)	5' GAACTGGTCCGGCAACTCCAGGA- AG 3'	5' TGCGGTCGACACCGATGATCA- C 3'
16S rRNA	5' GAGTGGCGAACGGGTGAGTAAC 3'	5' GGAGTCTGGGCCGTATCTCAG- TC 3'

Table 9. Oligonucleotides used for qRT-PCR of *M. tuberculosis* transcripts (Rv0225 study)

Gene	Forward Primer	Reverse Primer
16S rRNA	5' GAGTGGCGAACGGGTGAGTA- AC 3'	5' GGAGTCTGGGCCGTATCTCAG- TC 3'
<i>Rv0341</i> (<i>iniB</i>)	5' TCCTGAGCCTGTTCCGCAGCGA- AG 3'	5' ATTGGCGACGTCCTGCGCAAAG- C 3'
<i>Rv3862c</i> (<i>whiB6</i>)	5' GGCCTGATTTCGGGAATTAC 3'	5' CAACGCTTTCTGGAGGAAC 3'
<i>Rv0224c</i>	5' GAACGCCGTCGCGAAATACC 3'	5' TGCTGGCAGACTTCCGCTAC 3'
<i>Rv0225</i>	5' CATCGGGCATTGCAGTCAC 3'	5' GGTATCGACGACCACATCC 3'
<i>Rv0226c</i>	5' AAAGCGACCGCGAAGTCCTG 3'	5' GCTGGTCTTGGTGCTGCTGT- TG 3'
<i>Rv0227c</i>	5' AGCGAGGATCCGACCTGAAG- TG 3'	5' GCCCTGCTGCTGTGACCTAT- AC 3'
<i>Rv0228</i>	5' TTCGCCCGCAAACACCTCAC- AG 3'	5' AGATCGAAGCGGCCGAACAG 3'
<i>MSMEG0051</i>	5' TCGGGCAACAACCCGATGTG 3'	5' TCGCGTTTCGAGGTGATCCAG 3'
<i>MSMEG0311</i>	5' CGTGGTGATCGACACCCAGAAC 3'	5' ACAGCCACGACTCCACGAAC 3'
<i>Rv3130c</i> (<i>tgsl</i>)	5' AACCAGGTACAGGGACGTAG 3'	5' GACACTTGACGCCGGGTTTC 3'
<i>Rv3156</i> (<i>nuoL</i>)	5' CCGCAATCTTGCTGTTCCG 3'	5' AGCAGCACGAAGCACATGG 3'
<i>Rv1622c</i> (<i>cydB</i>)	5' GCGGTGATCAGCCAGACTTCGT- TG 3'	5' GCGCTGTTCTCGGTTTCTTCAT- CC 3'
<i>Rv1311</i> (<i>atpC</i>)	5' GGTGATGACGCCATGGTG 3'	5' GCCGACGGCGCGCAATCTG- GC 3'

5.3 Instruments, Kits and consumables

Table 10. Instruments, kits and consumables used in this study

Electroporator Pulser Microbial System™	BIO-RAD, München
Ice machine SVN 225	Nordcap, Ingelheim
Electrophoresis chamber	Hoefler, Amsterdam (NL)
Developer machine Cawomat 2000 IR	Cawo photochemical factory, Schrobenuhausen
ScalesCubis	Sartorius, Göttingen
Gel Doc™XR + Imaging System	BIO-RAD, München
Heating block	VWR International GmbH, Darmstadt
Heating stirrer MR3001	Heidolph, Schwabach
HYBAID Hybridization oven	Biometra, Göttingen
Incubator (BBD 6220)	Thermo Fisher Scientific, Bonn
Microwave	Bosch, Stuttgart
Milli-Q Purification Water System	Millipore, Schwabach
NanoDrop 1000	Thermo Fisher Scientific, Bonn
Orbital shaker 3005	GFL, Burgwedel
Spectrophotometer Genesys 10 UV	Thermo Fisher Scientific, Bonn
PCR-Cycler Mastercycler personal	Eppendorf, Hamburg
pH-Meter	Hanna Instruments, Bonn
Photometer	Thermo Fisher Scientific, Bonn
TissueLyser LT	Qiagen, Hilden
Ultrasound probe Labsonic U and TG1503	Bandelin
UV-Crosslinker CL1000	Biometra, Göttingen
Vortexer	VWR International, Darmstadt
Waterbath	Kottermann, Uetze/Hensingen
Centrifuge	Cooled tabletop centrifuge 5415 D, Eppendorf, Hamburg; Biofuge fresco, Heraeus, Hanau
CFX96 Real-Time System	Bio-Rad

Table 11. Kits

AlkPhos Direct Labelling Reagents	Amersham, Buckimhamshire (GB)
CDP-Star™ Detection Reagent	GE Healthcare, Dornstadt
MaxPlax™ Lambda Packaging Extracts	Epicentre, Biozym, Hessisch Oldendorf
peqGOLD Plasmid Miniprep Kit I	Peqlab, Biotechnologies GmbH, Erlangen
QIAquick® Gel Extraction Kit	Qiagen, Hilden
ZeroBlunt® TOPO® PCR Cloning Kits	Invitrogen, Karlsruhe
SuperScript III First-Strand Synthesis System	Invitrogen, Karlsruhe
GoTaq qPCR Master Mix	Promega

Table 12. Consumables

Formaldehyd, D(+)-Glucose, EDTA	AppiChem
Middlebrook 7H9, Middlebrook 7H10, Agar Noble, QADC, plastic pipettes	Becton Dickinson
Biozym LE Agarose, MaxPlax Packaging Extracts	Biozym Scientific
TRIS, Protein Kinase K	Carl Roth
FailSafe™ PCR 2x Premix	Epicentre
Safe-Lock Tubes (2.0 ml, 1.5 ml)	Eppendorf
Amersham Hybond-Nylonmembrane	GE Healthcare Lifescience
3 mm Glas Beads	Merck KG
NEB-5-alpha	New England Biolabs
Bovine Serum Albumin Fraction V	Roche
Cuvettes, PP centrifuge tubes (15, 50 ml), Petri Dishes	Sarstedt
Ethidium bromide, Resazurin (sodium salt), Tyloxapol, Lysomzyme, Calciumchloride, Anhydrotetracycline, Cetrimide, Isopropanol, Kanamycinsulfate, Trypanblue,	Sigma Aldrich

Electroporation Cuvettes, Apramycin, Hygromycin	
6x DNA Loading Buffer, GeneRuler, 1kb DNA Ladder	Thermo Scientific
Chlorform, Methanol, Ethanol, Glycerol, Magnesiumchloride-Hexahydrate, Sodiumchloride, Sodiumhydroxide, Inoculation loops, Spatula, Microtiter plates, Reagent Reservoirs, Sterile Filter, PCR Reaction Tubes, Screw-cap tubes, Roller Bottles	VWR International

5.4 Strains and growth conditions

5.4.1 Cultivation of mycobacterial strains

Cultivation of mycobacterial strains was mainly based on Larsen et al. 2007 [142]. All mycobacterial strains were grown aerobically at 37°C in Middlebrook 7H9 medium supplemented with 10% (v/v) OADC enrichment (Becton Dickinson Microbiology Systems) or ADS (see below), 0.5% (v/v) glycerol and 0.05% (v/v) Tyloxapol. Hygromycin (50 mg/l), apramycin (20 mg/l) and kanamycin (20 mg/l) were added for selection for appropriate strains. Shaking cultures were inoculated 1% (v/v) from glycerol stocks in 30 ml square bottles using an end volume of 10 ml. *M. smegmatis* cells were cultivated 3-5 days on solid medium and 24-48 h in liquid culture, cells of *M. tuberculosis* and *M. bovis* BCG for 21-28 days on solid and 6-14 days in liquid culture. For growth on solid medium, bacteria were incubated on petri dishes containing 7H10 medium (1.9% (w/v)) and ADS or OADC (10% (v/v)). All strains used for this study are listed in Table 2 and Table 5.

ADS (Albumine Dextrose Salt)

8.1 g NaCl

50g Bovine serum albumin (Fraction V)

20g Dextrose

950 ml dest H₂O

Substances were solved separately and subsequently sterile filtered.

5.4.2 Cultivation of *E. coli*

E. coli cells were cultivated on LB solid medium or in LB liquid medium: 1% LB-Casein hydrolysate (w/v), 0.5% yeast extract (w/v), sodium chloride 0.5% (w/v), adjusted to a pH-value of 7.2 in a total end volume of 1000 ml H₂O dest. For selection, antibiotics were used at the following final concentrations: Hyg (150 µg/ml), Kan (40 µg/ml), Apra (40 µg/ml). Solid medium was generated by addition of 1.2% (w/v) of agar before autoclaving.

5.4.3 Harvesting and washing of bacteria

After cultivation of the bacteria to an $OD_{600\text{ nm}} = 0.8\text{--}1.0$ for competent cells or for biomass production, cells were harvested by centrifugation. 5-10 ml cultures were pelleted at 4000 rpm/min for 10 min, smaller suspensions at 13000 rpm/min for 5 min. Two PBS washing steps served as purification steps, removing residual medium traces. Washing volumina corresponded to the total volume of the initial culture. Concentration of bacteria was performed achieving transformant competent bacteria (1/10 of end volume).

5.4.4 Generation of glycerol stocks of *Mycobacteria* and *E. coli*

Stocks of mycobacteria were generated under supplementation of glycerol to a final concentration of 16.6% (v/v) with densely grown bacteria. Similarly, *E. coli* stocks were prepared with addition of glycerol to a final concentration of 25% (v/v). Strains were stored at $-80\text{ }^{\circ}\text{C}$ in cryovials and thawed on ice when bacteria were used for inoculation of new cultures.

5.5 Genetical and analytical methods

5.5.1 Plasmid isolation

For plasmid isolation, repective *E. coli* strains were incubated over night in 5 ml LB-medium or on agar plates at $37\text{ }^{\circ}\text{C}$. Preparation followed by instructions of the manufacturer (Peqlab) using the Miniprep Kit. Bacteria were alkaline lysed under vigorous vortexing. This step dissolves hydrogen bonds between the complementary DNA strands of chromosomal DNA and plasmid DNA. Due to its conformation only the plasmid DNA is able to reanneal completely, by increasing the pH-value via acetate supplementation. The chromosomal DNA has been broken partially by exposition to shear forces during lysis. It is not able to reanneal and forms only short complementary regions in a predominant single stranded DNA coil. This coil is centrifuged together with precipitated NaOH, proteins and remaining cell debris, which have been formed during the neutralization step. The plasmid DNA is localized in the supernatant and transferred to a column. Plasmid DNA binds selectively to the silica matrix of the column. After washing, elution is performed by elution buffer of the manufacturer or water.

5.5.2 Polymerase chain reaction (PCR)

DNA-polymerases are able to use single strand DNA as a template for synthesis of a complementary double strand DNA. This characteristic attributes to the polymerase chain reaction (PCR), generating numerous copies of a specific DNA sequence. Within the PCR, the double stranded DNA is denatured, separating the DNA duplex in two single DNA strands. While the DNA is cooled down, primer can hybridize in a specific manner (Table 13) at the 5' and 3' flanking sequences of the DNA region of interest. The thermostable DNA polymerase *Phusion High Fidelity* (Fermentas) harbours a DNA binding domain, which is coupled to a *proofreading* polymerase. The polymerase synthesizes the complementary strand at $72\text{ }^{\circ}\text{C}$. Cyclic repeats of temperature changes (PCR programme) facilitate exponential fragment amplification. DNA

amplification was performed by Eppendorf PCR Cycler, using Failsafe Premix (Epicenter), 20 pmol specific primer pairs and 20 U/ml of described Phusion DNA polymerase. After an initial denaturation phase, several annealing and elongation steps were set up in the PCR program. A *Touchdown*-PCR was applied, which is characterized by a stepwise decrease of the annealing temperature. Hence, variable fragments of the flanking regions of respective *knock-outs* or *knock-ins* could be amplified efficiently.

Table 13. Overview of the used PCR-Protocol for defined DNA fragment amplification

Step	Temperature	Time	
Denaturation	98 °C	5 min	
Annealing	65 °C	30 sec	
	60 °C	30 sec	
	55 °C	30 sec	
	50 °C	30 sec	
	45 °C	30 sec	
Elongation	72 °C	~ 1 min/ kbp	
Denaturation	98 °C	30 sec	5 cycles
Annealing	50 °C	30 sec	
Elongation	72 °C	~ 1 min/ kbp	
Denaturation	98 °C	30 sec	5 cycles
Annealing	55 °C	30 sec	
Elongation	72 °C	~ 1 min/ kbp	
Denaturation	98 °C	30 sec	25 cycles
Annealing	60 °C	30 sec	
Elongation	72 °C	~ 1 min/ kbp	

Table 14. Quantitative real time PCR

Step	Temperature	Time	
Start	50 °C	10 min	
Denaturation	95 °C	2 min	
Denaturation	95 °C	30 sec	40 cycles
Annealing	55 °C	30 sec	
	50 °C	30 sec	
	45 °C	30 sec	
Elongation	72 °C	1 min	
Dissociation	95 °C	1 min	
	55 °C	55 sec	
	95 °C	30 sec	

Relative quantification of selected genes was performed employing the Mx3005P QPCR System with the MxPro3005P Software.

5.5.2.1 Quantitative real-time PCR reagents

For qRT-PCR, DNA-free total RNA samples were prepared from independent biological replicates essentially as described below in 5.5.21 with the omission of rRNA depletion, and were reverse transcribed with the SuperScript III First-Strand Synthesis System (Invitrogen). For the real-time reaction, each primer (250 nM) and 7.5 µl of template reaction (1:10 dilution) in 25 µl volume with GoTaq qPCR Master Mix (Promega) was used. Triplicate samples were run on a CFX96 Real-Time System (Bio-Rad). Threshold

cycles were normalized to those for 16S rRNA. Primer sequences used for qRT-PCR are listed in Table 8 and 9.

5.5.3 Agarose gel electrophoresis

In the agarose gel electrophoresis, DNA (DNA fragments, digested genomic DNA, PCR products, plasmids and phasmids) is separated according to its size, defined by its length. By comparison of its size with DNA standard ladders or other fragments of known length, the method helps to identify DNA molecules in regard to the experimental assays. Briefly, the agarose forms a gel, consisting of a network of agarose polymers. Using a constant voltage (typically 100 V), negatively charged nucleic acid molecules migrate through the gel matrix to the positive charged cathode, while smaller molecules move faster than bigger ones, resulting in separation of DNA molecules based on their length. In this study, 1% (w/v) agarose gels with TAE-buffer (Table 15) have been used. The agarose/TAE solution was melted using a microwave. Afterwards, ethidiumbromide was added to a final concentration of 0.5 µg/ml, the solution was mixed and filled into a gel chamber. A comb allowed to form pockets in the gel, which have been flushed with buffer before sample application followed. DNA samples were diluted in 6x sample buffer (Fermentas). The sample buffer consist of glycerol for weighing down the sample in order to avoid diffusion in the TAE-buffer filled gel chamber and allowing a sample manifestation in the gel pockets. Furthermore, low molecular dyes in the buffer are separated through electrophoresis, giving an indication of the running front of the samples.

Table 15. Tris-Acetate-EDTA-buffer (TAE-buffer)

Tris	242 g
EDTA	100 ml 9.5M
Acetic acid	57.1 ml
dH ₂ O	1000 ml

5.5.4 DNA extraction out of agarose gel

After the PCR-fragments or restriction-fragments in the agarose gel have been separated, respective bands were extracted using the QIAquick® Gel Extraction Kit according to the manufacturer. DNA bands were cut with a scalpel under UV light, gel fragments were weighed, buffer amount was adjusted and the excerpt were dissolved at 60 °C. The warm solution was transferred to a column, on which the DNA binds reversibly to a silica membrane in a salt-dependent manner. DNA elution followed in a small amount of elution buffer. During this purification step, primer, nucleotides, enzymes, agarose, ethidium bromide and other contaminating reagents or molecules can be removed. Finally, the purified DNA can be used for any downstream applications, like ligations and sequence verifications.

5.5.5 Sequencing for plasmid quality control

Plasmid DNA (~ 1000ng) was sequenced with suitable sequencing primer (5 pmol) employing the Extended-Hotshot method (Seqlab, Göttingen) with specialized treatment for GC-rich DNA. After data transfer, sequences were analyzed by Clone Manager 9 Software. The used sequencing primers are listed below.

Table 16. Oligonucleotides used for sequencing reactions for verification of plasmids.

Primer name	Sequence	Application
LL	5'GGCCCGATAATACGACTCAC-3'	<i>Knock-in and knock-out plasmid</i>
RR	5'AAACAAACCACCGCTGGTAG-3'	<i>Knock-in and knock-out plasmid</i>
LR	5' TCGACGACCCTAGAGTCCTG-3'	<i>Knock-out plasmid</i>
RL	5'AACTGGCGCAGTTCCTCTGG-3'	<i>Knock-out plasmid</i>
LR cohyg	5' AGGTGCCTCACTGATTAAGC-3'	<i>Knock-in plasmid</i>
RL tet-seq	5'AGGTGCCTCACTGATTAAGC-3'	<i>Knock-in plasmid</i>
pMV261/361 Kan Fw	5'CAGCGTAAGTAGCGGGGTTG-3'	Complementation plasmid harbouring Kan-resistance
pMV261/361 Kan Rev	5'GCCTCGAGCAAGACGTTTCC-3'	Complementation plasmid harbouring Kan-resistance
pMV261/361 Apra Rev	5'CTGATGGAGCTGCACATGAAC-3'	Complementation plasmid harbouring Apra-resistance

5.5.6 Restriction of DNA

In this study, DNA restriction was done by type II restriction endonucleases at specific recognition sites. Type II endonucleases recognition and restriction sites are identical. The DNA was treated with different restriction enzymes (Table 17). Genomic DNA was digested over night, plasmid and controls for 4-6 hours. PCR products and plasmids for ligations and double digestions were incubated over night as well, trying to achieve a complete restriction. Reaction volumes contained 10 µl for control digestions and 50 µl for restrictions, which have been used for downstream applications, including further cloning steps. Per 10 µg DNA, 10 U of the respective restriction enzyme was used. The restriction buffer for single- and double digestions was selected according to the manufacturer.

Table 17. Applied restriction enzymes.

Restriction enzyme	Recognition sequence and cutting site
<i>Bst</i> API (incubation at 60 °C)	5'-GCANNNN*NTGC-3'
<i>Eco</i> NI	5'-CCTNNNNAGG-3'
<i>Eco</i> RI	5'-GAA*TTC-3'
<i>Eco</i> RV	5'-GAT*ATC-3'
<i>Dra</i> III	5'-CAC*NNGTG-3'
<i>Hind</i> III	5'-AAG*CTT-3'
<i>Mlu</i> I	5'-ACG*CGT-3'
<i>Pac</i> I	5'-TTAA*TTAA-3'
<i>Pst</i> I	5'-CTG*CAG-3'
<i>Sma</i> I	5'-CCC*GGG-3'
<i>Van</i> 91I	5'-CCAANNNN*NTGG-3'
<i>Xho</i> I	5'-CTC*GAG-3'

Per µg DNA, 10 U enzyme was used. The incubation ranged from 4-6 h for a control digestion and overnight for further cloning purpose. Enzyme cutting sites are marked with *.

5.5.7 Ligation

The T4 ligase was selected to ligate DNA fragments into the respective vector. Both molecules have been subjected to restriction digestion before. Optimal insertion efficiency was obtained when using a vector:insert ratio of 1:5 to 1:7. The reaction mix was done according to the manufacturer (Fermentas). Incubation time at RT depended on the number of fragments to ligate: 2 h for ligation of two fragments, overnight for ligation of four fragments.

5.5.8 Generation of site-specific gene deletion mutants.

(This paragraph has been published in modified form in PLoS Pathog 12(12): e1006043)

Site-specific gene deletion mutants of *M. tuberculosis* H37Rv were generated by specialized transduction employing temperature-sensitive mycobacteriophages essentially as described previously [140, 141]. Briefly, for generation of allelic exchange constructs for gene replacement with a γ δres-sacB-hyg- γ δres cassette comprising a *sacB* as well as a hygromycin resistance gene flanked by *res*-sites of the γ δ-resolvase, upstream-and downstream-flanking DNA regions were amplified by PCR employing the oligonucleotides listed in Table 1. Subsequently, the upstream and downstream flanks were digested with the indicated restriction enzymes and ligated with *Van*91I-digested pYUB1471vector arms [3]. The resulting knock-out plasmids were then linearized with *PacI* and cloned and packaged into the temperature-sensitive phage phAE159 [3], yielding knock-out phages which were propagated in *M. smegmatis* at 30 °C. Allelic exchange in mycobacteria using the knock-out phages was achieved by specialized transduction using hygromycin (50 mg/l) for selection, resulting in gene deletion and replacement by the γ δres-sacB-hyg- γ δres cassette. For the generation of unmarked mutants, the γ δres-sacB-hyg- γ δres cassette was removed employing specialized transduction using the phage phAE7-1 expressing the γ δ-resolvase [3] using sucrose (3%, w/v) for counterselection. All obtained mutants were verified by Southern analysis of digested genomic DNA using appropriate restriction enzymes and probes (OtsB2 study: S1Fig/ S3 Fig, Rv0225 study: S11).

5.5.9 Generation of conditional mycobacterial mutants.

(This paragraph has been published in modified form in PLoS Pathog 12(12): e1006043)

For establishing regulated expression of the gene of interest (GOI), a synthetic gene cassette (hyg-*Pmyc1*-4x*tetO*) comprising a hygromycin resistance gene and the *Pmyc1* promoter from *M. smegmatis* engineered to contain four *tetO* operator sites, which are the DNA binding sites for the cognate repressor protein TetR,

was inserted immediately upstream of the GOI start codon in the respective mycobacterial strains used in this study. Targeted gene *knock-in* was achieved by specialized transduction employing temperature-sensitive mycobacteriophages. Briefly, for generation of allelic exchange constructs for site specific insertion in mycobacterial strains of the *hyg-Pmyc1-4xtetO* cassette, upstream-and downstream DNA regions flanking the GOI start codon were amplified by PCR employing the oligonucleotides listed in Table 1 and 4. Subsequently, the upstream and downstream flanks were digested with the indicated restriction enzymes (Table 2 and 5), and ligated with *Van91I*-digested *pcRv1327c-4xtetO* vector arms [4]. The resulting knock-in plasmid was then linearized with *PacI* and ligated into *PacI*-digested genomic DNA of phage *phAE159*, yielding a *knock-in* phage which was propagated in *M. smegmatis* at 30°C. Allelic exchange in mycobacteria using the *knock-in* phage at the nonpermissive temperature of 37°C was achieved by specialized transduction using hygromycin (50 mg/l) for selection, resulting in site -specific insertion of the *hyg-Pmyc1-4xtetO* cassette. The obtained *c-goi-4xtetO* knock-in mutant was verified by Southern analysis of digested genomic DNA using an appropriate restriction enzyme and probes (OtsB2 study: S2Fig , Rv0225 study: S10/ S12/S15/S17 Fig.).

For achieving controlled gene expression of the GOI, the *E. coli* Tn10 *tetR* gene encoding a repressor protein exhibiting high-binding affinity to *tetO* sites in absence of the inducer tetracycline was heterologously expressed in the *knock-in* mutant. The *tetR* gene was amplified by PCR employing the oligonucleotide primer pair 5'-TTTTTTGAATTCATGATGTCTAGATTAGATAAAAG-3' and 5'-TTTTTTAAGCTTAAGACCCACTTTTACATTTAAG-3' using an irrelevant *tetR*-harboring plasmid as a template and cloned using the restriction enzymes *EcoRI* and *HindIII* (underlined) into the episomal *E. coli-Mycobacterium* shuttle plasmid pMV261 [23] with different mutated ribosomal-binding-sites (pMV261-RBS-X) [56]. The resulting plasmid pMV261::*tetR*-X providing constitutive gene expression from the HSP60 promoter in mycobacteria was transformed by electroporation into the mycobacterial *c-GOI-4xtetO knock-in* mutant using solid medium containing 50 mg/l hygromycin and 20 mg/l kanamycin for selection. This yielded the conditional mutant *c-GOI-4xtetO pMV261::tetR-X* (referred to as *c-GOI-tet-on* mutant) allowing silencing of the GOI in absence of the inducer anhydrotetracycline (ATc). For regulated gene expression of the GOI in the $\Delta panCD$ mutant background, the *panC-panD* operon comprising the native ribosome binding sites was amplified by PCR employing the oligonucleotide primer pair 5'-TTTTTAAGCTTGAGGTTTTGACGGCATGACGATTC-3' and 5'-TTTTTAAGCTTCTATCCACACCGAGCCGGGGGTC-3' using wild-type *M. tuberculosis* H37Rv genomic DNA as a template and cloned using the restriction enzyme *HindIII* (underlined) into plasmid pMV261::*tetR*-X downstream of the *tetR* gene in collinear orientation, thereby establishing transcriptional coupling of the *tetR* and *panCD* genes all being expressed from the HSP60 promoter. The resulting plasmid pMV261::*tetR*-X::*panCD* was transformed by electroporation into the *M. tuberculosis* $\Delta panCD$ *c-GOI-4xtetO* knock-in mutant using solid medium containing 50 mg/l hygromycin, 20 mg/l kanamycin and no pantothenic acid supplementation for selection. This yielded the conditional mutant *M. tuberculosis* $\Delta panCD$ *c-GOI-4xtetO pMV261::tetR-X::panCD* (referred to as *M. tuberculosis* $\Delta panCD$ *c-GOI-tet-on* mutant). Two relevant *M.*

tuberculosis $\Delta panCD$ c-GOI-4xtetO pMV261::tetR-X::panCD strains have been generated: *M. tuberculosis* $\Delta panCD$ c-otsB2-4xtetO pMV261::tetR-G::panCD (referred to as *M. tuberculosis* $\Delta panCD$ c-otsB2-tet-on) and *M. tuberculosis* $\Delta panCD$ c-Rv0225-4xtetO pMV261::tetR-D::panCD (referred to as *M. tuberculosis* $\Delta panCD$ c-Rv0225-tet-on).

5.5.10 Genetic complementation.

For complementation of the conditional mycobacteria mutants and for generating a GOI merodiploid strain, the GOI gene was PCR amplified using the oligonucleotide pairs listed in Table 3 and 6 and cloned using the restriction enzymes *PacI* and *HindIII* into the single-copy integrative plasmid pMV361(Apr)-*PacI* or pMV361(Kan)-*PacI*, respectively, which are derivatives of pMV361(Kan) [143] engineered to contain a unique *PacI* restriction site and an apramycin resistance gene in case of pMV361(Apr)-*PacI*. This resulted in plasmids pMV361 (Apr):GOI and pMV361(Kan)::GOI, respectively, providing constitutive gene expression from the HSP60 promoter. The plasmids were transformed by electroporation into the conditional *M. tuberculosis* c-GOI-tet-on mutant or *M. tuberculosis* wild-type, respectively.

5.5.11 Hidden Markov Models (HMMs) for non-gene-centric comparative analysis of Tn-seq data

(This paragraph has been published in *PLoS Pathog* 12(12): e1006043)

A comparative analysis of the differentially essential regions in the $\Delta otsA$ library grown with- versus without trehalose was performed as follows. Two Hidden Markov Models (HMMs) were used. One was designed to identify regions where there is a clear difference in that the TA sites have insertions in one condition but not the other. The second HMM was designed to identify regions of quantitative differential essentiality, in that the relative level of insertion counts is significantly lower (but not necessarily zero) in one condition than the other. The advantage of using HMMs to analyze Tn-seq data is that differentially essential regions can be identified in a non-gene-centric way, i.e. not restricted to ORF boundaries.

HMM-1:

A 3-state HMM was implemented in Python to label each TA site as either Essential (ES), Non-essential (NE), or Missing (MI) based on insertion counts at TA sites. The intended interpretation of the MI state is for isolated TA sites where no insertions were observed in the middle of otherwise non-essential regions. The prior probabilities were set at 0.15 for ES, 0.85 for NE, and 0.001 for MI. The transition probability matrix was parameterized as: $[[0.001, 0.999, 0.0], [0.000000001, 0.9, 0.1], [0.0, 0.9999, 0.0001]]$. The likelihood function for counts in the ES state was given by a geometric distribution, $\text{Geom}(p=0.9)$, for the NE was given by a negative Binomial distribution, $\text{NegBinom}(r=1, p=0.01)$, and for MI states is $1e-6$ for counts > 1 and $1-1e-6$ otherwise. The state labels are assigned using the Viterbi algorithm.

HMM-2:

Regions with read-counts that were consistently higher in one condition relative to the other were determined using a HMM. The HMM consisted of three states representing regions that had consistently higher read-counts in condition A (S1), consistently higher read-counts in condition B (S3), or read-counts that were more or less evenly distributed (S2). The transition probabilities of the HMM were set so that there was high probability to stay within state ($[[0.98, 0.01, 0.01], [0.01, 0.98, 0.01], [0.01, 0.01, 0.98]]$). States S1 and S3 had a low prior-probability of being observed ($p(S)=0.1$ each), as most areas of the genome are not expected to be differentially essential. Observations at states S1 and S3 were modeled using a discrete distribution with the highest mass assigned to the sign of the direction in question: e.g.

$$P(-1 | S1) = 0.700$$

$$P(0 | S1) = 0.299$$

$$P(1 | S1) = 0.001$$

The observations at state S2, had a distribution that was closer to uniform as the sign in these regions may change back and forth:

$$P(-1 | S2) = 0.3$$

$$P(0 | S2) = 0.4$$

$$P(1 | S2) = 0.3$$

To determine the statistical significance of the difference in counts between the two datasets in each of the type-1 and type-2 segments identified above, a permutation test was performed [5]. Insertion counts at TA sites in each segment were randomly permuted between the datasets 10,000 times to generate a null-distribution for the difference in the sum of the counts between the two datasets, and a p-value for the observed difference was calculated from this. The p-values were then adjusted for multiple comparisons by the Benjamini-Hochberg procedure, and a threshold of adjusted p value <0.05 was applied. Bioinformatic analyses were performed by Prof. T. Ioerger, Department of Computer Science, Texas A&M University, College Station (USA).

5.5.12 Resazurin microplate assay (REMA) for growth quantification of ATc dependant mycobacterial growth.

Anhydrotetracycline (ATc)-dependent growth of conditional mycobacterial mutant strains was quantified using the resazurin microplate assay. A serial 2-fold ATc dilution was performed in a 96-Well plate format. Each well contained medium with increasing concentrations of ATc according to the construct, giving a range of 12 different ATc concentrations. After sonification and measurement of the OD_{600 nm} of densely grown 10 ml pre-cultures, which have been washed once with 10 ml PBS and resuspended in PBS, each well was inoculated with 4×10^6 cells/ml in a total final volume of 100 μ l medium/bacterial cells, considering an OD_{600 nm} of 1 corresponds to 3×10^8 cells/ml. In order to deplete possibly accumulated gene product, cells of the slow growers (*M. tuberculosis* and BCG-Pasteur) and the fast grower (*M. smegmatis*) were subcultivated at a certain incubation time at 37°C under previously identified ATc silencing conditions

(Table 18). After incubation of the first passage, 100 µl of the respective cell suspension was diluted in 2 ml medium in order to inoculate a second passage. Subsequently, 10 µl resazurin solution (100 µg/ml, Sigma-Aldrich) was added and cells were incubated for further 15 – 16 h at 37°C. Then cells were fixed at room temperature for 30 min after addition of formalin (5%, v/v, final concentration), and fluorescence was measured using an Infinite® 200 pro plate microplate reader (excitation 560 nm, emission 590 nm). Samples were run as triplicates.

Table 18. Anhydrotetracycline culturing conditions for dosis dependant gene silencing of conditional mycobacterial mutants

Strain	ATc concentration for silencing	Incubation time for silencing (1st passage)	Incubation time for silencing (2nd passage)	Resazurin incubation
<i>M. tuberculosis</i> c-Rv0225 tet-on	63 ng/ml	6 days	6 days	16 h
<i>M. tuberculosis</i> c-Rv0226c-tet-on	0 ng/ml	6 days	6 days	16 h
<i>M. bovis</i> c-Mb0230-tet-offmutant	640 ng/ml	6 days	6 days	16 h
c-MSMEG0311-tet-on	2 ng/ml	17 h at 37°C	6.5 h	15.5 h

ATc: Anhydrotetracycline.

5.5.13 Isolation of genomic DNA

Mycobacterial genomic DNA was isolated by the CTAB method. A growing culture was centrifuged, resuspended in 500 µl GTE-buffer (see below) with lysozym (10 mg/ml, see below) and incubated over night at 37°C in order to disrupt the cells. On the next day, the cell suspension was spiked with 150 µl of a 10% (w/v) SDS-solution with proteinase K (10 mg/ml) (composition, see below). For bacterial protein degradation, the mixed solution was incubated for 30 minutes at 55°C on a heating block. Afterwards, 200 µl of a 5 M NaCl solution was added. The complete solution was mixed carefully and 160 µl of pre-warmed CTAB-solution (see below) was added and carefully mixed. An incubation of 65 °C followed for 10 minutes.

DNA extraction followed by addition of 1 ml chloroform-isoamylalcohol (24:1, v/v). The suspension was carefully mixed. A following centrifugation (10 min, 4000 rpm) resulted in two phases, separated by an interphase containing proteins and cell debris. The upper aqueous phase containing the DNA was separated carefully avoiding any losses, and again treated with 1 ml chloroform-isoamylalcohol (24:1, v/v). After centrifugation, a faint interphase occurred. Again, the upper phase was removed. DNA precipitation followed by addition of 0.7 volumes isopropanol and inversion. In order to achieve a complete DNA precipitation, the mixture has been incubated 4°C for 15 minutes. The DNA was centrifuged (10 min, 13000 rpm) and became visible as a white pellet. The pellet was washed with 1 ml 70% (v/v) ethanol, the ethanol was removed carefully and the pellet was dried for some minutes at 40 °C on a heating block. Finally, the

DNA pellet was resuspended in 50-500 µl TE-buffer containing 1 µg/ml (w/v) RNase. DNA was stored at -20°C.

5.5.13.1 GTE buffer

25 mM Tris/HCl

10 mM EDTA

50 mM Glucose

pH adjusted with HCl to 8.0

5.5.13.2 Lysozym solution

10 mg Lysozym

10 ml H₂O

5.5.13.3 Proteinase K solution

10 mg Proteinase K

10 ml H₂O

5.5.13.4 SDS solution

10 g Natriumdodecylsulfate

100 ml H₂O

5.5.13.5 CTAB-solution

4.1 g NaCl

10 g Cetrimid (Cetyltrimethylammoniumbromide)

90 ml dest. H₂O

Cetrimid was added during an incubation at 65 °C on a heat block. During cooling, the suspension turned viscous.

5.5.14 Southern Blot

In order to validate the genotype of respective putative mutants, Southern blots were conducted using digested genomic DNA of the mutants in comparison to genomic DNA of the wild-type. DNA was isolated and incubated with a suitable restriction enzyme overnight and separated on an agarose gel electrophoresis system at 100 V. The DNA was transferred onto a nylon membrane using the Turboblotter Rapid Downward Transfer System according to the manufacturer. The DNA was crosslinked on the nylon membrane via UV radiation by 120 J/cm². Using the Amersham™ AlkPhos Direct Labeling Detection System, the blotting membrane was pre-incubated for one hour. As hybridization probes, PCR products of the left or right flank were used, which have also been used for the generation of the AES (see Table 1 and 4). The probes were labeled according to the manufacturer, either fresh or after mixture with 50% (v/v) glycerol at -20°C frozen for later usage. Hybridization was conducted largely as recommended by the manufacturer, but the incubation was 16 h and at 65 °C, improving the specificity. Signals on the membrane were detected by CDP-Star™ Detection Reagent and visualized by Amersham Hyperfilm™ MP with the developing machine Cawomat 2000 IR.

Digested mutant DNA was compared to the respective wild-type, ending up in diagnostic fragment sizes hybridizing with the probes. Due to the insertion of the resistance cassette, mutants typically showed a larger fragment than the wild-type.

5.5.15 Transformation of *E. coli* via heat shock

Competent *E. coli* NEB5-alpha (NEB) cells were thawed on ice and mixed with 5 µl ligation preparation or plasmid-DNA and incubated on ice for 30 minutes, which facilitated attachment of the DNA to the bacteria. The heat shock was performed at 42°C for 30 seconds on a waterbath, enabling the DNA uptake by the bacteria. After a short cooling, cells were able to regenerate in 500 µl SOC-medium (NEB) in order to express the antibiotic resistance encoded on the plasmid. The transformation mixture was plated on selective solid media, incubated overnight at 37°C, and a suitable amount (3-10) of clones were used for the further downstream processes and cultivated in liquid media.

5.5.16 Transformation of mycobacteria

M. bovis BCG, *M. tuberculosis* and *M. smegmatis* were cultivated to an OD_{600 nm} of 0.5-0.8. After harvesting the cells, the pellet was washed twice in cold 10% (v/v) glycerol with 0.05% (v/v) tyloxapol solution and resuspended in 1/10 of the original culture volume. The transformation was done using electroporation cuvettes with 0.2 cm gap at 2500 V, 1000 Ω and 25 µF. To establish the expression of the selection marker, cells were mixed with 1 ml Middlebrook 7H9 media (for phasmids: without tyloxapol, for normal plasmids: with 0.05% tyloxapol) and incubated for 1-2 hours (fast growing mycobacteria) or 18-20 hours (slow growing mycobacteria) at 37°C, before plating on solidified selection media.

5.5.17 Mouse infection: OtsB2 study.

(This paragraph has been published in *PLoS Pathog* 12(12): e1006043)

Aerosol infection of seven week old female C57BL/6 mice (Jackson Laboratory) was performed using an inhalation exposure system from Glas-Col and early log phase *M. tuberculosis* cultures prepared as single-cell suspensions in PBS to deliver 100–200 bacilli per mouse. Four mice were sacrificed per strain per time point. Serial dilutions of lung and spleen homogenates were plated on appropriate 7H10 agar plates that had been supplemented with 500 ng/ml ATc, 20 µg/ml kanamycin and 50 µg/ml hygromycin for the conditional *c-otsB2*-tet-on mutant. Aliquots of the conditional *c-otsB2*-tet-on mutant were plated in parallel on agar containing 20 µg/ml kanamycin and 50 µg/ml hygromycin but no ATc to determine the frequency of non-regulated suppressor mutants. Mouse infection studies were performed by Prof. S. Ehrt, Department of Microbiology and Immunology, Weill Cornell Medical College, New York, New York, USA.

5.5.18 Thin-layer chromatography (TLC) and ¹H-NMR analysis of carbohydrates for OtsB2.

Carbohydrates were extracted from equal amounts of cells with hot water (95°C for 4 h) and analyzed by TLC on Silica gel 60 (EMD Chemicals) plates using the solvent system 1-propanol:ethyl acetate:water (6:1:3, v/v/v). Substances were visualized by immersing TLC plates in 10% (v/v) sulfuric acid in ethanol followed by charring at 180°C for 10 min. The extracts were also subjected to ¹H-NMR spectroscopic analysis. Solution-state spectra were recorded on a Bruker Avance III 400 MHz spectrometer and analyzed using Bruker TopSpin 2.1 (Rheinstetten, Germany). Chemical shifts are reported with reference to residual water at δ_H 4.79 ppm and authentic trehalose and T6P were purchased from Sigma-Aldrich. ¹H-NMR analysis of carbohydrates for OtsB2 was performed by Dr. S. Bornemann, Department of Biological Chemistry, John Innes Centre, Norwich Research Park, Norwich, Norfolk, United Kingdom.

5.5.19 Extraction and TLC analysis of Mycolic Acid Methyl Esters (MAMEs)

Mycolic acids were extracted according to Besra [144]. Defatted cells have been weighted, and 50 mg of dried pellet were diluted in 2 ml 15% TBAH-solution and incubated at 100°C in the heating block over night. After cooling, the suspension was diluted with 2 ml ddH₂O. Per 50 mg dried pellet, 1 ml dichlormethane und 0.25 ml iodomethane was added. Test tubes were shaken radially for 30 min and centrifuged (4000 rpm, 1h). Die lower phase including the MAMEs was removed and lyophilized in HPLC-glasses. Extracted MAMEs were dissolved in 125 µl dichlormethane. For further experiments, MAMEs could be normalized to 0.5 mg of dried defatted cells. MAMEs were applied on a pre-warmed silica gel 60 TLC-plate, and the TLC plate was developed using the solvent system petroleum spirit/diethylether (95:5, vol/vol). Once the solving front reached the top of the TLC-plate, the plate was dried at room temperature. Separation of MAMEs on the same TLC plate was performed six times successively, exchanging the runnig solvent each time.

Finally, the dried TLC plate was stained with 5% molybdotophosphoric acid and bands became visible after heating up to 110 °C on a heating plate.

5.5.20 Extraction and TLC analysis of cell wall associated lipids in BCG

Thin-layer chromatography (TLC) for cell-wall associated lipids in *M. bovis* BCG was performed by our cooperation partner according to Besra [144].

5.5.21 Transcriptome profiling of conditional OtsB2 and Rv0225 mutants

(This paragraph has been published in modified form in *PLoS Pathog* 12(12): e1006043)

Cells of the conditional *M. tuberculosis* *c-otsB2* and conditional *Rv0225* mutant were grown from frozen stocks in 7H9 medium containing 1000 ng/ml (*c-otsB2*-tet-on) and 500 ng/ml (*c-Rv0225*-tet-on) ATc until they reached an OD_{600 nm} ~1. Cells were harvested, washed and then subcultured in 7H9 medium containing 100 ng/ml (*c-otsB2*-tet-on) and 63 ng/ml (*c-Rv0225*-tet-on) ATc for 7 days at 1% inoculation. Cells were subsequently harvested, washed, and used to inoculate 10–30 ml per replicate of 7H9 medium containing either 200 ng/ml (*c-otsB2*-tet-on) or 30 ng/ml (*c-otsB2*-tet-on) and 500 ng/ml (*c-Rv0225*-tet-on) and 10 ng/ml (*c-Rv0225*-tet-on) ATc, respectively, at 1% inoculation. Cells were harvested for RNA extraction after 7 days of incubation at 37°C, and cell pellets were fixed overnight in 5 ml RNA Protect reagent (Qiagen). Fixed cells were pelleted, resuspended in 1 ml RLT buffer (Qiagen) and lysed by bead beating to prepare lysates. Total RNA was extracted using the RNeasy Mini kit (Qiagen). Total RNA preparations were checked for RNA integrity by Agilent 2100 Bioanalyzer quality control. All samples in this study showed high quality RNA Integrity Numbers (RIN; mean 8.5). RNA was further analyzed by photometric Nanodrop measurement and quantified by fluorometric Qubit RNA assays (Life Technologies). After magnetic depletion of ribosomal RNA (Ribo-Zero rRNA Removal Kit, Gram-positive Bacteria; Epicentre), barcoded cDNA libraries were prepared according to the manufacturers protocol (Ion Total RNA-Seq Kit v2; Life Technologies). Emulsion PCR and subsequent IonProton sequencing were performed according to commercial kit protocols (Ion PI Template OT2 200 Kit v2, Ion PI Sequencing 200 Kit; Life Technologies). Demultiplexing was done using TorrentSuite software (vers. 4.0.2, Life Technologies). Raw sequencing reads were quality trimmed in CLC Genomics Workbench (vers. 6.5.2, CLCbio / Qiagen). After removal of short (< 50 nt) sequences, the remaining high quality reads were aligned against the *M. tuberculosis* H37Rv reference sequence NC_000962.3. RPKM [145] normalized read counts were log2 transformed for further analysis. Differential gene expression between two experimental conditions (three biological replicates each) was statistically determined by Student's T-test (FDR corrected). The significance threshold was set to p(corr) = 0.01. Regarding the published OtsB2 study, RNAseq data have been deposited in the NCBI Gene Expression Omnibus (GEO Series accession number GSE70291).

RNAseq sequencing and data analysis was performed by Dr. R. Deenen, Biological Medical Research Centre, Heinrich-Heine University Düsseldorf, Germany.

6 Results

6.1 Trehalose-6-phosphate-mediated toxicity determines essentiality of OtsB2 in *Mycobacterium tuberculosis* *in vitro* and in mice

(This chapter has been published in modified form in *PLoS Pathog* 12(12): e1006043)

The OtsA-OtsB2 pathway is the dominant route for trehalose formation *in vitro* and *in vivo*. Remarkable, the growth defect of the Δ *otsA* mutant led to the assumption of *otsA* dispensability in *M. tuberculosis*, whereas the *otsB2* gene (Rv3372) is strictly essential in *M. tuberculosis*, because the gene could not be inactivated even in the presence of exogenous trehalose to chemically complement the biosynthetic defect [108]. Strikingly, the T6P phosphatase has been shown to contribute to virulence in the pathogenic yeasts *Candida albicans* [71, 72, 108], *Cryptococcus neoformans* [73] and *Cryptococcus gattii* [74], the filamentous fungi *Aspergillus fumigatus* [76] and *Fusarium graminearum* [75]. While gene deletion mutants exhibit some growth deficiencies, T6P phosphatase is not strictly required for viability in these organisms under normal *in vitro* culture conditions in contrast to *M. tuberculosis*.

However, this points towards a peculiar vulnerability underlying the essential role of OtsB2 in *M. tuberculosis*. Thus, in this study, we generated a conditional *otsB2* Mutant in *M. tuberculosis* allowing regulated gene silencing in order to study the basis of OtsB2 essentiality *in vitro* and to assess the viability of the mutant *in vivo* in a mouse infection model.

6.1.1 OtsB2 is essential for the *in vitro* growth of *M. tuberculosis*

In order to test the possible essentiality of the *otsB2* gene in *M. tuberculosis*, we attempted gene deletion of *otsB2* in the wild type (WT) and in an isogenic merodiploid strain containing a second copy of *otsB2* provided on an integrative single-copy plasmid, using specialized transduction. Despite repeated attempts, we were unable to obtain transductants with a deleted *otsB2* gene in the haploid WT, corroborating previous observations [108]. In contrast, the endogenous *otsB2* gene could be readily deleted in the merodiploid strain, confirming that a functional copy of *otsB2* is strictly required for growth of *M. tuberculosis* under these conditions (S1 Fig).

In order to establish the basis of its proven genetic essentiality, we attempted conditional gene silencing of OtsB2 allowing the phenotypic characterization of partially silenced mutants. Based on a previously reported synthetic promoter cassette, which is predicated on the *E. coli* Tn10-derived tet regulatory system and comprises a strong promoter from *M. smegmatis* harboring two tet operator (*tetO*) sites (*Pmyc1*) [146],

we generated a modified promoter harboring four *tetO* sites. We reasoned that the higher number of *tetO* sites would allow more binding of tet repressor protein (TetR) to the promoter thereby increasing silencing efficacy. This promoter cassette (*Pmyc1-4×tetO*) was further engineered to include a hygromycin resistance gene for positive selection and was site-specifically inserted immediately upstream of the start codon of *otsB2* in the *M. tuberculosis* chromosome via specialized transduction (S2 Fig). The resulting knock-in mutant *M. tuberculosis* *c-otsB2-4×tetO* was subsequently transformed with the *E. coli* Tn10 *tetR* gene provided on an episomal plasmid, yielding strain *M. tuberculosis* *c-otsB2-4×tetO* pMV261::tetR-G. In this conditional mutant, hereafter referred to as the *M. tuberculosis* *c-otsB2-tet-on* mutant, expression of the target gene is repressed in the absence of the inducer anhydrotetracycline (ATc). As expected, growth of the *c-otsB2-tet-on* mutant on solid medium (Fig 8A) and in liquid culture (Fig 8B) was strictly dependent on presence of ATc, with the growth rate in liquid culture being modulated by ATc in a concentration-dependent manner. In contrast, growth of a vector control strain (i.e. the *c-otsB2-4×tetO* knock-in mutant transformed with an empty vector) that expresses *otsB2* constitutively, was not influenced by ATc (Fig 8B).

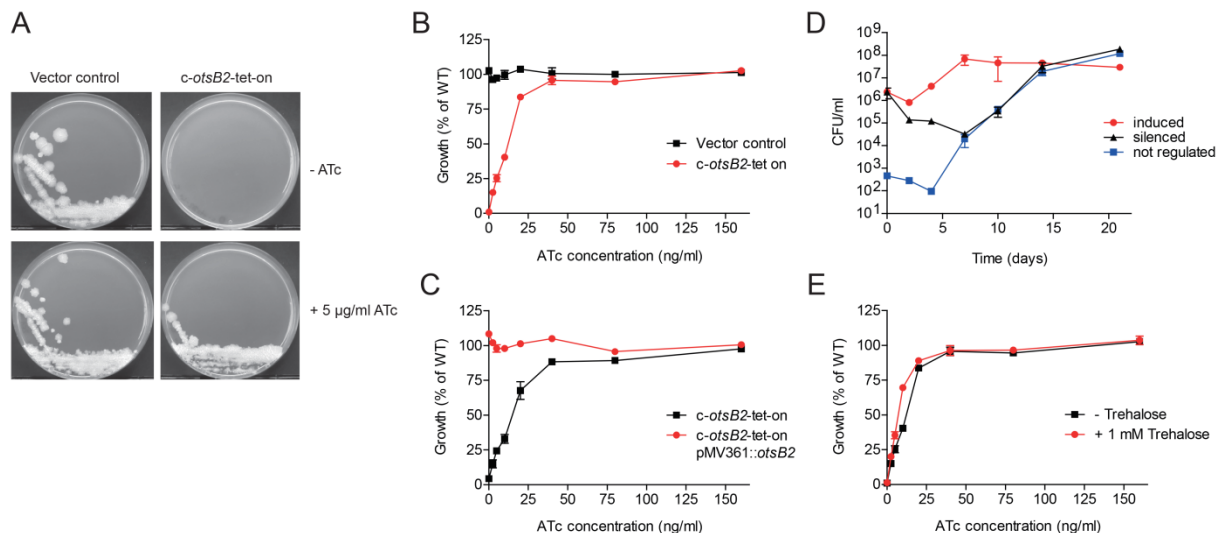


Fig 8. OtsB2 is essential for *in vitro* growth of *M. tuberculosis*.

(A) The *c-otsB2-tet-on* mutant strain and a non-regulated vector control strain were grown on Middlebrook 7H10 agar with or without 5 µg/ml ATc. Plates were incubated for 21 days. For the *c-otsB2-tet-on* mutant, only growth on plates containing ATc was observed. (B) The *c-otsB2-tet-on* mutant strain was grown in liquid medium containing increasing concentrations of ATc. Strict ATc-dependency demonstrates essentiality of *otsB2* for growth in liquid medium. (C) Genetic complementation with a constitutively expressed second copy of *otsB2* abrogates ATc-dependent growth of the *c-otsB2-tet-on* mutant, showing a lack of relevant polar effects or secondary mutations. (D) Silencing of *otsB2* has a bactericidal effect. Cells of the *c-otsB2-tet-on* mutant were grown in liquid culture containing either 200 ng/ml or 0 ng/ml ATc. Culture aliquots were taken at the indicated time points, serially diluted and plated on Middlebrook 7H10 agar containing 200 ng/ml ATc to determine viable bacterial cell counts. Aliquots were plated in parallel also on 7H10 agar containing no ATc to quantify the frequency of non-regulated suppressor mutants. (E) Supplementation with 1 mM trehalose cannot compensate for the growth defect during silencing of *otsB2* in liquid culture, indicating that lack of the pathway end product is not the reason for *otsB2* essentiality. Strains in B, C and E were grown in 96-well microtiter plates for 6 days, and growth was quantified using the resazurin microplate assay. Values in B, C, and E are means of triplicates \pm SEM, values in D are means of duplicates \pm SEM.

Next, as the integrated synthetic promoter cassette might have polar effects on neighboring genes, we complemented the *c-otsB2-tet-on* mutant with a second copy of the *otsB2* gene under control of the Hsp60

promoter provided on an integrative single-copy plasmid. In this complemented *M. tuberculosis* *c-otsB2-tet-on* mutant, which carries a constitutively expressed merodiploid *otsB2* allele, silencing of the endogenous *otsB2* allele in the absence of ATc had no effect on growth (Fig 8C). Together these data demonstrate that OtsB2 is strictly required for viability of *M. tuberculosis* and rule out polar effects or inadvertent secondary mutations that could influence the silencing phenotype. Growth kinetics of the *M. tuberculosis* *c-otsB2-tet-on* mutant in liquid cultures showed that silencing of *otsB2* was bactericidal and resulted in a moderate killing of ca. 1.5 logs within 7 days (Fig 8D). An apparent increase of viability of silenced cells after this time point was due to the outgrowth of suppressor mutants, which might have acquired spontaneous or stress-induced mutations compromising the function of the TetR protein or, more likely, the *tet* operator sites, leading to constitutive expression of the target gene and growth of the mutants independent from ATc. Furthermore, also loss-of-function mutations in the *otsA* gene might have given rise to mutants that can grow in absence of ATc as will be discussed below.

6.1.2 T6P-associated toxicity is the cause of OtsB2 essentiality

Although a Δ *otsA* mutant exhibited a growth defect *in vivo* probably due to trehalose bradytrophism [108], the *otsA* gene is in principle dispensable for *in vitro* growth of *M. tuberculosis*, indicating that the alternative TreX-TreY-TreZ pathway can produce sufficient amounts of trehalose to maintain viability under this condition. Therefore, we hypothesized that the essentiality of *otsB2* is not due to the limited formation of trehalose. To test this, we performed silencing experiments with the *M. tuberculosis* *c-otsB2-tet-on* mutant in the presence of 1 mM trehalose to chemically compensate for the possible biosynthetic defect. As expected, trehalose supplementation could not prevent growth inhibition upon *otsB2* silencing (Fig 8E), proving that lack of the pathway end product is not the basis of OtsB2 essentiality.

We have recently described the essential maltosyltransferase GlgE, which is the key enzyme in a novel alpha-glucan pathway in *M. tuberculosis* [147, 148]. Inactivation of GlgE causes intracellular accumulation of its phosphosugar substrate, maltose-1-phosphate (M1P), which is associated with direct or indirect toxicity leading to killing of bacterial cells *in vitro* and *in vivo* by eliciting pleiotropic stress responses [107, 149]. We speculated that a similar scenario might occur during *otsB2* silencing with hyper-accumulation of the OtsB2 substrate T6P, which might be associated with toxic effects. Therefore, cell extracts from fully induced and gradually silenced cells of the *M. tuberculosis* *c-otsB2-tet-on* mutant were prepared and analyzed by thin-layer chromatography. While no difference compared to WT cells was observed in the fully induced conditional mutant, gradual silencing of the *otsB2* gene at low ATc concentrations resulted in the accumulation of increasing amounts of a compound that co-migrated with an authentic T6P standard (Fig 9A). ¹H-NMR spectroscopic analyses of the same extracts confirmed the high abundance of T6P in the partially silenced conditional mutant, whereas this phosphosugar was not detectable in extracts of the fully induced conditional mutant or the WT (Fig 9B).

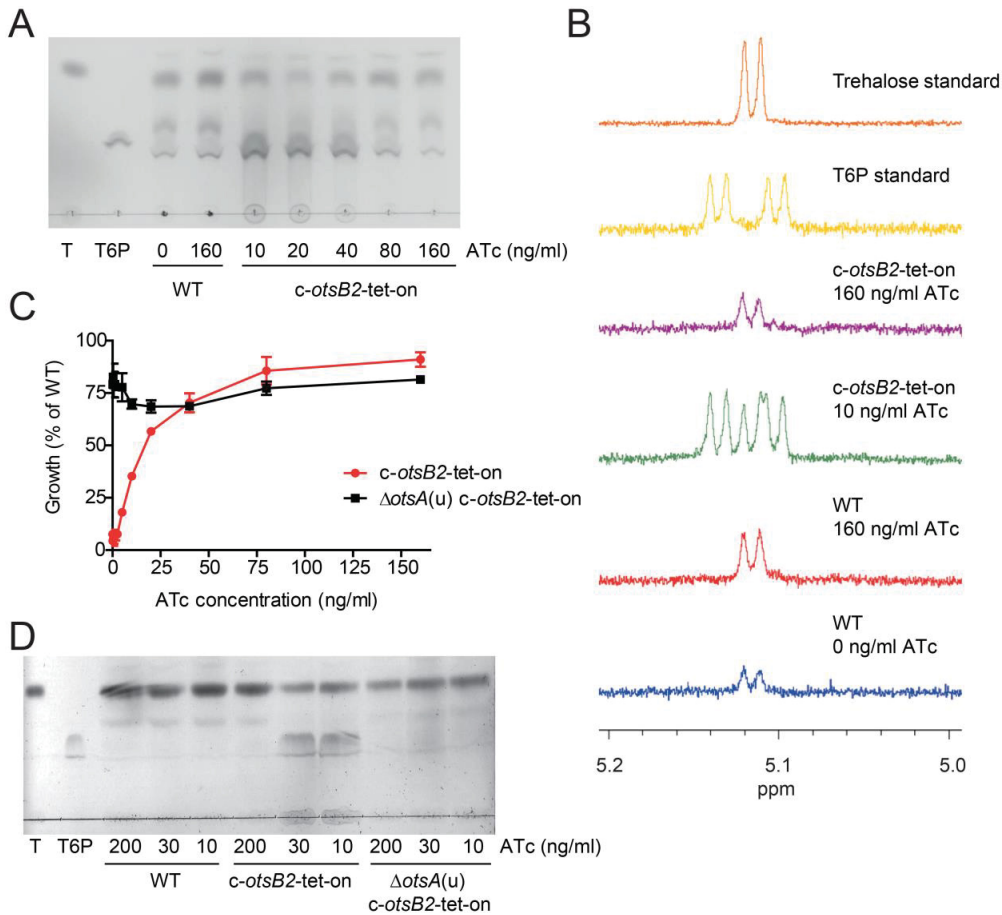


Fig 9. Silencing of *otsB2* leads to T6P accumulation in *M. tuberculosis*.

(A) Cells of *M. tuberculosis* wild-type and the *c-otsB2-tet-on* mutant were grown in Middlebrook 7H9 liquid medium at different ATc concentrations for 6 days. Hot water extracts obtained from 7.5×10^6 cells were analyzed by thin-layer chromatography, demonstrating the gradual accumulation of a substance co-migrating with an authentic T6P standard. Given that the volume of the cytosol of *M. tuberculosis* cells is $0.21 \mu\text{m}^3$ on average [150], the cytosolic T6P concentration in stressed cells can be estimated to be in the range from 5–10 mM. (B) ^1H -NMR spectroscopy confirms the presence of T6P in hot water extracts of partially silenced cells of the *c-otsB2-tet-on* mutant, whereas no T6P was detectable in extracts of fully induced cells of the *c-otsB2-tet-on* mutant or *M. tuberculosis* wild-type. (C) Silencing of *otsB2* in a $\Delta\text{otsA(u)}$ mutant does not result in a growth defect. Cells were grown in 96-well microtiter plates for 6 days, and growth was quantified using the resazurin microplate assay. Values are means of triplicates \pm SEM. (D) Silencing of *otsB2* in a $\Delta\text{otsA(u)}$ mutant does not result in T6P accumulation. Cells were grown in Middlebrook 7H9 liquid medium at different ATc concentrations for 6 days. Hot water extracts obtained from 7.5×10^6 cells were analyzed by thin-layer chromatography.

We hypothesized that similar to the reported toxic effects of M1P accumulation [106], intracellular T6P accumulation is toxic for *M. tuberculosis*. Consequently, the prevention of phosphosugar formation should avoid poisoning and abolish the essentiality of OtsB2. To block T6P synthesis, we first inactivated the T6P synthase gene *otsA* in *M. tuberculosis* and generated an unmarked gene deletion mutant ($\Delta\text{otsA(u)}$) (S3 Fig). We then attempted deletion of the *otsB2* gene in WT and in the $\Delta\text{otsA(u)}$ mutant. As observed before, we were unable to inactivate *otsB2* in the WT. In contrast, transductants with a deleted *otsB2* gene were readily obtained in the $\Delta\text{otsA(u)}$ genetic background (S1 Fig). We also generated a conditional *otsB2* mutant in the $\Delta\text{otsA(u)}$ background (S2 Fig). Silencing of *otsB2* in this *M. tuberculosis* $\Delta\text{otsA(u)}$ *c-otsB2-tet-on* mutant did not lead to growth impairment in liquid culture (Fig 9C) or to the accumulation of T6P as determined by thin-layer chromatography (Fig 9D). These results unambiguously show that the essentiality

of OtsB2 is dependent on the synthesis of T6P via OtsA and that the growth inhibitory consequence of *otsB2* inactivation relies on direct or indirect toxic effects associated with T6P accumulation. Exogenous T6P did not cause any growth inhibition of *M. tuberculosis* WT at concentrations up to 1 mM nor did it aggravate growth inhibition of the *c-otsB2*-tet-on mutant at low ATc concentrations (S4 Fig). However, this cannot be interpreted as lack of evidence for direct toxicity of T6P since this charged phosphosugar probably cannot penetrate the cells so that only endogenously formed T6P is toxic.

6.1.3 Insights into the T6P-induced stress response

Similar to what we have observed in *M. tuberculosis*, deletion of the T6P phosphatase gene results in T6P accumulation in various yeasts [70, 72, 73, 151] and filamentous fungi [75, 76]. In contrast to *M. tuberculosis*, however, these fungal mutants could tolerate this phosphosugar relatively well and remained viable, albeit with some growth deficiencies. Thus, *M. tuberculosis* exhibits unprecedented sensitivity toward T6P toxicity. In order to gain insights into the basis of toxicity, we analyzed the T6P-induced stress response by comparing the transcriptome profiles of fully induced and partially silenced cells of the *M. tuberculosis* *c-otsB2*-tet-on mutant employing RNAseq. In total, 877 genes were found to be significantly upregulated while only 37 genes were downregulated (≥ 2 -fold with $p < 0.01$) in T6P stressed cells. This unexpectedly biased global shift in gene expression levels suggests that differential RNA stability rather than transcriptional regulation might primarily drive the response. In fact, antitoxins (VapB7, VapB43), which neutralize cognate toxins exhibiting RNase activity (VapC7, VapC43), were among the strongest upregulated genes (36- and 160-fold induction, respectively, in T6P-stressed cells according to qRT-PCR analysis) (Fig 10A, Table 19), implying a reduction in RNase activity and an associated increase in RNA half-life in T6P-stressed cells.

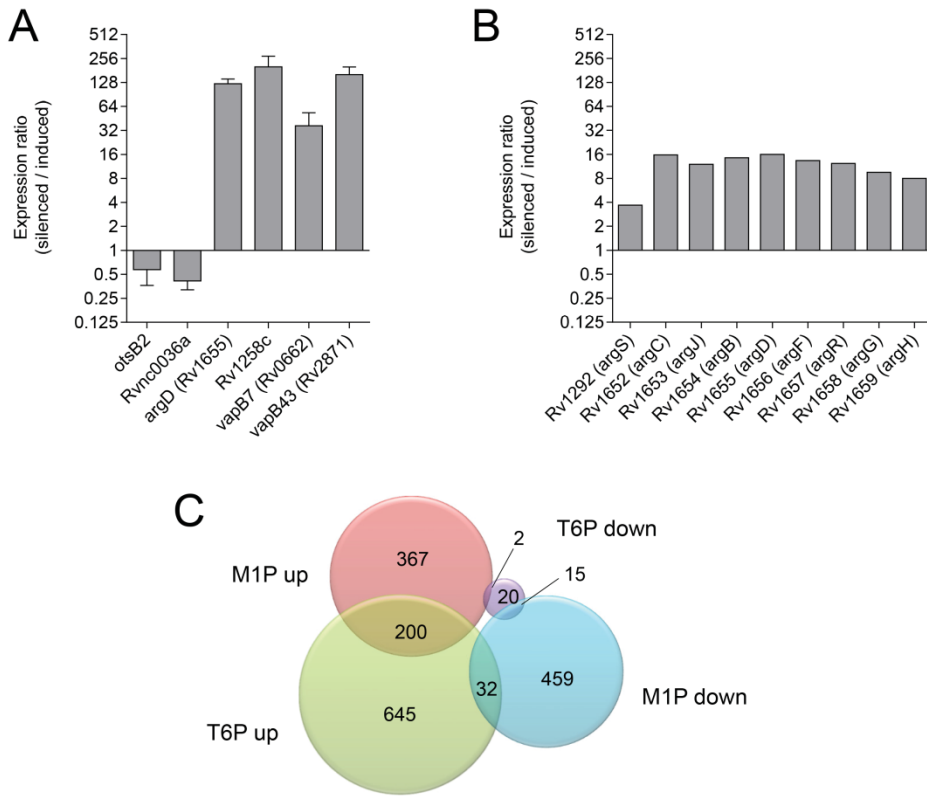


Fig 10. Genome-wide characterization of the T6P-elicited stress response profile.

(A) Quantitative real time PCR analyses of selected transcripts to corroborate RNAseq results. qRT-PCR data were normalized to 16S rRNA, and the expression ratios of partially silenced cells of the *M. tuberculosis* *c-otsB2*-tet-on mutant compared to fully induced cells are reported as means of triplicates \pm SEM. (B) Upregulation of arginine biosynthesis genes in T6P stressed cells of the partially silenced *c-otsB2*-tet-on mutant according to RNAseq data. (C) Diagram showing the overlap of the T6P stress response with the M1P stress response. Microarray data for M1P stress have been reported previously [106] and were obtained through NCBI Gene Expression Omnibus (GEO data set GSE18575). Only genes with a differential regulation of ≥ 2 are included.

Table 19. List of the ten most differentially up- and downregulated genes in T6P-stressed *M. tuberculosis* cells.

	Rv number	Gene	Fold change (silenced / induced)	Transformed p-value
Upregulated	Rv1258c	Rv1258c	27.12	0.00010
	Rv0662c	<i>vapB7</i>	23.29	0.00005
	Rv1257c	Rv1257c	19.22	0.00025
	Rv1655	<i>argD</i>	15.99	0.00018
	Rv2164c	Rv2164c	15.92	0.00041
	Rv1652	<i>argC</i>	15.72	0.00006
	Rv2165c	Rv2165c	15.54	0.00230
	Rv1654	<i>argB</i>	14.48	0.00017
	Rv1656	<i>argF</i>	13.38	0.00001
Downregulated	Rv1987	Rv1987	12.46	0.00009
	Rv2628	Rv2628	0.20	0.00066
	Rv2989	Rv2989	0.20	0.00004
	Rv2990c	Rv2990c	0.17	0.00162
	RVnc0035	MTS1082	0.16	0.00106
	Rv2988c	<i>leuC</i>	0.15	0.00009
	RVnc0036a	MTS2823	0.14	0.00021
	Rv2987c	<i>leuD</i>	0.14	0.00036
	Rv2056c	<i>rpsN2</i>	0.14	0.00030
	Rv0280	PPE3	0.09	0.00182
	RVnc0036	MTS1338	0.05	0.00008

doi:10.1371/journal.ppat.1006043.t001

Cells of the conditional *M. tuberculosis* *c-otsB2*-tet-on mutant were either induced in the presence of 200 ng/ml (100% growth relative to WT) or partially silenced in the presence of 30 ng/ml ATc (ca. 30% residual growth relative to WT).

The most upregulated gene Rv1258c (>200-fold induction in T6P-stressed cells according to qRT-PCR analysis) (Fig 10A, Table 19) encodes a putative efflux pump potentially involved in antibiotic resistance. However, T6P-stressed cells showed unaltered susceptibility to the first-line antibiotics rifampicin, ethambutol and isoniazid (S5 Fig), demonstrating that OtsB2 inactivation does not provoke general intrinsic drug resistance. Furthermore, genes involved in arginine biosynthesis were highly upregulated in response to T6P stress (Fig 10B, Table 19). A similar response has also been observed in M1P-stressed *M. tuberculosis* cells [106], suggesting that arginine might play a role in counteracting stress elicited by sugarphosphates. However, arginine supplementation (1 mM) didn't rescue growth of the *c-otsB2*-tet-on mutant at low ATc concentrations, providing no support for arginine having a direct protective effect during T6P stress (S6 Fig). Additionally, upregulation of several DNA damage-inducible genes including those belonging to the SOS regulon [152] were indicative of direct or indirect DNA damage caused by T6P stress (S7 Fig), again reminiscent of the M1P stress response [106]. Apart from these two common signatures, however, there was unexpectedly little overlap with the transcriptome profile elicited by M1P poisoning [106], indicating that these two phosphosugars induce remarkably different stress responses (Fig 10C). In addition to tRNAs, several non-coding RNAs were among the most abundant transcripts present in *M. tuberculosis* (S1 Table). One of these highly expressed non-coding RNAs, Rvnc0036a (= MTS2823), was one of the few genes significantly downregulated in response to T6P stress (Fig 11A, Table 19). While its expression appears to correlate with different stresses, its function is unknown [153]. However, the ultrahigh abundance in fully induced cells suggests an important physiological role under the tested culture

conditions, and its depletion in partially silenced cells might contribute to the inability to tolerate the toxic effects of T6P accumulation.

6.1.4 OtsB2 is essential for *M. tuberculosis* to establish an acute infection in mice

T6P is formed from intermediates of primary sugar metabolism (i.e. glucose-6-phosphate and ADP/UDP-glucose). However, *M. tuberculosis* primarily uses host lipids as sources of carbon and energy during infection given the limited carbohydrate availability [154]. It was therefore questionable whether sufficient amounts of T6P are produced by *M. tuberculosis* *in vivo* in a carbohydrate-poor environment to reach toxic intracellular concentrations. To address this question, silencing experiments in a mouse infection model were necessary.

With the genetic system described here, regulated gene expression relies on the presence of the episomal TetR expression plasmid. Loss of this plasmid would abrogate regulation and result in constitutive expression of the target gene. For stabilization of the episomal TetR expression plasmid in the absence of antibiotics *in vivo*, we employed auxotrophy complementation of the *M. tuberculosis* $\Delta panCD$ mutant, which requires pantothenic acid supplementation for *in vitro* growth. Importantly, this auxotrophic mutant is highly attenuated in mice, indicating that *M. tuberculosis* has virtually no access to pantothenic acid from the host during infection [155]. Thus, genetic complementation of the $\Delta panCD$ deletion from the episomal TetR expression vector should ensure plasmid stabilization during growth in a pantothenic acid-free environment even in the absence of antibiotic pressure. Toward this end, we first generated a *c-otsB2-4×tetO* knock-in mutant in a markerless *M. tuberculosis* $\Delta panCD$ mutant background via specialized transduction as described before (S2 Fig). Next, we constructed a plasmid in which the *panCD* operon from *M. tuberculosis* along with its native ribosome binding site was cloned downstream of the *tetR* gene under control of a single Hsp60 promoter, thereby transcriptionally coupling *panCD* and *tetR* expression. The resulting plasmid pMV261::*tetR*-G::*panCD* was subsequently transformed into the *M. tuberculosis* $\Delta panCD(u)$ *c-otsB2-4×tetO* knock-in mutant, yielding the *M. tuberculosis* $\Delta panCD(u)$ *c-otsB2-tet-on* strain. During culture in pantothenic acid-free media, this conditional mutant reproduced the relevant phenotypes of the *M. tuberculosis* *c-otsB2-tet-on* strain such as ATc-dependent growth (S8 Fig). Furthermore, the plasmid was stably maintained in this strain in the absence of antibiotic pressure even after extensive subculturing, suggesting that this conditional mutant was appropriate for testing in infection models.

To determine the role of OtsB2 for *M. tuberculosis* viability and virulence *in vivo*, mice were infected with the *M. tuberculosis* $\Delta panCD(u)$ *c-otsB2-tet-on* mutant via the aerosol route. Doxycycline provided in the food was used to induce *otsB2* expression. The *otsB2* gene was silenced by withdrawal of doxycycline either at day 0 or at day 28 post infection in order to assess the importance of OtsB2 for the acute or chronic infection phase, respectively (Fig. 11). While induction of *otsB2* led to full virulence of the conditional mutant

comparable to WT, silencing of *otsB2* following aerosol challenge resulted in an inability to establish an acute infection in mice and an inability of the bacterium to replicate *in vivo*. A bacteriostatic effect was observed in the lung with bacteria persisting at a very low organ burden after infection. Only a few bacteria disseminated to the spleen and were eventually eradicated from this organ. In contrast, when *otsB2* was silenced after day 28 when a chronic infection had already been established, no attenuation of the conditional mutant was detected in lungs and spleens. The efficiency of silencing during infection is difficult to be determined, and thus some residual *otsB2* expression in silenced cells cannot be ruled out. However, the presented data suggest that OtsB2 is much less important, if not fully dispensable, for the chronic infection phase in mice.

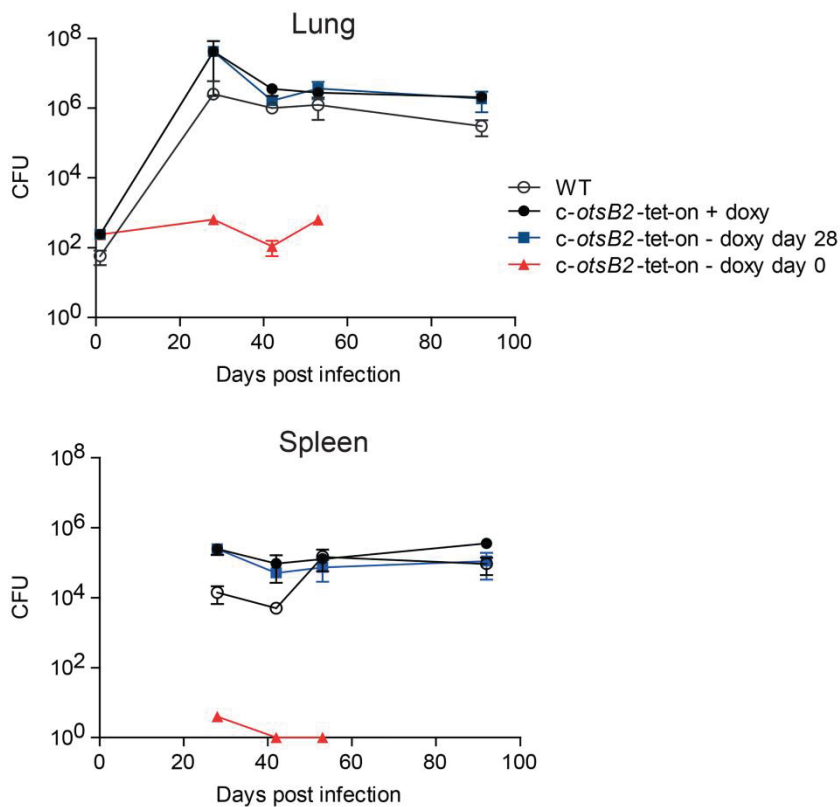


Fig 11. OtsB2 is required for *M. tuberculosis* to establish an acute infection in mice but dispensable for survival during the chronic phase.

Mice were infected with *M. tuberculosis* strains via the aerosol route. Mice received doxycycline via the mouse chow to induce *otsB2* in the conditional *M. tuberculosis* *c-otsB2-tet-on* mutant. Doxycycline treatment was stopped either 24 h or 28 d post-infection to silence *otsB2* during the acute or chronic infection phases, respectively. Bacterial loads in lungs and spleens of C57BL/6 mice infected with *M. tuberculosis* H37Rv wild-type and the *c-otsB2-tet-on* mutant strain were determined by plating serial dilutions of organ homogenates on 7H10 agar containing 200 ng/ml ATc to determine viable bacterial cell counts. Aliquots were plated in parallel also on 7H10 agar containing no ATc to quantify the frequency of non-regulated suppressor mutants of the conditional *c-otsB2-tet-on* mutant, which was <1% at all time points and conditions. Data are means \pm SD from four mice per group and time point (except *c-otsB2-tet-on*—doxy day 0, $n = 3$; at days 42 and 53). Data represent a single experiment. Silencing during the acute infection was repeated once to reproduce the bacteriostatic effect of OtsB2 inactivation (see S9 Fig).

6.1.5 Genome wide screen for synthetic lethal interactions

We have shown that the OtsA-OtsB2 pathway for trehalose biosynthesis appears to be much less active, if at all, during the chronic infection phase and that loss-of-function mutations in OtsA will mediate resistance against potential inhibitors of OtsB2. These observations reveal limitations to the drug target potential of OtsB2. We therefore performed a genome-wide screen to unravel synthetic lethal interactions with OtsA for the identification of additional targets, which would prevent resistance and result in synergistic killing when inhibited in combination with an OtsB2 inhibitor. For this, a saturated transposon mutant pool containing ~100,000 independent mutants was established in the *M. tuberculosis* Δ otsA(u) mutant in the presence of 500 μ M trehalose. After subcultivation in the presence or absence of trehalose, the relative composition of the complex mutant libraries was analyzed using transposon insertion sequencing (TnSeq) [155].

By comparing the mutant libraries grown in the absence or presence of trehalose using a Hidden Markov Model method to identify loci with significantly different transposon insertion counts (see 3.1.4), six genes were found to be differentially essential in the absence of trehalose (i.e. significantly fewer transposon insertions were detected in these genes in the Δ otsA(u) mutant background in absence of trehalose versus presence of trehalose) (Table 20). These included the genes *treX*, *treY* and *treZ*, as expected, since they mediate *de novo* synthesis of trehalose from α -glucans with their combined inactivation with *otsA* resulting in trehalose auxotrophy [107]. ADP-glucose pyrophosphorylase GlgC, which is involved in α -glucan production [56], was also found to be essential only in the absence of trehalose suggesting that inactivation of *glgC* in the Δ otsA(u) mutant results in glucan deficiency and depletes the TreX-TreY-TreZ pathway of its substrate. The nature of these genetic interactions implies that the two other identified genes, Rv0907 and Rv3160c of unknown function, might also play a direct or indirect role in α -glucan biosynthesis. Interestingly, one gene (Rv1845c) harbored significantly more transposon insertions in absence of trehalose. Thus, this gene, which is essential in WT [156], appears to become less essential in context of *otsA* deletion but only at low trehalose concentration. Rv1845c might be a sensor-transducer protein involved in sensing beta-lactams, but its precise function is unknown [157]. Thus, there is currently no obvious explanation for the differential gene essentiality and the nature of the interaction with OtsA.

Table 20. Genes differentially essential in the *M. tuberculosis* Δ otsA mutant in absence of trehalose supplementation.

Start nt	End nt	N of TA sites	Reads Δ otsA - trehalose	Reads Δ otsA + trehalose	p-value	Genes (% of ORF covered)	Segments type
1010144	1010572	10	0	140	0.00085	Rv0907 (25)	1
1010697	1011696	24	1	92	0.07207	Rv0907 (60)	1
1355864	1356654	28	69	591	0.00160	Rv1213-glgC (90)	2
1765353	1768480	55	1	1890	0.00000	Rv1561 (11) Rv1562c-treZ (100) Rv1563c-treY (47)	1
1769196	1769305	4	0	51	0.03122	Rv1563c-treY (11)	1
1770109	1771117	25	5	200	0.00879	Rv1564c-treX (51)	1
1771157	1771634	13	19	522	0.00140	Rv1564c-treX (22)	2
2095257	2096106	14	115	0	0.00772	Rv1845c (93)	1
3529246	3529897	10	0	50	0.03894	Rv3160c (100)	1

doi:10.1371/journal.ppat.1006043.t002

A saturated transposon mutant pool established in the *M. tuberculosis* Δ otsA mutant background was cultured either in the absence or presence of trehalose, subjected to transposon insertion sequencing (Tn-seq) and analyzed using a non-gene centric method. Genome areas harboring significantly less transposon insertions in absence of trehalose are shown. One genome area comprising most of gene Rv1845c harbored significantly more transposon insertions in absence of trehalose (i.e. appearing essential only in presence of trehalose) and is highlighted in grey.

In comparison to a published set of genes essential for *in vitro* growth of *M. tuberculosis* [156], 131 genes were found to be essential in the context of *otsA* deletion compared to WT irrespective of trehalose availability. Some of these may be due to use of different media (7H9 in this study versus minimal media in [156]) and might simply represent physiological differences rather than true differential genetic susceptibility based on lack of *otsA*. However, at least the observed effects on maltose-1-phosphate synthase *glgA* and components of a trehalose ABC transporter (*lpqY*, *sugA*, *sugC*) appear to be specific (S2 Table). We have very recently described the synthetic lethal interaction between *otsA* and *glgA* in *M. tuberculosis*, likely caused by toxic accumulation of the common precursor ADP-glucose. Furthermore, trehalose recycling via the ABC transporter LpqY-SugABC becomes essential when the OtsA-OtsB2 pathway is blocked, likely by further depleting intracellular trehalose levels via secretion of trehalose during cell wall assembly.

6.2 Characterization of the putative essential glycosyltransferase Rv0225 in a cell wall associated gene cluster in *Mycobacterium* species

MGLPs are suggested to regulate the fatty acid synthase I (FAS I) and mycolic acid metabolism in mycobacteria, although their exact function and biosynthesis remain elusive. As already highlighted before, a significant contribution in understanding the elongation of MGLPs was achieved by identification of the key glycosyltransferase Rv3032. However, despite to the fact that the key glycosyltransferase Rv3032 fulfills a major role in MGLP elongation (see 3.7.4), studies report the dispensability of Rv3032 for α -glucan biosynthesis [130] as well for mycobacterial growth [106]. Furthermore, absence of Rv3032 strongly

reduces, but does not completely abolish, MGLP formation in *M. tuberculosis* [127]. This indicates the presence of compensatory glycosyltransferases for MGLP synthesis in *M. tuberculosis*.

Hence, in a second project, we studied a conserved mycobacterial gene cluster (*Rv0224c-Rv0228*), which might also be involved in MGLP synthesis. According to public accessible TB databases, these genes encode a hypothetical methyltransferase (*Rv0224c*), hypothetical membrane proteins (*Rv0226c* and *Rv0227c*) and a hypothetical acyltransferase (*Rv0228*), potentially modifying MGLPs. All genes are suggested to be essential, indicated by a whole mycobacterial genome Himar-1 transposon library study [156].

Initially our experiments centered on *Rv0225*. Interestingly, *Rv0225* is a protein of unknown function and seems to be a completely uncharacterized glycosyltransferase. As described, MGLPs are predominantly composed of α -1,4-linked glucose units. We hypothesized that two glycosyltransferases must be involved its synthesis, since the absence of *Rv3032* leads to a strong decrease, albeit not a complete loss of the polysaccharide. The amino acid sequence of *Rv0225* shows some similarity with other α -glucan glycosyltransferases. Hence, we hypothesized that it plays a role in elongation of the oligomerization of alpha-1,4 chain of MGLPs .

The essentiality of the *Rv0225* locus in the *M. tuberculosis* strain was mainly investigated in the *M. tuberculosis* Δ *panCD* genetic background. This provides a mutant, which might be used for *in vivo* studies enabling plasmid stabilization via auxotrophic complementation (Fig S12, see also 5.5.9).

In addition to the conditional *Rv0225* *M. tuberculosis* mutant, the orthologues were also investigated in two further *Mycobacterium* species: the fast-growing species *M. smegmatis* strain mc²155 and the slow growing species *M. bovis* BCG-Pasteur. In order to generate the knock-in mutants of all strains, we inserted the promoter cassette site-specifically immediately upstream of the start codon of the respective *Rv0225* orthologous gene into the *M. smegmatis* (*MSMEG_0311*), *M. bovis* (*Mb0230*) and *M. tuberculosis* Δ *panCD* (*Rv0225*) chromosome via specialized transduction (Fig S12). The knock-in mutants *M. tuberculosis* c-*Rv0225-4xtetO*, *M. smegmatis* c-*MSMEG_0311-4xtetO* and *M. bovis* c-*Mb0230-4xtetO* were subsequently transformed with episomal plasmids harboring either the *E. coli* Tn10 *tetR* or the mutated *revtetR* gene and containing different ribosome binding sites. Optimal gene silencing efficiencies were achieved for the following conditional mutants: *M. tuberculosis* Δ *panCD* c-*Rv0225-4xtetO* pMV261::*tetR*-D (in the following referred to as *M. tuberculosis* c-*Rv0225-tet-on*), *M. smegmatis* c-*MSMEG0311-4xtetO* pMV261::*tetR*-D (in the following referred to as *M. smegmatis* c-*Rv0225-tet-on*) and the *M. bovis* c-*Mb0230-4xtetO* pMV261::*revtetR*-F (in the following referred to as *M. bovis* c-*Rv0225-tet-off*). In these conditional mutants, the expression of the target gene is repressed either in the absence of the inducer ATc (tet-on) or in the presence of ATc (tet-off). ATc dependent growth of respective mutants on solid medium and in liquid culture demonstrated essentiality of *Rv0225* and its homologues in all three strains.

Rv0225 gene expression was ATc dose dependent in the fast-growing *M. smegmatis* *c-Rv0225*-tet-on mutant on solid and liquid medium (Fig 12). As expected, growth of control strains harboring an extrachromosomal copy of the *Rv0225* gene from *M. tuberculosis* constitutively expressed from the HSP60 promoter on an integrative plasmid was constant and did not dependent on the ATc concentration. Hence,

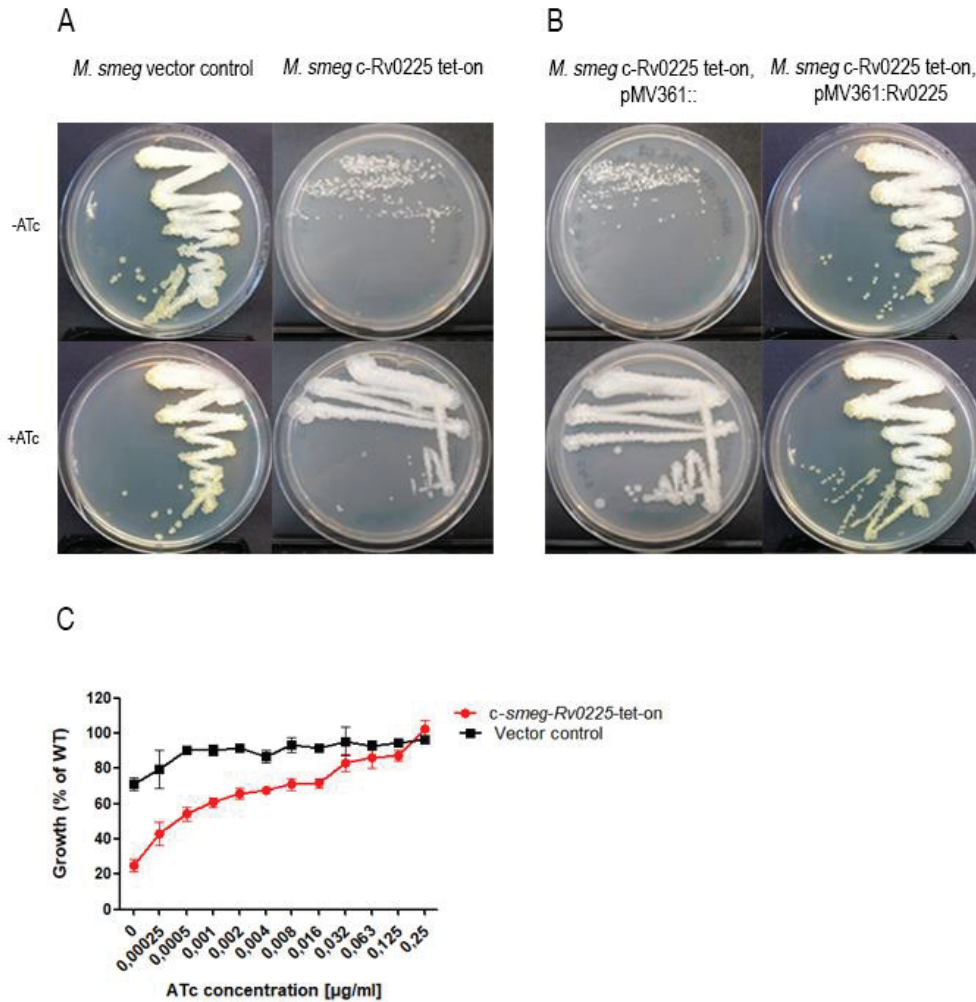


Fig12. The *Rv0225* homologue *MSMEG_0311* is essential for *in vitro* growth of *M. smegmatis*.

(A) The *M. smegmatis* *c-Rv0225*-tet-on strain and a non-regulated vector control strain were grown on Middlebrook 7H10 agar with or without 0.5 $\mu\text{g/ml}$ ATc. Plates were incubated for 3 days. For the *c-Rv0225*-tet-on mutant, only growth on plates containing ATc was observed. (B) (C) Genetic complementation with a constitutively expressed second copy of *Rv0225* abrogates ATc-dependent growth of the *M. smegmatis*-*Rv0225*-tet-on mutant, showing a lack of relevant polar effects or secondary mutations. (C) The *M. smegmatis*-*Rv0225*-tet-on strain was grown in liquid medium containing increasing concentrations of ATc. Strict ATc-dependency demonstrates essentiality of *Rv0225* for growth in liquid medium. Values are means of triplicates \pm SEM.

the observed silencing effect of the conditional *Rv0225* mutant was not influenced by polar effects or inadvertent secondary mutations potentially resulted from genetic manipulations. These findings were confirmed in the respective *M. bovis* *c-Rv0225*-tet-off mutant (Fig 13) and more importantly in the virulent *M. tuberculosis* strain (Fig 14). The bacterial growth on agar plates was significantly reduced within 3 weeks of silencing (Fig 14A). The silencing effect was also confirmed in a 96-well culture format (Fig 14B). Killing

kinetics of the *M. tuberculosis* c-Rv0225-tet-on mutant in liquid shaking cultures showed that silencing of Rv0225 was bactericidal and resulted in a moderate killing of ca. 1.0 log within 7 days (Fig 14C). The outgrowth of suppressor mutants after this time point might be caused by spontaneous mutations as discussed above (6.1.1).

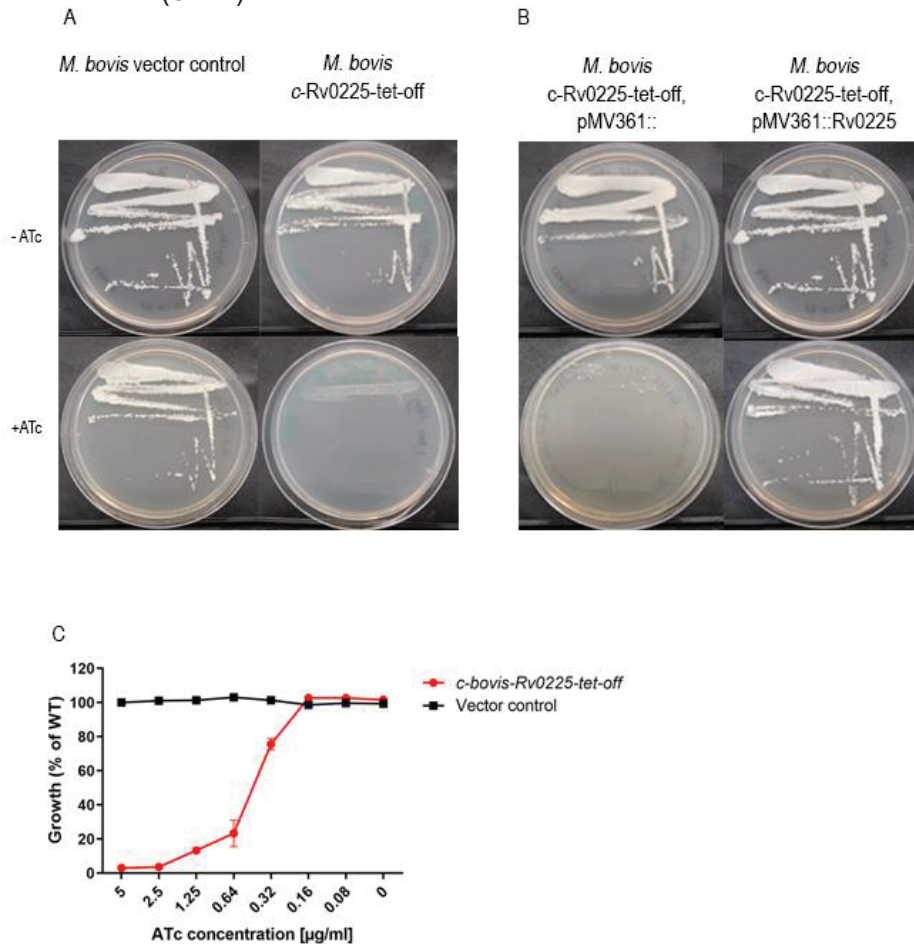


Fig 13. The Rv0225 homologue Mb0230 is essential for *in vitro* growth of *M. bovis*.

(A) The *M. bovis* c-Rv0225-tet-off strain and a non-regulated vector control strain were grown on Middlebrook 7H10 agar with or without 0.5 $\mu\text{g/ml}$ ATc. Plates were incubated for 21 days. *M. bovis* c-Rv0225-tet-off mutant, only growth on plates without ATc was observed. (B) Genetic complementation with a constitutively expressed second copy of Rv0225 abrogates ATc-dependent growth of the *M. bovis* c-Rv0225-tet-off mutant, showing a lack of relevant polar effects or secondary mutations. (C) The *M. bovis* c-Rv0225-tet-off strain was grown in liquid medium containing increasing concentrations of ATc. Strict ATc-dependency demonstrates essentiality of Rv0225 for growth in liquid medium. Values are means of triplicates \pm SEM.

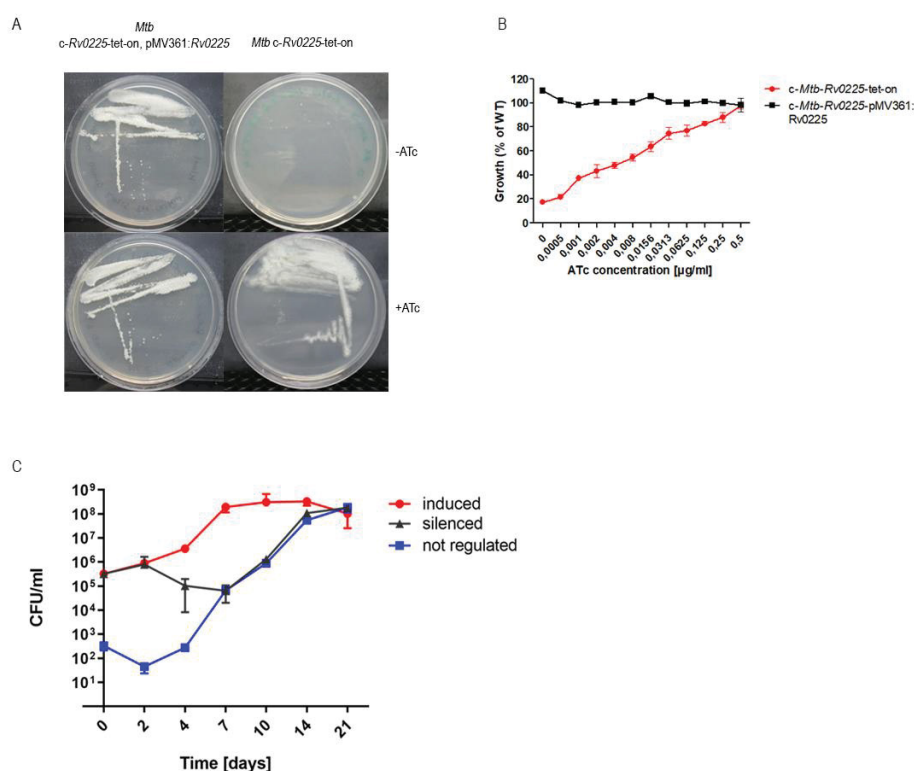


Fig 14. *Rv0225* is essential for *in vitro* growth of *M. tuberculosis*.

(A) The *M. tuberculosis*-*Rv0225*-tet-on mutant strain and a non-regulated complemented control strain were grown on Middlebrook 7H10 agar with or without 0.5 $\mu\text{g/ml}$ ATc. Plates were incubated for 21 days. For the *M. tuberculosis* c-*Rv0225*-tet-on mutant, only growth on plates containing ATc was observed. Genetic complementation with a constitutively expressed second copy of *Rv0225* abrogates ATc-dependent growth of the c-*Rv0225*-tet-on mutant, showing a lack of relevant polar effects or secondary mutations. (B) The c-*Rv0225*-tet-on mutant strain was grown in liquid medium containing increasing concentrations of ATc. Strict ATc-dependency demonstrates essentiality of *Rv0225* for growth in liquid medium. (C) Silencing of *Rv0225* has a bactericidal effect. Cells of the c-*Rv0225*-tet-on mutant were grown in liquid culture containing either 500 ng/ml or 0 ng/ml ATc. Culture aliquots were taken at the indicated time points, serially diluted and plated on Middlebrook 7H10 agar containing 500 ng/ml ATc to determine viable bacterial cell counts. Aliquots were plated in parallel also on 7H10 agar containing no ATc to quantify the frequency of non-regulated suppressor mutants. Values in B are means of triplicates \pm SEM, values in C are means of duplicates \pm SEM.

6.2.1 Sublethal *Rv0225* gene-silencing in conditional *Mycobacterium* species leads to an altered colony morphology and α -mycolic acid composition

The partially silenced conditional *M. smegmatis* (Fig 15) and BCG-Pasteur (S13 Fig.), but not the *M. tuberculosis* *Rv0225* mutant exhibited a different colony morphology in comparison to the fully induced mutant, indicative of an altered cell wall structure. The observed phenotype corroborates the hypothesis that the analyzed *Rv0225* gene plays a significant role in formation of the mycobacterial cell wall, possibly indirectly by participating in polymethylated polysaccharides (PMPS) biosynthesis, which in turn might regulate mycolic acid production. This effect on colony morphology was also observed in the *M. bovis* *Rv0226c*-tet-on mutant (S16 Fig.). This supports our hypothesis that at least the genes *Rv0225* and *Rv0226c* of the conserved gene cluster *Rv0224c*–*Rv0228* are part of the same pathway.



Fig 15. ATc dosis dependent partial gene silencing of the *Rv0225* homologous locus *MSMEG_0311* in *M. smegmatis* leads to differences in cell morphology.

In presence of ATc, the Tet-ON conditional mutant grows normally like wild-type, whereas under sublethal ATc conditions bacterial cell morphology changes.

6.2.2 Thin layer chromatography- and mass spectroscopy analysis on mycobacterial lipids

For investigating the morphological alterations observed in the conditional *Rv0225* *M. bovis* and the *M. smegmatis* mutants, cooperation partners at the University of Birmingham analyzed cellular lipid extracts of the conditional *M. bovis* c-*Rv0225-tet-off* mutant strain by one- and two-dimensional thin-layer chromatography (1D- and 2D-TLC) analysis. However, results led to no detectable alterations of the apolar and polar cell-wall lipid composition in the *M. bovis* mutant. In addition, no alterations in the mycolic acid-, LAMs and LMs composition were observed (S20 Fig). Independently from our cooperation partners, we also established a protocol for mycolic acid isolation in our lab and analyzed α -, keto and methoxy mycolic acids by 2D-TLC analysis and confirmed no detectable alterations between partial silenced and fully induced mutants (S19 Fig).

To prove this finding, a cooperation partner at the Research Center Borstel (Dr. Dominik Schwudke) investigated the mycolic acid composition with a more sensitive method in the genetic background of *M.*

tuberculosis. For this, solvent extracts of cells of the partially silenced *M. tuberculosis* *c-Rv0225-tet-on* mutant were analyzed by high-resolution electron spray ionisation-mass spectrometry (ESI-MS). Strikingly, this time prominent α -mycolic acids were slightly but significantly reduced under these suboptimal gene expression conditions (Fig 16), giving a further hint for a cell wall associated function of the putative glycosyltransferase Rv0225.

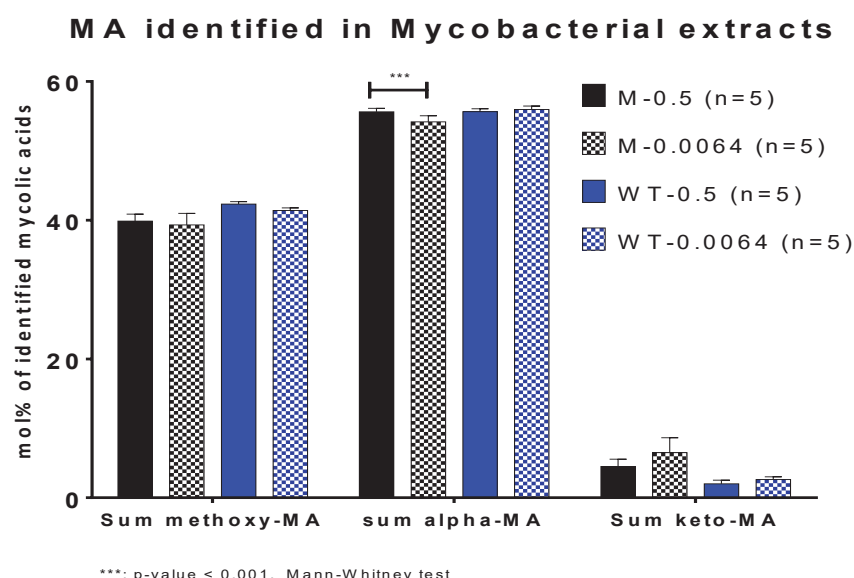


Fig 16. Mycolic acid analysis of *M. tuberculosis* *c-Rv0225-tet-on* via mass spectroscopy ESI-MS (electron spray ionisation-mass spectrometry).

For initial preparation, the partially silenced *M. tuberculosis* *c-Rv0225-tet-on* and the fully induced mutant were incubated in shaking cultures. Cultures were washed in PBS three times. After OD measurement, 5×10^8 cells were diluted in a total PBS volume of 1 ml. Cells were fixed by addition of 1 ml PFA and sent for analysis. Values show 5 replicates under each condition: mutant cultured with ATc 0.5 $\mu\text{g/ml}$ (M 0.5); mutant cultured with ATc 0.064 $\mu\text{g/ml}$ (M 0.064); controls *M. tuberculosis* wild-type without ATc (WT-0) and with 0.5 $\mu\text{g/ml}$ ATc (WT 0.5).

6.2.3 Genome-wide characterization of the *Rv0225*-elicited stress response profile.

In order to analyze the molecular response of suboptimal *Rv0225* gene expression, we compared the transcriptome profile of partially silenced cells to fully induced cells of the *M. tuberculosis* c-*Rv0225*-tet-on mutant (Fig 17). RNA-sequencing data analysis showed 629 significant differential regulated genes, comprising 376 up-regulated and 253 down-regulated genes (Fig 17A). 102 significantly regulated genes were associated to cell wall and cell processes (65 up; 37 down, Fig 17B), including the genes *Rv0225* (11-fold down) and *Rv0226c* (3-fold down). Since we analyzed RNA expression levels of *M. tuberculosis* c-*Rv0225*-tet-on partially silenced cells, down-regulation of *Rv0225* was expected and in agreement with our genetic model. Interestingly, *Rv0226c* was also downregulated, which might suggest a functional correlation to *Rv0225* in a commonly regulated gene cluster. In contrast, further neighboring genes (*Rv0224c*, *Rv0227c*, and *Rv0228*) were not significantly differentially expressed (Fig 17C).

Strikingly, the transcriptional response of partially silenced *Rv0225* cells included an up-regulation of the *iniBAC* gene cluster (isoniazid-induced genes *iniB*, *iniA* und *iniC*, Fig 17D), which is known to be strongly induced in *M. tuberculosis* cells after antibiotic treatment with the first-line antibiotic isoniazid [158]. Since isoniazid targets the mycobacterial cell wall assembly, this points towards a cell wall associated function of the putative glycosyltransferase *Rv0225*.

Typical transcriptional stress responses such as the upregulation of the translational apparatus and DNA damage response were not significantly differential expressed. Surprisingly, genes involved in the electron transport chain/ATP synthase and the *dosR* regulon were globally downregulated for unknown reason (S23 Fig). Furthermore, the triacylglycerol synthase gene (*tgs1*) was down regulated (27-fold down). *M. tuberculosis* primarily uses host lipids, including TAGs, as sources of carbon and energy during infection with only limited carbohydrate availability. Tgs1 accounts for most of the triacylglycerol (TAG) synthetic activity *in vitro*. The most significant up-regulated gene *whiB6* (120-fold up) has been described as a strong stress regulatory protein with regard to cell wall-active agents (e.g. isoniazid, ethambutol, cycloserine) and oxidative stress responses [159].

By selection of a few genes, we confirmed the transcriptome profile by qRT-PCR analysis (Fig 18B). Differential gene expression of the cytochrome bd oxidase subunit *Rv1622c* (*cydB*), *nuoL* and the ATP synthase epsilon chain *Rv1311* (*atpC*), all involved in the respiratory chain, were confirmed by qRT-PCR analysis. The gene *iniB* has been chosen as a representative gene for the *iniBAC* operon. Also, the strongest upregulated gene in the partially silenced *M. tuberculosis* mutant, *whiB6* (fold change: 120), has been validated by qRT-PCR. Also, non-significantly regulated genes of the *Rv0225* gene cluster (*Rv0224c*, *Rv0227c*, *Rv0228*) were confirmed (Fig 18B).

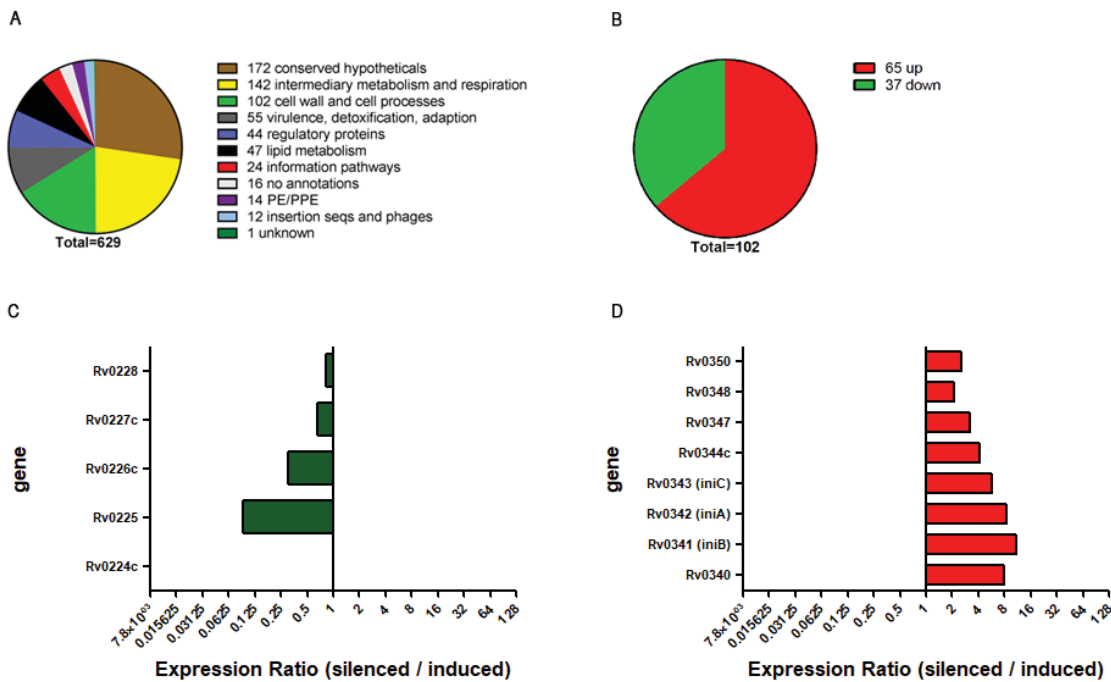


Fig 17. Insights into the *Rv0225*-induced stress response in *M. tuberculosis* using RNAseq.

Three RNA-samples of fully induced and partially silenced cells were reverse transcribed in cDNA, after depletion of ribosomal RNA. Transcripts in cDNA-libraries were quantified and tested for significant gene regulation ($p < 0.01$). Significantly regulated genes (≥ 2 -fold) in partially silenced cells were analyzed by gene annotations and pathway mappings of a *M. tuberculosis* H37Rv database (TubercuList). RNA-quality and concentration have been tested by an Agilent 2100 Bioanalyzer and Qubit-Quantification. (A) Pathway analysis of significant regulated genes (≥ 2 -fold with $p < 0.01$) in *Rv0225* partially silenced (10 ng/ml ATc) *M. tuberculosis* cells in comparison to fully induced (500 ng/ml ATc) ones. (B) Among 102 significant regulated genes involved in cell wall and cell processes, 65 were up-regulated and 37 down-regulated. (C) Two genes of the conserved mycobacterial gene cluster (Rv0224c - Rv0228), which might be involved in MGLP synthesis, were significantly down-regulated. As expected, the essential putative glycosyltransferase gene *Rv0225* (10.9-fold down) and further the hypothetically transmembrane protein Rv0226 (3.3-fold down). (D) Significant induction of the *iniBAC* operon, which is known as a specific response to cell wall inhibition [160].

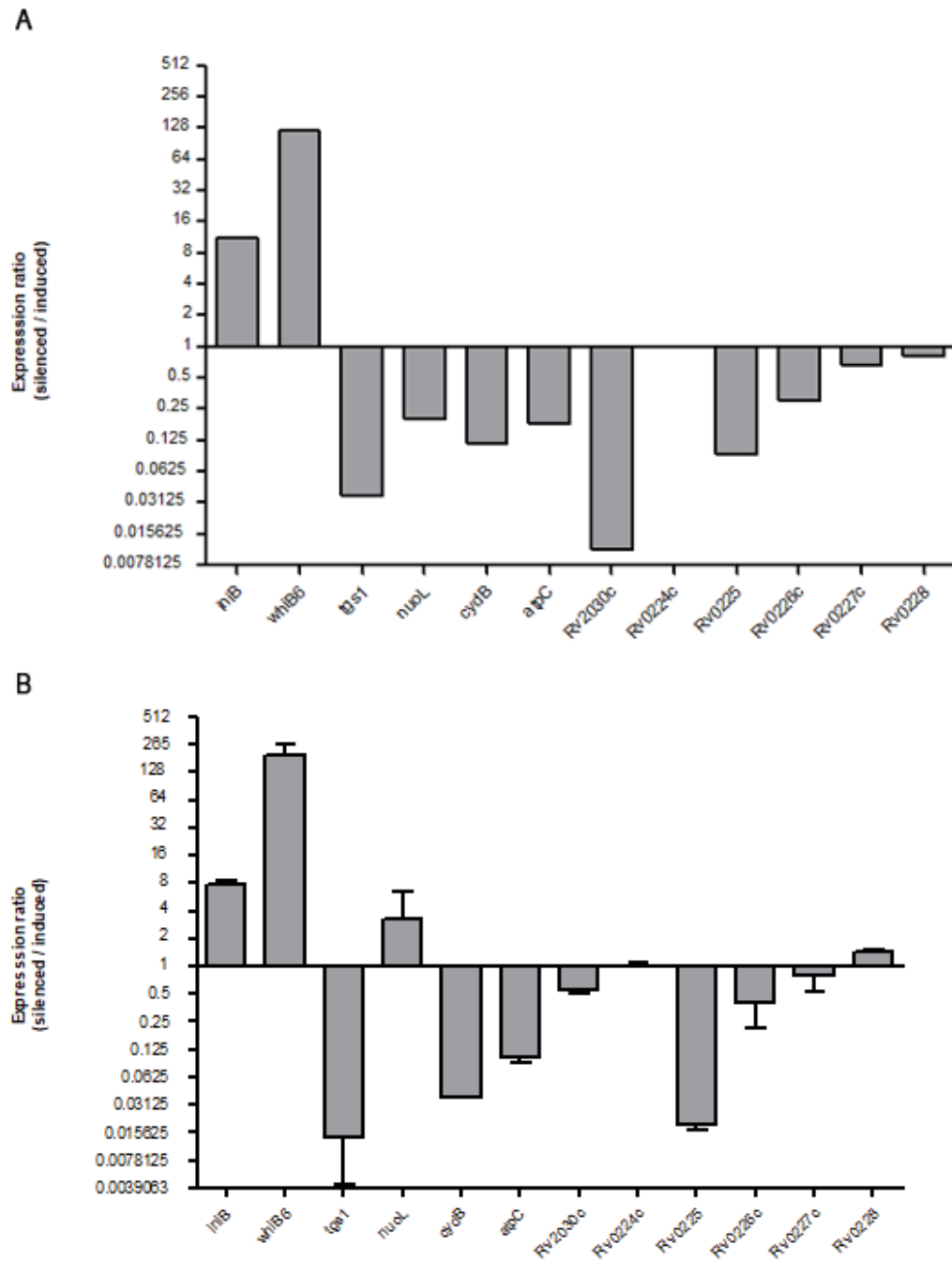


Fig 18. Confirmation of RNAseq via qRT-PCR.

(A) Selection of significantly regulated genes in stressed cells of the partially silenced *c-Rv0225-tet-on* mutant according to RNAseq data. (B) Quantitative real time PCR analyses of selected transcripts to corroborate RNAseq results. qRT-PCR data were normalized to 16S rRNA, and the expression ratios of partially silenced cells of the *M. tuberculosis c-Rv0225-tet-on* mutant compared to fully induced cells are reported as means of triplicates \pm SEM.

7 Discussion

7.1 Trehalose-6-phosphate-mediated toxicity determines essentiality of OtsB2 in *Mycobacterium tuberculosis* in vitro and in mice

(This chapter has been published in modified form in *PLoS Pathog* 12(12): e1006043)

Many potential candidates for target-based approaches in antibacterial drug discovery are selected only based on apparent genetic essentiality *in vitro*, while there is often a lack of knowledge of their relevance *in vivo* during different infection phases. The present study exemplifies that not only is *in vitro* gene essentiality a poor predictor of drug target suitability *in vivo* but also that the vulnerability of a target can change dramatically during the course of an infection. Thus, knowledge of the consequences of inactivation of potential targets during all relevant infection phases is imperative to make realistic predictions of target suitability and efficacy. Accordingly, we assessed OtsB2 as a drug target candidate in *M. tuberculosis* employing conditional gene silencing *in vitro* and in mice. Despite technical advances in recent years, the study of strictly essential genes in *M. tuberculosis* using conditional mutants is still a challenging endeavor, particularly in the context of animal infection models. So far, only 13 conditional *M. tuberculosis* mutants have been studied in mice (reviewed in [161]), but just seven of them were made for genes being strictly essential for *in vitro* growth. Six of these essential genes have been shown to be required during both the acute and the chronic infection phase in mice (*nadE* [154], *card* [162], *pptT* [163], *pimA* [32], *bioA* [164], *glum* [165], while *ideR* is also essential for acute infection, but has not specifically been silenced during the chronic phase [166]. As revealed in this study, *otsB2* is the first example of an essential *M. tuberculosis* gene shown to be specifically required only during the acute infection phase in mice.

Differential OtsB2 essentiality during two infection stages indicates that trehalose metabolism of *M. tuberculosis* is substantially remodeled *in vivo*. The OtsA-OtsB2 pathway for trehalose biosynthesis dominates in culture and during the acute infection phase. In contrast, this pathway is surprisingly dispensable to maintain viability of *M. tuberculosis* during the chronic infection phase. This implies that flux through the OtsA-OtsB2 pathway is significantly reduced at later infection stages. This could be achieved by downregulating trehalose production altogether. However, there is evidence that the chronic infection phase in mice does not represent a static equilibrium of slow or nonreplicating bacilli. Rather, *M. tuberculosis* seems to continue replicating at least at basic level, while counteracting immune killing results in no net increase in organ burden of viable bacteria [167]. Since trehalose is essential for cell wall assembly during mycobacterial replication, trehalose biosynthesis probably continues at some rate also during chronic infection. Thus, it is more likely that the alternative TreX-TreY-TreZ pathway becomes activated during chronic infection to release trehalose from intracellular α -glucan storage molecules.

Silencing of *otsB2* in culture has a bactericidal effect whereas it is bacteriostatic *in vivo* during the acute infection phase. A likely explanation for this is a reduced flux through the OtsA-OtsB2 route *in vivo* compared to *in vitro* conditions, so that the level of toxic T6P that accumulates is somewhat less *in vivo*. Thus, while the OtsA-OtsB2 route clearly dominates during the acute infection phase, the alternative TreX-TreY-TreZ pathway might be already more active early during infection than under *in vitro* conditions. This is not unusual as we have recently described a similar *in vitro-in vivo* difference in flux through alternative sugar metabolic pathways for biosynthesis of maltose-1-phosphate in *M. tuberculosis* [56].

Our data conclusively show that essentiality of OtsB2 relies on direct or indirect toxic effects associated with OtsA-mediated T6P accumulation. While this apparent phosphosugar-related toxicity resembles a previous example in *M. tuberculosis* concerning M1P [149], we were surprised to observe a very different transcriptome profile in T6P-stressed cells, and little overlap with the stress response elicited by M1P. Two notable examples of a common signature in T6P- and M1P-stressed cells were the global upregulation of the *arg* operon required for *de novo* biosynthesis of L-arginine and induction of DNA damage-responsive genes including those of the SOS regulon [149]. Induction of arginine production has been described as a stress response upon hyperosmotic stress in yeast [168] and upon internalization of *Candida albicans* cells by macrophages [169]. Likewise, genes involved in arginine biosynthesis are also induced under hyperosmotic conditions in *M. tuberculosis* [170]. Therefore, it is conceivable that arginine may play a role as a general small-molecule stress protectant in *M. tuberculosis*, very similar to trehalose [57], to counteract various stresses that may be encountered in the host during infection. However, arginine could not confer any noticeable protective effects during stress associated with T6P accumulation, so this could represent a general, unspecific stress response that provides no advantage in this particular case. Further experiments involving *otsB2* silencing in arginine auxotrophic mutants are needed to address the role of arginine biosynthesis in phosphosugar stress response. T6P stress led to a strong upregulation of the putative efflux pump Rv1258c, which has been implicated in antibiotic resistance. However, this did not lead to a decreased susceptibility of stressed *M. tuberculosis* cells to the first-line anti-tuberculosis drugs isoniazid, rifampicin and ethambutol. While it cannot be ruled out that this efflux pump might be specific for other antibiotics, this suggests that OtsB2 inhibitors could be included in tuberculosis chemotherapy without impairing the efficacy of standard drugs. Whether upregulation of Rv1258c represents a specific mechanism to alleviate T6P stress or not is unknown. However, it is tempting to speculate that this could mediate efflux of T6P or downstream products to decrease the intracellular concentration. While we have not tested for potential secretion of T6P in silenced cells, the high levels of intracellular T6P accumulation implies that T6P cannot be exported at a substantial rate. Although not being overrepresented among the many genes induced in T6P stressed cells, upregulation of several DNA damage-inducible genes including those of the SOS regulon indicates that T6P accumulation might lead to DNA damage in a direct or indirect way, very similar to that described for M1P. While this probably explains the bactericidal effect of both T6P and M1P accumulation in *M. tuberculosis*, the molecular mechanisms of phosphosugar-mediated DNA damage are unclear in each case. Two intriguing features of the T6P-elicited transcriptome profile are the

upregulation of *vapB* antitoxin genes, which might cause increased RNA half-life via enhanced neutralization of the RNase activity of VapC toxins whose specific RNA substrates have yet to be identified, and downregulation of highly-abundant non-coding RNAs of unknown functions. Whether these features contribute to the loss of viability upon OtsB2 inactivation or constitute responses that aim to mitigate and/or counteract the T6P stress needs to be addressed in the future.

The strict essentiality of OtsB2 to establish an acute infection in mice highlights that it might represent a new potential drug target candidate. However, conditional gene silencing *in vivo* has revealed several limitations of OtsB2 in terms of its suitability as a potential drug target. First, although the efficacy of gene silencing *in vivo* is unclear, it appears that inhibition of OtsB2 can maximally achieve bacteriostatic growth inhibition in the lung. Thus, monotherapy with OtsB2 inhibitors would not be sufficient to eradicate the pathogen, necessitating combination therapy with other drugs. Second, loss-of-function mutations in OtsA would abolish the efficacy of OtsB2 inhibitors by preventing T6P accumulation, thereby readily giving rise to resistance. And third, OtsB2 inhibitors would only be appropriate to treat acute infections because they become ineffective during the chronic infection phase. Nevertheless, a genome-wide screen for synthetic lethal interactions with OtsA has revealed several opportunities for the design of combination therapies that would suppress resistance and boost the efficacy of drugs targeting OtsB2. Since, in the absence of the OtsA-OtsB2 pathway, trehalose is synthesized via the TreX-TreY-TreZ pathway from α -glucans, targeting either the TreX-TreY-TreZ pathway or reactions required for α -glucan formation (e.g. GlgC, GlgA) in a combination therapy will prevent resistance that might arise through loss-of-function mutations in OtsA. Additionally, targeting both trehalose synthesis pathways simultaneously will likely enhance the growth inhibitory effect during the acute infection phase and might render *M. tuberculosis* cells susceptible towards OtsB2 inhibitors also during the chronic infection phase.

7.2 Characterization of the putative essential glycosyltransferase Rv0225 in a cell wall associated gene cluster in *Mycobacterium* species

In this study, we investigated the essentiality of the conserved mycobacterial gene cluster *Rv0224c-Rv0228*. Via generation of gene deletion and conditional mutants, we found that *Rv0225* is strictly essential for mycobacterial growth *in vitro*, not only for the non-pathogenic *M. smegmatis* and *M. bovis* strains, but more importantly also for *M. tuberculosis*, the causative agent for tuberculosis disease.

Contrary to a *himar1* based transposon library generated by Long et al. [155], postulating essential roles of *Rv0224c* and *Rv0226c* for *M. tuberculosis* growth *in vitro*, we were able to generate a *Rv0224c* gene deletion mutant in the genetic background of *M. bovis* and *M. tuberculosis*. The *Rv0224c* knock out proves its dispensability for mycobacterial growth *in vitro*. Since the *Rv0226c* gene deletion experiments resulted in no positive clones after specialized transduction of the knock-out constructs, we generated conditional

Rv0226c *M. bovis* and *M. tuberculosis* mutants. Bacterial growth was not completely restricted under gene silencing conditions in both backgrounds. Conclusively, we claim that *Rv0226c* is only partial essential for mycobacterial growth *in vitro*.

However, due to our primary results of *Rv0225* showing the strict essentiality *in vitro*, *Rv0225* caught our attention. We observed changes in the colony morphology of *Rv0225* homologues in *M. smegmatis* and *M. bovis* under partial gene silencing conditions, pointing towards a cell wall associated role. In general, various studies have been published describing morphological abnormalities associated with alterations in the cell wall composition. These experiments involving the characterization of different gene deletion mutants disclosed many potential drug targets and vaccines. It has been reported that a FASII β -ketoacyl-ACP synthase (*kasB*) gene deletion mutant, coding for an enzyme involved in mycolic acid synthesis, showed a loss of acid-fast staining. The authors observed abnormalities in colony morphology, and light microscopy revealed the deficiency in cording known as a classical serpentine growth of *M. tuberculosis*, forming tight bundles of *M. tuberculosis* cells. Strikingly, the abnormal cellular morphology of the Δ *kasB* mutant strain is caused by the synthesis of mycolates with shorter chain lengths. Further, *in vivo* experiments in immunocompetent mice showed the ability of the mutant to persist for up to 600 days without causing disease or mortality. Based on these findings, the Δ *kasB* mutant strain might be valuable vaccine candidate against tuberculosis [171]. In another study, a *M. tuberculosis* double knockout strain lacking *pknI* and *dacB2* revealed a smoother colony morphology on solid agar and an irregular shape in transmission electron microscopy. The double-knock out strain was shown to be defective in cord formation, and it was twofold more susceptible to the first-line antibiotic isoniazid than the wild type H37Rv strain. The authors suggest a functional role of these two genes within the synthesis of the peptidoglycan layer in the mycobacterial cell wall [46, 172, 173]. The gene *pcaA* is likely required for the synthesis of a proximal cyclopropane ring of alpha mycolic acids in *M. bovis* BCG Pasteur and *M. tuberculosis*. Inactivation of *pcaA* in these strains led to an altered microscopic cording, forming disordered aggregates without tightly packed cords visible in wild type. Mice infected with the mutant revealed a less severe pulmonary damage, and all mice survived more than 219 days post infection compared to all control groups. The authors suggested that *pcaA* contributes to establishing a lethal chronic *M. tuberculosis* infection in mice [46]. Russell-Goldman et al showed that a resuscitation-promoting factors (rpfs) Δ *rpfAB* double mutant is smoother and more regular compared to the used *M. tuberculosis* Erdman wild-type strain. Additionally, the mutant colonies are described to be more prominent translucent. Rpf's are associated with peptidoglycan hydrolases and reactivation of dormant bacteria by modulating innate immune responses to the bacterium [172].

Studies on the mammalian cell entry operon 1 (*mce1*) mutants highlight the fact that changes in the mycolic acid composition do not necessarily have an impact on the cell morphology *per se*. The *mce1* operon (*mce1-4*) encodes an ATP-binding cassette transporter (ABC transporter). Although a *mce1* mutant did not show any obvious morphological abnormalities, the disruption of the *mce1* operon resulted in a *M. tuberculosis* mutant that accumulated several-fold more free mycolic acids in its cell wall than wild-type

bacteria. Mouse studies revealed a hypervirulent phenotype of the *mce1* mutants since they were unable to induce a strong T-helper 1 (Th1) type T cell immune response, and granuloma formation in lungs was significantly impaired. Interestingly, due to the lack of *mce1* operon expression in the wild-type strain during the first 4-8 weeks of infection in mice, the authors postulate a switch in the mycolic acid composition during the course of infection. Expression of the *mce1* operon might “fine-tune” a latent infection without causing active disease in the host [173].

Taken together, alterations in the colony morphology due to gene editing studies can certainly be a promising indicator for direct or indirect participation of the studied gene in the regulatory network of the mycobacterial cell wall formation. However, slight alterations in the cell wall composition do not automatically result in apparent changes in the colony morphology as illustrated by the investigations on the *mce1* operon.

Following our observations of the smooth colony morphology under partial silenced gene expression conditions observed for the conditional *Rv0225 M. smegmatis* and *M. bovis* BCG Pasteur mutants, but not for the conditional *Rv0225 M. tuberculosis* mutant, we analyzed the mycolic acid composition of the partial silenced compared to the fully induced *Rv0225 M. tuberculosis* mutant. Strikingly, we found a subtle, yet statistically significant, reduction of alpha mycolic acids in partially silenced mutant cells. Alpha mycolic acids are the most representative mycolic acid species in *M. tuberculosis*. This could lead to more insights into the biological function of *Rv0225*, which likely participates in the regulation of the biosynthesis of mycolic acids. Interestingly, the colony morphology was not altered in the partially silenced *Rv0225 M. tuberculosis* mutant compared to the other species. One possible reason could be that the dose response for the inducer ATc needs to be investigated in more detail including more concentrations. The *tetO* promoter upstream of *Rv0225* has been shown to be very sensitive to increasing concentrations of ATc. Even small alterations of ATc concentrations in the nanogram range had an impact on induction of the gene. Thus, fine tuning of a suitable amount of tet repressor molecules leading to a change in the colony morphology could be hard to achieve, while concentrations below and above this specific range might either result in a non-discernable subtle alteration or too strong pleiotropic effects, respectively, both possibly masking the cell wall effect.

So far, the binding domain of the *Rv0225* glycosyltransferase has not been revealed, but protein modeling could provide hints towards the enzyme's substrate. The glycosyltransferase *Rv3032* involved in the elongation of the MGLP backbone utilizes ADP-glucose as well as UDP-glucose as activated donor substrates [56, 127]. However, a $\Delta Rv3032$ mutant of *M. tuberculosis* only exhibited a reduced content but not a complete loss of MGLP, strongly pointing toward the involvement of one or more redundant glycosyltransferases. As shown in this study, *Rv0225* is strictly essential for mycobacterial growth. Conclusively, we hypothesize that *Rv0225* might play a dominant role in elongation of the proximal part of the MGLP glucan backbone, whereas *Rv3032* might only mediate the distal elongation. The role of

compensatory effects would be interesting to investigate, e.g. by isolation and a quantitative and structural comparison of MGLPs obtained from fully induced and partially silenced cells of the conditional *Rv0225 M. tuberculosis* mutant and from a *Rv3032* gene deletion mutant. This will reveal whether Rv0225 plays any role in MGLP formation as hypothesized. Further, incubation of radiolabel UDP-glucose with native crude extracts obtained from fully induced and partially silenced cells of the conditional *Rv0225 M. tuberculosis* mutant and subsequent comparative TLC analysis could provide indications whether this nucleotide-bound sugar can serve as a Rv0225 donor substrate and what the potential reaction products might be. Additionally, enzyme-substrate bioactivity studies of purified Rv0225 protein with nucleotide activated sugars could also shed light on its preferred substrate.

On a molecular level, we observed completely different pattern in the RNAseq data from *Rv0225* stressed cells compared to trehalose-6-phosphate (T6P) and maltose-1-phosphate (M1P) one. We couldn't identify a common signature in the data, which explains the diversity of stress responses, as shown for the sugar intermediate T6P and the glycosyltransferase Rv0225. However, we could identify significantly different expressed gene clusters and profiles in the partially silenced conditional *Rv0225 M. tuberculosis* mutant compared to the fully induced mutant. Downregulation of *Rv0225* led to an increased expression of the *iniBAC* operon, which is known to be strongly induced in *M. tuberculosis* cells after antibiotic treatment with isoniazid [158]. Briefly, the first-line antibiotic isoniazid targets mycobacterial cell wall assembly via affecting the mycolic acid biosynthesis, leading to a bactericidal effect. Due to the common upregulation of the *iniBAC* operon in isoniazid treated *M. tuberculosis* cells and partially silenced *Rv0225* cells, Rv0225 could have a cell wall associated function. As a further hint toward a role of Rv0225 in cell wall formation or integrity, the most significant up-regulated gene in the partially silenced conditional *Rv0225 M. tuberculosis* mutant, *whiB6* (120-fold up), has been described as a stress regulatory protein strongly responsive to treatment with cell wall-active agents (e.g. isoniazid, ethambutol, cycloserine) and oxidative stress responses [159].

Taken together, we have shown in the recent study that *Rv0225* is essential for growth and viability of the fast growing *M. smegmatis* as well as for the slow growing *M. bovis* BCG Pasteur and *M. tuberculosis* strains. As shown for other gene modulation studies targeting different genes, alterations in the cell morphology strongly indicates a cell wall associated function. A small but significant reduction of alpha mycolic acids in the partially silenced *Rv0225 M. tuberculosis* mutant as detected by ESI-MS provides further corroboration towards this hypothesis. The transcriptome analysis revealed gene expression signatures of stressed *M. tuberculosis* cells, potentially associated with impaired cell wall biosynthesis. The hypothesis that Rv0225 has an impact on MGLP synthesis needs to be evaluated by further experiments. Investigations on the enzymes structure and its substrate are crucial to identify the donor and acceptor substrate of Rv0225. Finally, although we have found out that silencing of *Rv0225* has a bactericidal effect *in vitro* similar to what we have shown for *otsB2*, the question is whether *Rv0225* is also essential *in vivo*? Does it fulfill an essential role in the acute phase of infection, comparable to *OtsB2*, rather than in the

chronic infection phase or are even both infection phases affected in mice? Obtaining these results would provide more detailed information on its relevance as a potential drug target.

8 Supplementary Information

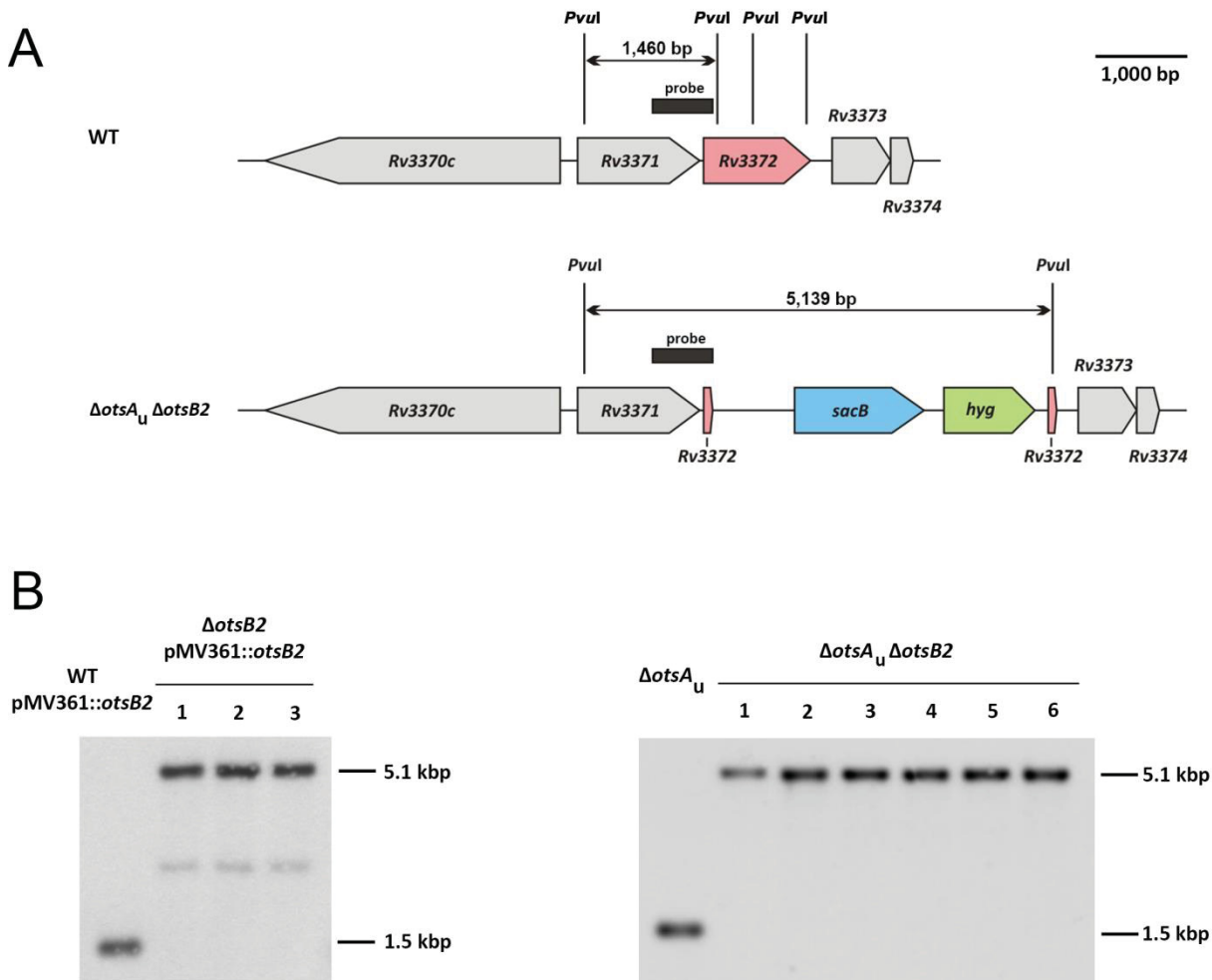
8.1 List of Figures (Supplementary Information)

S1 Fig. Generation of <i>M. tuberculosis</i> <i>otsB2</i> gene deletion mutants.....	88
S2 Fig. Generation of <i>M. tuberculosis</i> <i>c-otsB2-4xtetO</i> gene knock-in mutants.	89
S3 Fig. Generation of a marked and unmarked <i>M. tuberculosis</i> <i>otsA</i> gene deletion mutants.	90
S4 Fig. Exogenous T6P has no toxic effect on <i>M. tuberculosis</i> cells.	91
S5 Fig. Drug susceptibility of induced and partially silenced cells of the conditional <i>M. tuberculosis</i> <i>c-otsB2-tet-on</i> mutant.....	91
S6 Fig. Arginine supplementation does not rescue growth of the conditional <i>M. tuberculosis</i> <i>c-otsB2-tet-on</i> mutant under silencing conditions.	92
S7 Fig. Differential gene expression of the DNA-damage-responsive genes in induced and partially silenced cells of the conditional <i>M. tuberculosis</i> <i>c-otsB2-tet-on</i> mutant.	93
S8 Fig. Anhydrotetracycline- (ATc-) dependent growth of the conditional <i>M. tuberculosis</i> Δ <i>panCD</i> <i>c-otsB2-tet-on</i> mutant.....	94
S9 Fig. Independent silencing experiment to reproduce the bacteriostatic effect of <i>otsB2</i> silencing during the acute infection phase in mice.....	94
S10 Fig. Generation of mycobacterial <i>Rv0224c-4xtetO</i> gene knock-in mutants and conditional <i>M. tuberculosis</i> <i>Rv0224c-tet-on</i> mutant.	99
S11 Fig. Generation of <i>M. tuberculosis</i> and <i>M. bovis</i> <i>Rv0224c</i> gene deletion mutants.....	100
S12 Fig. Generation of <i>Mycobacterium</i> <i>c-Rv0225-4xtetO</i> gene knock-in mutants.....	102
S13 Fig. ATc dosis dependent partial gene silencing of locus <i>Rv0225</i> in BCG-Pasteur leads to differences in cell morphology.	103
S14 Fig. Growth kinetics of conditional mycobacterial <i>Rv0225</i> mutants in shaking culture.	104
S15 Fig. Generation of <i>M. tuberculosis</i> and <i>M. bovis</i> <i>Rv0226c-4xtetO</i> gene knock-in mutants.....	105
S16 Fig. <i>Rv0226c</i> is not strictly essential for mycobacterial <i>in vitro</i> growth, whereas the <i>M. bovis</i> conditional <i>Mb0231c-tet-off</i> mutant shows morphological abnormalities under silenced gene expression conditions.....	106
S17 Fig. Organization of the <i>Rv0228</i> locus in <i>M. tuberculosis</i> wild-type as well as in a <i>c-Rv0228-i4xtetO</i> gene knock-in mutant.....	108
S18 Fig. <i>Rv0228</i> is not essential for <i>in vitro</i> growth of <i>M. tuberculosis</i> and <i>M. bovis</i>	108
S19 Fig. Thin layer chromatography (TLC) of mycolic acid methyl esters (MAMEs), prepared from <i>M. spec.</i>	109
S20 Fig. Thin layer chromatography analysis of dried <i>M. bovis</i> <i>c-Rv0225-tet-off</i> mutant cells under fully induced and partially silenced conditions show no differences in organic soluble cellular-envelope lipid composition, mycolic acids and lipoarabinomannan/ lipomannan.	111
S21 Fig. Liquid chromatography coupled with mass spectrometry (LC-MS) analysis of <i>M. tuberculosis</i> <i>c-Rv0225-tet-on</i> mutant methanol fractions.....	112
S22 Fig. Electrospray ionization mass spectrometry analysis (ESI-MS) of <i>M. tuberculosis</i> <i>c-Rv0225-tet-on</i> mutant petroleum ether fractions lead to identification of significant differences in cardiolipin and sulfolipid composition.	113
S23 Fig. Differential gene expression of pathway responsive genes in induced and partially silenced cells of the conditional <i>M. tuberculosis</i> <i>c-Rv0225-tet-on</i> mutant.....	118

8.2 Table Directory (Supplemental Information)

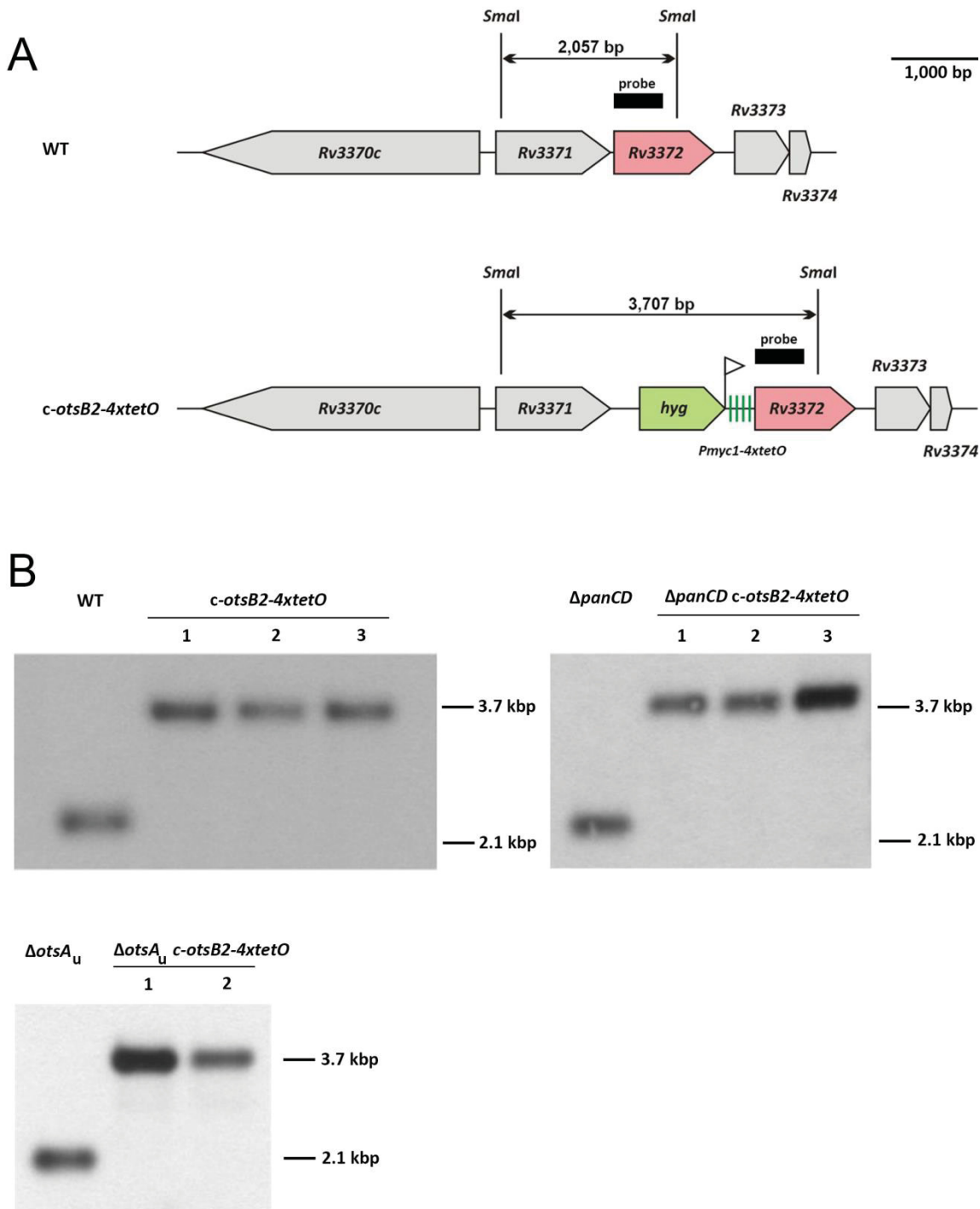
S1 Table. Most abundant transcripts in induced and partially silenced cells of the conditional <i>M. tuberculosis</i> c-otsB2-tet-on mutant.....	95
S2 Table. Differentially essential genes in the <i>M. tuberculosis</i> Δ otsA mutant compared to wild- type.	96

8.3 OtsB2 study



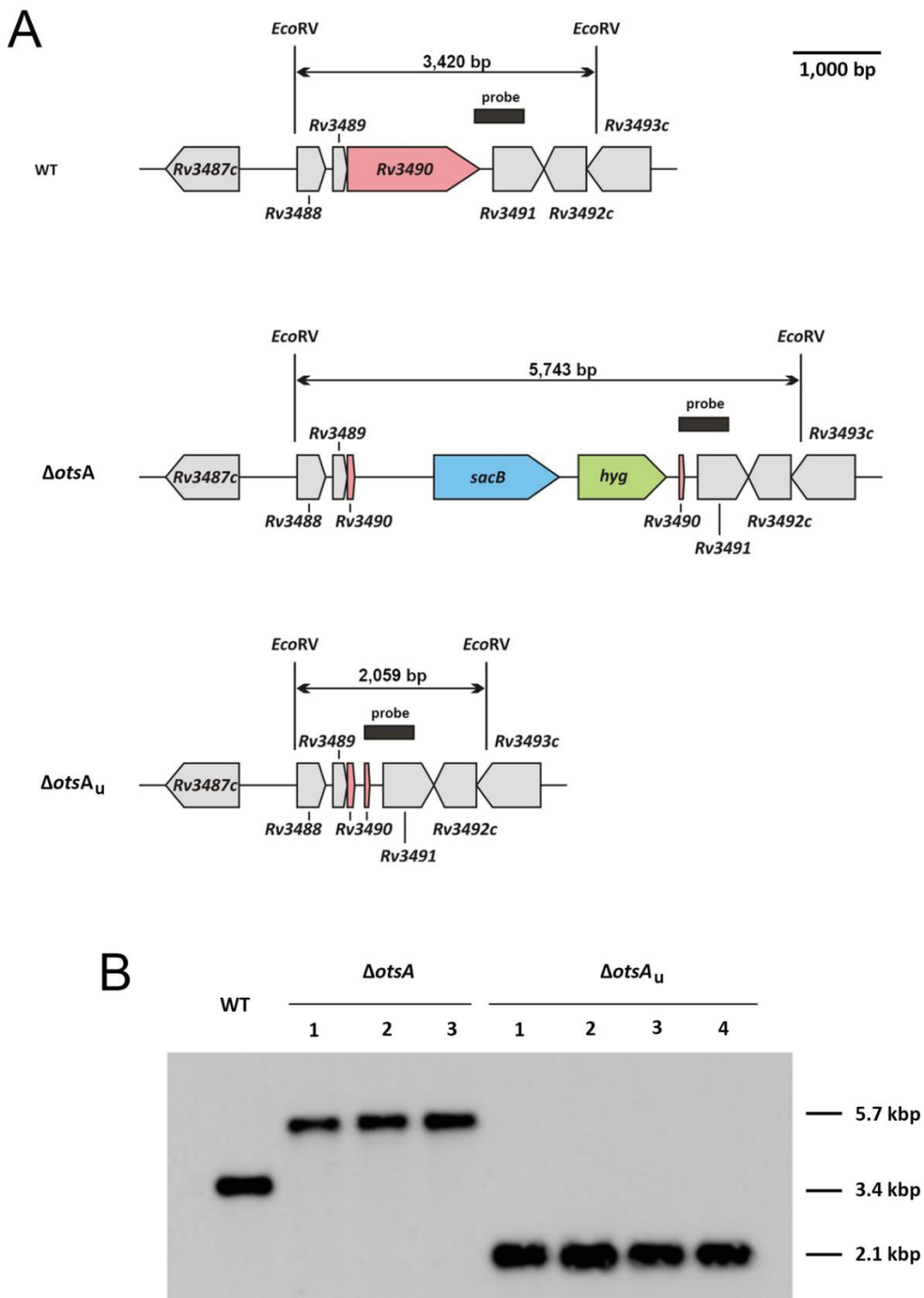
S1 Fig. Generation of *M. tuberculosis* *otsB2* gene deletion mutants.

(A) Organization of the *otsB2* locus in *M. tuberculosis* wild-type as well as in a marked *otsB2* gene deletion mutant. The sizes of relevant fragments as well as the location of the probe used for Southern analyses are indicated. WT, wild-type; (u), unmarked locus; $\gamma\delta\text{res}$, *res*-sites of the $\gamma\delta$ -resolvase; *hyg*, hygromycin resistance gene; *sacB*, levansucrase gene from *Bacillus subtilis*. (B) Southern analyses of *PvuI*-digested genomic DNA using a probe hybridizing to the position indicated in A, showing *otsB2* gene deletion in an *otsB2* merodiploid strain (left) and in an unmarked *otsA* mutant.



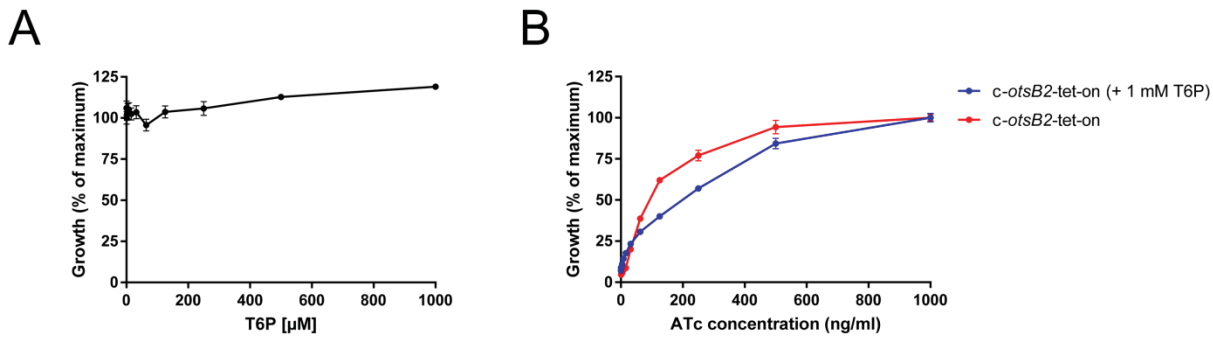
S2 Fig. Generation of *M. tuberculosis* *c-otsB2-4xtetO* gene knock-in mutants.

(A) Organization of the *otsB2* locus in *M. tuberculosis* wild-type as well as in a *c-otsB2-4xtetO* gene knock-in mutant. The sizes of relevant fragments as well as the location of the probe used for Southern analyses are indicated. WT, wild-type; (u), unmarked locus; *hyg*, hygromycin resistance gene; *Pmyc1-4xtetO*, promoter cassette containing 4 *tetO* sites. (B) Southern analyses of *Smal*-digested genomic DNA using a probe hybridizing to the position indicated in A, showing promoter cassette insertion in wild-type (upper left panel), in a $\Delta panCD$ gene deletion mutant (upper right panel), and in an unmarked *otsA* gene deletion mutant (lower left panel).



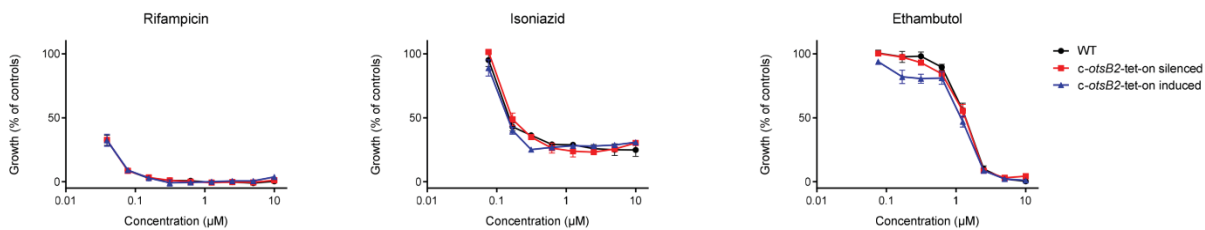
S3 Fig. Generation of a marked and unmarked *M. tuberculosis* *otsA* gene deletion mutants.

(A) Organization of the *otsA* locus in *M. tuberculosis* wild-type as well as in a marked and unmarked *otsA* gene deletion mutant. The sizes of relevant fragments as well as the location of the probe used for Southern analyses are indicated. WT, wild-type; (u), unmarked locus; $\gamma\delta$ res, res-sites of the $\gamma\delta$ -resolvase; *hyg*, hygromycin resistance gene; *sacB*, levansucrase gene from *Bacillus subtilis*. (B) Southern analyses of *EcoRV*-digested genomic DNA using a probe hybridizing to the position indicated in A, showing *otsA* gene deletion and marker cassette removal.



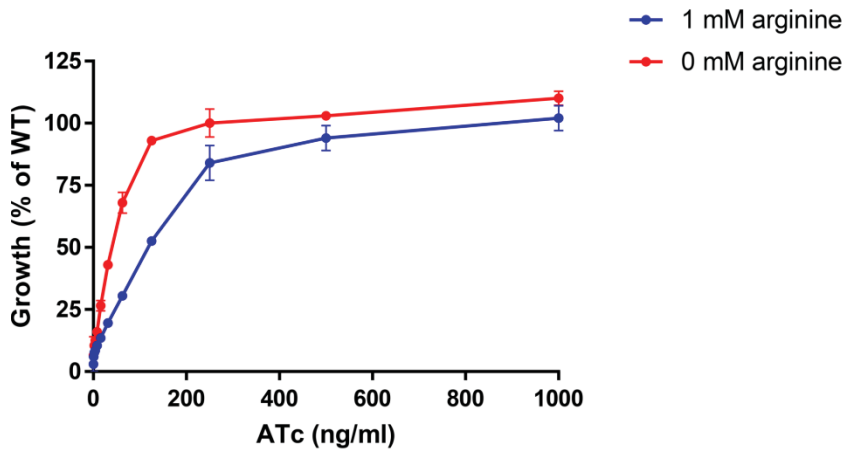
S4 Fig. Exogenous T6P has no toxic effect on *M. tuberculosis* cells.

(A) WT cells were grown in liquid medium containing increasing concentrations of T6P, revealing no growth inhibitory effect. (B) Cells of the conditional *M. tuberculosis* *c-otsB2-tet-on* mutant were cultivated in liquid medium containing increasing concentrations of ATc either in presence or absence of 1 mM T6P. ATc-dependent growth was not substantially altered by the presence of T6P, revealing no toxic effect of exogenous T6P. Growth in A and B was determined employing the resazurin microplate assay. Values are means of triplicates \pm SEM.



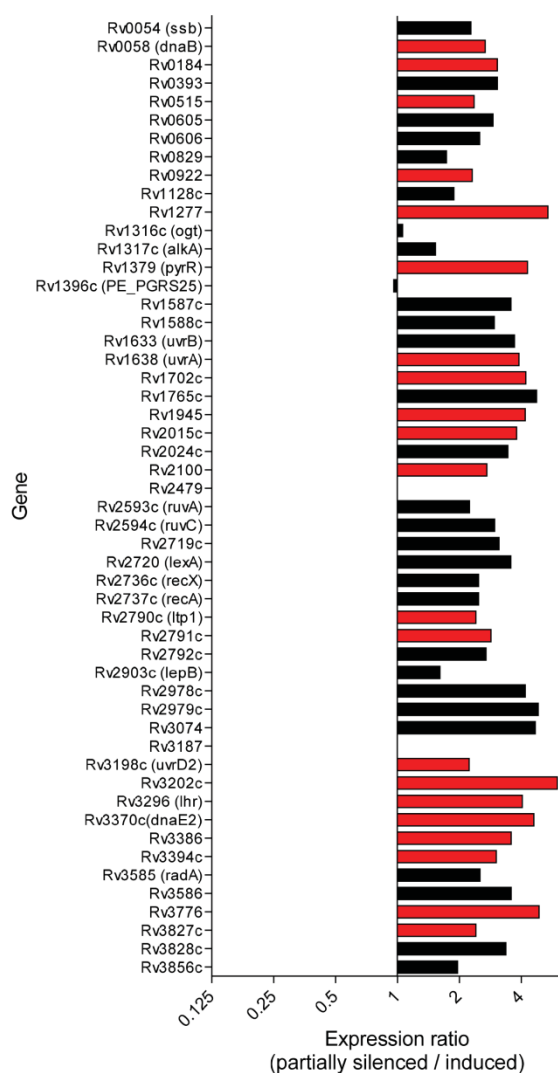
S5 Fig. Drug susceptibility of induced and partially silenced cells of the conditional *M. tuberculosis* *c-otsB2-tet-on* mutant.

Cells of the conditional *M. tuberculosis* *c-otsB2-tet-on* mutant were either induced in presence of 200 ng/ml or partially silenced in presence of 30 ng/ml ATc and incubated with the indicated concentrations of either rifampicin, isoniazid, or ethambutol for 5 days. Growth was determined employing the resazurin microplate assay using non-inoculated medium (0% growth) and solvent treated cells (DMSO; 100% growth) as controls. WT, wild-type.



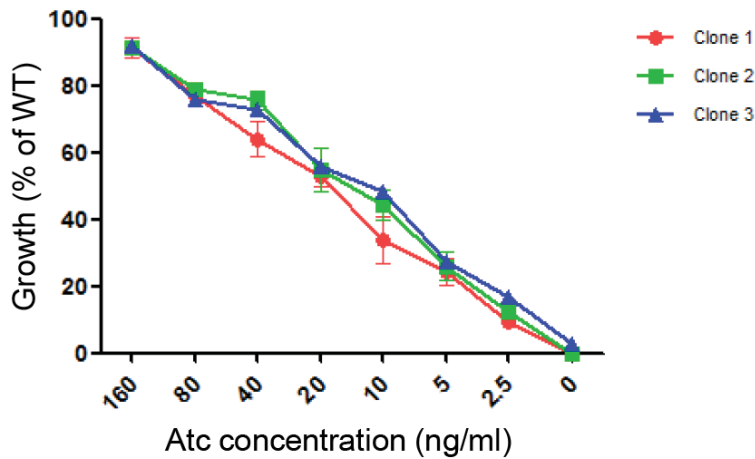
S6 Fig. Arginine supplementation does not rescue growth of the conditional *M. tuberculosis* c-otsB2-tet-on mutant under silencing conditions.

Cells of the conditional *M. tuberculosis* c-otsB2-tet-on mutant were cultivated in liquid medium containing increasing concentrations of ATc either in presence or absence of 1 mM arginine. ATc-dependent growth was not substantially altered by the presence of arginine, revealing no stress-protective effect of exogenous arginine during T6P accumulation. Growth was determined employing the resazurin microplate assay. Values are means of triplicates \pm SEM.



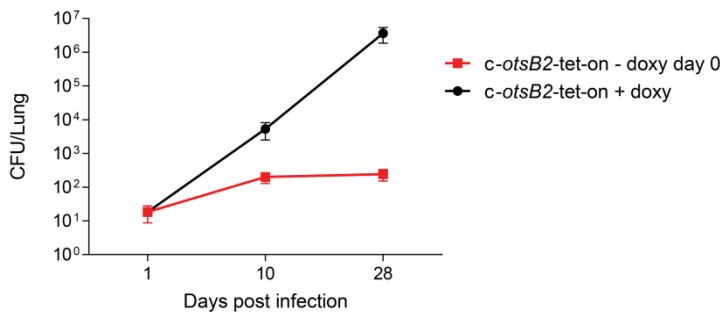
S7 Fig. Differential gene expression of the DNA-damage-responsive genes in induced and partially silenced cells of the conditional *M. tuberculosis* *c-otsB2-tet-on* mutant.

Cells were cultivated either in presence of 200 ng/ml (100% growth relative to WT) or 30 ng/ml ATc (ca. 30% residual growth relative to WT) for 7 days. rRNA-depleted samples were analyzed by RNAseq. Genes with corrected p-values < 0.01 are shown in red. The data indicate global upregulation of DNA damage responsive genes including those of the SOS regulon in partially silenced, trehalose-6-phosphate stressed cells. DNA damage-responsive genes in *M. tuberculosis* have been defined as those that respond to DNA damage as a result of treatment with DNA damaging agents such as fluoroquinolones, UV irradiation, H₂O₂, and mitomycin C.



S8 Fig. Anhydrotetracycline- (ATc-) dependent growth of the conditional *M. tuberculosis* Δ panCD *c-otsB2*-tet-on mutant.

Growth of three independent clones was measured using the resazurin microplate assay.



S9 Fig. Independent silencing experiment to reproduce the bacteriostatic effect of *otsB2* silencing during the acute infection phase in mice.

Mice were infected with the conditional *M. tuberculosis* *c-otsB2*-tet-on mutant via the aerosol route. Mice received doxycycline via the mouse chow to induce *otsB2* in the conditional *M. tuberculosis* *c-otsB2*-tet-on mutant. Doxycycline treatment was stopped in one group 24 h post-infection to silence *otsB2* during the acute infection phase. Bacterial loads in lungs of infected C57BL/6 mice were determined by plating serial dilutions of organ homogenates on 7H10 agar containing 200 ng/ml ATc to determine viable bacterial cell counts. Aliquots were plated in parallel also on 7H10 agar containing no ATc to quantify the frequency of non-regulated suppressor mutants of the conditional *c-otsB2*-tet-on mutant, which was <1% at all time points and conditions. Data are means \pm SD from four mice per group and time point.

S1 Table. Most abundant transcripts in induced and partially silenced cells of the conditional *M. tuberculosis* c-otsB2-tet-on mutant.

	Rv ID	Description	Size (bp)	Average trimmed RPKM	
				partially silenced	induced
Most abundant in partially silenced cells	RVnc0046	ssr	368	151348.7	301903.6
	RVnc0036a	MTS2823	300	123055.7	856824.6
	Rvnt03	leuT	83	45327.2	152403.1
	Rvns01	rnpB	307	21422.5	66901.6
	Rv1398c	vapB10	258	17890.8	13075.9
	RVnc0006	C8	128	15441.2	122028.7
	RVnc0036	MTS1338	117	13833.1	277857.0
	Rvnt12	aspT	74	13515.8	44517.0
	Rvnt38	metU	74	11107.0	15902.2
	Rv1872c	lIdD2	1245	11023.0	7265.6
	Rvnt44	serT	89	9276.9	27669.3
	RVnc0024	mcr7	350	6370.0	5655.6
	Rvnr03	rrf	115	6344.6	11202.3
	RVnc0004	B11	93	5964.1	17216.6
	Rvnt37	alaU	73	5085.8	16496.5
Most abundant in induced cells	RVnc0036a	MTS2823	300	123055.7	856824.6
	RVnc0046	ssr	368	151348.7	301903.6
	RVnc0036	MTS1338	117	13833.1	277857.0
	Rvnt03	leuT	83	45327.2	152403.1
	RVnc0006	C8	128	15441.2	122028.7
	Rvns01	rnpB	307	21422.5	66901.6
	Rvnt12	aspT	74	13515.8	44517.0
	Rvnt44	serT	89	9276.9	27669.3
	RVnc0004	B11	93	5964.1	17216.6
	Rvnt37	alaU	73	5085.8	16496.5
	Rvnt38	metU	74	11107.0	15902.2
	Rv1398c	vapB10	258	17890.8	13075.9
	Rvnr03	rrf	115	6344.6	11202.3
	RVnc0013	mcr11	131	3149.4	7376.8
	Rv1872c	lIdD2	1245	11023.0	7265.6

Cells were cultivated in presence of 200 ng/ml (100% growth relative to WT) or 30 ng/ml ATc (ca. 30% residual growth relative to WT) for 7 days. rRNA-depleted samples were analyzed by RNAseq. RPKM, reads per kilobase of transcript per million mapped reads.

S2 Table. Differentially essential genes in the *M. tuberculosis* Δ otsA mutant compared to wild-type.

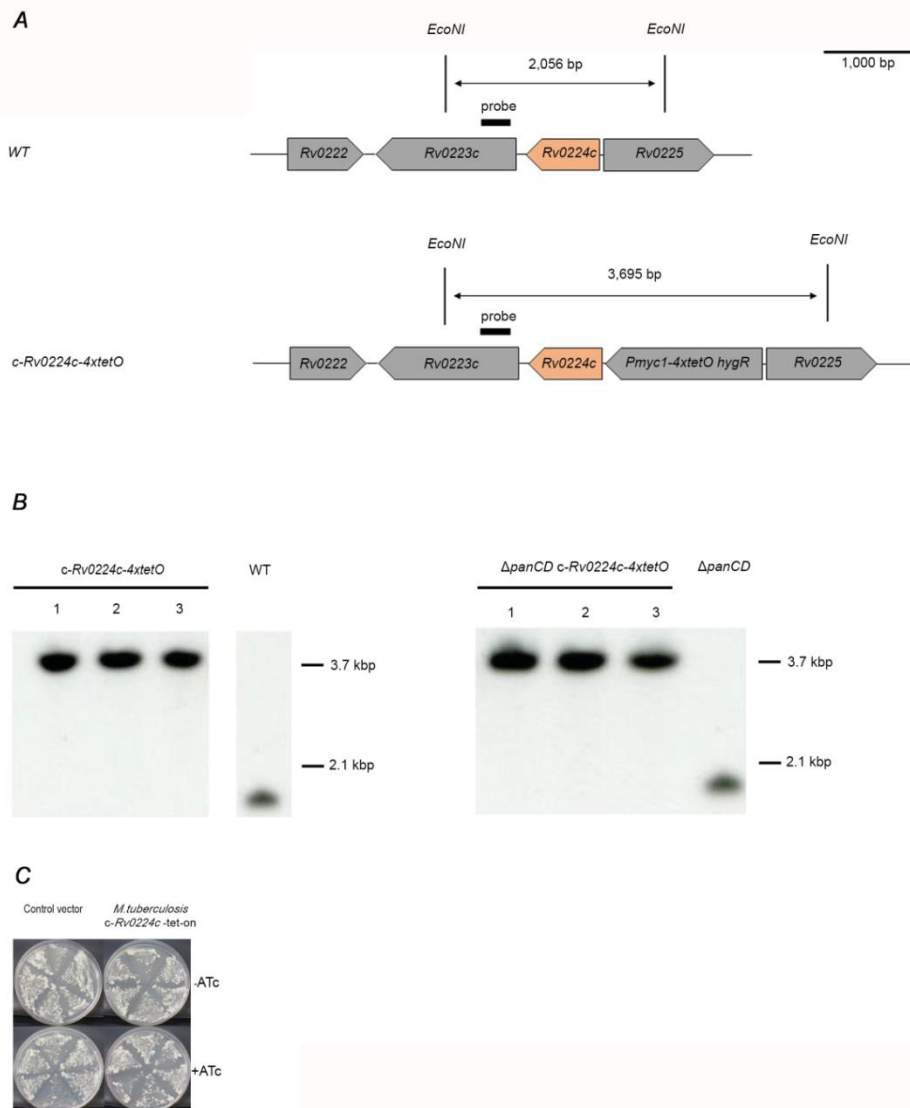
Rv number	Gene	N of TA sites	TAs Hit	Avg Reads Δ otsA	Avg Reads		p-adj
					WT[156]	Delta Reads	
Rv1212c	-	31	22	0	3194.4	3194.4	0
Rv1235	lpqY	30	17	0	1496.1	1496.1	0
Rv1238	sugC	25	9	0	1084.3	1084.3	0
Rv2074	-	6	5	0	1068.1	1068.1	0.0072
Rv0746	PE_PGRS9	15	8	0	862.2	862.2	0.0072
Rv1795	-	22	8	0	1068.4	1068.4	0.0197
Rv1796	mycP5	36	15	6.4	879.9	873.6	0
Rv1236	sugA	19	10	6.4	1109.7	1103.3	0
Rv3512	PE_PGRS56	27	13	6.4	770.4	764	0.0072
Rv1562c	treZ	37	15	6.4	716.4	710.1	0.0072
Rv3664c	dppC	14	6	6.4	285.5	279.1	0.0124
Rv1745c	idi	14	9	6.4	1243.9	1237.5	0.0232
Rv3657c	-	8	6	6.4	434	427.6	0.0249
Rv1262c	-	4	4	6.4	659.5	653.2	0.0415
Rv3590c	PE_PGRS58	21	14	12.7	1815.4	1802.7	0
Rv2236c	cobD	12	6	12.7	1031.3	1018.6	0.0124
Rv1823	-	15	11	12.7	790.7	778	0.0456
Rv3414c	sigD	9	7	19.1	1266.8	1247.7	0.0072
Rv1840c	PE_PGRS34	16	8	19.1	824.1	805	0.0472
Rv2967c	pca	63	19	25.4	1213.1	1187.6	0.0072
Rv1244	lpqZ	8	6	25.4	839.2	813.8	0.0249
Rv1710	-	15	10	25.4	756.3	730.8	0.0429
Rv3388	PE_PGRS52	19	13	31.8	942	910.2	0.0197
Rv2487c	PE_PGRS42	25	15	38.1	2048.8	2010.7	0
Rv0234c	gabD1	23	14	38.1	1095.4	1057.3	0.035
Rv2065	cobH	8	6	38.1	1301.8	1263.6	0.0362
Rv2564	glnQ	14	12	44.5	1396.7	1352.2	0
Rv2159c	-	6	6	50.9	2525.5	2474.6	0.0197
Rv0747	PE_PGRS10	16	11	63.6	2568.7	2505.1	0.0072
Rv3345c	PE_PGRS50	47	25	69.9	2481.5	2411.6	0
Rv1727	-	6	5	69.9	1195.9	1126	0.0249
Rv1564c	treX	49	23	76.3	3404.2	3327.9	0
Rv3563	fadE32	11	11	76.3	1291.9	1215.6	0.0472
Rv0782	ptrBb	45	18	82.6	1406.1	1323.5	0.0197
Rv1991c	-	6	6	82.6	1009.5	926.9	0.0249
Rv2615c	PE_PGRS45	17	9	89	2230.9	2141.9	0
Rv0861c	ercc3	26	16	89	1054.2	965.2	0.0326
Rv1232c	-	11	8	95.4	2506.1	2410.7	0.0232
Rv0279c	PE_PGRS4	19	16	101.7	1886.2	1784.5	0
Rv0012	-	16	12	108.1	2506.8	2398.8	0.0124
Rv2859c	-	17	16	114.4	2384.5	2270	0.0232
Rv3308	pmmB	20	13	114.4	2076.5	1962	0.0276
Rv2800	-	20	17	120.8	2516	2395.2	0
Rv0281	-	14	13	120.8	2232.5	2111.7	0
Rv1283c	oppB	21	14	133.5	2404.3	2270.8	0.0197
Rv0263c	-	16	10	139.9	2938.7	2798.8	0.0072
Rv3787c	-	10	8	146.2	1869.1	1722.9	0.0276
Rv0244c	fadE5	23	18	152.6	1921.6	1769.1	0.0072

Rv0767c	-	14	9	152.6	2695.8	2543.2	0.0232
Rv1910c	-	13	11	158.9	2197.9	2039	0
Rv0092	ctpA	30	22	165.3	3141.6	2976.3	0
Rv0727c	fucA	12	11	171.6	2071.9	1900.2	0.0301
Rv0976c	-	20	17	178	3279.1	3101.1	0.0072
Rv3649	-	33	23	178	1944.7	1766.7	0.035
Rv0889c	citA	12	12	178	2836.6	2658.6	0.0472
Rv1864c	-	10	9	184.4	4396	4211.6	0.0072
Rv1737c	narK2	15	14	190.7	2305.1	2114.4	0.0362
Rv2328	PE23	12	12	190.7	2096.6	1905.9	0.0389
Rv2559c	-	15	13	190.7	3023.3	2832.6	0.0415
Rv3507	PE_PGRS53	41	23	203.4	2805.7	2602.2	0.0362
Rv1180	pkS3	25	14	209.8	4939.7	4729.9	0.0389
Rv0613c	-	16	14	235.2	4539.8	4304.6	0
Rv3575c	-	18	15	241.6	1827.3	1585.8	0.0249
Rv3196	-	9	8	241.6	3087.2	2845.7	0.035
Rv0501	galE2	25	18	241.6	2361.3	2119.7	0.0362
Rv0914c	-	16	15	247.9	2206.1	1958.2	0.035
Rv1632c	-	11	11	254.3	3572.3	3318	0.0249
Rv1206	fadD6	37	30	260.6	7149.9	6889.2	0
Rv2681	-	19	15	267	3904.8	3637.8	0
Rv0574c	-	20	15	267	2367.9	2101	0.0072
Rv3220c	-	21	19	273.4	3362.6	3089.3	0.0168
Rv0492c	-	17	14	273.4	3209.5	2936.1	0.0168
Rv3119	moaE1	12	12	273.4	2834.6	2561.2	0.0197
Rv3450c	-	15	13	273.4	4483.1	4209.7	0.0301
Rv2896c	-	20	15	279.7	4269.9	3990.2	0.0168
Rv0630c	recB	34	23	286.1	2913.7	2627.6	0.0472
Rv2066	cobI	22	18	317.8	3836.9	3519.1	0.0124
Rv0210	-	13	9	330.6	2677.7	2347.1	0.0276
Rv2241	aceE	57	18	381.4	0	-381.4	0
Rv2052c	-	21	19	394.1	3413.2	3019.1	0
Rv3312c	-	17	14	400.5	3704.6	3304.1	0.0362
Rv1971	mce3F	20	20	413.2	2890.1	2476.9	0.0498
Rv2860c	glnA4	31	22	432.3	4491.1	4058.8	0.0362
Rv2214c	ephD	31	26	438.6	4148.2	3709.6	0.0072
Rv3731	ligC	18	16	438.6	3293.9	2855.2	0.0124
Rv0877	-	15	13	438.6	4350.2	3911.5	0.0429
Rv3479	-	39	33	445	4758.4	4313.4	0
Rv2458	mmuM	17	14	445	3878.5	3433.5	0.0124
Rv3329	-	21	19	445	4262.3	3817.3	0.0276
Rv0166	fadD5	27	22	451.3	6274.6	5823.3	0
Rv1266c	pknH	29	26	451.3	4400.8	3949.5	0
Rv0443	-	14	12	451.3	4880.1	4428.7	0.0249
Rv0280	PPE3	26	23	457.7	4779.1	4321.4	0
Rv1768	PE_PGRS31	21	20	457.7	6355.1	5897.4	0.0072
Rv2224c	-	29	26	464.1	3149.5	2685.5	0.0362
Rv2329c	narK1	28	24	470.4	5846.8	5376.4	0
Rv2636	-	18	12	476.8	6190.6	5713.8	0.0232
Rv0570	nrdZ	37	28	495.8	3511.3	3015.5	0.0429
Rv1323	fadA4	14	12	514.9	4778.5	4263.6	0.0326
Rv1908c	katG	39	15	534	0	-534	0.0168
Rv0270	fadD2	25	22	540.3	5182.7	4642.4	0.0072
Rv1820	ilvG	20	18	578.5	5790	5211.5	0.0301
Rv1902c	nanT	33	23	616.6	3945.6	3328.9	0.0301
Rv3903c	-	51	33	635.7	4610.3	3974.6	0.0124
Rv2394	ggtB	30	26	654.8	4081.5	3426.8	0.0326
Rv2917	-	25	23	724.7	6088.2	5363.5	0.0429
Rv3822	-	39	26	781.9	6029	5247	0.0197
Rv0191	-	19	16	807.3	8150.2	7342.8	0.0168
Rv0449c	-	23	20	826.4	4807.5	3981.1	0
Rv1770	-	17	14	883.6	6425.9	5542.3	0.0249

Rv1442	bisC	37	33	915.4	7626.5	6711.1	0.0249
Rv1181	pks4	70	50	921.8	14037.9	13116.1	0
Rv3263	-	29	26	921.8	7973.3	7051.6	0.0326
Rv3728	-	32	28	1010.8	5081.7	4070.9	0.0197
Rv2941	fadD28	46	34	1023.5	14827.2	13803.7	0
Rv2000	-	35	30	1023.5	6677.4	5653.9	0.0124
Rv0754	PE_PGRS11	31	22	1029.8	8158.8	7129	0.0197
Rv3296	lhr	55	42	1055.3	10366.7	9311.5	0
Rv3824c	papA1	46	31	1106.1	9284.5	8178.4	0.0276
Rv2209	-	25	19	1195.1	7032.1	5837	0.0197
Rv0386	-	44	36	1246	7395.2	6149.2	0.0249
Rv2115c	-	29	20	1284.1	6.5	-1277.6	0.0124
Rv3059	cyp136	24	22	1411.3	8455.7	7044.5	0.0168
Rv0483	lprQ	29	26	1659.2	12510.2	10851	0
Rv2930	fadD26	40	26	1729.1	19620.4	17891.3	0.0301
Rv0169	mce1A	39	33	1900.7	8807.3	6906.5	0.0429
Rv2931	ppsA	81	62	2027.9	27715.8	25687.9	0
Rv2932	ppsB	71	56	2104.2	19681.6	17577.5	0
Rv0890c	-	48	40	2161.4	10043.3	7881.9	0.0168
Rv2934	ppsD	67	50	2472.9	20525.3	18052.4	0
Rv1836c	-	42	28	3108.6	35.1	-3073.5	0.0072
Rv2690c	-	32	22	3140.4	0.6	-3139.7	0
Rv2933	ppsC	84	66	3324.7	25042.7	21718	0
Rv2935	ppsE	68	58	4303.7	36153.8	31850.1	0
Rv3825c	pks2	116	97	4914	29179.9	24265.9	0
Rv2940c	mas	81	71	8098.8	42390.1	34291.3	0

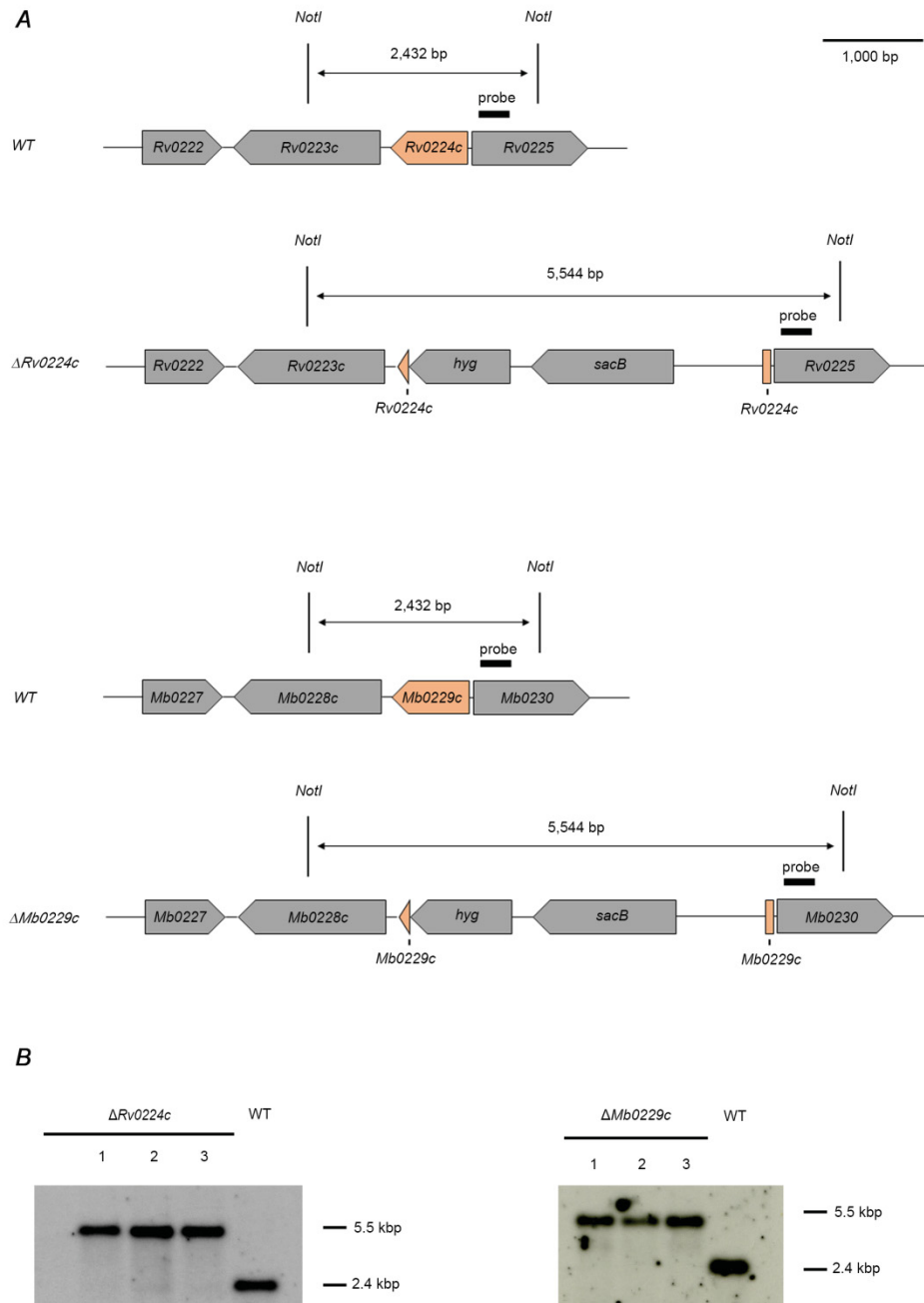
A saturated transposon mutant pool was generated in the *M. tuberculosis* Δ *otsA* mutant background, cultured in the absence of trehalose and subjected to transposon insertion sequencing (Tn-seq). Genes harboring significantly less transposon insertions compared to a transposon mutant library established in *M. tuberculosis* H37Rv wild-type [156] are shown ($p < 0.05$). Few genes harboring significantly more transposon insertions compared to a transposon mutant library established in *M. tuberculosis* H37Rv wild-type [156] (i.e. genes appearing less essential in context of *otsA* gene deletion) are highlighted in grey.

8.4 Rv0225 study



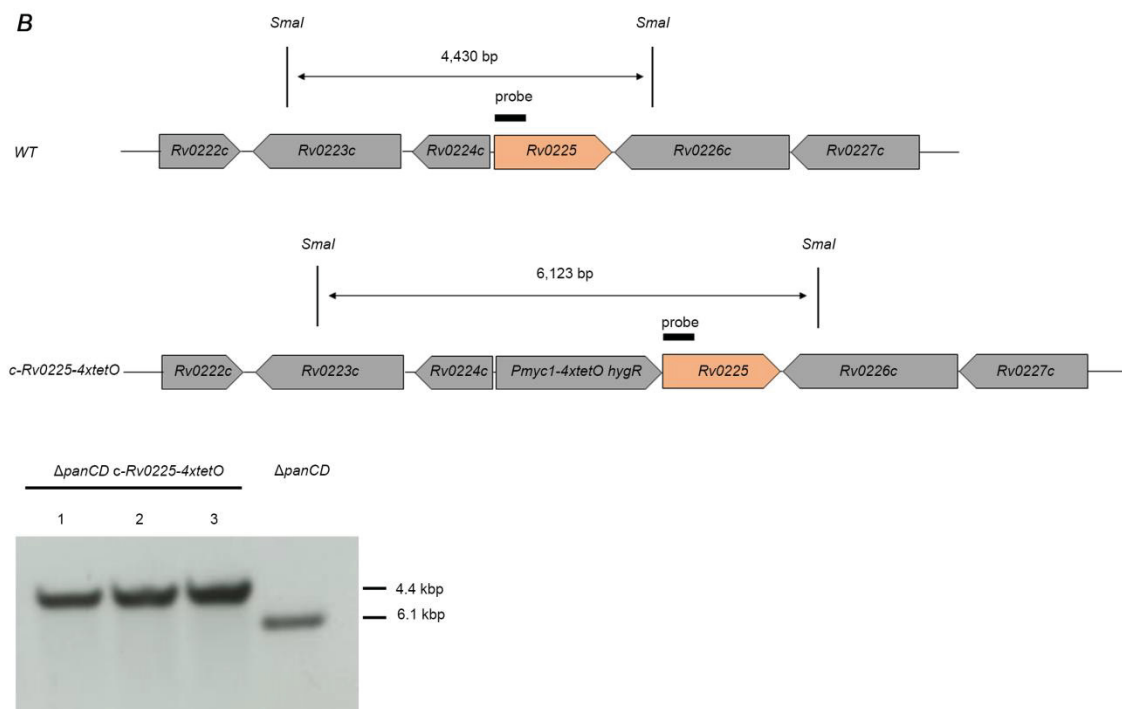
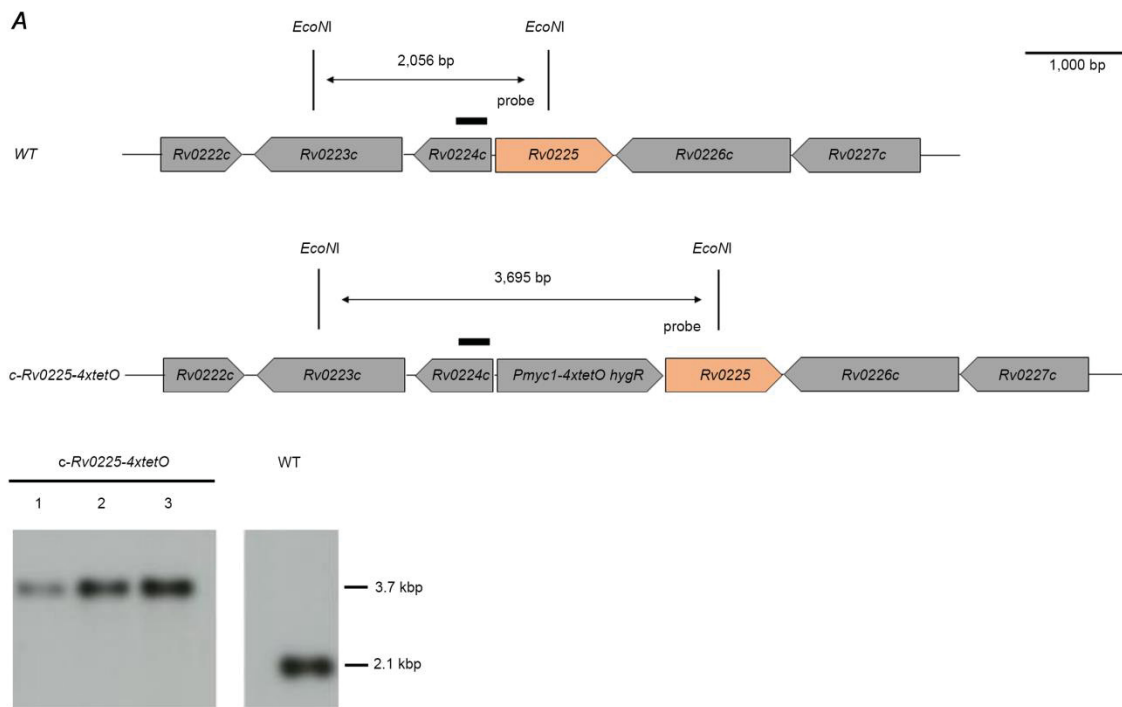
S10 Fig. Generation of mycobacterial *Rv0224c-4xtetO* gene knock-in mutants and conditional *M. tuberculosis Rv0224c-tet-on* mutant.

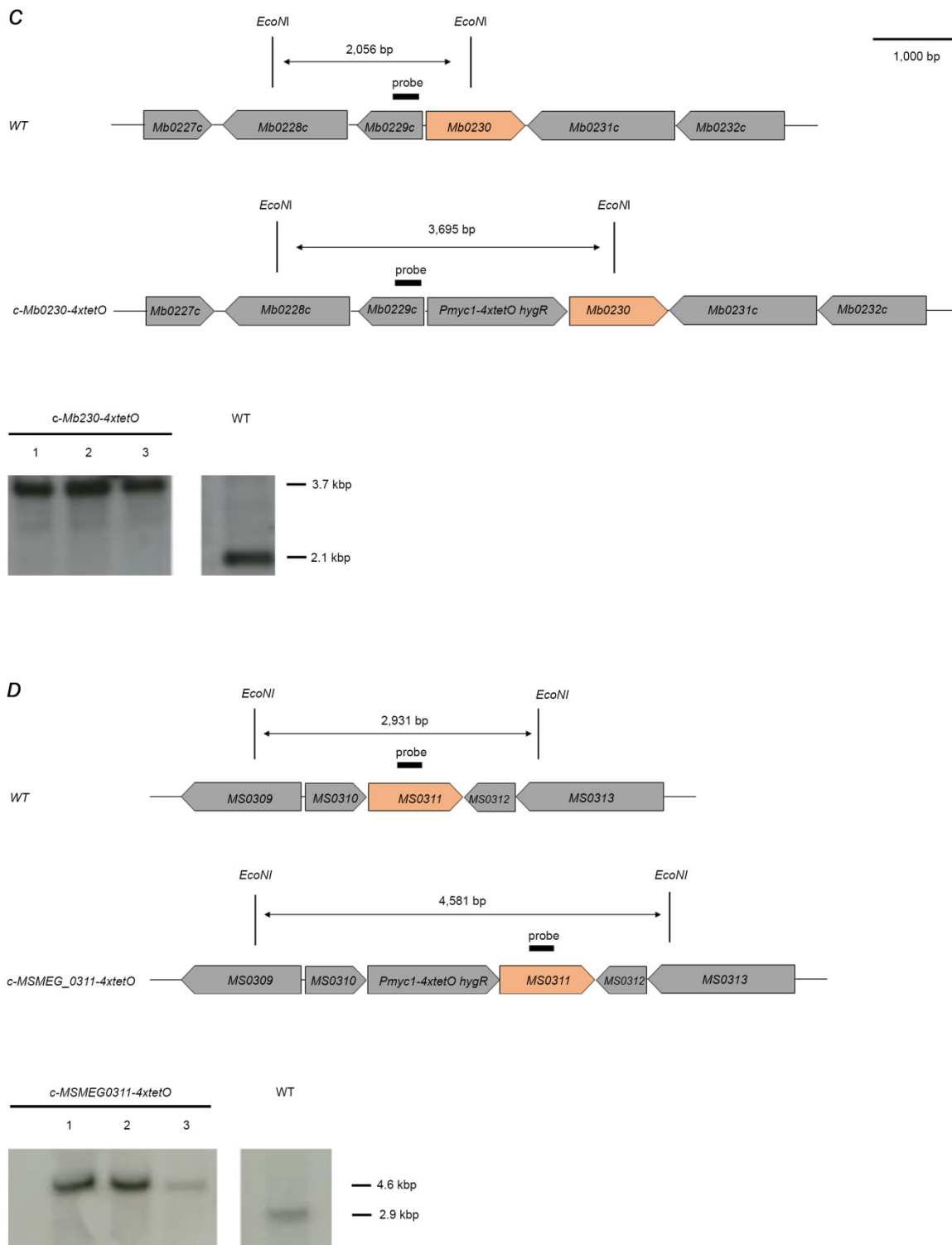
(A) Organization of the *Rv0224c* locus in *M. tuberculosis* wild-type as well as in a *c-Rv0224c-4xtetO* gene knock-in mutant. The sizes of relevant fragments as well as the location of the probe used for Southern analyses are indicated. WT, wild-type; *hyg*, hygromycin resistance gene; *Pmyc1-4xtetO*, promoter cassette containing 4 *tetO* sites. (B) Southern analyses of *EcoNI*-digested genomic DNA using a probe hybridizing to the position indicated in A, showing promoter cassette insertion in *M. tuberculosis* wild-type (lower left panel), and in a *M. tuberculosis ΔpanCD* gene deletion mutant (lower right panel). (C) The *M. tuberculosis c-Rv0224c-tet-on* mutant in the wild-type background as well as a non-regulated vector control strain were grown on Middlebrook 7H10 agar with or without 5 μg/ml ATc. Plates were incubated for 21 days. For each *c-Rv0224c-tet-on* mutant strain, growth on plates containing ATc and without the inducer, was observed (upper panel). Several clones were picked from knock-in transductants plates and plated on sector plates.



S11 Fig. Generation of *M. tuberculosis* and *M. bovis* *Rv0224c* gene deletion mutants.

(A) Organization of the *Rv0224c* locus in *M. tuberculosis* wild-type strain as well as in a marked *Rv0224c* gene deletion mutant (upper panel). The corresponding homologous *Mb0229c* locus in *M. bovis* strains is also illustrated (lower panel). The sizes of relevant fragments as well as the location of the probe used for Southern analyses are indicated. WT, wild-type; *hyg*, hygromycin resistance gene; *sacB*, levansucrase gene from *Bacillus subtilis*. (B) Southern analyses of *NotI*-digested genomic DNA using a probe hybridizing to the position indicated in A (upper panel), showing *Rv0224c* gene deletion in *M. tuberculosis* and in A (lower panel) *Mb0229c* gene deletion in *M. bovis*.

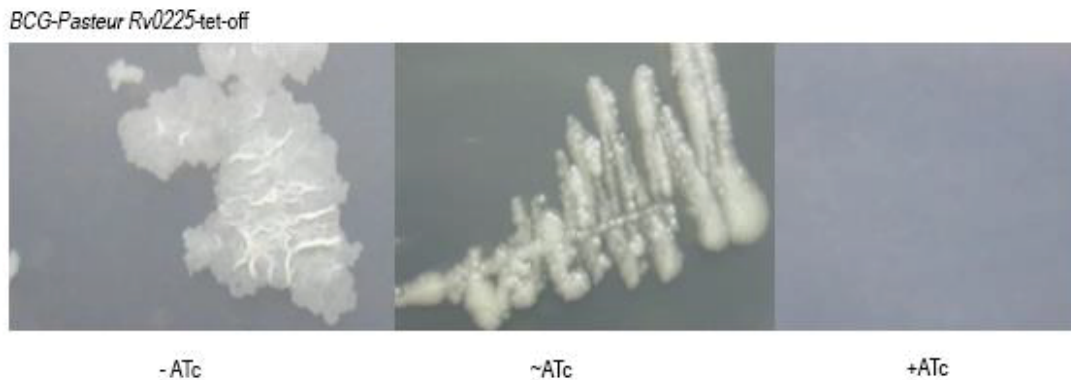




S12 Fig. Generation of *Mycobacterium c-Rv0225-4×tetO* gene knock-in mutants.

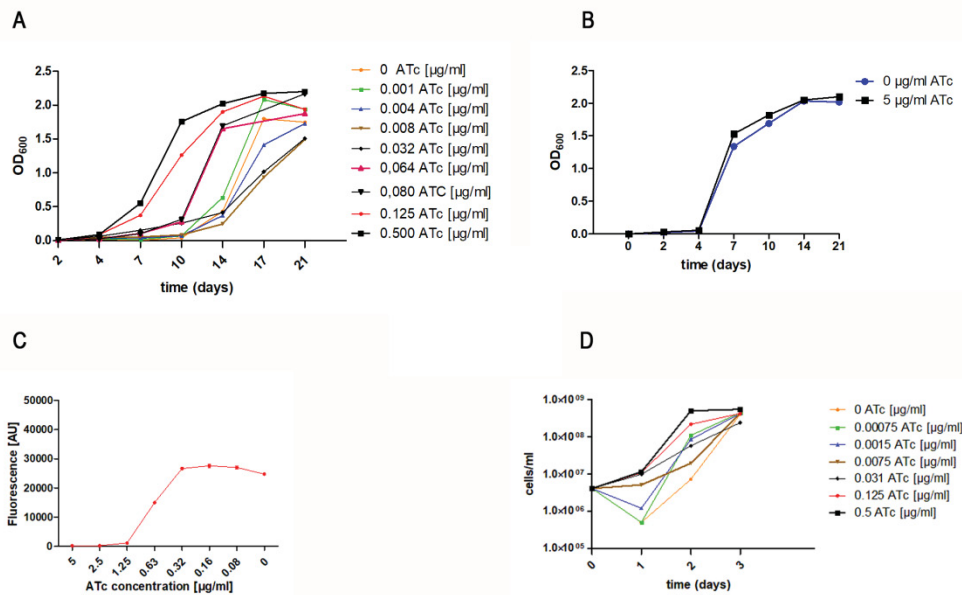
(A) Organization of the *Rv0225* locus in *M. tuberculosis* wild-type as well as in a *c-Rv0225-4×tetO* gene knock-in mutant. The sizes of relevant fragments as well as the location of the probe used for Southern analyses are indicated. Southern analyses of *Eco*NI-digested genomic DNA using a probe hybridizing to the position indicated in the restriction panel, showing promoter cassette

insertion in. WT, wild-type. (B) Organization of the *Rv0225* locus in *M. tuberculosis* $\Delta panCD$ gene deletion mutant as well as in a *M. tuberculosis* $\Delta panCD$ c-*Rv0225*-4×*tetO* gene knock-in mutant. The sizes of relevant fragments as well as the location of the probe used for Southern analyses are indicated. Southern analyses of *Sma*I-digested genomic DNA using a probe hybridizing to the position indicated in the restriction panel, showing promoter cassette insertion in the $\Delta panCD$ gene deletion mutant. (C) Organization of the *Mb0230* locus in *M. bovis* wild-type as well as in a c-*Mb0230*-4×*tetO* gene knock-in mutant. The sizes of relevant fragments as well as the location of the probe used for Southern analyses are indicated. Southern analyses of *Sma*I-digested genomic DNA using a probe hybridizing to the position indicated in the restriction panel, showing promoter cassette insertion in wild-type. (D) Organization of the *MSMEG_0311* locus in *M. smegmatis* wild-type as well as in a c-*MSMEG_0311*-4×*tetO* gene knock-in mutant. The sizes of relevant fragments as well as the location of the probe used for Southern analyses are indicated. Southern analyses of *Eco*NI-digested genomic DNA using a probe hybridizing to the position indicated in the restriction panel, showing promoter cassette insertion in wild-type WT, wild-type; *hyg*, hygromycin resistance gene; 4×*tetO*, Pmyc1-promoter cassette containing 4 *tetO* sites.



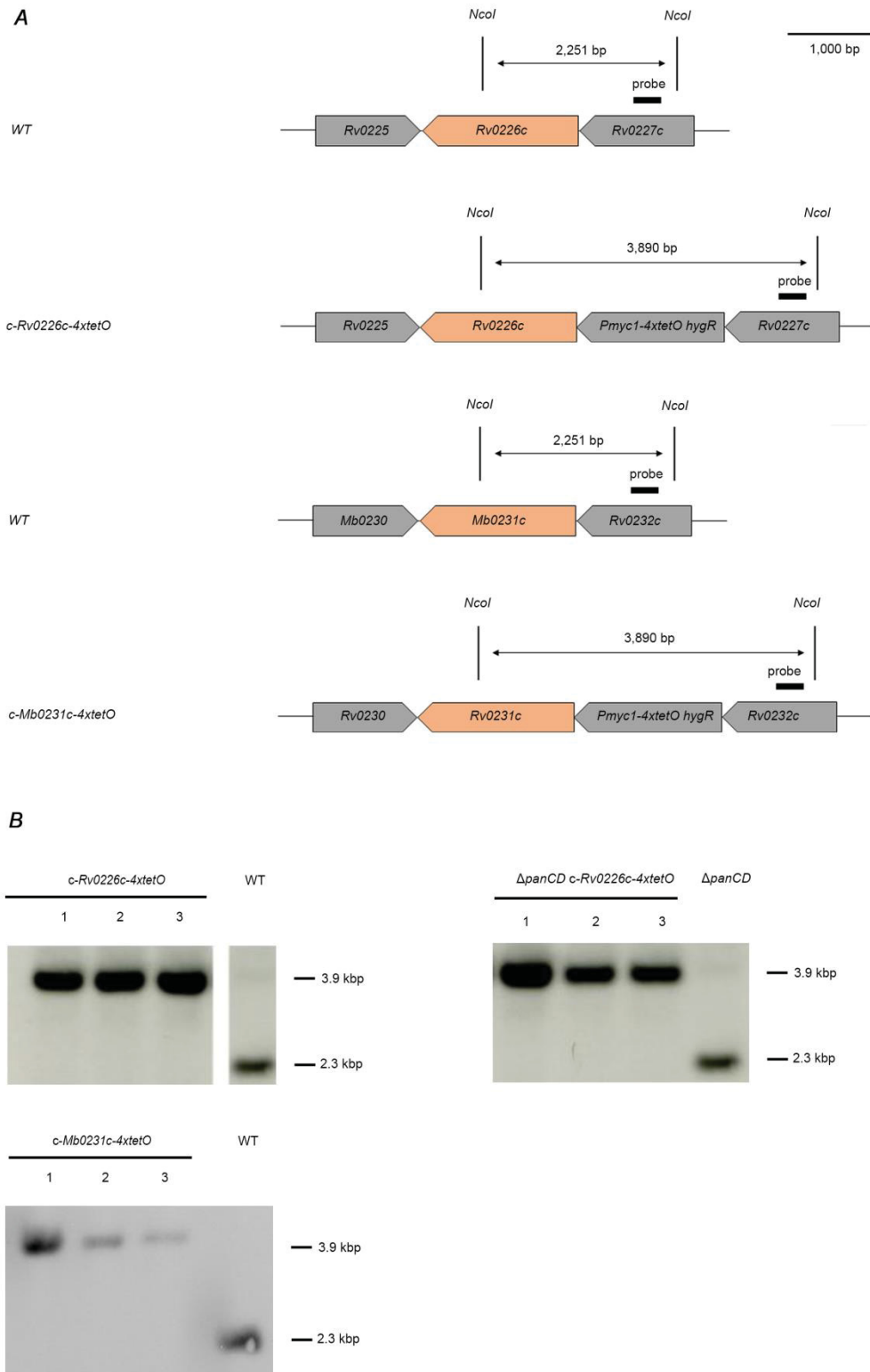
S13 Fig. ATc dose dependent partial gene silencing of locus *Rv0225* in BCG-Pasteur leads to differences in cell morphology.

Without ATc, the Tet-OFF conditional mutant grows normally like wild-type whereas on 5 µg/ml ATc agar plates gene transcription is completely inhibited. Strikingly, on 0.5 µg/ml ATc agar plates the bacterial cell morphology changes. Bacteria grew on 7H10 agar plates for a period of three weeks.



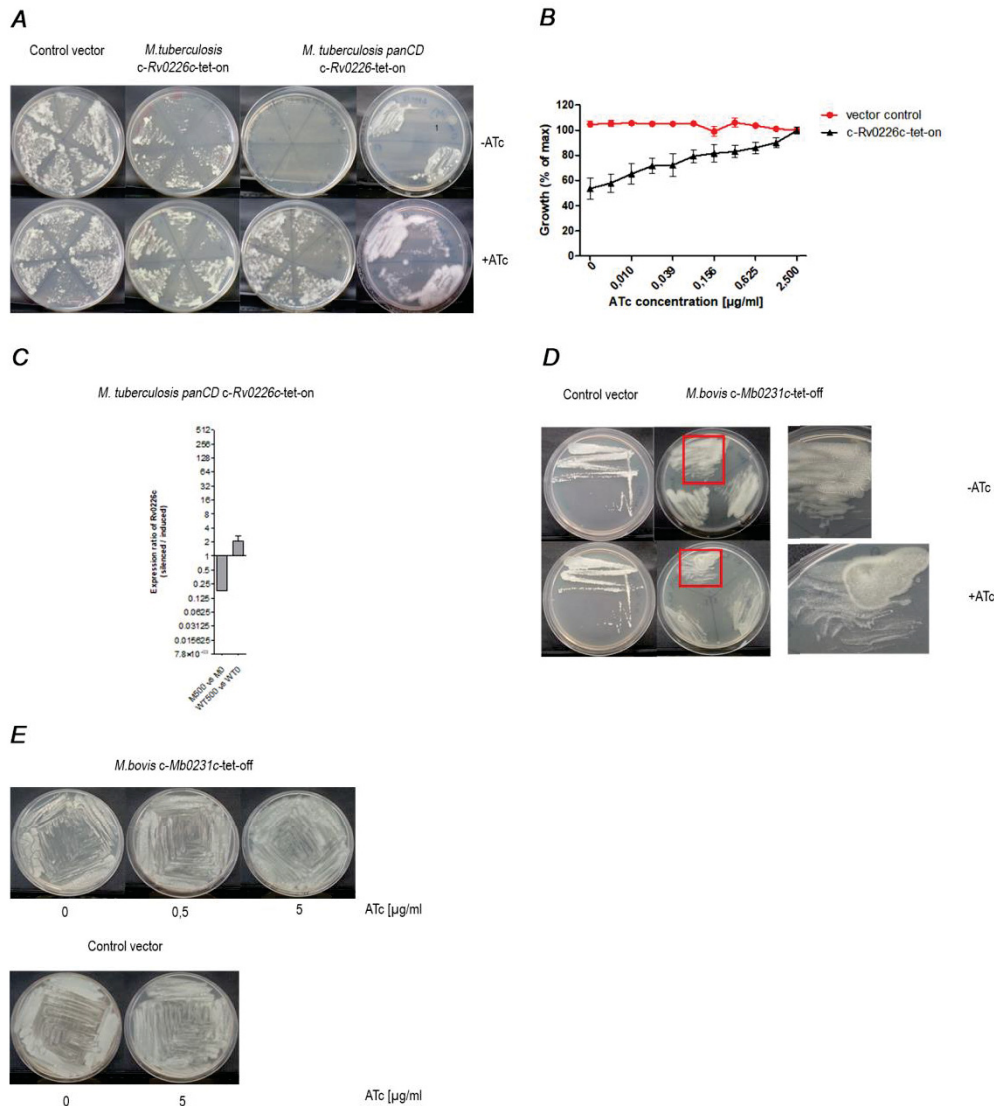
S14 Fig. Growth kinetics of conditional mycobacterial *Rv0225* mutants in shaking culture.

(A) The conditional *M. tuberculosis* *c-Rv0225-tet-on* mutant was cultivated for two weeks under fully expressed gene conditions, by addition of 0.5 µg/ml ATc to the culture medium. The culture was washed two times with PBS. A new culture was inoculated 1% under 0.064 µg/ml ATc and incubated for 1 week. Accumulated intracellular protein was depleted. 9 new cultures with different concentrations of the inducer were inoculated 1% and incubated for 21 days. Growth kinetics shows enhanced bacterial growth in comparison to lower amounts of ATc, whereas bacterial growth was observed after 10-14 days under completely silenced expression conditions. This might be due to mutations in the tet regulatory (B) *M. tuberculosis* wild-type was incubated by addition and withdrawal of ATc. (C) The respective *M. bovis* *c-Rv0225-tet-off* mutant was cultivated under fully induced gene expression conditions (0 µg/ml ATc) in a shaking culture. After reaching an OD_{600 nm} of 1 of a period of two weeks, cells were partially silenced by addition of 0.32 µg/ml ATc. Afterwards media was inoculated under given concentrations with ATc for one week and measured by Resazurin on 96-well plate. Optimal conditions to harvest cells from a shaking culture were determined: 3 passage, 1x10 ml square bottle (fully induced gene expression, OD_{600 nm}=1); 3x10 ml square bottle (each OD_{600 nm}=.4). (D) The pre-culture of the *M. smegmatis* *c-Rv0225-tet-on* mutant was incubated for 24 hours with 1.5 ng/ml ATc. From the pre-culture, different cultures with different ATc concentration were inoculated 1%. OD_{600 nm} was measured after 24 h, 48 h and 72 h.



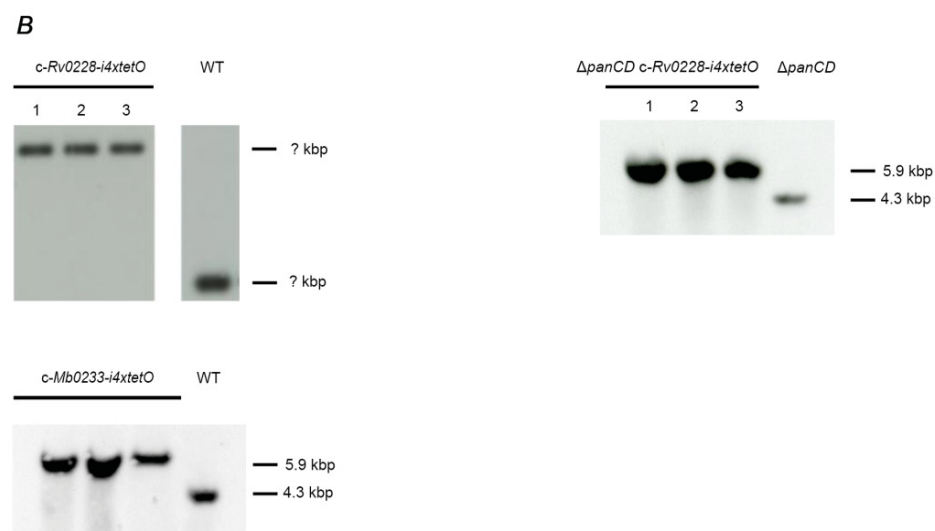
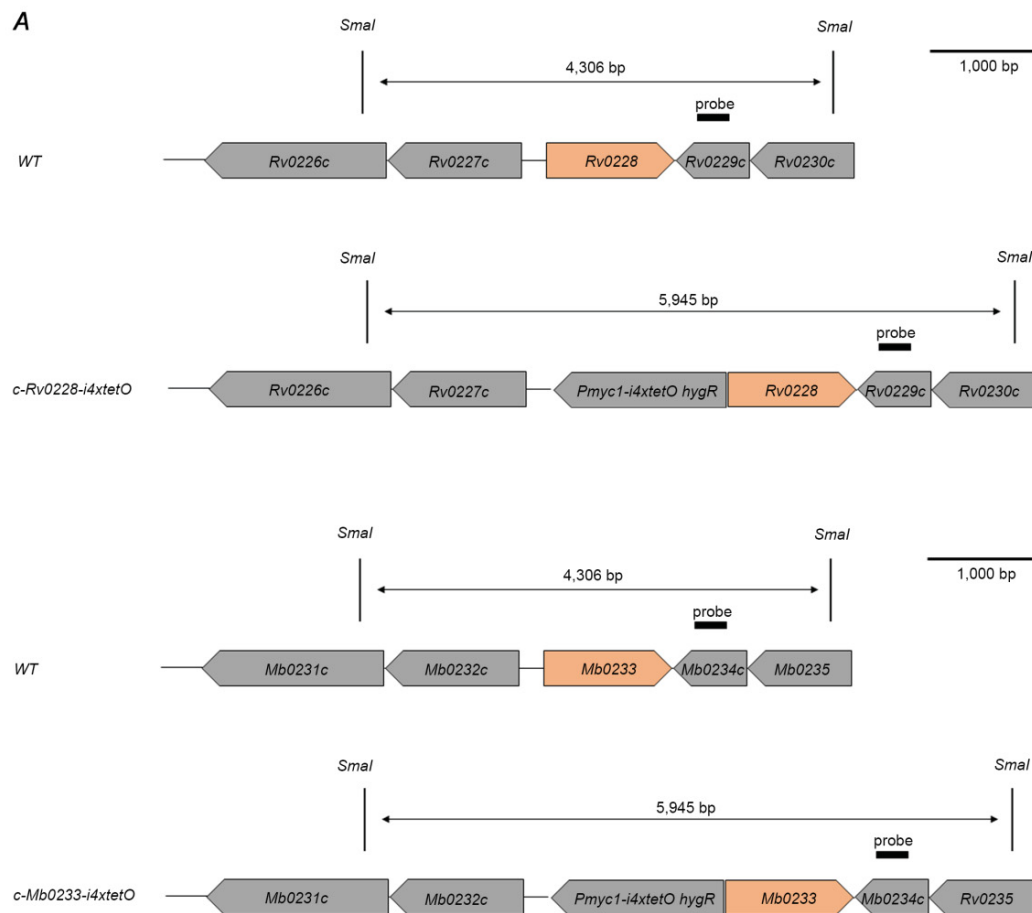
S15 Fig. Generation of *M. tuberculosis* and *M. bovis* *Rv0226c-4xtetO* gene knock-in mutants.

(A) Organization of the *Rv0226c* locus in *M. tuberculosis* wild-type as well as in a *c-Rv0226c-4xtetO* gene knock-in mutant. Corresponding, homologues *Mb0231* locus is illustrated in *M. bovis* strains (lower panel). The sizes of relevant fragments as well as the location of the probe used for Southern analyses are indicated. WT, wild-type; *hyg*, hygromycin resistance gene; *Pmyc1-4xtetO*, promoter cassette containing 4 *tetO* sites. (B) Southern analyses of *NcoI*-digested genomic DNA using a probe hybridizing to the position indicated in A, showing promoter cassette insertion in *M. tuberculosis* wild-type (upper left panel), and in a *M. tuberculosis* *ΔpanCD* gene deletion mutant (upper right panel), and in a *M. bovis* wild-type mutant (lower left panel).



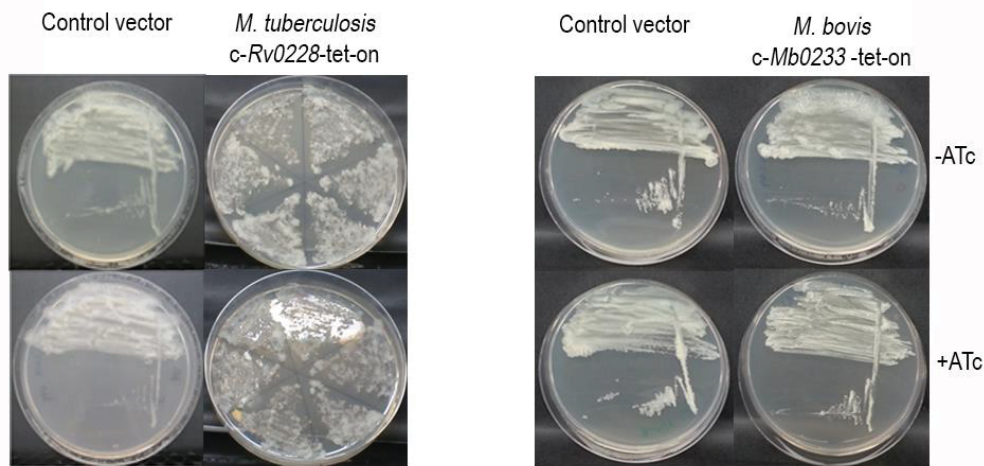
S16 Fig. *Rv0226c* is not strictly essential for mycobacterial *in vitro* growth, whereas the *M. bovis* conditional *Mb0231c*-tet-off mutant shows morphological abnormalities under silenced gene expression conditions.

(A) The *M. tuberculosis* c-Rv0226c-tet-on mutant in the wild-type and in the Δ panCD gene deletion background as well as a non-regulated vector control strain were grown on Middlebrook 7H10 agar with or without 5 µg/ml ATc. Plates were incubated for 21 days. For each c-Rv0226c-tet-on mutant strain, growth on plates containing ATc and without the inducer, was observed (upper panel). Several clones were picked from knock-in transductants plates (not shown) and plated on sector plates. Two clones were picked from the sector plates and plated. (B) The c-Rv0226c-tet-on mutant strain was grown in liquid medium containing increasing concentrations of ATc. Limited ATc-dependency demonstrates partial essentiality of *Rv0226c* for growth in liquid medium. Cells were grown in 96-well microtiter plates for 6 days, and growth was quantified using the resazurin microplate assay. Values are means of triplicates \pm SEM. (C) Verification of *Rv0226c* gene transcription in the silenced *M. tuberculosis* c-Rv0226c-tet-on mutant. Quantitative real time PCR analyses of *Rv0226c* transcripts results corroborate to *Rv0226c* downregulation in the silenced c-Rv0226c-tet-on mutant. qRT-PCR data were normalized to 16S rRNA, and the expression ratios of partially silenced cells of the *M. tuberculosis* c-otsB2-tet-on mutant compared to fully induced cells are reported as means of at least duplicates \pm SEM. (D) The *M. bovis* c-Mb0231c-tet-off mutant was equally incubated as in A. Similarly to the silenced *M. tuberculosis* mutant, ATc has a partial impact on Mb0231c gene regulation in the *M. bovis* wild-type strain. Strikingly, silenced clones showed an altered cell morphology in comparison to the fully induced mutant. A representative vector control clone was isolated and plated out under same conditions. (E). Biomass accumulation of the *M. bovis* c-Rv0231c-tet-off mutant for cell wall analysis. The *M. bovis* c-Rv0231c-tet-on mutant as well as a non-regulated vector control strain were grown on Middlebrook 7H10 agar without, with 0.5 and 5 µg/ml ATc. Biomass was removed and stored at -20°C for further analysis.



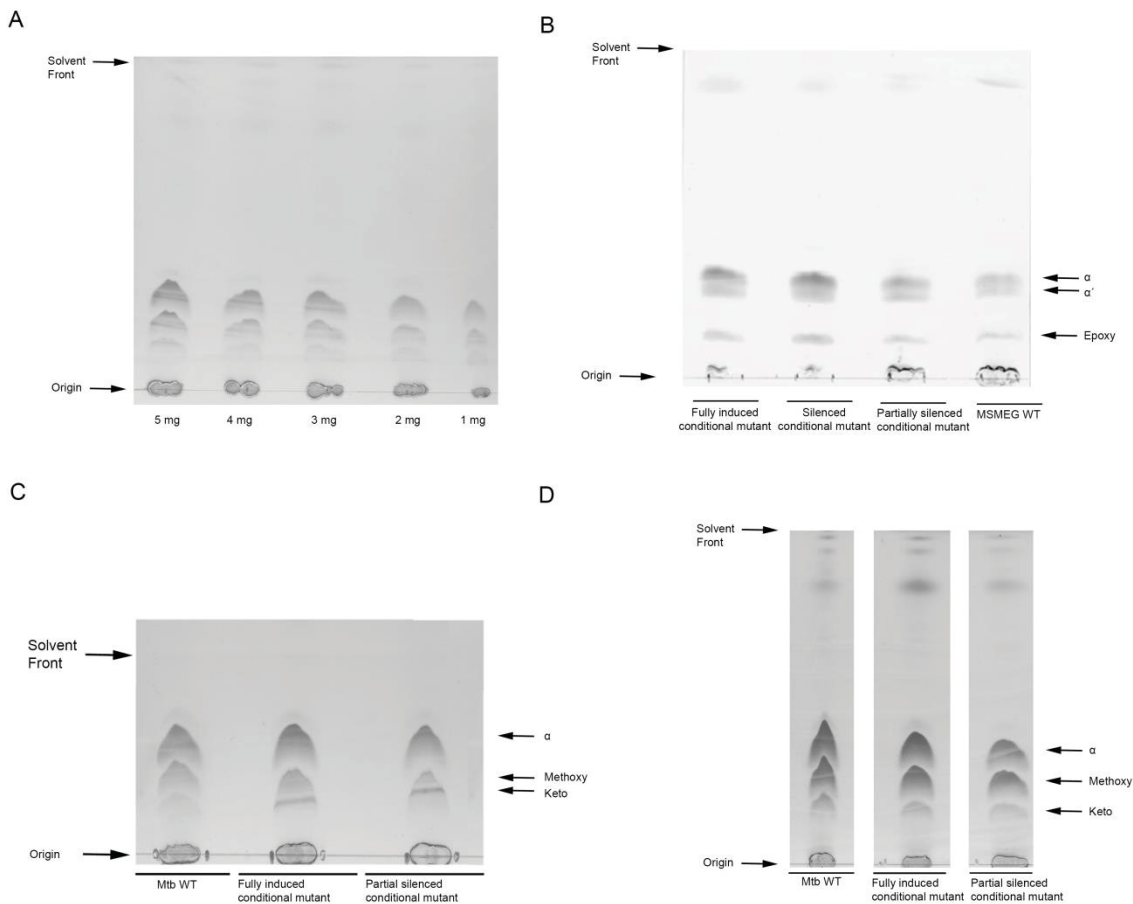
S17 Fig. Organization of the *Rv0228* locus in *M. tuberculosis* wild-type as well as in a *c-Rv0228-i4xtetO* gene knock-in mutant.

Corresponding, homologues *Mb0233* locus is illustrated in *M. bovis* strains (lower panel). The sizes of relevant fragments as well as the location of the probe used for Southern analyses are indicated. WT, wild-type; *hyg*, hygromycin resistance gene; Pmyc1-i4×*tetO*, promoter cassette containing 4 inverted *tetO* sites. (B) Southern analyses of *Sma*I-digested genomic DNA using a probe hybridizing to the position indicated in A, showing promoter cassette insertion in *M. tuberculosis* wild-type (upper left panel), and in a *M. tuberculosis* Δ *panCD* gene deletion mutant (upper right panel), and in a *M. bovis* wild-type mutant (lower left panel).



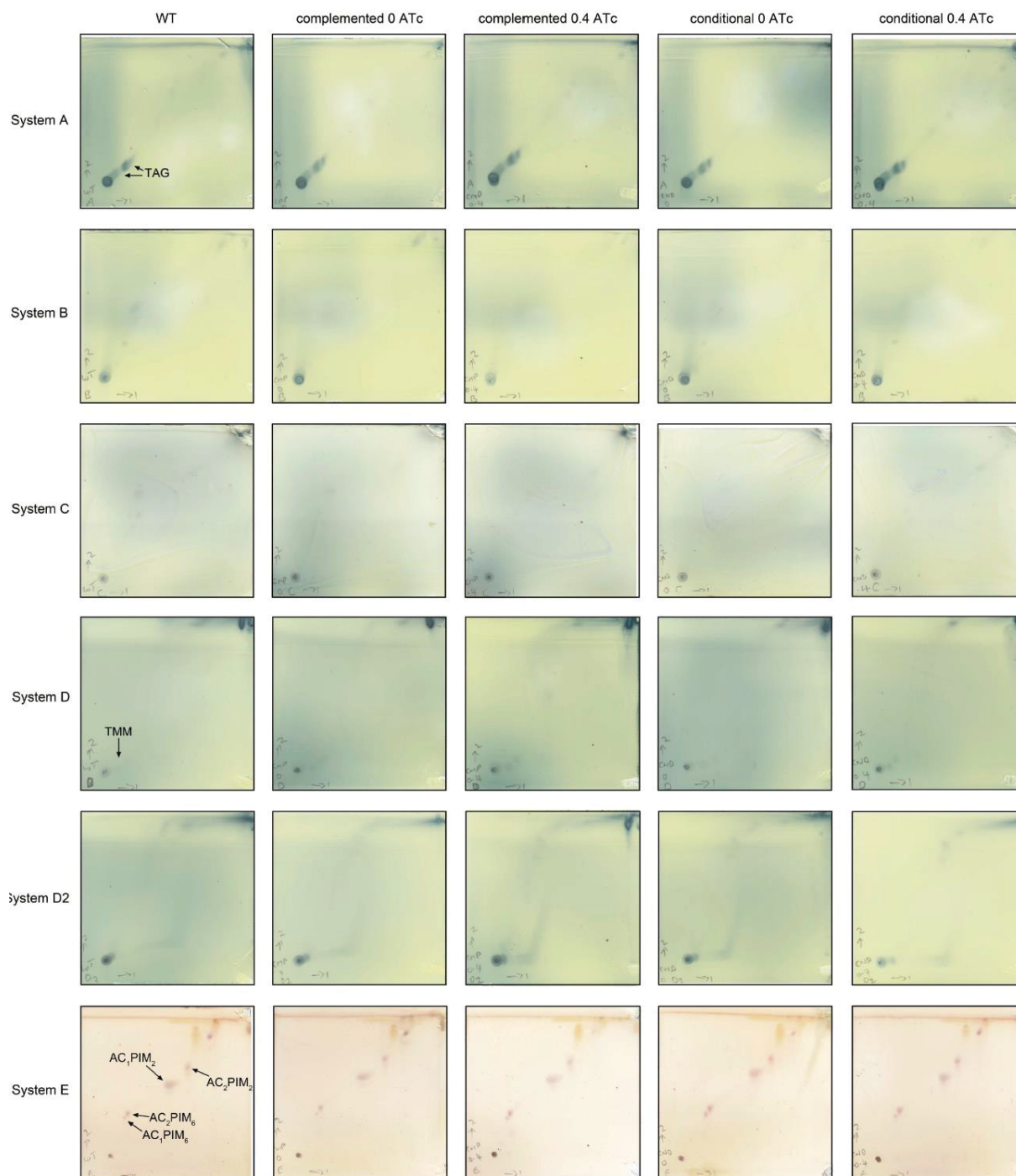
S18 Fig. *Rv0228* is not essential for in vitro growth of *M. tuberculosis* and *M. bovis*.

The *M. tuberculosis* *c-Rv0228c-tet-on* mutant in the wild-type background as well as a non-regulated vector control strain were grown on Middlebrook 7H10 agar with or without 5 µg/ml ATc. Plates were incubated for 21 days. For each *c-Rv0228-tet-on* mutant strain, growth on plates containing ATc and without the inducer, was observed. Several clones were picked from knock-in transductants plates and plated on sector plates (left panel). A representative single isolated clone of the *M. bovis* *c-Mb0233-tet-on* mutant show same results, ATc independent growth (right panel).

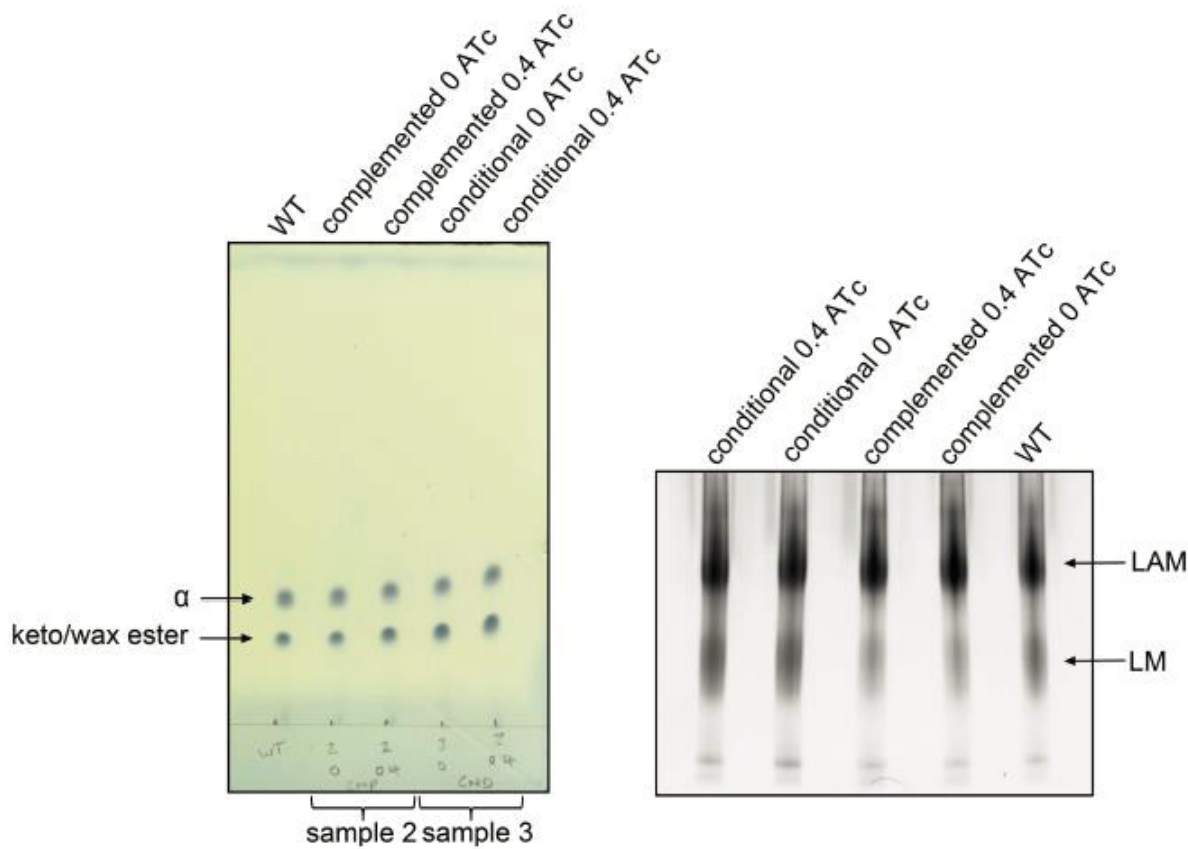


S19 Fig. Thin layer chromatography (TLC) of mycolic acid methyl esters (MAMEs), prepared from *M. spec.*

(A) Extract is normalized by dried mass of defatted cells. In terms of determining the detection level a titration curve has been performed. Thin layer chromatography (TLC) of lipid extracts from the fully induced and partially silenced conditional *M. smegmatis* Rv0225-tet-on (B), *M. bovis* Rv0225-tet-off (C) and *M. tuberculosis* Rv0225-tet-on mutant reveals no altered mycolic acid pattern. Biomass was obtained from cells grown on 7H10 plates as described for mycolic acids were extracted from defatted cells by alkaline hydrolysis and converted to the corresponding methyl esters. As a control, mycolic acid methyl esters from *M. tuberculosis* were applied on the TLC-plate. Extracts were normalized by dried mass of defatted cells. To compare MAME pattern, see: Yuan Y et al: The effect of oxygenated mycolic acid composition on cell wall function and macrophage growth in Mycobacterium tuberculosis. Molecular Microbiology, 6, 1449-58 (1998)[174].

A

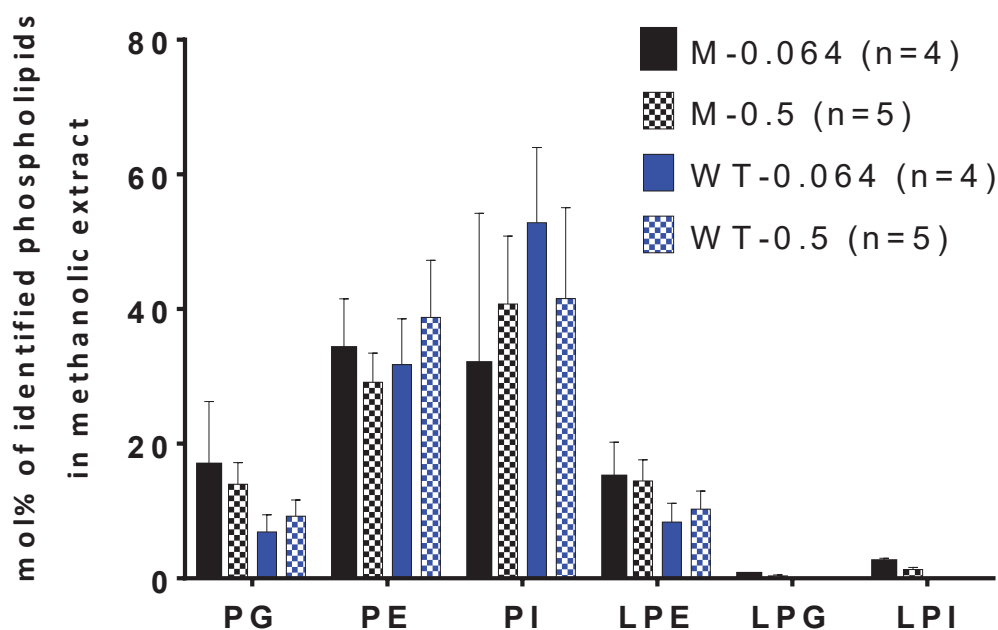
B



S20 Fig. Thin layer chromatography analysis of dried *M. bovis* c-*Rv0225*-tet-off mutant cells under fully induced and partially silenced conditions show no differences in organic soluble cellular-envelope lipid composition, mycolic acids and lipoarabinomannan/ lipomannan.

The *M. bovis* c-*Rv0225*-tet-off mutant was grown in a shaking culture under fully induced conditions without supplementation of ATc and partial silenced gene expression conditions (0.4 µg/ml ATc) for 2 weeks. Control strains, including the complemented *M. bovis* *Rv0225*-tet-off-strain with a constitutively expressed second copy of *Rv0225* and the *M. bovis* wild-type strain, were grown under the same conditions. Subsequently, TLC analysis followed by the protocol of Besra et al „Preparation of cell-wall fractions from mycobacteria“, Methods Mol Biol 1998. (A) Two-dimensional TLC analysis of the organic soluble cellular-envelope lipids was performed by using solvent systems A-E. (B) One-dimensional TLC analysis of three types of mycolic acids (left panel) and lipoarabinomannan/ lipomannan. Abbreviations: TAG, triacylglyceride; TMM, trehalose monomycolate; AC_nPIM_n, acylphosphatidylinositol mannosides; α,keto/wax ester, types of mycolic acids in *M. bovis*; LAM, lipoarabinomannan; LM, lipomannan. Several cell wall associated structures were purified and applied on TLC plates according to Besra et al (1998).

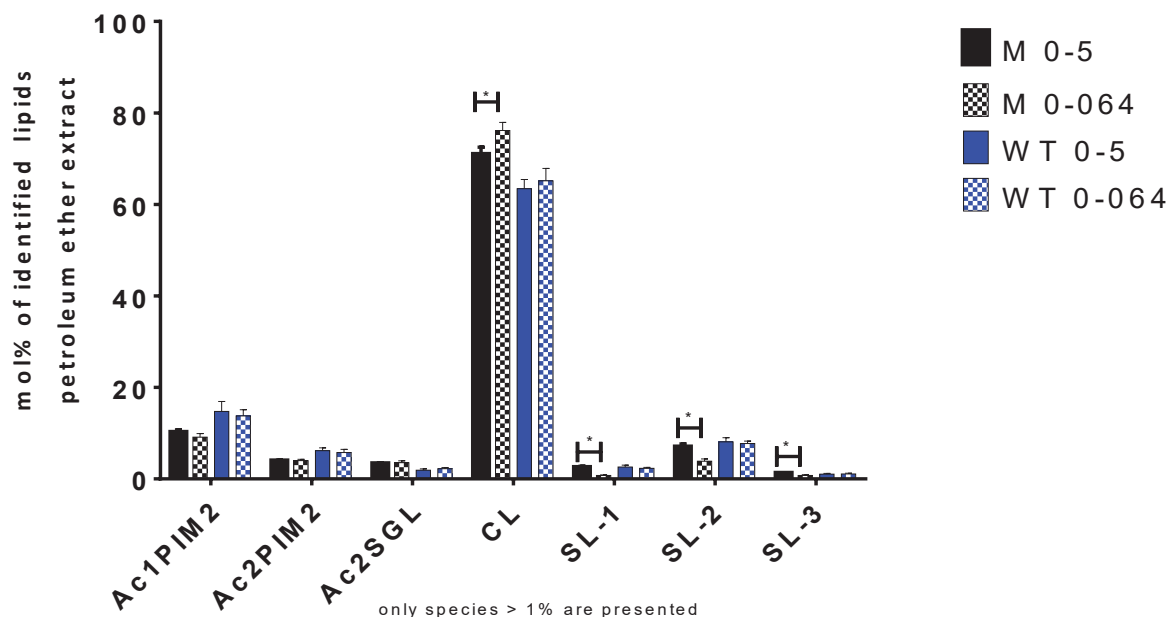
Phospholipids in methanolic mycobacterial lipid extracts



S21 Fig. Liquid chromatography coupled with mass spectrometry (LC-MS) analysis of *M. tuberculosis* c-Rv0225-tet-on mutant methanol fractions.

126 phospholipids were identified. No significant differences in lipid class distribution of fully induced and partially silenced mutant has been detected. Multiple t-test, FDR 1%; performed by the Department of Bioanalytical Chemistry, The German Center for Infection Research (DZIF) in Borstel (GER), Dominik Schwudke.

Identified Lipids in Petroleum ether Phase

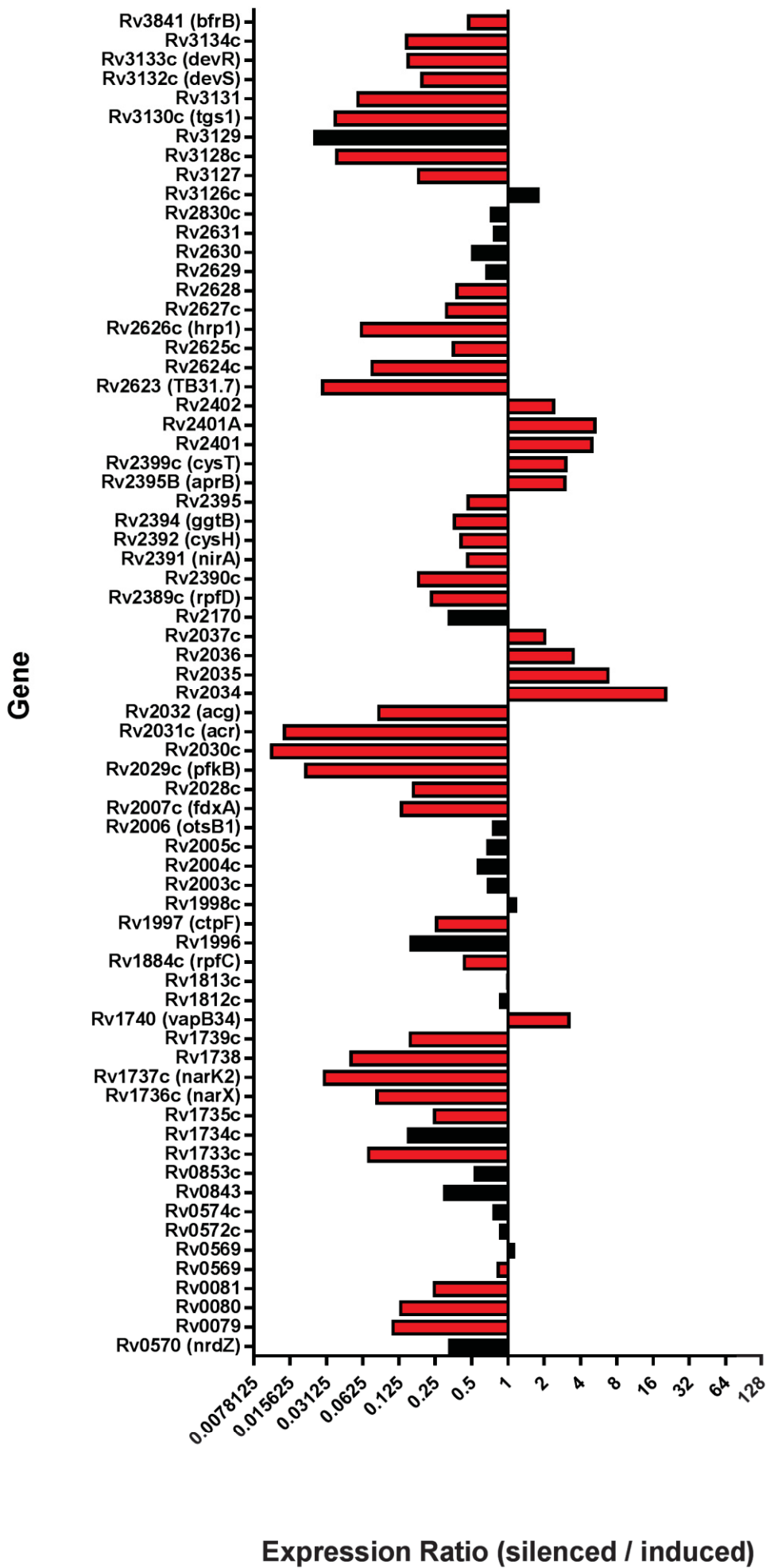


S22 Fig. Electrospray ionization mass spectrometry analysis (ESI-MS) of *M. tuberculosis* c-Rv0225-tet-on mutant petroleum ether fractions lead to identification of significant differences in cardiolipin and sulfolipid composition.

293 lipid species (25 different lipid classes) were identified. Significant increases have been found in the CL composition of the silenced mutant in comparison to the fully induced mutant, whereas diverse SLs were significant increased in the fully induced mutant. Abbreviations: PG, phosphatidylglycerol; PE, phosphatidyl-ethanolamine; PI, phosphatidylinositol; LPE, lysophosphatidylethanolamine; LPG, lysophosphatidyl-glycerol; LPI, Lysophosphatidylinositol; SL-1, Sulfolipid-1; SL-2, Sulfolipid-2; SL-3, Sulfolipid-3; ACnPI Mn, acylphosphatidylinositolmannosides*; CL, cardiolipin*; free methoxy Mycolic acids*; PIM6, phosphatidylinositolmannoside 6*; *not shown (below 1mol%); multiple t tests FDR 1%. Values are means of triplicates \pm SEM. Performed by the Department of Bioanalytical Chemistry, The German Center for Infection Research (DZIF) in Borstel (GER), Dominik Schwudke.

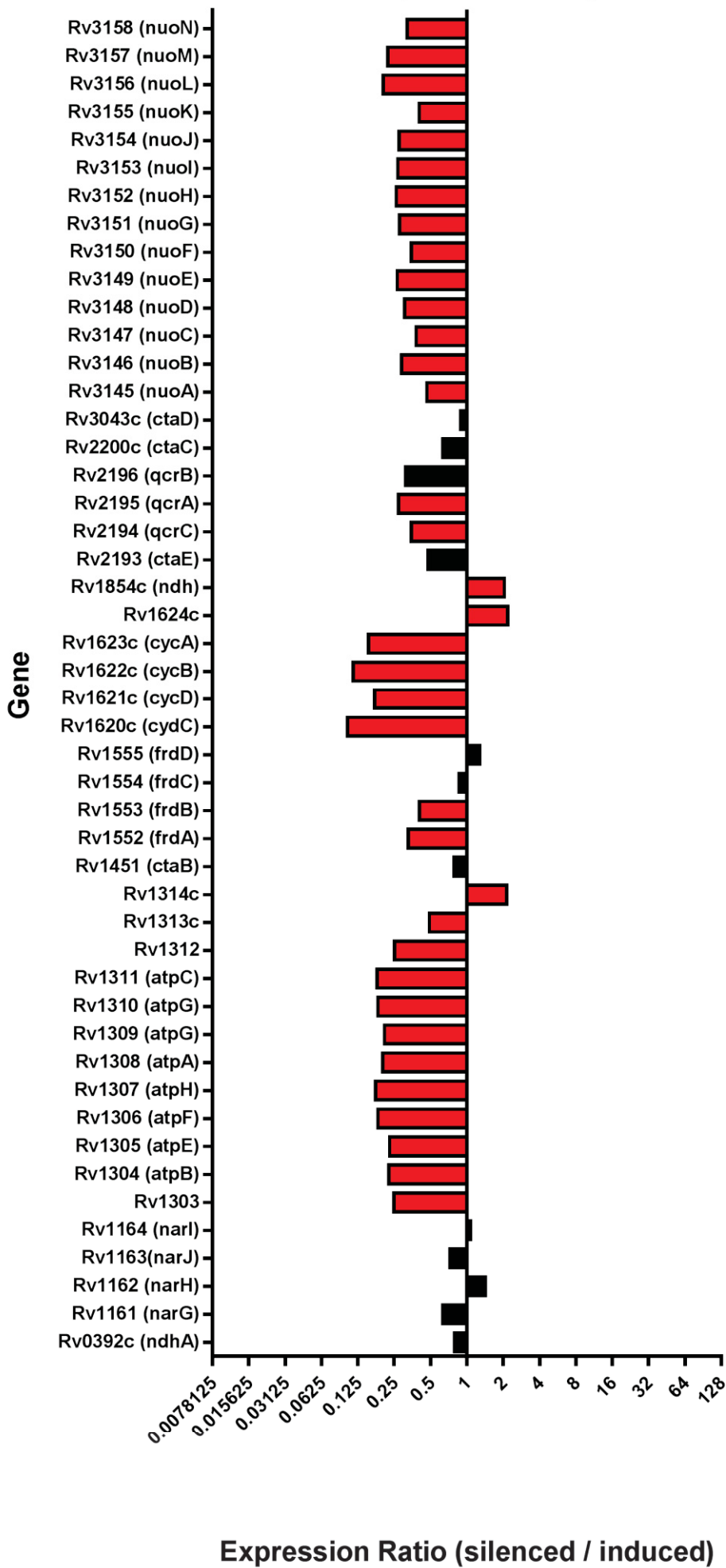
A

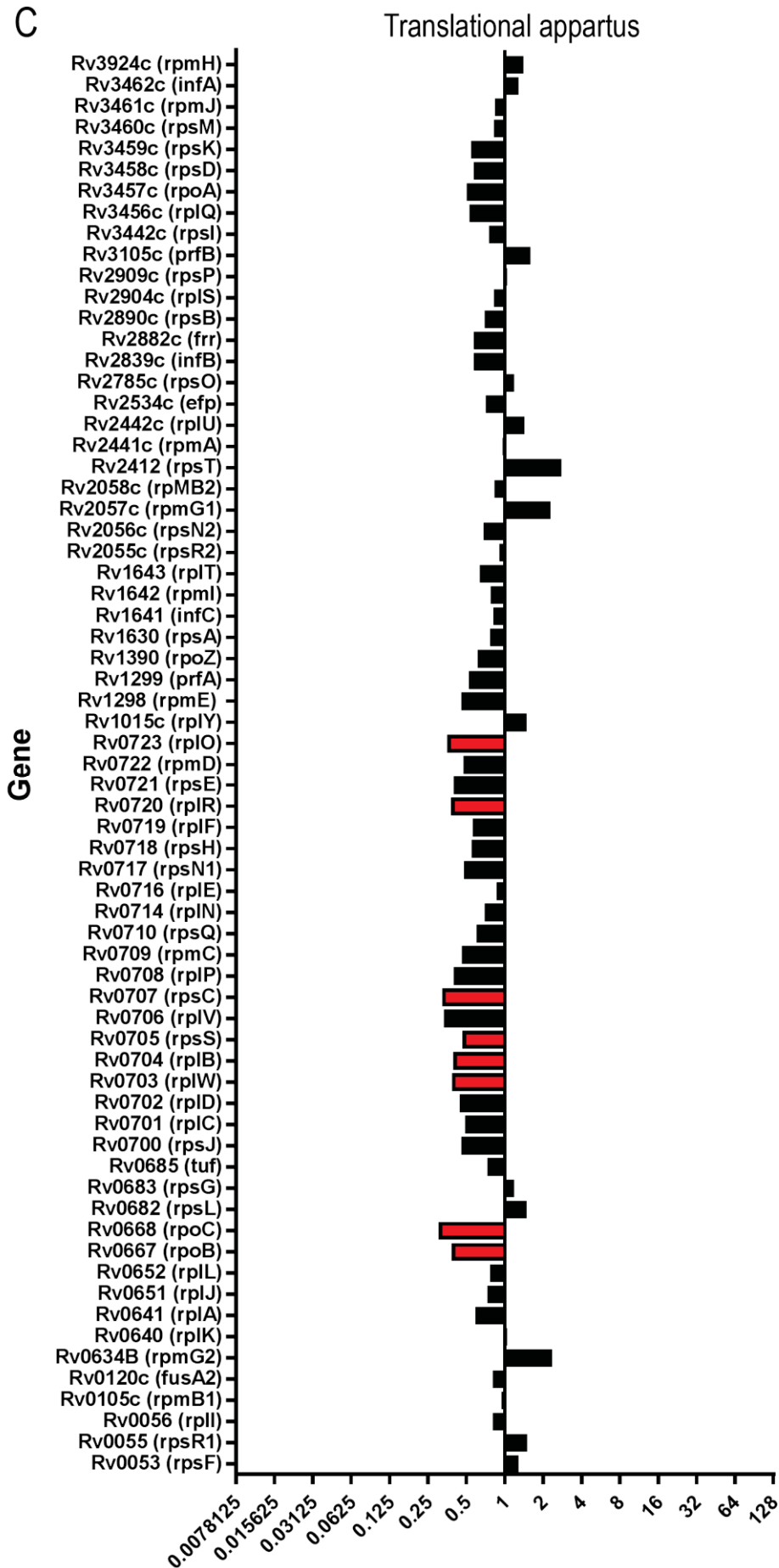
DosR regulon



B

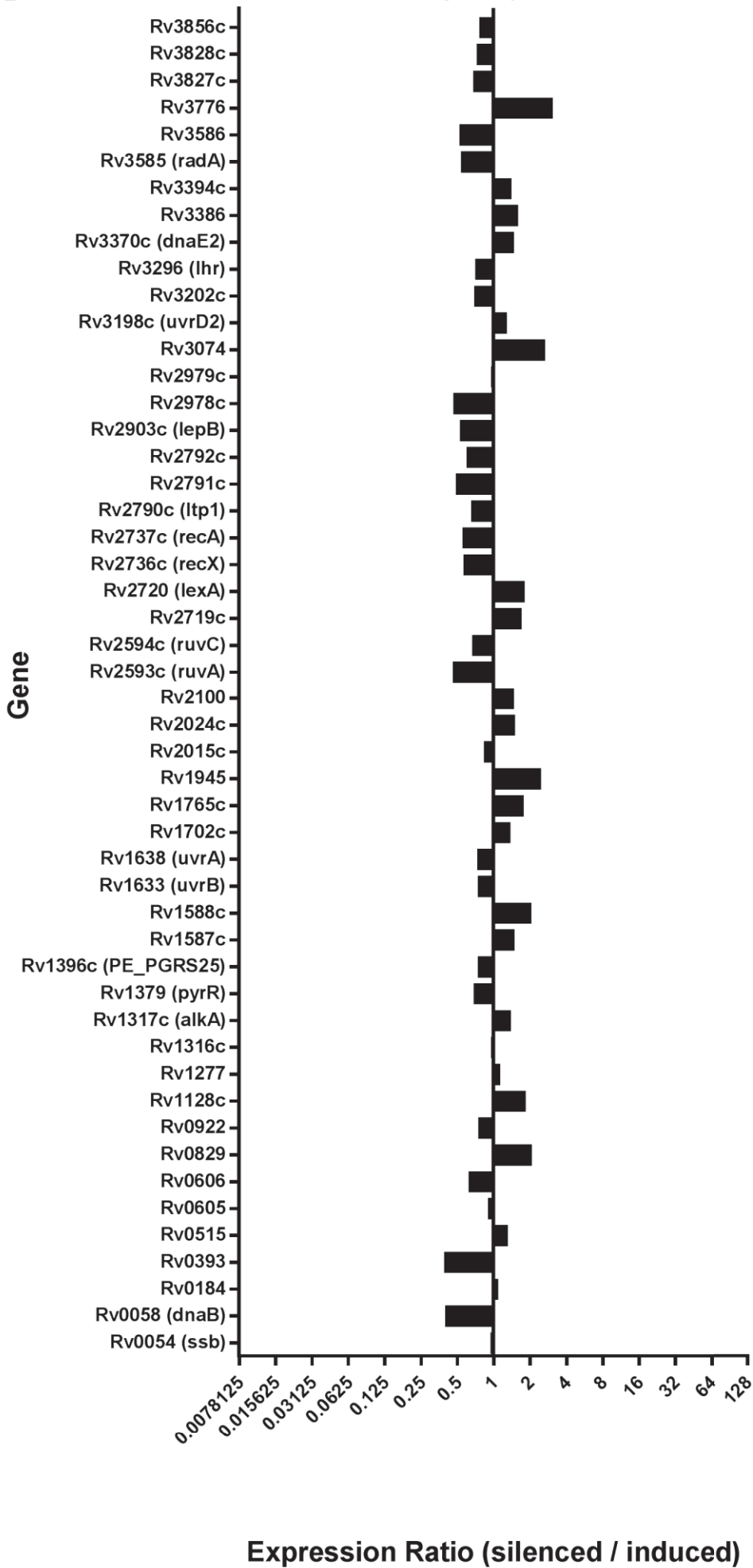
Electron transport chain: ATP synthesis





D

DNA-damage-response



S23 Fig. Differential gene expression of pathway responsive genes in induced and partially silenced cells of the conditional *M. tuberculosis* c-Rv0225-tet-on mutant.

Cells were cultivated either in presence of 100 ng/ml (100% growth relative to WT) or 10 ng/ml ATc (ca. 30% residual growth relative to WT) for 7 days. rRNA-depleted samples were analyzed by RNAseq. Genes with corrected p-values <0.01 are shown in red. Black are not significantly regulated genes.

9 References

1. Cambau E, Drancourt M. Steps towards the discovery of *Mycobacterium tuberculosis* by Robert Koch, 1882. *Clin Microbiol Infect*. 2014;20(3):196-201. doi: 10.1111/1469-0691.12555. PubMed PMID: 24450600.
2. Pai M, Behr MA, Dowdy D, Dheda K, Divangahi M, Boehme CC, et al. Tuberculosis. *Nat Rev Dis Primers*. 2016;2:16076. doi: 10.1038/nrdp.2016.76. PubMed PMID: 27784885.
3. Dorhoi A, Kaufmann SH. Perspectives on host adaptation in response to *Mycobacterium tuberculosis*: modulation of inflammation. *Semin Immunol*. 2014;26(6):533-42. doi: 10.1016/j.smim.2014.10.002. PubMed PMID: 25453228.
4. Modlin RL, Bloom BR. TB or not TB: that is no longer the question. *Sci Transl Med*. 2013;5(213):213sr6. doi: 10.1126/scitranslmed.3007402. PubMed PMID: 24285487.
5. Manzanillo PS, Shiloh MU, Portnoy DA, Cox JS. *Mycobacterium Tuberculosis* Activates the DNA-Dependent Cytosolic Surveillance Pathway within Macrophages. *Cell Host & Microbe*. 2012;11(5):469-80. doi: 10.1016/j.chom.2012.03.007. PubMed PMID: WOS:000304794500008.
6. Pieters J. *Mycobacterium tuberculosis* and the macrophage: maintaining a balance. *Cell Host Microbe*. 2008;3(6):399-407. doi: 10.1016/j.chom.2008.05.006. PubMed PMID: 18541216.
7. Gengenbacher M, Kaufmann SH. *Mycobacterium tuberculosis*: success through dormancy. *FEMS Microbiol Rev*. 2012;36(3):514-32. doi: 10.1111/j.1574-6976.2012.00331.x. PubMed PMID: 22320122; PubMed Central PMCID: PMC3319523.
8. Ramakrishnan L. Revisiting the role of the granuloma in tuberculosis. *Nat Rev Immunol*. 2012;12(5):352-66. doi: 10.1038/nri3211. PubMed PMID: 22517424.
9. Lin PL, Flynn JL. Understanding latent tuberculosis: a moving target. *J Immunol*. 2010;185(1):15-22. doi: 10.4049/jimmunol.0903856. PubMed PMID: 20562268; PubMed Central PMCID: PMC3311959.
10. Ndlovu H, Marakalala MJ. Granulomas and Inflammation: Host-Directed Therapies for Tuberculosis. *Front Immunol*. 2016;7:434. doi: 10.3389/fimmu.2016.00434. PubMed PMID: 27822210; PubMed Central PMCID: PMC45075764.
11. Manabe YC, Bishai WR. Latent *Mycobacterium tuberculosis*-persistence, patience, and winning by waiting. *Nat Med*. 2000;6(12):1327-9. doi: 10.1038/82139. PubMed PMID: 11100115.
12. Organisation WH. Global Tuberculosis Report 2016.
13. Zhao Y, Xu S, Wang L, Chin DP, Wang S, Jiang G, et al. National survey of drug-resistant tuberculosis in China. *N Engl J Med*. 2012;366(23):2161-70. doi: 10.1056/NEJMoa1108789. PubMed PMID: 22670902.
14. Organisation WH. Global Tuberculosis Report 2015.
15. Udwadia ZF, Amale RA, Ajbani KK, Rodrigues C. Totally drug-resistant tuberculosis in India. *Clin Infect Dis*. 2012;54(4):579-81. doi: 10.1093/cid/cir889. PubMed PMID: 22190562.
16. Pawlowski A, Jansson M, Skold M, Rottenberg ME, Kallenius G. Tuberculosis and HIV co-infection. *PLoS Pathog*. 2012;8(2):e1002464. doi: 10.1371/journal.ppat.1002464. PubMed PMID: 22363214; PubMed Central PMCID: PMC3280977.
17. Prezzemolo T, Guggino G, La Manna MP, Di Liberto D, Dieli F, Caccamo N. Functional Signatures of Human CD4 and CD8 T Cell Responses to *Mycobacterium tuberculosis*. *Front Immunol*. 2014;5:180. doi: 10.3389/fimmu.2014.00180. PubMed PMID: 24795723; PubMed Central PMCID: PMC4001014.
18. Maartens G, Celum C, Lewin SR. HIV infection: epidemiology, pathogenesis, treatment, and prevention. *Lancet*. 2014;384(9939):258-71. doi: 10.1016/S0140-6736(14)60164-1. PubMed PMID: 24907868.
19. Cohen T, Murray M, Wallengren K, Alvarez GG, Samuel EY, Wilson D. The Prevalence and Drug Sensitivity of Tuberculosis among Patients Dying in Hospital in KwaZulu-Natal, South Africa: A Postmortem Study. *Plos Medicine*. 2010;7(6). doi: ARTN e1000296
- 10.1371/journal.pmed.1000296. PubMed PMID: WOS:000279400000016.
20. Dowdy DW, Golub JE, Chaisson RE, Saraceni V. Heterogeneity in tuberculosis transmission and the role of geographic hotspots in propagating epidemics. *Proc Natl Acad Sci U S A*. 2012;109(24):9557-62. doi: 10.1073/pnas.1203517109. PubMed PMID: 22645356; PubMed Central PMCID: PMC3386125.
21. Hawgood BJ. Albert Calmette (1863-1933) and Camille Guérin (1872-1961): the C and G of BCG vaccine. *J Med Biogr*. 2007;15(3):139-46. PubMed PMID: 17641786.

22. Zwerling A, Behr MA, Verma A, Brewer TF, Menzies D, Pai M. The BCG World Atlas: a database of global BCG vaccination policies and practices. *PLoS Med*. 2011;8(3):e1001012. doi: 10.1371/journal.pmed.1001012. PubMed PMID: 21445325; PubMed Central PMCID: PMC3062527.
23. Pereira SM, Dantas OM, Ximenes R, Barreto ML. [BCG vaccine against tuberculosis: its protective effect and vaccination policies]. *Rev Saude Publica*. 2007;41 Suppl 1:59-66. PubMed PMID: 18038092.
24. Nuttall JJ, Eley BS. BCG Vaccination in HIV-Infected Children. *Tuberc Res Treat*. 2011;2011:712736. doi: 10.1155/2011/712736. PubMed PMID: 22567268; PubMed Central PMCID: PMC3335547.
25. Campbell EA, Korzheva N, Mustaev A, Murakami K, Nair S, Goldfarb A, et al. Structural mechanism for rifampicin inhibition of bacterial rna polymerase. *Cell*. 2001;104(6):901-12. PubMed PMID: 11290327.
26. Organisation WH. Guidelines for treatment of drug-susceptible tuberculosis and patient care (2017).
27. Organisation WH. WHO consolidated guidelines on drug-resistant tuberculosis treatment (2018).
28. Jankute M, Cox JA, Harrison J, Besra GS. Assembly of the Mycobacterial Cell Wall. *Annu Rev Microbiol*. 2015;69:405-23. doi: 10.1146/annurev-micro-091014-104121. PubMed PMID: 26488279.
29. Marrakchi H, Laneelle MA, Daffe M. Mycolic acids: structures, biosynthesis, and beyond. *Chem Biol*. 2014;21(1):67-85. doi: 10.1016/j.chembiol.2013.11.011. PubMed PMID: 24374164.
30. Angala SK, Belardinelli JM, Huc-Claustre E, Wheat WH, Jackson M. The cell envelope glycoconjugates of *Mycobacterium tuberculosis*. *Crit Rev Biochem Mol Biol*. 2014;49(5):361-99. doi: 10.3109/10409238.2014.925420. PubMed PMID: 24915502; PubMed Central PMCID: PMC34436706.
31. Abrahams KA, Besra GS. Mycobacterial cell wall biosynthesis: a multifaceted antibiotic target. *Parasitology*. 2016;1-18. doi: 10.1017/S0031182016002377. PubMed PMID: 27976597.
32. Boldrin F, Ventura M, Degiacomi G, Ravishankar S, Sala C, Svetlikova Z, et al. The phosphatidyl-myo-inositol mannosyltransferase PimA is essential for *Mycobacterium tuberculosis* growth in vitro and in vivo. *J Bacteriol*. 2014;196(19):3441-51. doi: 10.1128/JB.01346-13. PubMed PMID: 25049093; PubMed Central PMCID: PMC4187664.
33. Ortalo-Magne A, Lemassu A, Laneelle MA, Bardou F, Silve G, Gounon P, et al. Identification of the surface-exposed lipids on the cell envelopes of *Mycobacterium tuberculosis* and other mycobacterial species. *J Bacteriol*. 1996;178(2):456-61. PubMed PMID: 8550466; PubMed Central PMCID: PMC177678.
34. Guerin ME, Kordulakova J, Alzari PM, Brennan PJ, Jackson M. Molecular basis of phosphatidyl-myo-inositol mannoside biosynthesis and regulation in mycobacteria. *J Biol Chem*. 2010;285(44):33577-83. Epub 2010/08/31. doi: 10.1074/jbc.R110.168328. PubMed PMID: 20801880; PubMed Central PMCID: PMC2962455.
35. Maeda N, Nigou J, Herrmann JL, Jackson M, Amara A, Lagrange PH, et al. The cell surface receptor DC-SIGN discriminates between *Mycobacterium* species through selective recognition of the mannose caps on lipoarabinomannan. *Journal of Biological Chemistry*. 2003;278(8):5513-6. doi: 10.1074/jbc.C200586200. PubMed PMID: WOS:000181129400006.
36. Mishra AK, Driessen NN, Appelmeik BJ, Besra GS. Lipoarabinomannan and related glycoconjugates: structure, biogenesis and role in *Mycobacterium tuberculosis* physiology and host-pathogen interaction. *FEMS Microbiol Rev*. 2011;35(6):1126-57. doi: 10.1111/j.1574-6976.2011.00276.x. PubMed PMID: 21521247; PubMed Central PMCID: PMC3229680.
37. Nigou J, Gilleron M, Rojas M, Garcia LF, Thurnher M, Puzo G. Mycobacterial lipoarabinomannans: modulators of dendritic cell function and the apoptotic response. *Microbes Infect*. 2002;4(9):945-53. PubMed PMID: 12106787.
38. Schlesinger LS, Hull SR, Kaufman TM. Binding of the terminal mannosyl units of lipoarabinomannan from a virulent strain of *Mycobacterium tuberculosis* to human macrophages. *J Immunol*. 1994;152(8):4070-9. PubMed PMID: 8144972.
39. Schleifer KH, Kandler O. Peptidoglycan Types of Bacterial Cell-Walls and Their Taxonomic Implications. *Bacteriological Reviews*. 1972;36(4):407-77. PubMed PMID: WOS:A1972O878300001.
40. van Heijenoort J. Formation of the glycan chains in the synthesis of bacterial peptidoglycan. *Glycobiology*. 2001;11(3):25R-36R. PubMed PMID: 11320055.
41. Mcneil M, Daffe M, Brennan PJ. Evidence for the Nature of the Link between the Arabinogalactan and Peptidoglycan of Mycobacterial Cell-Walls. *Journal of Biological Chemistry*. 1990;265(30):18200-6. PubMed PMID: WOS:A1990EE20100031.
42. Mcneil M, Wallner SJ, Hunter SW, Brennan PJ. Demonstration That the Galactosyl and Arabinosyl Residues in the Cell-Wall Arabinogalactan of *Mycobacterium-Leprae* and *Mycobacterium-Tuberculosis* Are Furanoid.

- Carbohydrate Research. 1987;166(2):299-308. doi: Doi 10.1016/0008-6215(87)80065-4. PubMed PMID: WOS:A1987K397400011.
43. Draper P, Khoo KH, Chatterjee D, Dell A, Morris HR. Galactosamine in walls of slow-growing mycobacteria. *Biochem J.* 1997;327 (Pt 2):519-25. PubMed PMID: 9359425; PubMed Central PMCID: PMCPMC1218825.
 44. Bhamidi S, Scherman MS, Rithner CD, Prenni JE, Chatterjee D, Khoo KH, et al. The identification and location of succinyl residues and the characterization of the interior arabinan region allow for a model of the complete primary structure of *Mycobacterium tuberculosis* mycolyl arabinogalactan. *J Biol Chem.* 2008;283(19):12992-3000. doi: 10.1074/jbc.M800222200. PubMed PMID: 18303028; PubMed Central PMCID: PMCPMC2442352.
 45. Liu J, Barry CE, 3rd, Besra GS, Nikaido H. Mycolic acid structure determines the fluidity of the mycobacterial cell wall. *J Biol Chem.* 1996;271(47):29545-51. PubMed PMID: 8939881.
 46. Glickman MS, Cox JS, Jacobs WR. A novel mycolic acid cyclopropane synthetase is required for cording, persistence, and virulence of *Mycobacterium tuberculosis*. *Molecular Cell.* 2000;5(4):717-27. doi: Doi 10.1016/S1097-2765(00)80250-6. PubMed PMID: WOS:000086790000012.
 47. Takayama K, Wang C, Besra GS. Pathway to synthesis and processing of mycolic acids in *Mycobacterium tuberculosis*. *Clin Microbiol Rev.* 2005;18(1):81-101. doi: 10.1128/CMR.18.1.81-101.2005. PubMed PMID: 15653820; PubMed Central PMCID: PMCPMC544180.
 48. Qureshi N, Takayama K, Jordi HC, Schnoes HK. Characterization of the purified components of a new homologous series of alpha-mycolic acids from *Mycobacterium tuberculosis* H37Ra. *J Biol Chem.* 1978;253(15):5411-7. PubMed PMID: 97292.
 49. Barry CE, 3rd, Lee RE, Mdluli K, Sampson AE, Schroeder BG, Slayden RA, et al. Mycolic acids: structure, biosynthesis and physiological functions. *Prog Lipid Res.* 1998;37(2-3):143-79. PubMed PMID: 9829124.
 50. Gavalda S, Leger M, van der Rest B, Stella A, Bardou F, Montrozier H, et al. The Pks13/FadD32 crosstalk for the biosynthesis of mycolic acids in *Mycobacterium tuberculosis*. *J Biol Chem.* 2009;284(29):19255-64. doi: 10.1074/jbc.M109.006940. PubMed PMID: 19436070; PubMed Central PMCID: PMCPMC2740550.
 51. Kalscheuer R, Koliwer-Brandl H. Genetics of *Mycobacterial* Trehalose Metabolism. *Microbiol Spectr.* 2014;2(3). doi: 10.1128/microbiolspec.MGM2-0002-2013. PubMed PMID: 26103976.
 52. Ishikawa E, Mori D, Yamasaki S. Recognition of *Mycobacterial* Lipids by Immune Receptors. *Trends Immunol.* 2017;38(1):66-76. doi: 10.1016/j.it.2016.10.009. PubMed PMID: 27889398.
 53. Day TA, Mittler JE, Nixon MR, Thompson C, Miner MD, Hickey MJ, et al. *Mycobacterium tuberculosis* strains lacking surface lipid phthiocerol dimycocerosate are susceptible to killing by an early innate host response. *Infect Immun.* 2014;82(12):5214-22. doi: 10.1128/IAI.01340-13. PubMed PMID: 25287926; PubMed Central PMCID: PMCPMC4249296.
 54. Kaur D, Guerin ME, Škovierová H, Brennan PJ, Jackson M. Chapter 2 Biogenesis of the Cell Wall and Other Glycoconjugates of *Mycobacterium tuberculosis*. 2009;69:23-78. doi: 10.1016/s0065-2164(09)69002-x.
 55. Sambou T, Dinadayala P, Stadthagen G, Barilone N, Bordat Y, Constant P, et al. Capsular glucan and intracellular glycogen of *Mycobacterium tuberculosis*: biosynthesis and impact on the persistence in mice. *Mol Microbiol.* 2008;70(3):762-74. doi: 10.1111/j.1365-2958.2008.06445.x. PubMed PMID: 18808383; PubMed Central PMCID: PMCPMC2581643.
 56. Koliwer-Brandl H, Syson K, van de Weerd R, Chandra G, Appelmelk B, Alber M, et al. Metabolic Network for the Biosynthesis of Intra- and Extracellular alpha-Glucans Required for Virulence of *Mycobacterium tuberculosis*. *PLoS Pathog.* 2016;12(8):e1005768. doi: 10.1371/journal.ppat.1005768. PubMed PMID: 27513637; PubMed Central PMCID: PMCPMC4981310.
 57. Elbein AD, Pan YT, Pastuszak I, Carroll D. New insights on trehalose: a multifunctional molecule. *Glycobiology.* 2003;13(4):17R-27R. doi: 10.1093/glycob/cwg047. PubMed PMID: 12626396.
 58. M. B. Sur le trehalose, nouvelle espece de sucre. *Compt Rend Hebd Seanc Acad Sci, Paris* 1858;(46):1276-9.
 59. Liebl M, Nelius V, Kamp G, Ando O, Wegener G. Fate and effects of the trehalase inhibitor trehazolin in the migratory locust (*Locusta migratoria*). *J Insect Physiol.* 2010;56(6):567-74. doi: 10.1016/j.jinsphys.2009.11.021. PubMed PMID: 19958774.
 60. Arguelles JC. Physiological roles of trehalose in bacteria and yeasts: a comparative analysis. *Arch Microbiol.* 2000;174(4):217-24. PubMed PMID: 11081789.
 61. Jain NK, Roy I. Effect of trehalose on protein structure. *Protein Sci.* 2009;18(1):24-36. doi: 10.1002/pro.3. PubMed PMID: 19177348; PubMed Central PMCID: PMCPMC2708026.

62. Kandror O, DeLeon A, Goldberg AL. Trehalose synthesis is induced upon exposure of *Escherichia coli* to cold and is essential for viability at low temperatures. *Proceedings of the National Academy of Sciences of the United States of America*. 2002;99(15):9727-32. doi: 10.1073/pnas.142314099. PubMed PMID: WOS:000177042400025.
63. Singer MA, Lindquist S. Multiple effects of trehalose on protein folding in vitro and in vivo. *Mol Cell*. 1998;1(5):639-48. PubMed PMID: 9660948.
64. Lu H, Zhu ZY, Dong LL, Jia XM, Sun XR, Yan L, et al. Lack of Trehalose Accelerates H₂O₂-Induced *Candida albicans* Apoptosis through Regulating Ca²⁺ Signaling Pathway and Caspase Activity. *Plos One*. 2011;6(1). doi: ARTN e15808
10.1371/journal.pone.0015808. PubMed PMID: WOS:000286511200015.
65. Cardoso FS, Castro RF, Borges N, Santos H. Biochemical and genetic characterization of the pathways for trehalose metabolism in *Propionibacterium freudenreichii*, and their role in stress response. *Microbiology-Sgm*. 2007;153:270-80. doi: 10.1099/mic.0.29262-0. PubMed PMID: WOS:000243545300028.
66. Djonovic S, Urbach JM, Drenkard E, Bush J, Feinbaum R, Ausubel JL, et al. Trehalose biosynthesis promotes *Pseudomonas aeruginosa* pathogenicity in plants. *PLoS Pathog*. 2013;9(3):e1003217. doi: 10.1371/journal.ppat.1003217. PubMed PMID: 23505373; PubMed Central PMCID: PMC3591346.
67. Grzegorzewicz AE, Pham H, Gundi VA, Scherman MS, North EJ, Hess T, et al. Inhibition of mycolic acid transport across the *Mycobacterium tuberculosis* plasma membrane. *Nat Chem Biol*. 2012;8(4):334-41. doi: 10.1038/nchembio.794. PubMed PMID: 22344175; PubMed Central PMCID: PMC3307863.
68. Kalscheuer R, Weinrick B, Veeraraghavan U, Besra GS, Jacobs WR. Trehalose-recycling ABC transporter LpqY-SugA-SugB-SugC is essential for virulence of *Mycobacterium tuberculosis*. *Proceedings of the National Academy of Sciences of the United States of America*. 2010;107(50):21761-6. doi: 10.1073/pnas.1014642108. PubMed PMID: WOS:000285521500096.
69. Marrero J, Rhee KY, Schnappinger D, Pethe K, Ehrt S. Gluconeogenic carbon flow of tricarboxylic acid cycle intermediates is critical for *Mycobacterium tuberculosis* to establish and maintain infection. *Proc Natl Acad Sci U S A*. 2010;107(21):9819-24. Epub 2010/05/05. doi: 10.1073/pnas.1000715107. PubMed PMID: 20439709; PubMed Central PMCID: PMC2906907.
70. Martinez-Esparza M, Martinez-Vicente E, Gonzalez-Parraga P, Ros JM, Garcia-Penarrubia P, Arguelles JC. Role of trehalose-6P phosphatase (TPS2) in stress tolerance and resistance to macrophage killing in *Candida albicans*. *Int J Med Microbiol*. 2009;299(6):453-64. doi: 10.1016/j.ijmm.2008.12.001. PubMed PMID: 19231283.
71. Van Dijck P. Disruption of the *Candida albicans* TPS2 Gene Encoding Trehalose-6-Phosphate Phosphatase Decreases Infectivity without Affecting Hypha Formation. *Infection and Immunity*. 2002;70(4):1772-82. doi: 10.1128/iai.70.4.1772-1782.2002.
72. Zaragoza O, de Virgilio C, Ponton J, Gancedo C. Disruption in *Candida albicans* of the TPS2 gene encoding trehalose-6-phosphate phosphatase affects cell integrity and decreases infectivity. *Microbiology*. 2002;148(Pt 5):1281-90. doi: 10.1099/00221287-148-5-1281. PubMed PMID: 11988502.
73. Petzold EW, Himmelreich U, Mylonakis E, Rude T, Toffaletti D, Cox GM, et al. Characterization and regulation of the trehalose synthesis pathway and its importance in the pathogenicity of *Cryptococcus neoformans*. *Infect Immun*. 2006;74(10):5877-87. doi: 10.1128/IAI.00624-06. PubMed PMID: 16988267; PubMed Central PMCID: PMC1594924.
74. Ngamskulrungron P, Himmelreich U, Breger JA, Wilson C, Chayakulkeeree M, Krockenberger MB, et al. The trehalose synthesis pathway is an integral part of the virulence composite for *Cryptococcus gattii*. *Infect Immun*. 2009;77(10):4584-96. doi: 10.1128/IAI.00565-09. PubMed PMID: 19651856; PubMed Central PMCID: PMC2747965.
75. Song XS, Li HP, Zhang JB, Song B, Huang T, Du XM, et al. Trehalose 6-phosphate phosphatase is required for development, virulence and mycotoxin biosynthesis apart from trehalose biosynthesis in *Fusarium graminearum*. *Fungal Genet Biol*. 2014;63:24-41. doi: 10.1016/j.fgb.2013.11.005. PubMed PMID: 24291007.
76. Puttikamonkul S, Willger SD, Grahl N, Perfect JR, Movahed N, Bothner B, et al. Trehalose 6-phosphate phosphatase is required for cell wall integrity and fungal virulence but not trehalose biosynthesis in the human fungal pathogen *Aspergillus fumigatus*. *Mol Microbiol*. 2010;77(4):891-911. doi: 10.1111/j.1365-2958.2010.07254.x. PubMed PMID: 20545865; PubMed Central PMCID: PMC2954268.
77. Farelli JD, Galvin BD, Li Z, Liu C, Aono M, Garland M, et al. Structure of the trehalose-6-phosphate phosphatase from *Brugia malayi* reveals key design principles for anthelmintic drugs. *PLoS Pathog*.

- 2014;10(7):e1004245. doi: 10.1371/journal.ppat.1004245. PubMed PMID: 24992307; PubMed Central PMCID: PMC4081830.
78. Belisle JT. Role of the Major Antigen of *Mycobacterium tuberculosis* in Cell Wall Biogenesis. *Science*. 1997;276(5317):1420-2. doi: 10.1126/science.276.5317.1420.
 79. Varela C, Rittmann D, Singh A, Krumbach K, Bhatt K, Eggeling L, et al. MmpL genes are associated with mycolic acid metabolism in mycobacteria and corynebacteria. *Chem Biol*. 2012;19(4):498-506. doi: 10.1016/j.chembiol.2012.03.006. PubMed PMID: 22520756; PubMed Central PMCID: PMC3370651.
 80. Takeuchi O, Akira S. Pattern recognition receptors and inflammation. *Cell*. 2010;140(6):805-20. doi: 10.1016/j.cell.2010.01.022. PubMed PMID: 20303872.
 81. Means TK, Wang S, Lien E, Yoshimura A, Golenbock DT, Fenton MJ. Human toll-like receptors mediate cellular activation by *Mycobacterium tuberculosis*. *J Immunol*. 1999;163(7):3920-7. PubMed PMID: 10490993.
 82. Werninghaus K, Babiak A, Gross O, Holscher C, Dietrich H, Agger EM, et al. Adjuvanticity of a synthetic cord factor analogue for subunit *Mycobacterium tuberculosis* vaccination requires FcRgamma-Syk-Card9-dependent innate immune activation. *J Exp Med*. 2009;206(1):89-97. doi: 10.1084/jem.20081445. PubMed PMID: 19139169; PubMed Central PMCID: PMC2626670.
 83. Schoenen H, Bodendorfer B, Hitchens K, Manzanero S, Werninghaus K, Nimmerjahn F, et al. Cutting edge: Mincle is essential for recognition and adjuvanticity of the mycobacterial cord factor and its synthetic analog trehalose-dibehenate. *J Immunol*. 2010;184(6):2756-60. doi: 10.4049/jimmunol.0904013. PubMed PMID: 20164423; PubMed Central PMCID: PMC2642336.
 84. Ishikawa E, Ishikawa T, Morita YS, Toyonaga K, Yamada H, Takeuchi O, et al. Direct recognition of the mycobacterial glycolipid, trehalose dimycolate, by C-type lectin Mincle. *J Exp Med*. 2009;206(13):2879-88. doi: 10.1084/jem.20091750. PubMed PMID: 20008526; PubMed Central PMCID: PMC2806462.
 85. Sueoka E, Nishiwaki S, Okabe S, Iida N, Suganuma M, Yano I, et al. Activation of protein kinase C by mycobacterial cord factor, trehalose 6-monomycolate, resulting in tumor necrosis factor- α release in mouse lung tissues. *Jpn J Cancer Res*. 1995;86(8):749-55. PubMed PMID: 7559098.
 86. Desel C, Werninghaus K, Ritter M, Jozefowski K, Wenzel J, Russkamp N, et al. The Mincle-activating adjuvant TDB induces MyD88-dependent Th1 and Th17 responses through IL-1R signaling. *PLoS One*. 2013;8(1):e53531. doi: 10.1371/journal.pone.0053531. PubMed PMID: 23308247; PubMed Central PMCID: PMC3538599.
 87. Matsunaga I, Naka T, Talekar RS, McConnell MJ, Katoh K, Nakao H, et al. Mycolyltransferase-mediated glycolipid exchange in *Mycobacteria*. *J Biol Chem*. 2008;283(43):28835-41. doi: 10.1074/jbc.M805776200. PubMed PMID: 18703502; PubMed Central PMCID: PMC2570876.
 88. Middlebrook G, Coleman CM, Schaefer WB. Sulfolipid from Virulent Tubercle Bacilli. *Proc Natl Acad Sci U S A*. 1959;45(12):1801-4. PubMed PMID: 16590578; PubMed Central PMCID: PMC222804.
 89. Goren MB, Brokl O, Das BC, Lederer E. Sulfolipid I of *Mycobacterium tuberculosis*, strain H37RV. Nature of the acyl substituents. *Biochemistry*. 1971;10(1):72-81. PubMed PMID: 4992189.
 90. Layre E, Paepe DC, Larrouy-Maumus G, Vaubourgeix J, Mundayoor S, Lindner B, et al. Deciphering sulfoglycolipids of *Mycobacterium tuberculosis*. *J Lipid Res*. 2011;52(6):1098-110. doi: 10.1194/jlr.M013482. PubMed PMID: 21482713; PubMed Central PMCID: PMC3090231.
 91. Chatterjee D, Brennan PJ. Glycosylated components of the mycobacterial cell wall. 2010:147-67. doi: 10.1016/b978-0-12-374546-0.00009-2.
 92. Daffe M, Papa F, Laszlo A, David HL. Glycolipids of recent clinical isolates of *Mycobacterium tuberculosis*: chemical characterization and immunoreactivity. *J Gen Microbiol*. 1989;135(10):2759-66. doi: 10.1099/00221287-135-10-2759. PubMed PMID: 2517299.
 93. Goren MB, Das BC, Brokl O. Sulfatide-III of *Mycobacterium-Tuberculosis* Strain H37rv. *Nouveau Journal De Chimie-New Journal of Chemistry*. 1978;2(4):379-84. PubMed PMID: WOS:A1978FH75200016.
 94. Lemassu A, Laneelle MA, Daffe M. Revised structure of a trehalose-containing immunoreactive glycolipid of *Mycobacterium tuberculosis*. *FEMS Microbiol Lett*. 1991;62(2-3):171-5. PubMed PMID: 1904042.
 95. Baer HH. The structure of an antigenic glycolipid (SL-IV) from *Mycobacterium tuberculosis*. *Carbohydrate Research*. 1993;240:1-22. doi: 10.1016/0008-6215(93)84167-5.
 96. Cruaud P, Yamashita JT, Casabona NM, Papa F, David HL. Evaluation of a novel 2,3-diacyl-trehalose-2'-sulphate (SL-IV) antigen for case finding and diagnosis of leprosy and tuberculosis. *Res Microbiol*. 1990;141(6):679-94. PubMed PMID: 2284503.

97. Gangadharam PRJ, Cohn ML, Middlebrook G. Infectivity, pathogenicity and sulpholipid fraction of some Indian and British strains of tubercle bacilli. *Tubercle*. 1963;44(4):452-5. doi: 10.1016/s0041-3879(63)80087-2.
98. Goren MB, Brokl O, Schaefer WB. Lipids of putative relevance to virulence in *Mycobacterium tuberculosis*: correlation of virulence with elaboration of sulfatides and strongly acidic lipids. *Infect Immun*. 1974;9(1):142-9. PubMed PMID: 4202886; PubMed Central PMCID: PMCPMC414778.
99. Kato M, Goren MB. Synergistic action of cord factor and mycobacterial sulfatides on mitochondria. *Infect Immun*. 1974;10(4):733-41. PubMed PMID: 4214779; PubMed Central PMCID: PMCPMC423014.
100. Rousseau C, Turner OC, Rush E, Bordat Y, Sirakova TD, Kolattukudy PE, et al. Sulfolipid Deficiency Does Not Affect the Virulence of *Mycobacterium tuberculosis* H37Rv in Mice and Guinea Pigs. *Infection and Immunity*. 2003;71(8):4684-90. doi: 10.1128/iai.71.8.4684-4690.2003.
101. Okamoto Y, Fujita Y, Naka T, Hirai M, Tomiyasu I, Yano I. Mycobacterial sulfolipid shows a virulence by inhibiting cord factor induced granuloma formation and TNF-alpha release. *Microb Pathog*. 2006;40(6):245-53. doi: 10.1016/j.micpath.2006.02.002. PubMed PMID: 16626929.
102. Goren MB, D'Arcy Hart P, Young MR, Armstrong JA. Prevention of phagosome-lysosome fusion in cultured macrophages by sulfatides of *Mycobacterium tuberculosis*. *Proc Natl Acad Sci U S A*. 1976;73(7):2510-4. PubMed PMID: 821057; PubMed Central PMCID: PMCPMC430628.
103. Pabst MJ, Gross JM, Brozna JP, Goren MB. Inhibition of macrophage priming by sulfatide from *Mycobacterium tuberculosis*. *J Immunol*. 1988;140(2):634-40. PubMed PMID: 2826597.
104. Zhang L, English D, Andersen BR. Activation of human neutrophils by *Mycobacterium tuberculosis*-derived sulfolipid-1. *J Immunol*. 1991;146(8):2730-6. PubMed PMID: 1849937.
105. Zhang L, Goren MB, Holzer TJ, Andersen BR. Effect of *Mycobacterium tuberculosis*-derived sulfolipid I on human phagocytic cells. *Infect Immun*. 1988;56(11):2876-83. PubMed PMID: 2844675; PubMed Central PMCID: PMCPMC259665.
106. Kalscheuer R, Syson K, Veeraraghavan U, Weinrick B, Biermann KE, Liu Z, et al. Self-poisoning of *Mycobacterium tuberculosis* by targeting GlgE in an alpha-glucan pathway. *Nat Chem Biol*. 2010;6(5):376-84. Epub 2010 Mar 21. doi: 10.1038/nchembio.340. PubMed PMID: 20305657; PubMed Central PMCID: PMCPMC3256575.
107. Miah F, Koliwer-Brandl H, Rejzek M, Field RA, Kalscheuer R, Bornemann S. Flux through Trehalose Synthase Flows from Trehalose to the Alpha Anomer of Maltose in *Mycobacteria*. *Chemistry & Biology*. 2013;20(4):487-93. doi: 10.1016/j.chembiol.2013.02.014. PubMed PMID: WOS:000318201700007.
108. Murphy HN, Stewart GR, Mischenko VV, Apt AS, Harris R, McAlister MS, et al. The OtsAB pathway is essential for trehalose biosynthesis in *Mycobacterium tuberculosis*. *J Biol Chem*. 2005;280(15):14524-9. doi: 10.1074/jbc.M414232200. PubMed PMID: 15703182.
109. Chapman GB, Hanks JH, Wallace JH. An electron microscope study of the disposition and fine structure of *Mycobacterium lepraemurium* in mouse spleen. *J Bacteriol*. 1959;77(2):205-11. PubMed PMID: 13630872; PubMed Central PMCID: PMCPMC290351.
110. Lemassu A, Daffe M. Structural features of the exocellular polysaccharides of *Mycobacterium tuberculosis*. *Biochem J*. 1994;297 (Pt 2):351-7. PubMed PMID: 8297342; PubMed Central PMCID: PMCPMC1137836.
111. Sani M, Houben EN, Geurtsen J, Pierson J, de Punder K, van Zon M, et al. Direct visualization by cryo-EM of the mycobacterial capsular layer: a labile structure containing ESX-1-secreted proteins. *PLoS Pathog*. 2010;6(3):e1000794. doi: 10.1371/journal.ppat.1000794. PubMed PMID: 20221442; PubMed Central PMCID: PMCPMC2832766.
112. Ortalo-Magne A, Dupont MA, Lemassu A, Andersen AB, Gounon P, Daffe M. Molecular composition of the outermost capsular material of the tubercle bacillus. *Microbiology*. 1995;141 (Pt 7):1609-20. Epub 1995/07/01. doi: 10.1099/13500872-141-7-1609. PubMed PMID: 7551029.
113. Lemassu A, Ortalo-Magne A, Bardou F, Silve G, Laneelle MA, Daffe M. Extracellular and surface-exposed polysaccharides of non-tuberculous mycobacteria. *Microbiology*. 1996;142 (Pt 6):1513-20. Epub 1996/06/01. doi: 10.1099/13500872-142-6-1513. PubMed PMID: 8704991.
114. Geurtsen J, Chedammi S, Mesters J, Cot M, Driessen NN, Sambou T, et al. Identification of mycobacterial alpha-glucan as a novel ligand for DC-SIGN: involvement of mycobacterial capsular polysaccharides in host immune modulation. *J Immunol*. 2009;183(8):5221-31. Epub 2009/09/29. doi: 10.4049/jimmunol.0900768. PubMed PMID: 19783687.

115. Cywes C1 HH, Daffé M, Ehlers MR. Nonopsonic Binding of *Mycobacterium tuberculosis* to Complement Receptor Type 3 Is Mediated by Capsular Polysaccharides and Is Strain Dependent. *Infection and Immunity*. 1997;65(10):4258–66. PubMed Central PMCID: PMC175611.
116. Gagliardi MC, Lemassu A, Teloni R, Mariotti S, Sargentini V, Pardini M, et al. Cell wall-associated alpha-glucan is instrumental for *Mycobacterium tuberculosis* to block CD1 molecule expression and disable the function of dendritic cell derived from infected monocyte. *Cellular Microbiology*. 2007;9(8):2081-92. doi: 10.1111/j.1462-5822.2007.00940.x. PubMed PMID: WOS:000248534700019.
117. Bittencourt VC, Figueiredo RT, da Silva RB, Mourao-Sa DS, Fernandez PL, Sasaki GL, et al. An alpha-glucan of *Pseudallescheria boydii* is involved in fungal phagocytosis and Toll-like receptor activation. *J Biol Chem*. 2006;281(32):22614-23. Epub 2006/06/13. doi: 10.1074/jbc.M511417200. PubMed PMID: 16766532.
118. Gagliardi MC, Lemassu A, Teloni R, Mariotti S, Sargentini V, Pardini M, et al. Cell wall-associated alpha-glucan is instrumental for *Mycobacterium tuberculosis* to block CD1 molecule expression and disable the function of dendritic cell derived from infected monocyte. *Cell Microbiol*. 2007;9(8):2081-92. Epub 2007/04/20. doi: 10.1111/j.1462-5822.2007.00940.x. PubMed PMID: 17441985.
119. Caner S, Nguyen N, Aguda A, Zhang R, Pan YT, Withers SG, et al. The structure of the *Mycobacterium smegmatis* trehalose synthase reveals an unusual active site configuration and acarbose-binding mode. *Glycobiology*. 2013;23(9):1075-83. doi: 10.1093/glycob/cwt044. PubMed PMID: 23735230; PubMed Central PMCID: PMC3724413.
120. Roy R, Usha V, Kermani A, Scott DJ, Hyde EI, Besra GS, et al. Synthesis of alpha-glucan in mycobacteria involves a hetero-octameric complex of trehalose synthase TreS and Maltokinase Pep2. *ACS Chem Biol*. 2013;8(10):2245-55. doi: 10.1021/cb400508k. PubMed PMID: 23901909; PubMed Central PMCID: PMC3805332.
121. Fraga J, Maranha A, Mendes V, Pereira PJ, Empadinhas N, Macedo-Ribeiro S. Structure of mycobacterial maltokinase, the missing link in the essential GlgE-pathway. *Sci Rep*. 2015;5:8026. doi: 10.1038/srep08026. PubMed PMID: 25619172; PubMed Central PMCID: PMC4306142.
122. Mendes V, Maranha A, Lamosa P, da Costa MS, Empadinhas N. Biochemical characterization of the maltokinase from *Mycobacterium bovis* BCG. *BMC Biochem*. 2010;11:21. doi: 10.1186/1471-2091-11-21. PubMed PMID: 20507595; PubMed Central PMCID: PMC2885305.
123. Syson K, Stevenson CE, Rashid AM, Saalbach G, Tang M, Tuukkanen A, et al. Structural insight into how *Streptomyces coelicolor* maltosyl transferase GlgE binds alpha-maltose 1-phosphate and forms a maltosyl-enzyme intermediate. *Biochemistry*. 2014;53(15):2494-504. doi: 10.1021/bi500183c. PubMed PMID: 24689960; PubMed Central PMCID: PMC4048318.
124. Syson K, Stevenson CE, Rejzek M, Fairhurst SA, Nair A, Bruton CJ, et al. Structure of *Streptomyces* maltosyltransferase GlgE, a homologue of a genetically validated anti-tuberculosis target. *J Biol Chem*. 2011;286(44):38298-310. doi: 10.1074/jbc.M111.279315. PubMed PMID: 21914799; PubMed Central PMCID: PMC3207445.
125. Chandra G, Chater KF, Bornemann S. Unexpected and widespread connections between bacterial glycogen and trehalose metabolism. *Microbiology-Sgm*. 2011;157:1565-72. doi: 10.1099/mic.0.044263-0. PubMed PMID: WOS:000292356200002.
126. Preiss J. Bacterial glycogen synthesis and its regulation. *Annu Rev Microbiol*. 1984;38:419-58. doi: 10.1146/annurev.mi.38.100184.002223. PubMed PMID: 6093684.
127. Stadthagen G, Sambou T, Guerin M, Barilone N, Boudou F, Kordulakova J, et al. Genetic basis for the biosynthesis of methylglucose lipopolysaccharides in *Mycobacterium tuberculosis*. *J Biol Chem*. 2007;282(37):27270-6. doi: 10.1074/jbc.M702676200. PubMed PMID: 17640872.
128. Kaur D, Pham H, Larrouy-Maumus G, Riviere M, Vissa V, Guerin ME, et al. Initiation of methylglucose lipopolysaccharide biosynthesis in mycobacteria. *PLoS One*. 2009;4(5):e5447. doi: 10.1371/journal.pone.0005447. PubMed PMID: 19421329; PubMed Central PMCID: PMC2674218.
129. Mendes V, Maranha A, Alarico S, Empadinhas N. Biosynthesis of mycobacterial methylglucose lipopolysaccharides. *Nat Prod Rep*. 2012;29(8):834-44. doi: 10.1039/c2np20014g. PubMed PMID: 22678749.
130. Jackson M, Brennan PJ. Polymethylated polysaccharides from *Mycobacterium* species revisited. *J Biol Chem*. 2009;284(4):1949-53. doi: 10.1074/jbc.R800047200. PubMed PMID: 18786916; PubMed Central PMCID: PMC2629103.

131. Lee YC. Isolation and characterization of lipopolysaccharides containing 6-O-methyl-D-glucose from *Mycobacterium* species. *J Biol Chem*. 1966;241(8):1899-908. PubMed PMID: 4957728.
132. Machida Y, Bloch K. Complex-Formation between Mycobacterial Polysaccharides and Fatty Acyl-CoA Derivatives. *Proceedings of the National Academy of Sciences of the United States of America*. 1973;70(4):1146-8. doi: DOI 10.1073/pnas.70.4.1146. PubMed PMID: WOS:A1973P380700042.
133. Keller J, Ballou CE. The 6-O-methylglucose-containing lipopolysaccharide of *Mycobacterium phlei*. Identification of the lipid components. *J Biol Chem*. 1968;243(11):2905-10. doi: 243, 2905-2910. . PubMed PMID: 4968183.
134. De P, McNeil M, Xia M, Boot CM, Hesser DC, Deneff K, et al. Structural determinants in a glucose-containing lipopolysaccharide from *Mycobacterium tuberculosis* critical for inducing a subset of protective T cells. *J Biol Chem*. 2018;293(25):9706-17. doi: 10.1074/jbc.RA118.002582. PubMed PMID: 29716995; PubMed Central PMCID: PMC6016469.
135. Machida Y, Bergeron R, Flick P, Bloch K. Effects of cyclodextrins on fatty acid synthesis. *J Biol Chem*. 1973;248(17):6246-7. PubMed PMID: 4726303.
136. Kamisango K, Dell A, Ballou CE. Biosynthesis of the mycobacterial O-methylglucose lipopolysaccharide. Characterization of putative intermediates in the initiation, elongation, and termination reactions. *J Biol Chem*. 1987;262(10):4580-6. PubMed PMID: 3558356.
137. Zhang Y, Chen C, Liu J, Deng H, Pan A, Zhang L, et al. Complete genome sequences of *Mycobacterium tuberculosis* strains CCDC5079 and CCDC5080, which belong to the Beijing family. *J Bacteriol*. 2011;193(19):5591-2. doi: 10.1128/JB.05452-11. PubMed PMID: 21914894; PubMed Central PMCID: PMC3187387.
138. Empadinhas N, da Costa MS. Diversity, biological roles and biosynthetic pathways for sugar-glycerate containing compatible solutes in bacteria and archaea. *Environ Microbiol*. 2011;13(8):2056-77. doi: 10.1111/j.1462-2920.2010.02390.x. PubMed PMID: 21176052.
139. Pereira PJ, Empadinhas N, Albuquerque L, Sa-Moura B, da Costa MS, Macedo-Ribeiro S. *Mycobacterium tuberculosis* glucosyl-3-phosphoglycerate synthase: structure of a key enzyme in methylglucose lipopolysaccharide biosynthesis. *PLoS One*. 2008;3(11):e3748. doi: 10.1371/journal.pone.0003748. PubMed PMID: 19015727; PubMed Central PMCID: PMC2581804.
140. Bardarov S, Bardarov S, Jr., Pavelka MS, Jr., Sambandamurthy V, Larsen M, Tufariello J, et al. Specialized transduction: an efficient method for generating marked and unmarked targeted gene disruptions in *Mycobacterium tuberculosis*, *M. bovis* BCG and *M. smegmatis*. *Microbiology*. 2002;148(Pt 10):3007-17. doi: 10.1099/00221287-148-10-3007. PubMed PMID: 12368434.
141. Jain P, Hsu T, Arai M, Biermann K, Thaler DS, Nguyen A, et al. Specialized transduction designed for precise high-throughput unmarked deletions in *Mycobacterium tuberculosis*. *MBio*. 2014;5(3):e01245-14. doi: 10.1128/mBio.01245-14. PubMed PMID: 24895308; PubMed Central PMCID: PMC4049104.
142. Larsen MH, Biermann K, Jacobs WR, Jr. Laboratory maintenance of *Mycobacterium tuberculosis*. *Curr Protoc Microbiol*. 2007;Chapter 10:Unit 10A 1. Epub 2008/09/05. doi: 10.1002/9780471729259.mc10a01s6. PubMed PMID: 18770602.
143. Stover CK, de la Cruz VF, Fuerst TR, Burlein JE, Benson LA, Bennett LT, et al. New use of BCG for recombinant vaccines. *Nature*. 1991;351(6326):456-60. doi: 10.1038/351456a0. PubMed PMID: 1904554.
144. Besra GS. Preparation of cell-wall fractions from mycobacteria. *Methods Mol Biol*. 1998;101:91-107. doi: 10.1385/0-89603-471-2:91. PubMed PMID: 9921472.
145. Mortazavi A, Williams BA, McCue K, Schaeffer L, Wold B. Mapping and quantifying mammalian transcriptomes by RNA-Seq. *Nat Methods*. 2008;5(7):621-8. doi: 10.1038/nmeth.1226. PubMed PMID: 18516045.
146. Ehrt S, Guo XV, Hickey CM, Ryou M, Monteleone M, Riley LW, et al. Controlling gene expression in mycobacteria with anhydrotetracycline and Tet repressor. *Nucleic Acids Res*. 2005;33(2):e21. doi: 10.1093/nar/gni013. PubMed PMID: 15687379; PubMed Central PMCID: PMC548372.
147. Bornemann S. alpha-Glucan biosynthesis and the GlgE pathway in *Mycobacterium tuberculosis*. *Biochem Soc Trans*. 2016;44(1):68-73. doi: 10.1042/BST20150181. PubMed PMID: 26862190.
148. Rashid AM, Batey SF, Syson K, Koliwer-Brandl H, Miah F, Barclay JE, et al. Assembly of alpha-Glucan by GlgE and GlgB in *Mycobacteria* and *Streptomyces*. *Biochemistry*. 2016;55(23):3270-84. doi: 10.1021/acs.biochem.6b00209. PubMed PMID: 27221142.

149. Kalscheuer R, Jacobs WR, Jr. The significance of GlgE as a new target for tuberculosis. *Drug News Perspect.* 2010;23(10):619-24. doi: 10.1358/dnp.2010.23.10.1534855. PubMed PMID: 21180647.
150. Yamada H, Yamaguchi M, Chikamatsu K, Aono A, Mitarai S. Structome analysis of virulent *Mycobacterium tuberculosis*, which survives with only 700 ribosomes per 0.1 fl of cytoplasm. *PLoS One.* 2015;10(1):e0117109. doi: 10.1371/journal.pone.0117109. PubMed PMID: 25629354; PubMed Central PMCID: PMC4309607.
151. De Virgilio C, Burckert N, Bell W, Jenö P, Boller T, Wiemken A. Disruption of TPS2, the gene encoding the 100-kDa subunit of the trehalose-6-phosphate synthase/phosphatase complex in *Saccharomyces cerevisiae*, causes accumulation of trehalose-6-phosphate and loss of trehalose-6-phosphate phosphatase activity. *Eur J Biochem.* 1993;212(2):315-23. PubMed PMID: 8444170.
152. Boshoff HI, Myers TG, Copp BR, McNeil MR, Wilson MA, Barry CE, 3rd. The transcriptional responses of *Mycobacterium tuberculosis* to inhibitors of metabolism: novel insights into drug mechanisms of action. *J Biol Chem.* 2004;279(38):40174-84. doi: 10.1074/jbc.M406796200. PubMed PMID: 15247240.
153. Arnvig K, Young D. Non-coding RNA and its potential role in *Mycobacterium tuberculosis* pathogenesis. *RNA Biol.* 2012;9(4):427-36. doi: 10.4161/rna.20105. PubMed PMID: 22546938; PubMed Central PMCID: PMC3384566.
154. Kim JH, O'Brien KM, Sharma R, Boshoff HI, Rehren G, Chakraborty S, et al. A genetic strategy to identify targets for the development of drugs that prevent bacterial persistence. *Proc Natl Acad Sci U S A.* 2013;110(47):19095-100. Epub 2013/11/06. doi: 10.1073/pnas.1315860110. PubMed PMID: 24191058; PubMed Central PMCID: PMC3839782.
155. Long JE, DeJesus M, Ward D, Baker RE, Ioerger T, Sassetti CM. Identifying essential genes in *Mycobacterium tuberculosis* by global phenotypic profiling. *Methods Mol Biol.* 2015;1279:79-95. doi: 10.1007/978-1-4939-2398-4_6. PubMed PMID: 25636614.
156. Griffin JE, Gawronski JD, DeJesus MA, Ioerger TR, Akerley BJ, Sassetti CM. High-resolution phenotypic profiling defines genes essential for mycobacterial growth and cholesterol catabolism. *PLoS Pathog.* 2011;7(9):e1002251. doi: 10.1371/journal.ppat.1002251. PubMed PMID: 21980284; PubMed Central PMCID: PMC3182942.
157. Sala C, Haouz A, Saul FA, Miras I, Rosenkrands I, Alzari PM, et al. Genome-wide regulon and crystal structure of Blal (Rv1846c) from *Mycobacterium tuberculosis*. *Mol Microbiol.* 2009;71(5):1102-16. doi: 10.1111/j.1365-2958.2008.06583.x. PubMed PMID: 19154333.
158. JR WRJ. Characterization of the *Mycobacterium tuberculosis* iniBAC Promoter, a Promoter That Responds to Cell Wall Biosynthesis Inhibition. *JOURNAL OF BACTERIOLOGY.* 2000;182(7):1802-11. doi: 10.1128/JB.182.7.1802-1811.2000
159. Geiman DE, Raghunand TR, Agarwal N, Bishai WR. Differential gene expression in response to exposure to antimycobacterial agents and other stress conditions among seven *Mycobacterium tuberculosis* whiB-like genes. *Antimicrob Agents Chemother.* 2006;50(8):2836-41. doi: 10.1128/AAC.00295-06. PubMed PMID: 16870781; PubMed Central PMCID: PMC1538666.
160. Colangeli R, Helb D, Sridharan S, Sun J, Varma-Basil M, Hazbon MH, et al. The *Mycobacterium tuberculosis* iniA gene is essential for activity of an efflux pump that confers drug tolerance to both isoniazid and ethambutol. *Mol Microbiol.* 2005;55(6):1829-40. doi: 10.1111/j.1365-2958.2005.04510.x. PubMed PMID: 15752203.
161. Evans JC, Mizrahi V. The application of tetracycline-regulated gene expression systems in the validation of novel drug targets in *Mycobacterium tuberculosis*. *Front Microbiol.* 2015;6:812. doi: 10.3389/fmicb.2015.00812. PubMed PMID: 26300875; PubMed Central PMCID: PMC4523840.
162. Stallings CL, Stephanou NC, Chu L, Hochschild A, Nickels BE, Glickman MS. CarD is an essential regulator of rRNA transcription required for *Mycobacterium tuberculosis* persistence. *Cell.* 2009;138(1):146-59. doi: 10.1016/j.cell.2009.04.041. PubMed PMID: 19596241; PubMed Central PMCID: PMC2756155.
163. Leblanc C, Prudhomme T, Tabouret G, Ray A, Burbaud S, Cabantous S, et al. 4'-Phosphopantetheinyl transferase PptT, a new drug target required for *Mycobacterium tuberculosis* growth and persistence in vivo. *PLoS Pathog.* 2012;8(12):e1003097. doi: 10.1371/journal.ppat.1003097. PubMed PMID: 23308068; PubMed Central PMCID: PMC3534377.
164. Park SW, Klotzsche M, Wilson DJ, Boshoff HI, Eoh H, Manjunatha U, et al. Evaluating the Sensitivity of *Mycobacterium tuberculosis* to Biotin Deprivation Using Regulated Gene Expression. *Plos Pathogens.* 2011;7(9). doi: ARTN e1002264

- 10.1371/journal.ppat.1002264. PubMed PMID: WOS:000295409000064.
165. Soni V, Upadhyay S, Suryadevara P, Samla G, Singh A, Yogeewari P, et al. Depletion of *M. tuberculosis* GlmU from Infected Murine Lungs Effects the Clearance of the Pathogen. *PLoS Pathog.* 2015;11(10):e1005235. Epub 2015/10/22. doi: 10.1371/journal.ppat.1005235. PubMed PMID: 26489015; PubMed Central PMCID: PMC4619583.
166. Pandey R, Rodriguez GM. IdeR is required for iron homeostasis and virulence in *Mycobacterium tuberculosis*. *Mol Microbiol.* 2014;91(1):98-109. doi: 10.1111/mmi.12441. PubMed PMID: 24205844; PubMed Central PMCID: PMC43902104.
167. Gill WP, Harik NS, Whiddon MR, Liao RP, Mittler JE, Sherman DR. A replication clock for *Mycobacterium tuberculosis*. *Nat Med.* 2009;15(2):211-4. Epub 2009/02/03. doi: 10.1038/nm.1915. PubMed PMID: 19182798; PubMed Central PMCID: PMC2779834.
168. Xu S, Zhou J, Liu L, Chen J. Arginine: A novel compatible solute to protect *Candida glabrata* against hyperosmotic stress. *Process Biochemistry.* 2011;46(6):1230-5. doi: 10.1016/j.procbio.2011.01.026.
169. Lorenz MC, Bender JA, Fink GR. Transcriptional response of *Candida albicans* upon internalization by macrophages. *Eukaryot Cell.* 2004;3(5):1076-87. Epub 2004/10/08. doi: 10.1128/EC.3.5.1076-1087.2004. PubMed PMID: 15470236; PubMed Central PMCID: PMC43902104.
170. Hatzios SK, Baer CE, Rustad TR, Siegrist MS, Pang JM, Ortega C, et al. Osmosensory signaling in *Mycobacterium tuberculosis* mediated by a eukaryotic-like Ser/Thr protein kinase. *Proc Natl Acad Sci U S A.* 2013;110(52):E5069-77. Epub 2013/12/07. doi: 10.1073/pnas.1321205110. PubMed PMID: 24309377; PubMed Central PMCID: PMC3876250.
171. Bhatt A, Fujiwara N, Bhatt K, Gurucha SS, Kremer L, Chen B, et al. Deletion of *kasB* in *Mycobacterium tuberculosis* causes loss of acid-fastness and subclinical latent tuberculosis in immunocompetent mice. *Proc Natl Acad Sci U S A.* 2007;104(12):5157-62. Epub 2007/03/16. doi: 10.1073/pnas.0608654104. PubMed PMID: 17360388; PubMed Central PMCID: PMC1829279.
172. Russell-Goldman E, Xu J, Wang X, Chan J, Tufariello JM. A *Mycobacterium tuberculosis* Rpf double-knockout strain exhibits profound defects in reactivation from chronic tuberculosis and innate immunity phenotypes. *Infect Immun.* 2008;76(9):4269-81. doi: 10.1128/IAI.01735-07. PubMed PMID: 18591237; PubMed Central PMCID: PMC2519441.
173. Shimono N, Morici L, Casali N, Cantrell S, Sidders B, Ehrt S, et al. Hypervirulent mutant of *Mycobacterium tuberculosis* resulting from disruption of the *mce1* operon. *Proc Natl Acad Sci U S A.* 2003;100(26):15918-23. doi: 10.1073/pnas.2433882100. PubMed PMID: 14663145; PubMed Central PMCID: PMC307668.
174. Yuan Y, Zhu Y, Crane DD, Barry CE, 3rd. The effect of oxygenated mycolic acid composition on cell wall function and macrophage growth in *Mycobacterium tuberculosis*. *Mol Microbiol.* 1998;29(6):1449-58. Epub 1998/10/22. PubMed PMID: 9781881.

10 Statement of project contribution

Both projects have been performed in cooperation. In the following, my own contributions are described in detail and quantified.

Project 1: „Trehalose-6-phosphate-mediated toxicity determines essentiality of OtsB2 in *Mycobacterium tuberculosis* in vitro and in mice.“

Involved cooperation partners:

Dipl. Biol. M. Alber, Dr. Hendrik-Koliwer Brandl (Kalscheuer lab); Dr. S. Bornemann, Dr. K. Syson (Department of Biological Chemistry, John Innes Centre, Norwich Research Park, Norwich, Norfolk, United Kingdom); Dr. CM. Trujillo, Prof. S. Ehrt (Department of Microbiology and Immunology, Weill Cornell Medical College, New York, New York, USA); Dr. R. Deenen, Prof. Dr. K. Köhrer (Biological Medical Research Centre, Heinrich-Heine University Düsseldorf, Germany); Dr. MA De Jesus, Prof. T. Ioerger (Department of Computer Science, Texas A&M University, College Station, USA); Dr. T. Hartman, Prof. Dr. WR Jacobs Jr. (Albert Einstein College of medicine, Bronx, USA).

Own contributions:

Growth kinetics

- *M. tuberculosis* c-otsB2-tet-on mutant in liquid shaking cultures and CFU-plating under silenced and induced gene expression conditions.
- Resazurin microplate assays of *M. tuberculosis* c-otsB2-tet-on/- complemented mutant- and *M. tuberculosis* Δ otsA(u) c-otsB2-tet-on cells under induced and partially silenced gene expression conditions in static cultures, as well under supplementation of exogenous T6P and arginine.

Thin-layer chromatography

- Thin-layer chromatography of hot water extracts obtained from *M. tuberculosis* wild-type, *M. tuberculosis* c-otsB2-tet-on- and *M. tuberculosis* otsB2 in a Δ otsA(u)- mutant cells.

Isolation of total genomic RNA

- RNA extraction of mutant of partially silenced and fully induced *M. tuberculosis* c-otsB2-tet-on cells for RNAseq analysis.

Quantitative real-time PCR/ validation of RNAseq data

- qRT-PCR of c-otsB2-tet-on mutant of partially silenced and fully induced cells

Evaluation of RNAseq data

- Transcriptome analysis and compilation of significantly regulated genes based on the RNAseq analysis.

Percentage of my own contribution to the total project was 40%.

Project 2: “Characterization of the putative essential glycosyltransferase Rv0225 in a cell wall associated gene cluster in *Mycobacterium* species.”

Involved cooperation partners:

Dipl. Biol. M. Alber and Dr. Hendrik-Koliwer Brandl (Kalscheuer lab); Dr. R. Deenen, Prof. Dr. K. Köhrer (Biological Medical Research Centre, Heinrich-Heine University Düsseldorf, Germany); Prof. Dr. G. Besra (School of Bioscience, University of Birmingham, United Kingdom); Dr. D. Schwudke (Department of Bioanalytical Chemistry, The German Center for Infection Research (DZIF) in Borstel, Germany).

Own contributions:

Generation of conditional *M. tuberculosis* mutants in the $\Delta panCD$ background

- *Rv0224c*, *Rv0225*, *Rv0226c* and *Rv0228*

Generation of *M. tuberculosis*- and *M. bovis* knockout mutants

- *Rv0224c*

Generation of conditional *M. bovis* mutants

- *Rv0224c*, *Rv0226c* and *Rv0228*

Generation of conditional *M. smegmatis* mutant

- *M. smegmatis* c-*Rv0225*-tet-on

Generation of complemented mutants

- *M. tuberculosis* c-*Rv0225*-tet-on, pMV361: *Rv0225*
- *M. smegmatis* c-*Rv0225*-tet-on, pMV361: *Rv0225*
- *M. bovis* c-*Rv0225*-tet-on, pMV361: *Rv0225*

Growth kinetics of conditional *Rv0225* mutants in the genetic background of *M. tuberculosis*-/ *M. bovis*- and *M. smegmatis*

- *M. tuberculosis* c-Rv0225-tet-on CFU-plating under silenced and induced gene expression conditions.
- *M. bovis* c-Rv0225 tet-off mutant in liquid shaking cultures.
- Resazurin microplate assays of conditional Rv0225 and complemented mutants under induced and partially silenced gene expressing conditions in static cultures
- Growth kinetics on solid medium

Growth kinetics of other conditional mutants

- Resazurin microplate assays of conditional *M. tuberculosis* Rv0224c, Rv0226c and Rv0228 mutants and growth kinetics on solid medium

Thin-layer chromatography

- Mycolic acid profile of *M. tuberculosis* c-Rv0225-tet-on-mutant.

ESI-MS (electron spray ionisation-mass spectrometry)

- Sample preparation of partially silenced *M. tuberculosis* c-Rv0225-tet-on and the fully induced mutant cells as well as wild-type cells.

Isolation of total genomic RNA

- RNA extraction of mutant of partially silenced and fully induced *M. tuberculosis* c-Rv0225-tet-on cells for RNAseq analysis.

Quantitative real-time PCR/ validation of RNAseq data

- qRT-PCR of c-Rv0225-tet-on mutant of partially silenced and fully induced cells

Evaluation of RNAseq data



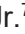
- Transcriptome analysis and compilation of significantly regulated genes based on the RNAseq analysis.

Percentage of my own contribution to the total project was 80%.

11 Research contributions


11.1 Journal publications

Trehalose-6-Phosphate-Mediated Toxicity Determines Essentiality of OtsB2 in Mycobacterium tuberculosis In Vitro and in Mice

Jan Korte^{1,2}, Marina Alber², Carolina M. Trujillo³, Karl Syson⁴, Hendrik Koliwer-Brandl², René Deenen⁵, Karl Köhrer⁵, Michael A. DeJesus⁶, Travis Hartman⁷, William R. Jacobs, Jr.⁷, Stephen Bornemann⁴, Thomas R. Ioerger⁶, Sabine Ehrlich³, Rainer Kalscheuer^{1,2*}

1 Institute for Pharmaceutical Biology and Biotechnology, Heinrich-Heine-University Düsseldorf, Düsseldorf, Germany, **2** Institute for Medical Microbiology and Hospital Hygiene, Heinrich-Heine-University Düsseldorf, Düsseldorf, Germany, **3** Department of Microbiology and Immunology, Weill Cornell Medical College, New York, New York, United States of America, **4** Department of Biological Chemistry, John Innes Centre, Norwich Research Park, Norwich, Norfolk, United Kingdom, **5** Biological and Medical Research Center (BMFZ), Cluster of Excellence on Plant Sciences (CEPLAS), Heinrich-Heine-University Düsseldorf, Düsseldorf, Germany, **6** Department of Computer Science, Texas A&M University, College Station, Texas, United States of America, **7** Department of Microbiology and Immunology, Howard Hughes Medical Institute, Albert Einstein College of Medicine, Bronx, New York, United States of America

 These authors contributed equally to this work.

 Current address: Department of Medicine, Weill Cornell Medical College, New York, New York, United States of America

[*rainer.kalscheuer@uni-duesseldorf.de](mailto:rainer.kalscheuer@uni-duesseldorf.de)

PLoS Pathog. 2016;12(12):e1006043. doi: 10.1371/journal.ppat.1006043. PubMed PMID: 27936238; PubMed Central PMCID: PMC45148154.

11.2 Talks and Poster

“Tuberculosis Co-Morbidities and Immuno-pathogenesis” in Keystone (2016, Colorado. USA)

12 Curriculum Vitae

	Personal Data
Place of Birth	Coesfeld
Date of Birth	22.10.1985
Nationality	German
Family status	Married
	Doctorate (Dr. rer. nat.)
Since 02/2013	Institute of Pharmaceutical Biology and Biotechnology, Heinrich Heine University, Düsseldorf Thesis: Key Roles of Essential Genes in Mycobacterial Glycoconjugate Biosynthesis: otsB2 and Rv0225
	University Education (Dipl.-Biol.)
WS/ 2008 – SS/ 2012	Diploma in Biology, University of Rostock External Diploma Thesis at the Center for Biochemistry, Medical Faculty, University of Cologne Thesis: Validation of Differential Expressed Genes of Insulinreceptor (Insr) and Insulinreceptor-substrate-1 (Irs-1) in Double Heterozygous Mice Versus Wildtype Animals During Aging“
WS/ 2006-SS/2008	Diploma in Biology; Karlsruhe Institute of Technology (KIT)
	School Education (General Qualification for University Entrance)
1995 - 2005	Rupert-Neudeck Gymnasium, Nottuln, Germany
	Publications
12/ 2016	Trehalose-6-phosphate mediated toxicity determines essentiality of OtsB2 in <i>Mycobacterium tuberculosis in vitro</i> and in mice”. Korte J. , Alber M., Carolina M. Trujillo, Karl Syson, Hendrik Koliwer-Brandl, René Deenen, Karl Köhrer, Travis Hartman, William R. Jacobs Jr., Stephen Bornemann, Thomas R. Ioerger, Sabine Ehrt, and Rainer Kalscheuer (09.12.2016, PLOS Pathogens).
Talks and Poster	“Tuberculosis Co-Morbidities and Immuno-pathogenesis“ in Keystone (2016, Colorado. USA)
	Career
05/ 2017 – 10/ 2017	Scientific Support Specialist, GE Healthcare, Chicago, United States
Since 10/2017	Scientific Support Specialist, Horizon Discovery, Cambridge, United Kingdom

13 Eidesstattliche Erklärung

Hiermit erkläre ich, Herr Dipl.-Biol. Jan Korte, gemäß §5 Absatz 1 der Promotionsordnung der Mathematisch-Naturwissenschaftlichen Fakultät der Heinrich-Heine-Universität Düsseldorf des Eides Statt, dass die Dissertation von mir selbstständig und ohne unzulässige fremde Hilfe unter Beachtung der „Grundsätze zur Sicherung guter wissenschaftlicher Praxis an der Heinrich-Heine-Universität Düsseldorf“ erstellt worden ist und dass ich diese in der vorgelegten oder in ähnlicher Form noch bei keiner anderen Institution eingereicht habe.

Düsseldorf, den

Jan Korte